NASA/TM—2005-213649

Forging of Advanced Disk Alloy LSHR

Timothy P. Gabb and John Gayda
Glenn Research Center, Cleveland, Ohio

John Falsey
Cleveland State University, Cleveland, Ohio

June 2005

The NASA STI Program Office . . . in Profile

Since its founding, NASA has been dedicated to the advancement of aeronautics and space science. The NASA Scientific and Technical Information (STI) Program Office plays a key part in helping NASA maintain this important role.

The NASA STI Program Office is operated by Langley Research Center, the Lead Center for NASA's scientific and technical information. The NASA STI Program Office provides access to the NASA STI Database, the largest collection of aeronautical and space science STI in the world. The Program Office is also NASA's institutional mechanism for disseminating the results of its research and development activities. These results are published by NASA in the NASA STI Report Series, which includes the following report types:

- TECHNICAL PUBLICATION. Reports of completed research or a major significant phase of research that present the results of NASA programs and include extensive data or theoretical analysis. Includes compilations of significant scientific and technical data and information deemed to be of continuing reference value. NASA's counterpart of peer-reviewed formal professional papers but has less stringent limitations on manuscript length and extent of graphic presentations.

- TECHNICAL MEMORANDUM. Scientific and technical findings that are preliminary or of specialized interest, e.g., quick release reports, working papers, and bibliographies that contain minimal annotation. Does not contain extensive analysis.

- CONTRACTOR REPORT. Scientific and technical findings by NASA-sponsored contractors and grantees.

- CONFERENCE PUBLICATION. Collected papers from scientific and technical conferences, symposia, seminars, or other meetings sponsored or cosponsored by NASA.

- SPECIAL PUBLICATION. Scientific, technical, or historical information from NASA programs, projects, and missions, often concerned with subjects having substantial public interest.

- TECHNICAL TRANSLATION. English-language translations of foreign scientific and technical material pertinent to NASA's mission.

Specialized services that complement the STI Program Office's diverse offerings include creating custom thesauri, building customized databases, organizing and publishing research results . . . even providing videos.

For more information about the NASA STI Program Office, see the following:

- Access the NASA STI Program Home Page at ***http://www.sti.nasa.gov***

- E-mail your question via the Internet to help@sti.nasa.gov

- Fax your question to the NASA Access Help Desk at 301–621–0134

- Telephone the NASA Access Help Desk at 301–621–0390

- Write to:
  NASA Access Help Desk
  NASA Center for AeroSpace Information
  7121 Standard Drive
  Hanover, MD 21076

NASA/TM—2005-213649

Forging of Advanced Disk Alloy LSHR

Timothy P. Gabb and John Gayda
Glenn Research Center, Cleveland, Ohio

John Falsey
Cleveland State University, Cleveland, Ohio

National Aeronautics and
Space Administration

Glenn Research Center

June 2005

Acknowledgments

The tests and heat treatments were performed at PCC-Wyman-Gordon Forgings, Houston R&D Laboratory, by James Arnold, under the direction of Ian Dempster.

Available from

NASA Center for Aerospace Information
7121 Standard Drive
Hanover, MD 21076

National Technical Information Service
5285 Port Royal Road
Springfield, VA 22100

Available electronically at http://gltrs.grc.nasa.gov

Forging of Advanced Disk Alloy LSHR

Timothy P. Gabb and John Gayda
National Aeronautics and Space Administration
Glenn Research Center
Cleveland, Ohio 44135

John Falsey
Cleveland State University
Cleveland, Ohio 44115–2214

Introduction

The powder metallurgy disk alloy LSHR was designed with a relatively low γ' solvus temperature and high refractory element content to allow versatile heat treatment processing combined with high tensile, creep and fatigue properties (ref. 1). When processed to produce microstructures with fine grains near 10 μm in diameter, the alloy can exhibit high tensile strength, creep resistance, and fatigue resistance at temperatures up to 650 °C. When alternatively processed to produce microstructures with coarser grains near 50 μm in diameter, the alloy can exhibit high tensile strength, creep resistance, and fatigue crack propagation resistance to temperatures exceeding 700 °C. Grain size is predominantly controlled by the solution heat treatment temperature in relationship to the γ' solvus temperature (ref. 2). "Subsolvus" solution heat treatments below the solvus temperature allow coarse remnant "primary" γ' particles 1 to 5 μm in diameter to remain and constrain grain growth. "Supersolvus" solution heat treatments above the solvus temperature dissolves the coarse remnant "primary" γ' particles, and grains can grow significantly larger.

However, forging process conditions can also significantly affect solution heat treatment-grain size response. Forging process conditions influence the as-forged grain size of the microstructure. Furthermore, the forging process conditions also introduce varying amounts of dislocations and associated internal energy within the microstructure, which drives grain growth during solution heat treatments (ref. 3). Therefore, it is necessary to understand the relationships between forging process conditions and the eventual grain size of solution heat treated material. This would allow selection of appropriate forging conditions having sufficient tolerances for production processes, in order to produce uniform fine grain and coarse grain microstructures. This is especially important for low cycle fatigue resistance, where fatigue life can be sensitive to both mean and as-large-as (ALA) grain size (refs. 4 and 7).

The objective of this study was to perform forging and heat treatment experiments ("thermomechanical processing" or "TMP" experiments) on small compression test specimens of extruded LSHR material, in order to identify viable forging process conditions allowing uniform fine grain and coarse grain microstructures after the appropriate heat treatments. Selected forging conditions could then be applied to a production-size forging.

Material and Procedure

Specimen machining, testing, and heat treatments were performed by Wyman-Gordon Forgings, Houston, Texas. A 28 mm thick cross-section of a 15.3 cm diameter extrusion was removed using an abrasive disk saw. Specimen blanks were then electrodischarge machined along a 7.6 cm diameter circle centered in the cross section. Fifteen right circular cylinder (RCC) specimens having a diameter

of 12.3 mm and length of 19 mm were then machined. RCC specimens have fairly uniform strain and strain rate as a function of location within the specimen interior when compression tested. Two double cone (DC) specimens were also machined according to figure 1 (ref. 4). DC specimens have varying strains and strain rates as a function of interior location when compression tested. The matrix of test conditions for the RCC and DC specimens is illustrated in figure 2. RCC specimens were tested at three temperatures of 1050, 1080, and 1110 °C using 3 strain rates of 0.0003, 0.003, and 0.03 sec^{-1}, after being presoaked at the test temperature for times of 1 to 8 h. This design of experiments (DOE) represents a central composite statistical test matrix, but includes no repeats of the center point. All RCC tests were continued to an upset of at least 50 percent, and true strain of 0.70. DC specimens were tested at 1080 °C and two extreme approximate strain rates of 0.0003 and 0.03 sec^{-1} after a 3h presoak. All DC tests were also continued to an upset of 50 percent.

After the tests, all specimens were sliced into four quarters. Single quarters of each specimen were heat treated together on a tray in a resistance heated furnace using subsolvus heat treatments of 1135 °C for 1 and 4h. Second quarters were given simple supersolvus heat treatments of 1171 °C for 1 and 4 h. Third quarters were give a compound heat treatment consisting of a subsolvus solution heat treatment of 1135 °C/1h, followed by supersolvus treatments of 1171 °C for 1 and 4h. Heat treated and as-forged quarters were then sectioned, metallographically prepared, and swab etched using Kallings reagent. Five fields near the center of the forging specimen were measured to determine mean grain size (G) in each case, using a circular overlay grid according to ASTM E112. The largest grain observed on each metallographic section was measured for ALA grain size according to ASTM E930. Statistical evaluations of flow stress and grain sizes were then performed. Controlled variables were orthogonally scaled to standardized form in all cases, using the relationship $v_i' = (v_i - v_{mid})/(0.5*(v_{max} - v_{min}))$. This produced a range for each standardized variable of −1 to +1, and gave standardized variables for temperature (T′), log presoak time (log(P′)), log strain rate (log(R)′), and log solution time (log(S)′) of:

$$T' = (T - 1080)/30$$
$$\log(P)' = (\log(P) - 4.5)/3.5$$
$$\log(R)' = (\log(R) + 2.523)/1$$
$$\log(S)' = (\log(S) - 2.5)/1.5$$

Regression model equations were derived by comparing the results of both forward and reverse stepwise term selection, with a 90 percent probability of significance required for term inclusion. After model selection, analysis of variance and residuals were examined to assess goodness of fit and normality. The effect of each significant variable on the response after adjustment for other variables ("adjusted effects") was then directly assessed. Finally, predicted responses and confidence intervals were also examined for each response at centerpoint and extreme variable values.

Results and Discussion

Forging Stress-Strain Response

Typical engineering stress-strain curves are shown for RCC tests, and load-displacement curves for DC tests are shown in figures 3 to 6. Stress at a given strain clearly increased with increasing strain rate and presoak temperature, and decreased with increasing temperature. Flow stress at a true strain of 0.5 for each RCC test was employed for regression analyses. Plots of this flow stress (S) vs. log (strain rate) are shown for the various test temperatures and presoak times in figure 7. A strong dependence of flow stress with strain rate and temperature is obvious. Reverse stepwise selection linear regression of log (stress) on temperature, log (presoak time), log (strain rate), and their interactive products were performed. The resulting linear regression equation was:

$$\log(\text{stress}) = 1.595152 - 0.08334T' + 0.056251\log(P)' + 0.431000\log(R)', \quad (1)$$

with a correlation coefficient $R^2_{adj} = 0.9759$ and rms error = 0.05867. The complete statistical output is included in appendix A–1. This equation indicated flow stress moderately decreased with increasing temperature, strongly increased with increasing strain rate, and moderately increased with increasing presoak time for the range of conditions investigated. This result is favorable for producibility, as average and local strain rate can be well-controlled and modeled in modern isothermal forging operations, while small variations in the actual presoak time and temperature of each forging would be permissible without large influence on flow stress. A plot of the predicted and actual flow stress indicated very good agreement, figure 8.

It is highly preferable that the alloy exhibit superplastic flow during a forging process. This allows complete flow of the material into all forging die cavities with uniform strain and strain rates in the disk, while minimizing the buildup of stresses in the dies. Superplastic flow is present when a material exhibits high strain rate sensitivity (m), as usually defined by the relationship $\sigma = K(d\varepsilon/dt)^m$. A material is considered superplastic in deformation conditions where a strain rate sensitivity m of at least 0.3 is observed. The strain rate sensitivity m was evaluated by fitting linear regression equations to the log (stress) data as a function of log (strain rate) at constant temperatures and presoak times, according to the equation:

$$\log(\sigma) = \log K + m \log(d\varepsilon/dt) \quad (2)$$

The resulting plot and equations are shown in figure 9. The strain rate sensitivity m was defined by the slope of each line and remained well above 0.3 for all conditions. The material therefore exhibited superplastic flow for the evaluated conditions.

Grain Size Response

1. As-Forged.—Images of the typical microstructures observed for all specimens in the as-forged state are compared in figures 10 to 12, and suggest only minor variations in grain size with forging conditions. The images are arranged as isotherms of the DOE in order to indicate the prior forging temperatures, strain rates, and presoak times. The macrostructures of as-forged RCC and DC specimens appeared uniform in all cases. Mean grain size at the center of DC specimens in figure 13 appeared comparable to that of RCC specimens tested at the equivalent approximated strain and strain rate conditions. Plots of as-forged mean grain size (AFG) versus log (strain rate) at various temperatures (T) and presoak times (P) of the RCC specimens are shown in figure 14. Mean grain size number appeared to moderately decrease with increasing temperature. Stepwise linear regression of mean ASTM grain size number on temperature, log (presoak time), log (strain rate), and their interactive products was performed. The resulting linear regression equation indicated as-forged grain size number (AFG) only significantly decreased with increasing temperature for the range of conditions investigated, according to the equation:

$$\text{AFG} = 12.1 - 0.39\,T', \quad (3)$$

with a correlation coefficient $R^2_{adj} = 0.3938$ and rms error = 0.3882. The complete statistical output is given in appendix A–2. A plot of the predicted and actual mean grain size indicated reasonable agreement, figure 15.

2. Subsolvus Heat Treatment Response.—Images of the typical microstructures produced after subsolvus solution heat treatments of 1135 °C for 1 and 4 hours are shown in figures 16 to 21. Mean grain size at the center of DC specimens in figure 22 again appeared comparable to that of RCC specimens tested at the equivalent approximate strain and strain rate conditions. Plots of mean grain size versus

log (strain rate) at various temperatures, presoak times, and solution heat treat times of the RCC specimens are shown in figure 23. Mean grain size number appeared to decrease with increasing temperature and solution heat treatment time. Stepwise linear regression of mean grain size number on temperature, log (presoak time), log (strain rate) and log (solution time) was performed. The resulting equation indicated subsolvus mean grain size number (SBG) strongly decreased with increasing log(solution time), and moderately decreased with increasing temperature, log (strain rate), and log (presoak time) for the range of conditions investigated, according to the equation:

$$\mathrm{SBG} = 10.803077 - 0.120\,T' - 0.0120009\,\log(R)' - 0.165107\,\log(P)' - 0.560037\,\log(S)' - 0.2125\,T'\,\log(R)' - 0.140009\,\log(R)'\,\log(S)', \tag{4}$$

with a correlation coefficient of $R^2_{adj} = 0.8755$ and rms error = 0.2355. The T' log(R)' interaction term indicated enhanced subsolvus grain growth for combinations of high temperature and high log (strain rate). The log (R)' log (S)' interaction term indicated enhanced subsolvus grain growth for combinations of high log (strain rate) and high log (solution time). The complete statistical output is given in appendix A–3. A plot of predicted and actual mean grain size indicated very good agreement, figure 25.

The macrostructures of subsolvus heat treated specimens were appeared uniform in all cases, suggesting well-controlled grain size. Plots of observed ALA subsolvus grain size versus log (strain rate) at various temperatures, presoak times, and solution times for the RCC specimens are shown in figure 24. No consistent trends are visually apparent. The results of linear regression with stepwise selection of terms indicated (appendix A–4) ALA subsolvus grain size number (SBALA) only significantly decreased with increasing log (strain rate) for the range of conditions investigated:

$$\mathrm{SBALA} = 7.65 - 0.525\,\log(R)', \tag{5}$$

with a poor correlation coefficient of $R^2_{adj} = 0.1920$ and rms error = 0.8359. A plot of predicted and actual grain size number indicated only modest agreement, figure 25.

Supersolvus Heat Treatment Response.—The microstructures of supersolvus heat treated specimens are shown in figures 26 to 32. Mean grain size at the center of DC specimens again appeared comparable to that of RCC specimens tested at the equivalent approximated strain and strain rate conditions. Plots of mean grain size number vs. log (strain rate) are shown for the various temperatures, presoaks, and solution heat treat times of the RCC specimens in figure 33. Mean grain size number appeared to decrease with increasing forging temperature. Linear regression using stepwise selection of terms indicated (appendix A–5) supersolvus mean grain size number (SPG) only moderately decreased with increasing temperature, log(presoak time), and log(solution time) for the range of conditions investigated according to the equation:

$$\mathrm{SPG} = 5.966475 - 0.275\,T' - 0.167369\,\log(P)' - 0.0223348\,\log(S)', \tag{6}$$

with a relatively low correlation coefficient of $R^2_{adj} = 0.3439$ and rms error = 0.4429. This suggested a relatively stable mean grain size for the ranges of conditions tested. However, inspection of figure 33 indicates more divergence in grain size at the highest forging temperature of 1110 °C. A plot of predicted and actual grain size number showed fair agreement, figure 34.

The macrostructures of supersolvus heat treated specimens are shown in figures 35 to 41. Reduced uniformity and large grains are evident for specimens forged at 1110 °C and a strain rate of 0.03 s^{-1}. The “rims” of DC specimens tested at 1080 °C and 0.03 s^{-1} approximated average strain rate also show large grains. Plots of ALA grain size number vs. log(strain rate) at various presoaks and solution times for the RCC specimens are shown in figure 42. Stable ALA grain sizes are evident for all specimens forged at 1050 and 1080 °C. However, very low ALA grain size numbers corresponding to large grain are present for specimens forged at 1110 °C and a strain rate of 0.03 s^{-1}. Linear regression would be expected to have

difficulty handling such sharp, isolated changes in response. However, a relationship for supersolvus ALA grain size number (SPALA) could be derived by stepwise selection (appendix A–6):

$$\begin{aligned} \text{SPALA} = {} & 1.696504 - 1.166139\ T' - 1.191710 \log(R)' - 0.698321 \log(P)' \\ & - 1.3125\ T' \log(R)' - 0.783\ T' \log(P)' - 0.732556 \log(R)' \log(P)', \end{aligned} \tag{7}$$

with a correlation coefficient of $R^2_{adj} = 0.5347$ and rms error = 1.689. In this equation, SPALA number decreased with increasing temperature, log (strain rate) and log (presoak time). The T' log (R)' interaction term indicated enhanced ALA grain growth for combinations of high temperature and high log (strain rate). The T' log (P)' interaction term indicated enhanced ALA grain growth for combinations of high temperature and high log (presoak time). The log (R)' log (P)' interaction term indicated enhanced ALA grain growth for combinations of high log (strain rate) and high log (presoak time). This equation fit was strongly influenced by the critical grain growth occurrences, and a plot of predicted and actual grain size number showed only fair agreement, figure 43. However, the equation clearly signifies that the combination of 1110 °C and strain rate of 0.03 s^{-1} should be avoided.

Combined Subsolvus + Supersolvus Heat Treatment Response.—The microstructures of subsolvus + supersolvus heat treated specimens are shown in figures 44 to 50. Mean grain size at the center of DC specimens again appeared comparable to that of RCC specimens tested at the equivalent approximated strain and strain rate conditions. Plots of mean grain size number vs. log (strain rate) are shown for the various temperatures, presoaks, and solution heat treatment times of the RCC specimens in figure 51. No consistent trends are visually obvious in these figures. Linear regression with stepwise selection of terms indicated (appendix A–7) mean subsolvus + supersolvus grain size number (SBPG) varied for the range of conditions investigated according to the equation:

$$\text{SBPG} = 5.91332 - 0.193346 \log(S)' + 0.31875\ T' \log(R)', \tag{8}$$

with a correlation coefficient of $R^2_{adj} = 0.3733$ and rms error = 0.3775. This again suggested a relatively stable mean grain size for the ranges of conditions tested. The equation indicated SBPG number decreased with increasing log (solution time). The T' log (R)' interaction term indicated enhanced grain growth for combinations of low log (strain rate) with high temperature, and high log(strain rate) with low temperature. A plot of predicted versus actual mean grain size in figure 52 showed reasonable agreement.

The macrostructures of subsolvus + supersolvus heat treated specimens are shown in figures 53 to 59. Plots of ALA grain size number vs. log (strain rate) at various presoaks and solution times for the RCC specimens are shown in figure 60. As for supersolvus heat treated specimens, ALA grain size was relatively stable for most conditions. The "rims" of DC specimens tested at 1080 °C and 0.03 s^{-1} approximated average strain rate also now showed stable ALA grain growth with the combined subsolvus plus supersolvus heat treatment, unlike the supersolvus heat treatment case. However, for the combination of 8h forging presoak, 1110 °C, and 0.03 s^{-1} strain rate, very low ALA grain size numbers corresponding to very large grains are evident in the plots and macrostructures. These few critical grain growth occurrences in RCC specimens again strongly influenced the linear regression, producing a complex relationship (appendix A–8) for subsolvus + supersolvus ALA grain size number (SBPALA) for the range of conditions investigated:

$$\begin{aligned} \text{SBPALA} = {} & 1.862922 - 0.66806\ T' - 0.542313 \log(R)' - 0.685123 \log(P)' \\ & - 0.613291\ T' \log(P)' - 0.679285 \log(R)' \log(P)', \end{aligned} \tag{9}$$

with a relatively low correlation coefficient of $R^2_{adj} = 0.3039$ and rms error = 1.466. This indicated ALA grain size number decreased with increasing temperature, log (strain rate), and log (presoak time). The log (R)' log (P)' interaction term again indicated enhanced ALA grain growth for combinations of high log (strain rate) and high log (presoak time). This equation fit was again strongly influenced by the critical

grain growth occurrences, but a plot of predicted and actual grain size number showed fair agreement, figure 61. However, the equation produced less satisfactory ALA grain size predictions for critical grain growth conditions than in the supersolvus heat treatment case.

Selection of Appropriate Forging Conditions for Uniform Microstructures.—In general terms, as-forged, subsolvus, supersolvus, and subsolvus plus supersolvus mean and as-large-as grain sizes were smallest for the lowest forging temperature of 1050 °C, and were relatively insensitive to strain rate and presoak time at that temperature. As-forged, subsolvus, supersolvus, and subsolvus plus supersolvus mean and as-large-as grain sizes were largest for the highest forging temperature of 1110 °C, and were more sensitive to strain rate and presoak time. The intermediate forging temperature of 1080 °C allowed intermediate mean and as-large-as grain sizes, with still relatively low strain rate and presoak time sensitivity. This would generally argue for a forging temperature range of 1050 to 1080 °C, to insure uniform microstructures while allowing some random variations in exact temperature and presoak times expected during production runs, and systematic variations in strain rate expected within forging dies.

The microstructures of subsolvus heat treated specimens were generally quite uniform over the entire range of forging conditions investigated. However, mean subsolvus grain size was least sensitive to strain rate and presoak time for the forging temperature range of 1050 to 1080 °C. As-large-as subsolvus grain size was also minimized over this forging temperature range. Therefore selection of this forging temperature range for material intended for subsolvus heat treatment would allow full latitude in strain rate and presoak time within the range of conditions investigated. Increasing subsolvus solution heat treat time from 1 to 4 hours allowed some coarsening of mean grain size number from near 11.5 (6.7 μm) to near 10.5 (9.4 μm), without adversely increasing as-large-as grain size.

The microstructures of supersolvus heat treated specimens were generally uniform over the temperature range of 1050 to 1080 °C for the forging conditions investigated. Mean supersolvus grain size remained near 6.0 (45 μm) and was not usually sensitive to strain rate and presoak time for this forging temperature range. As-large-as supersolvus grain size was also minimized to near 2 (180 μm) over this forging temperature range for the right circular cylinder specimens. For double cone specimens tested at 1080°C and an approximated strain rate of 0.03 s^{-1}, a divergence in response was observed between supersolvus and subsolvus plus supersolvus heat treatments. Supersolvus heat treated DC specimens exhibited critical grain growth to produce very large grains up to –6 (3100 μm) in the rims of DC specimens, while subsolvus plus supersolvus heat treatments minimized their as-large-as grain size to 2 (180 μm). The highest localized strain rates induced in the rims of DC specimens apparently encouraged enhanced deformation in the microstructure, to encourage the critical grain growth in direct supersolvus heat treatments as observed for Rene′ 88DT (ref 4). Addition of a prior subsolvus heat treatment step before the supersolvus heat treatment apparently helps anneal out some of this localized forging deformation (ref. 3). For these reasons, forging at 1050 to 1080 °C would be advisable, followed by a subsolvus plus supersolvus heat treatment to achieve a uniform microstructure with mean grain size near 6.0 (45 μm) and as-large-as grain size minimized to 2.0 (180 μm). This would allow forging presoaks of 1 to 8 hours and strain rates of 0.0003 to 0.03 s^{-1} without adverse effects.

At 1110 °C, mean supersolvus grain size was more sensitive to strain rate and presoak time. Slower strain rates and longer presoak times allowed coarser mean supersolvus grain size near 5 (65 μm). This trend of coarser mean supersolvus grain size with higher forging temperature, slower strain rates, and longer presoak times has been previously observed in another powder metallurgy disk superalloy (ref. 6). As-large-as grain size remained near 2 (180 μm) at strain rates of 0.0003 to 0.003 s^{-1}, but critical grain growth produced very large grains for a forging strain rate of 0.03 s^{-1}. Therefore, forging at this temperature followed by a subsolvus plus supersolvus heat treatment could be used to achieve a coarser mean grain size near 5.0, provided that the forging strain rates are maintained between 0.0003 and 0.003 s^{-1}. Forging presoak times between 1 and 8 h would be allowable in these conditions.

Comparison of TMP Specimen and Disk Forging Results.—The forging condition recommendations based on TMP test results were compared to disk forging results for the supersolvus

case, where grain size control can be more critical for high temperature applications. Grain size control can be especially important in low cycle fatigue resistance, where coarser grain size can reduce fatigue life (refs. 4 and 7). An extrusion mult 16.5 cm in diameter and 20 cm long was forged at 1080 °C after a presoak time of 3 hours, using an average strain rate of 0.003 s^{-1}. The mult was forged to a final height of 4 cm, representing an 80 percent upset. This forged disk was then given a subsolvus solution heat treatment of 1135 °C/1h, followed by a supersolvus treatment of 1171 °C for 3 hours. Equation 8 predicted a mean grain size of 5.8 (48 μm) for these conditions, while equation 9 predicted an as-large-as grain size of 1.8 (190 μm). Measurements on duplicate specimens extracted from the disk indicated mean grain sizes of 6.7 (35 μm) and 7.2 (30 μm). As-large-as grain sizes were 2.5 (150 μm) and 3.0 (125 μm). The experimental forging grain size results were conservatively finer than those predicted using the TMP specimen data, and quite satisfactory. The finer grain sizes observed in the disk could be related to the much greater forging upset of 80 percent and true strain of 1.6 in the disk forging, compared to the 50 percent upset and true strain of 0.7 percent incurred in TMP test specimens. The higher strains within the forging could encourage more grain recrystallization, for finer resulting heat treated grain sizes.

Summary and Conclusions

A series of forging experiments were performed with subsequent subsolvus and supersolvus heat treatments, in search of suitable forging conditions for producing uniform fine grain and coarse grain microstructures. Forging temperatures of 1050 to 1110 °C and strain rates of 0.0003 to 0.03 s^{-1} were used, after presoaks of 1h to 8h. Subsolvus, supersolvus, and combined subsolvus plus supersolvus heat treatments were then applied with final solution times of 1h or 4h. The findings over this range of test conditions can be summarized as follows:

1) The material displayed the desired superplastic response under these compression testing conditions.
2) Forging flow stress strongly increased with increasing strain rate, but only moderately increased with decreasing temperature and increasing presoak time.
3) As-forged grain size number varied between 13.0 and 11.4 (4.0 and 7.0 μm), and only moderately coarsened with increasing temperature.
4) Subsolvus heat treated mean grain size number varied between 12 and 9.5 (5.6 and 13 μm), strongly coarsened with increasing log (solution time), and moderately coarsened with increasing temperature, log (strain rate), and log (presoak time).
5) Subsolvus as-large-as grain size number was very well controlled at between 9.5 and 5.5 (13 and 55 μm), and only significantly coarsened with increasing log (strain rate).
6) Supersolvus heat treated mean grain size number varied between 6.6 and 4.2 (36 and 85 μm), and substantially coarsened with increasing temperature, log (presoak time), and log (solution time).
7) Supersolvus as-large-as grain size number varied between 4.0 and –6.5 (90 and 3100 μm), and substantially coarsened with increasing temperature, log (strain rate) and log (presoak time).
8) Subsolvus plus supersolvus heat treated mean grain size number varied between 6.8 and 5.0 (34 and 65 μm), and coarsened with increasing log (solution time).
9) Subsolvus plus supersolvus heat treated as-large-as grain size number varied between 3.5 and –6.0 (105 and 2600 μm), and coarsened with increasing temperature, log (strain rate), and log (presoak time).
10) Forging conditions combining high temperature, high presoak time, and high strain rate produced very large, macroscopic grains.

It can be concluded from this work that:

1) Forging at temperatures of 1050 to 1080 °C over the full range of presoak times and strain rates investigated is recommended to achieve mean grain sizes of 10.5 to 11.5 and ALA grain sizes of 6.5 for applications utilizing subsolvus heat treatments.
2) Forging at temperatures of 1050 to 1080 °C over the full range of presoak times and strain rates investigated is recommended to achieve mean grain size near 6.0 and as-large-as grain size of 2.0, for applications utilizing a subsolvus plus supersolvus heat treatment.
3) Alternatively forging near 1110 °C over the full range of presoak times and strain rates of 0.0003 to 0.003 s^{-1} is recommended to achieve coarser mean grain size near 5.0 and as-large-as grain size of 2.0, when using a subsolvus plus supersolvus heat treatment.
4) Forging at 1050 to 1080 °C and strain rates of 0.0003 to 0.003 s^{-1} is recommended for material intended for direct supersolvus heat treatments, in order to avoid critical grain growth.

References

1. Enabling Propulsion Materials Program Final Technical Report, Vol. 5: Task K—Long Life Compressor/Turbine Disk Material, Contract NAS3–26385, NASA Glenn Research Center, May 2000.
2. K.R. Bain, "Development of Damage Tolerant Microstructures in Udimet 720", Superalloys 1984, ed. M. Gell, et al., The Minerals, Metals, and Materials Society, Warrendale, PA, 1984, pp. 13–22.
3. C.P. Blankenship, Jr., M.F. Henry, J.M. Hyzak, R.B. Rohling, E.L. Hall, "Hot-Die Forging of P/M Ni-Base Superalloys," Superalloys 1996, ed. R.D. Kissinger, D.J. Deye, D.L. Anton, A.D. Cetel, M.V. Nathal, T.M. Pollock, D.A. Woodford, The Minerals, Metals, and Materials Society, Warrendale, PA, 1996, pp. 653–662.
4. E. Huron, S. Srivatsa, E. Raymond, "Control of Grain Size Via Forging Strain Rate Limits for R′88DT," Superalloys 2000, ed. T.M. Pollock, R.D. Kissinger, R.R. Bowman, K.A. Green, M. McLean, S.L. Olson, J.J. Schirra, The Minerals, Metals, and Materials Society, Warrendale, PA, 2000, pp. 49–58.
5. M. Soucail, M. Harty, H. Octor, "The Effect of High Temperature Deformation on Grain Growth in a P/M Nickel-Base Superalloy," Superalloys 1996, ed. R.D. Kissinger, D.J. Deye, D.L. Anton, A.D. Cetel, M.V. Nathal, T.M. Pollock, D.A. Woodford, The Minerals, Metals, and Materials Society, Warrendale, PA, 1996, pp. 663–666.
6. T.P. Gabb, K. O'Connor, "High Temperature, Slow Strain Rate Forging of Advanced Disk Alloy ME3," NASA/TM—2001-210901, National Aeronautics and Space Administration, Washington, D.C., 2001.
7. T.P. Gabb, J. Gayda, J. Telesman, P.T. Kantzos, "Thermal and Mechanical Property Characterization of the Advanced Disk Alloy LSHR," NASA/TM—2005-213645, National Aeronautics and Space Administration, Washington, D.C., June 2005.

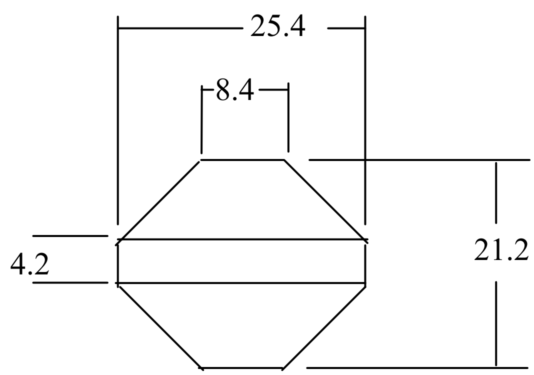

Figure 1.—Double cone specimen configuration, with dimensions in millimeters.

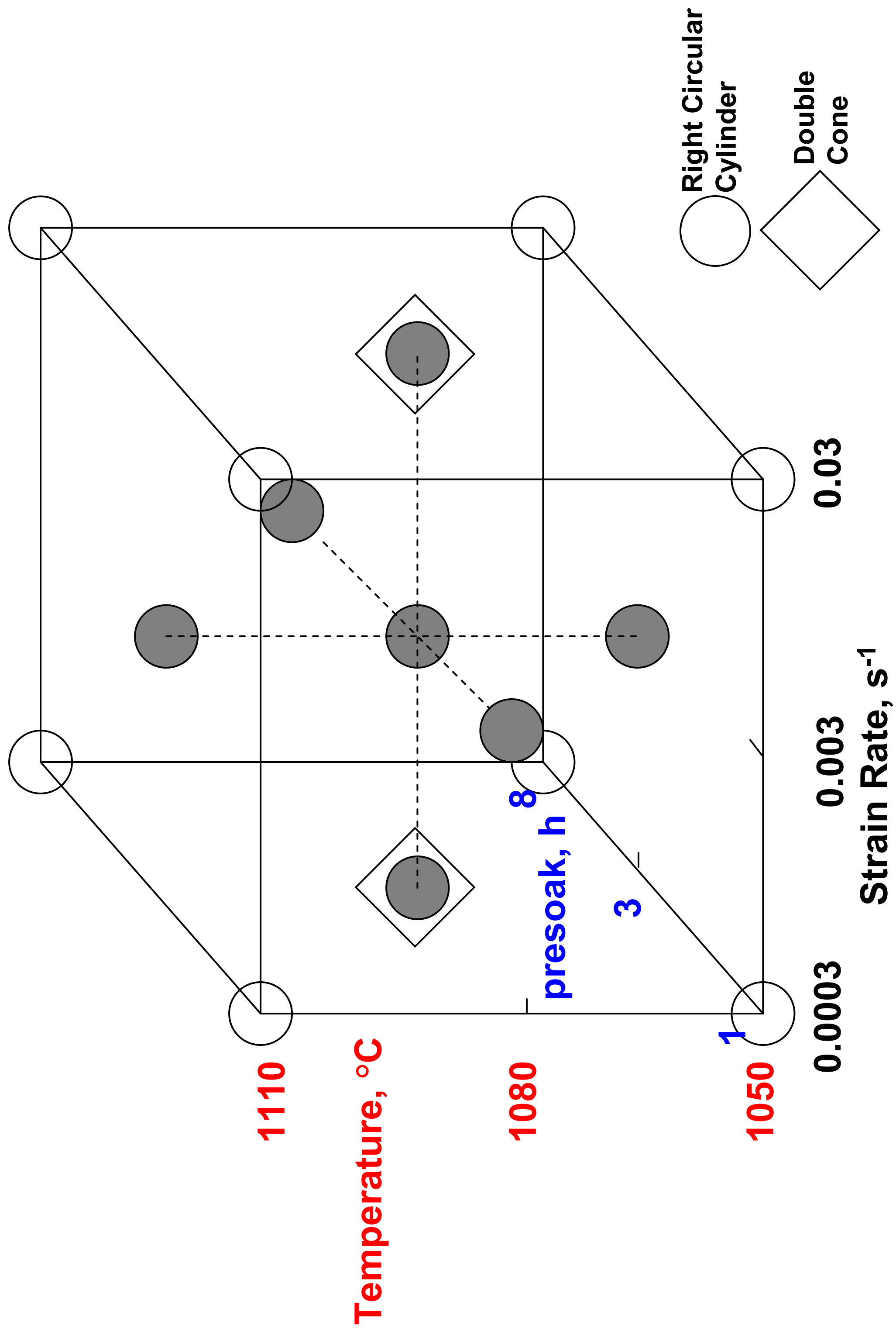

Figure 2.—Diagram showing the design of experiments with experimental conditions.

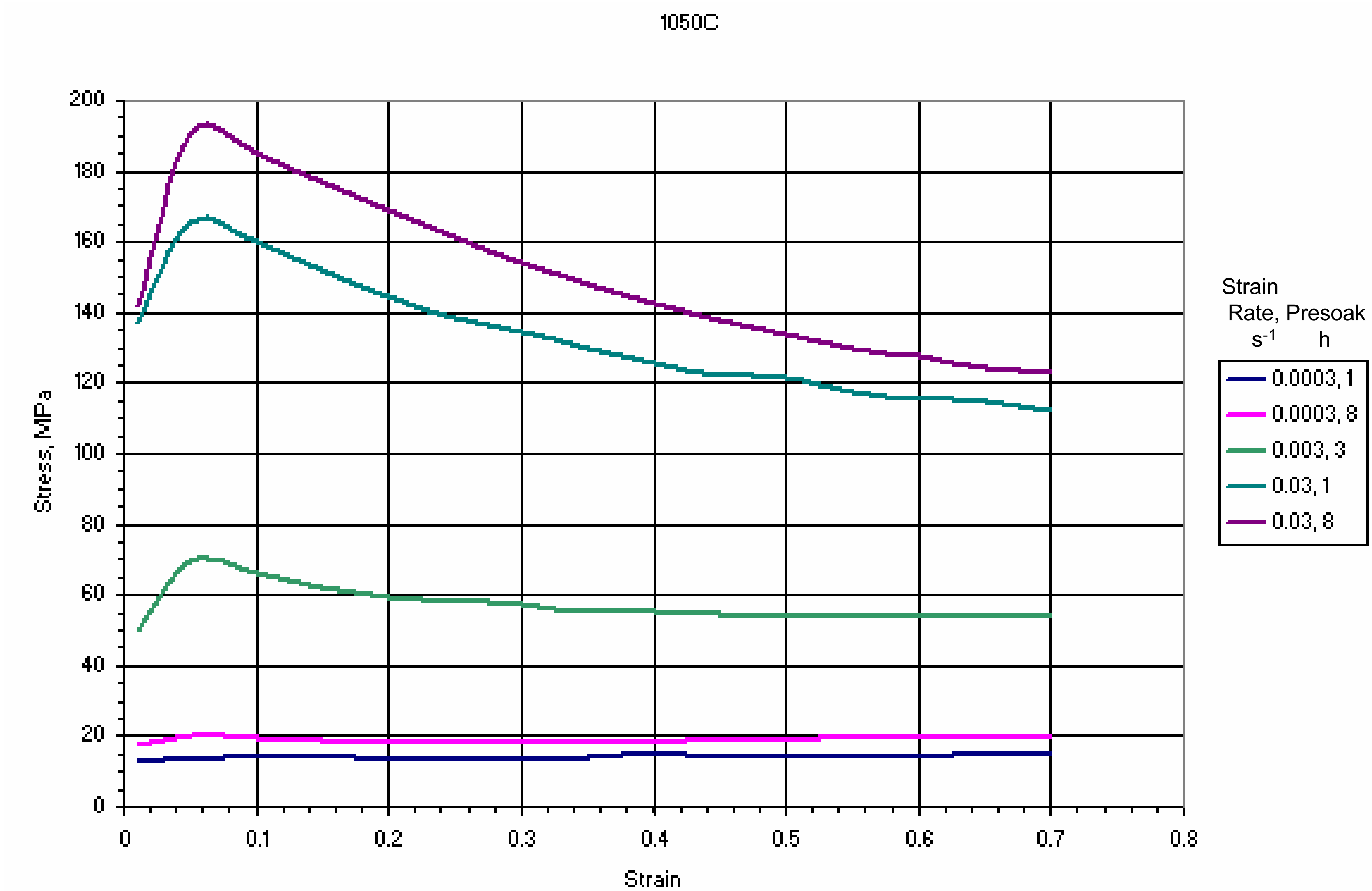

Figure 3.—Compression test stress-strain responses at 1050 °C.

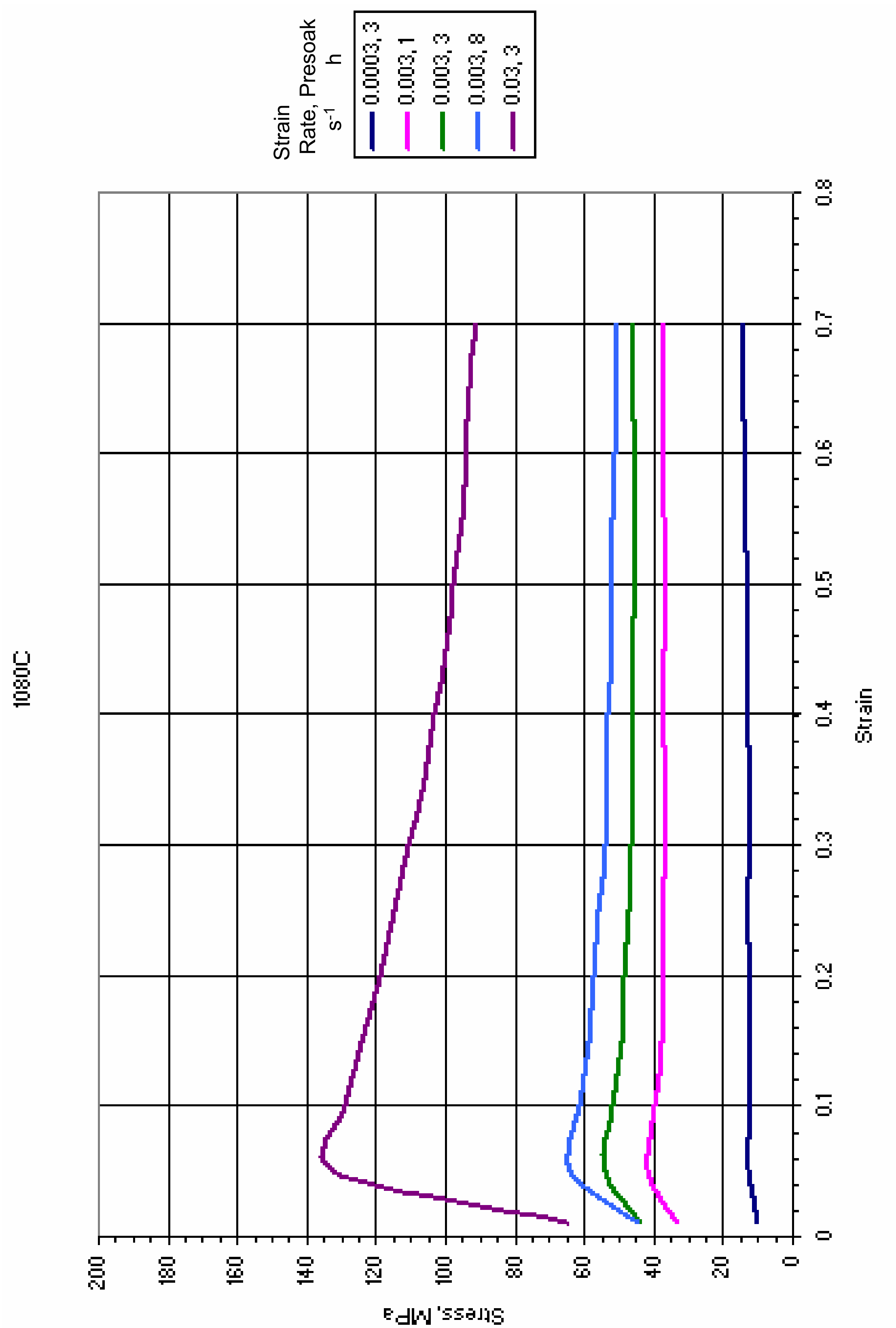

Figure 4.—Compression test stress-strain responses at 1080 °C.

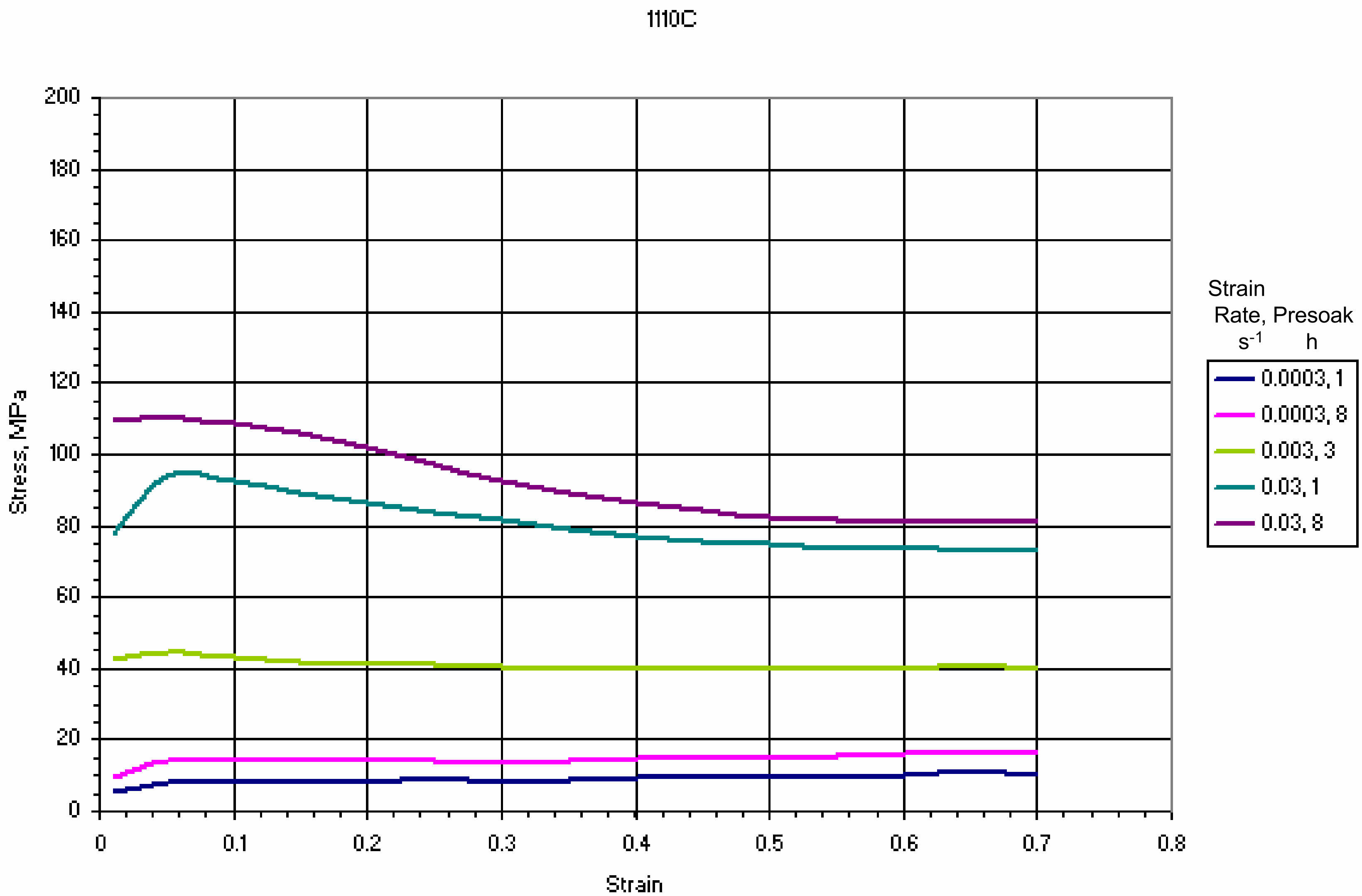

Figure 5.—Compression test stress-strain responses at 1110 °C.

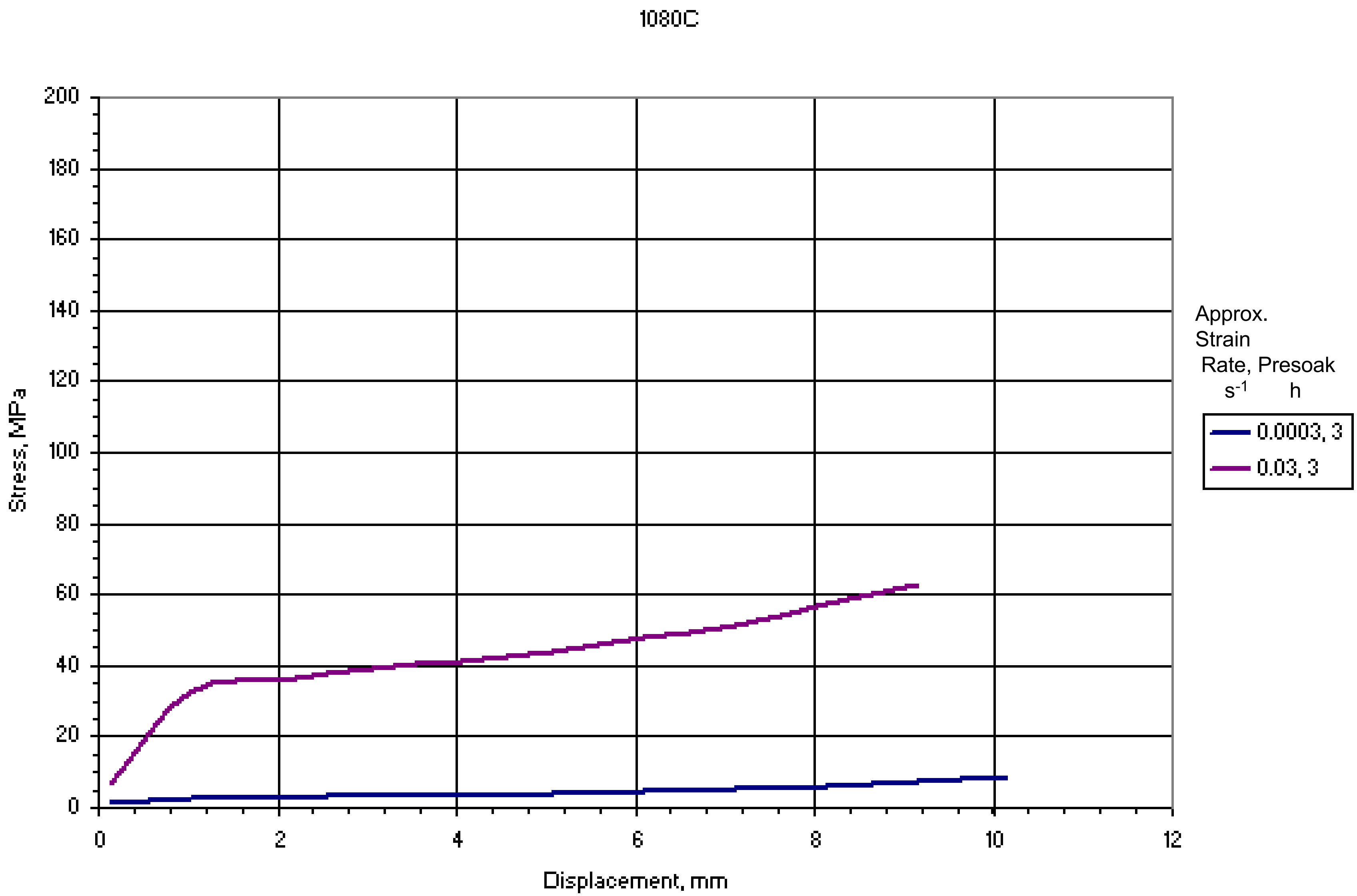

Figure 6.—Compression test stress-displacement responses for double cone specimens at 1080 °C.

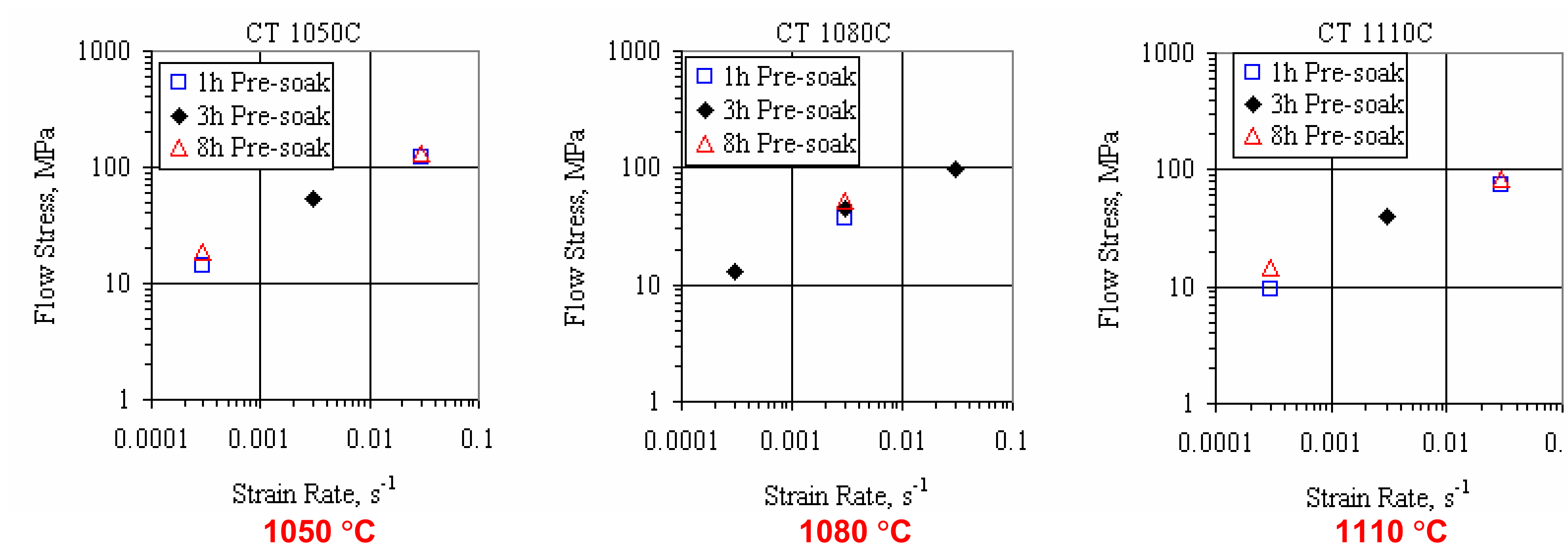

Figure 7.—Compression test true flow stress vs. strain rate.

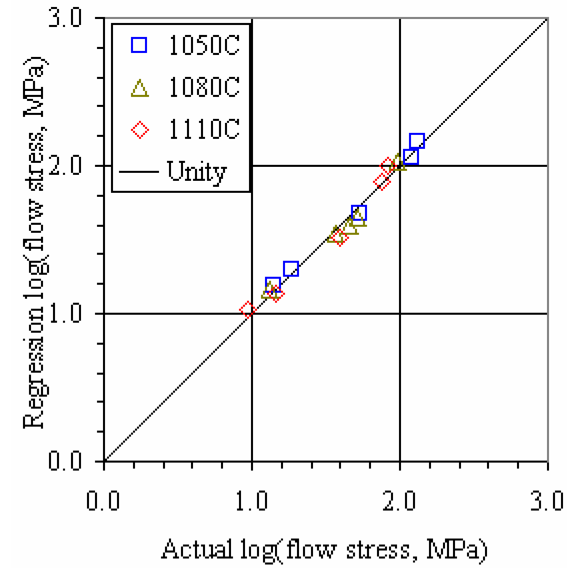

Figure 8.—Comparison of actual vs. regression flow stresses.

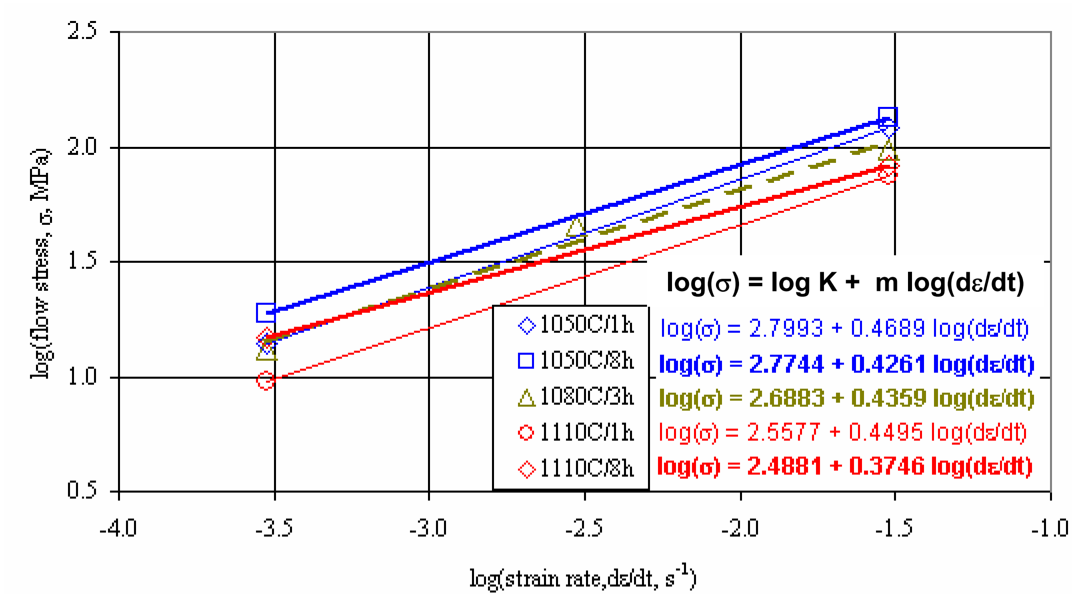

Figure 9.—Log (flow stress) vs. log (strain rate) plots with superplasticity (m) determinations.

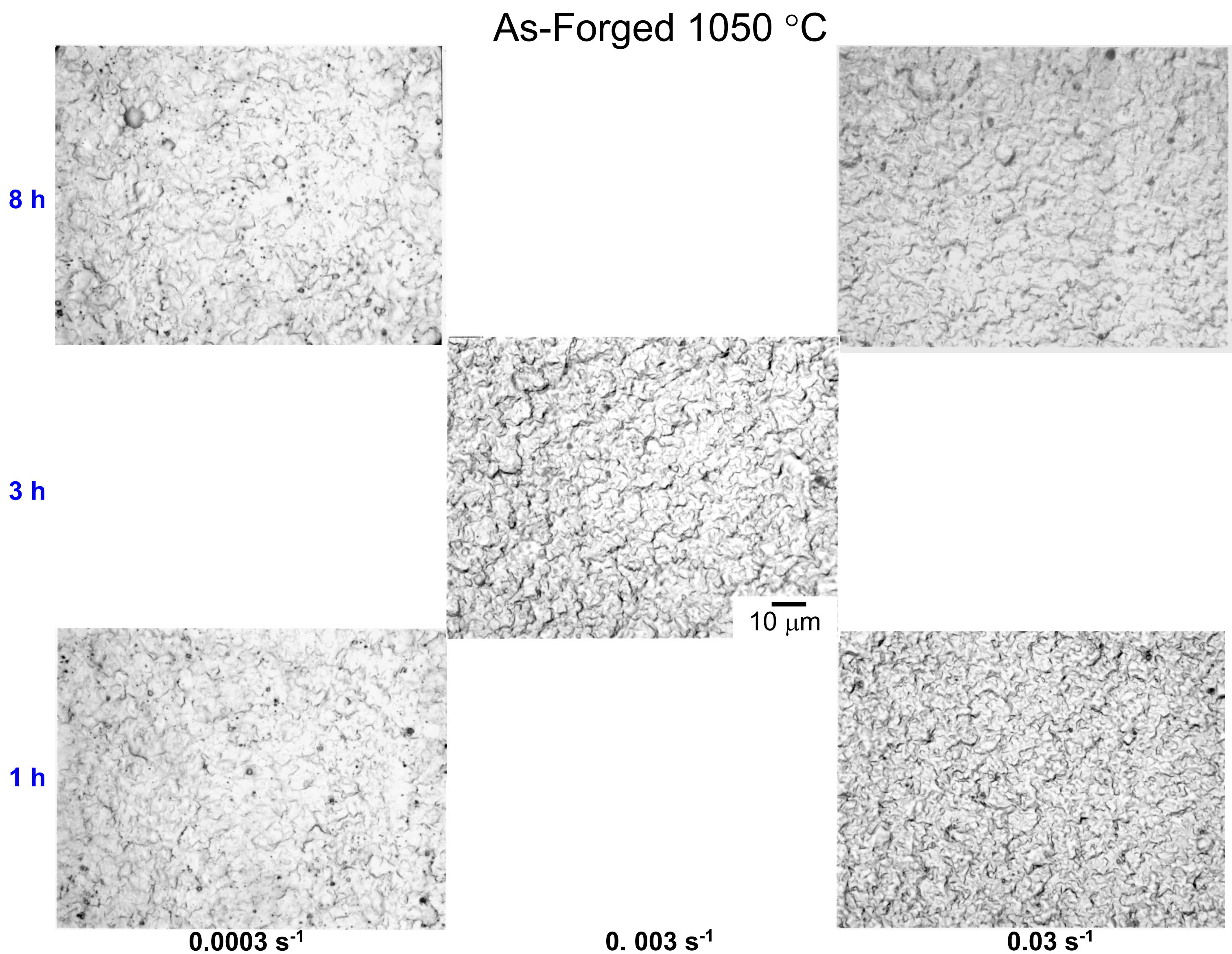

Figure 10.—Typical microstructures of specimens forged at 1050 °C with the indicated presoak times and strain rates.

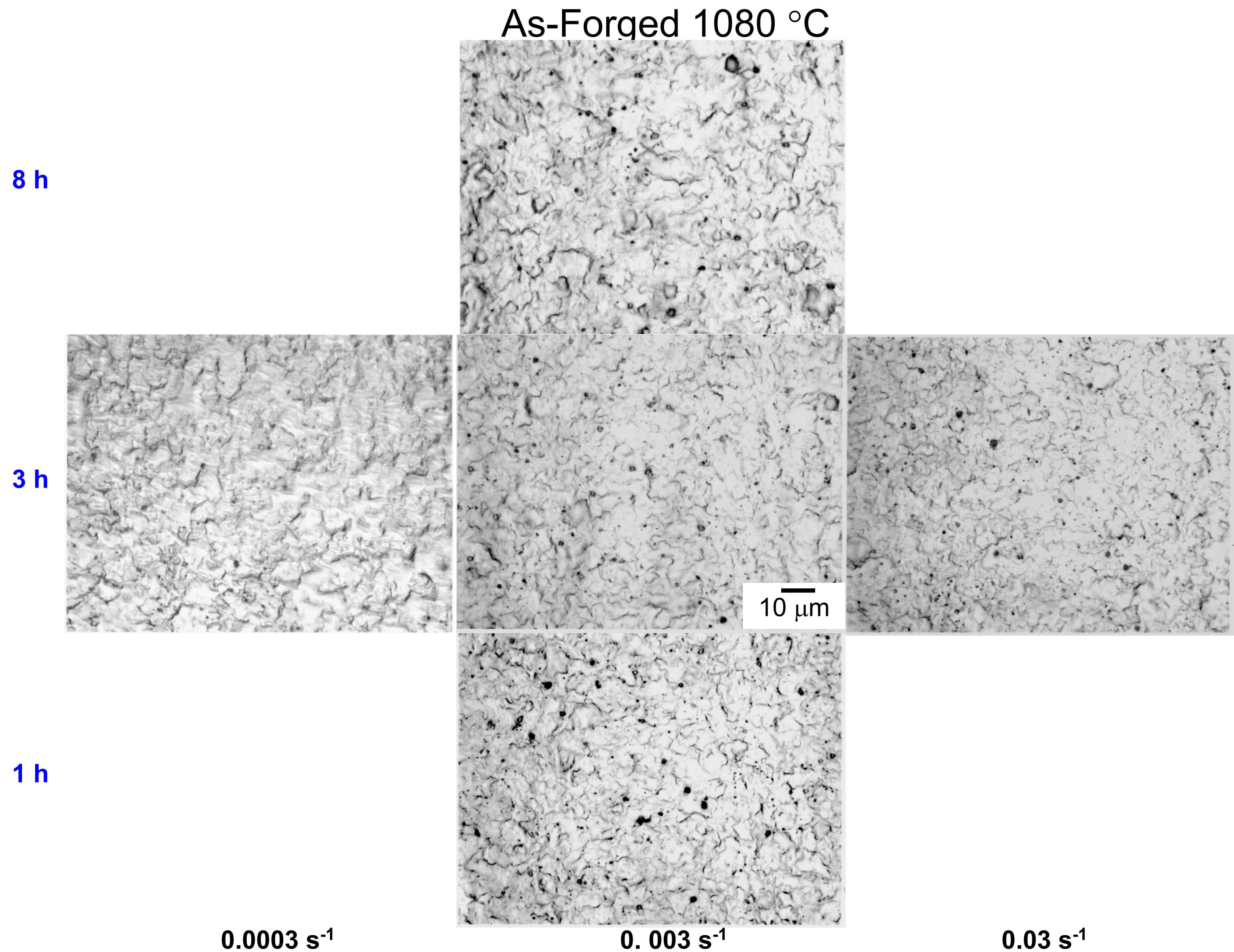

Figure 11.—Typical microstructures of specimens forged at 1080 °C with the indicated presoak times and strain rates.

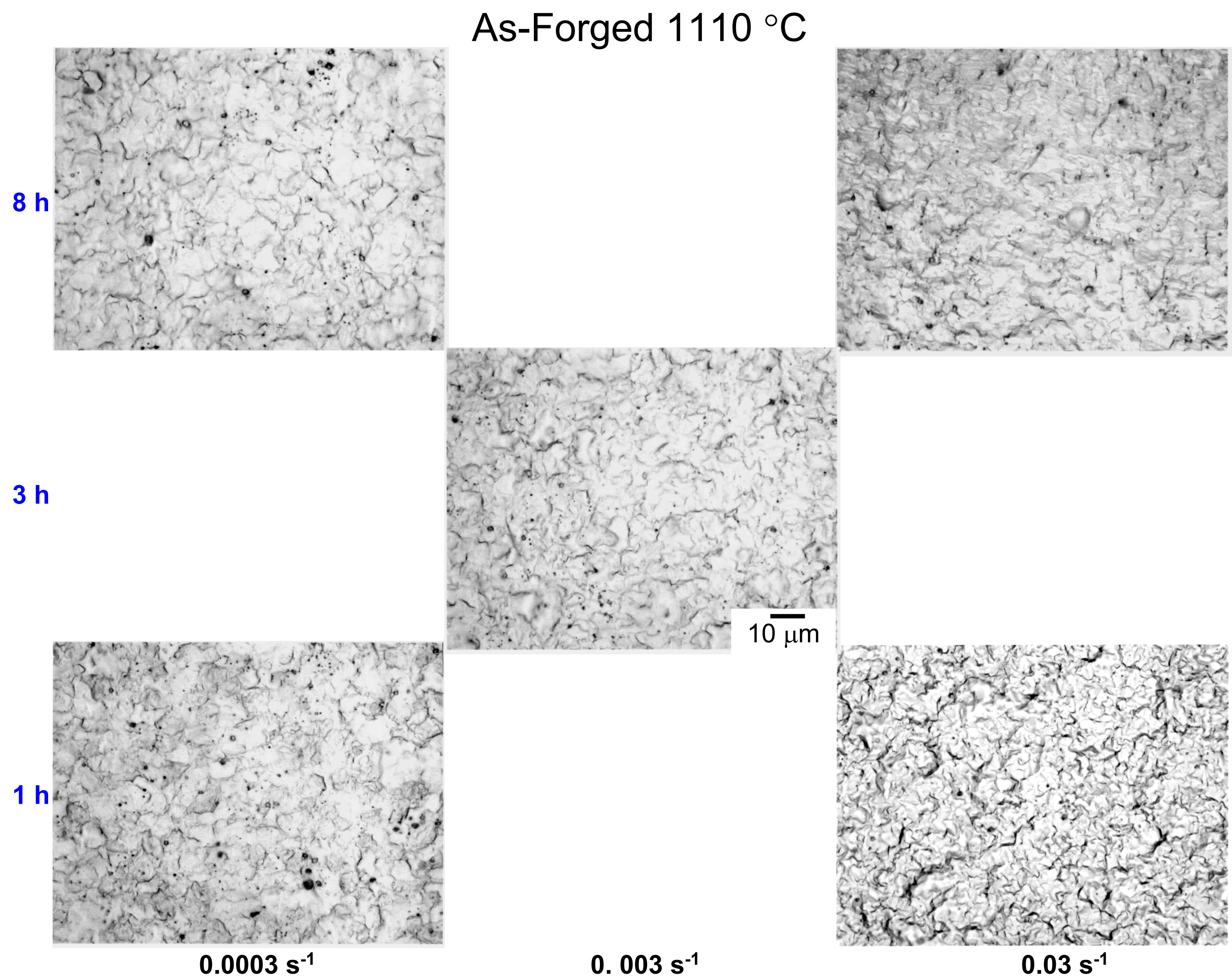

Figure 12.—Typical microstructures of specimens forged at 1110 °C with the indicated presoak times and strain rates.

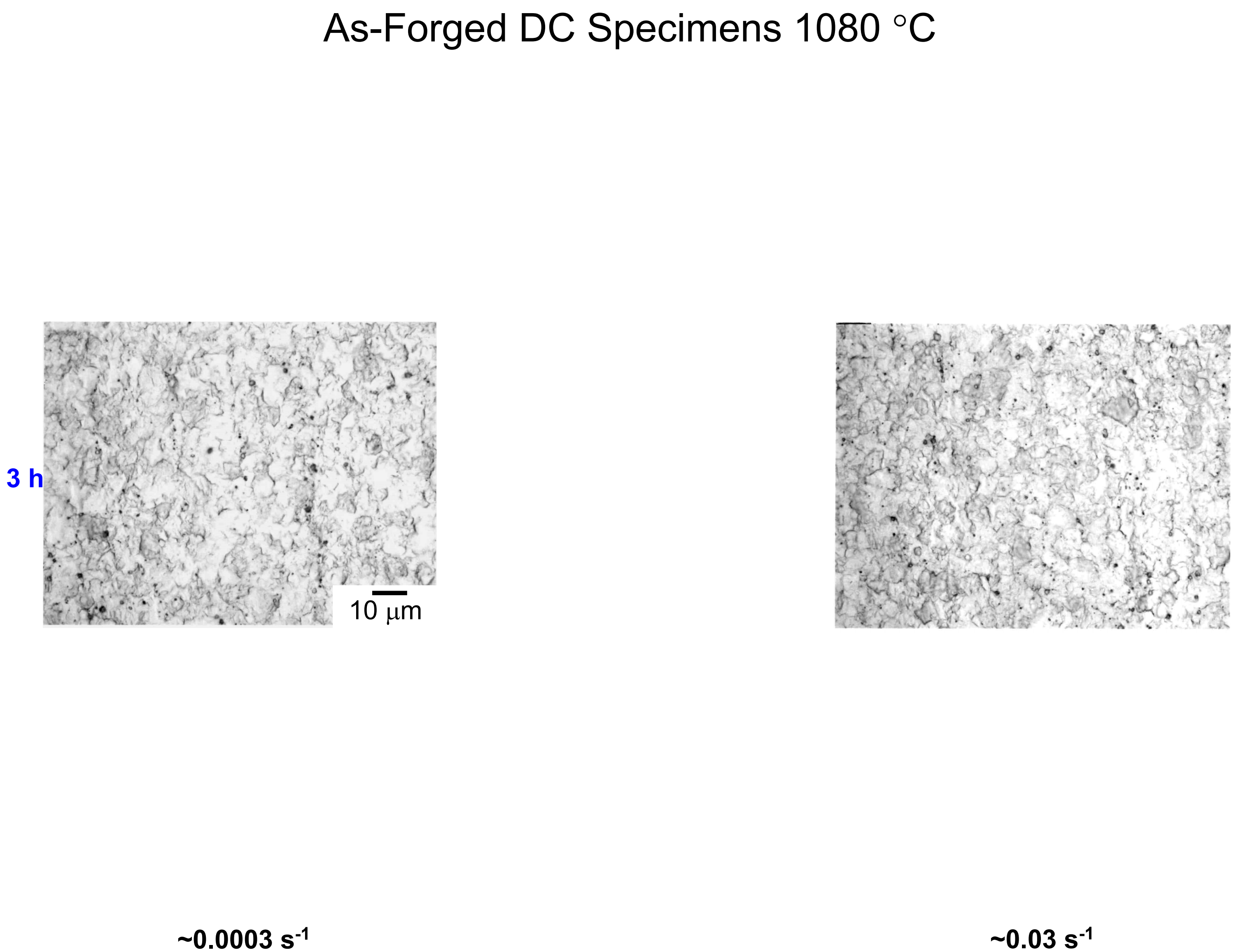

Figure 13.—Typical microstructures of specimens forged at 1080 °C with the indicated presoak times and approximate average strain rates.

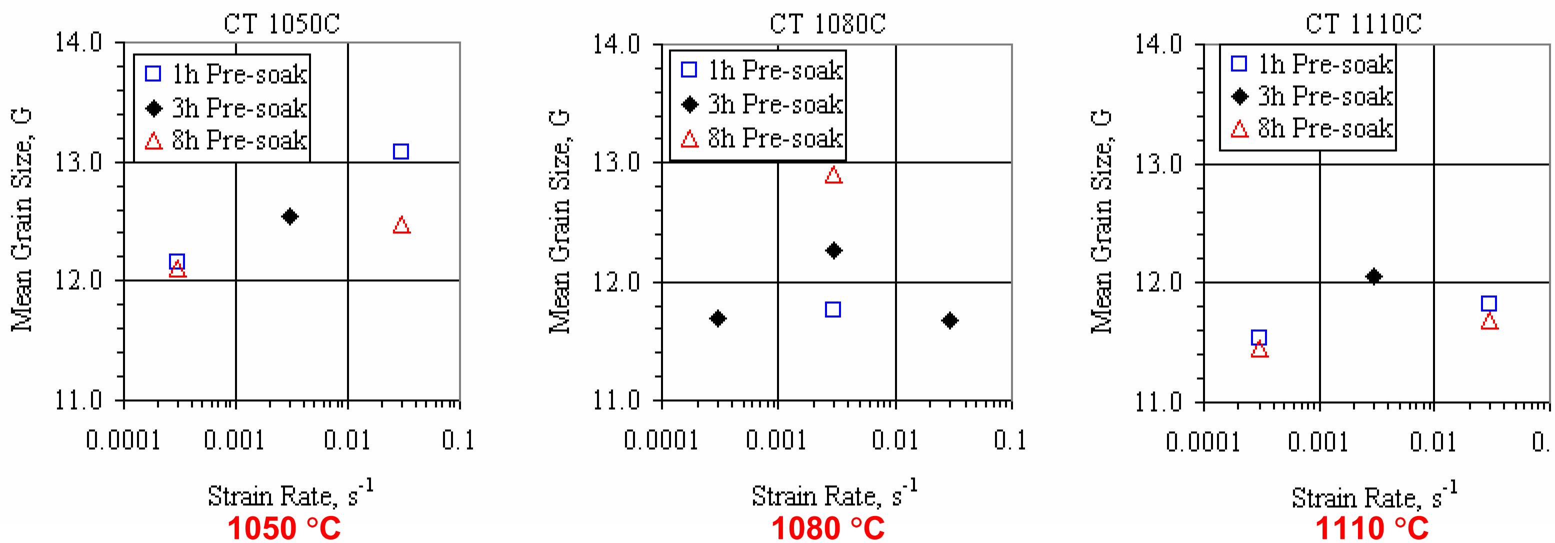

Figure 14.—Mean as-forged grain size vs. strain rate for the indicated forging presoak times and temperatures.

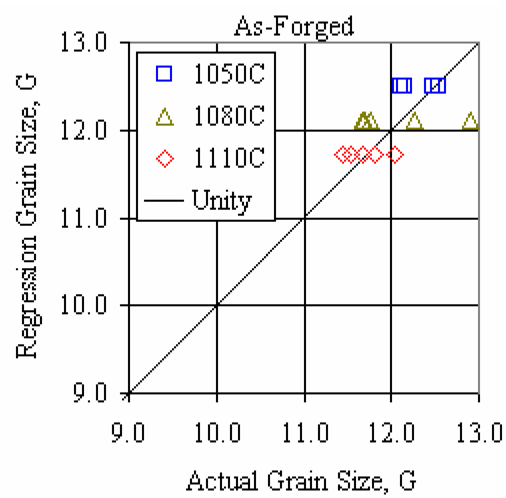

Figure 15.—Comparison of actual vs. regression as-forged mean grain sizes.

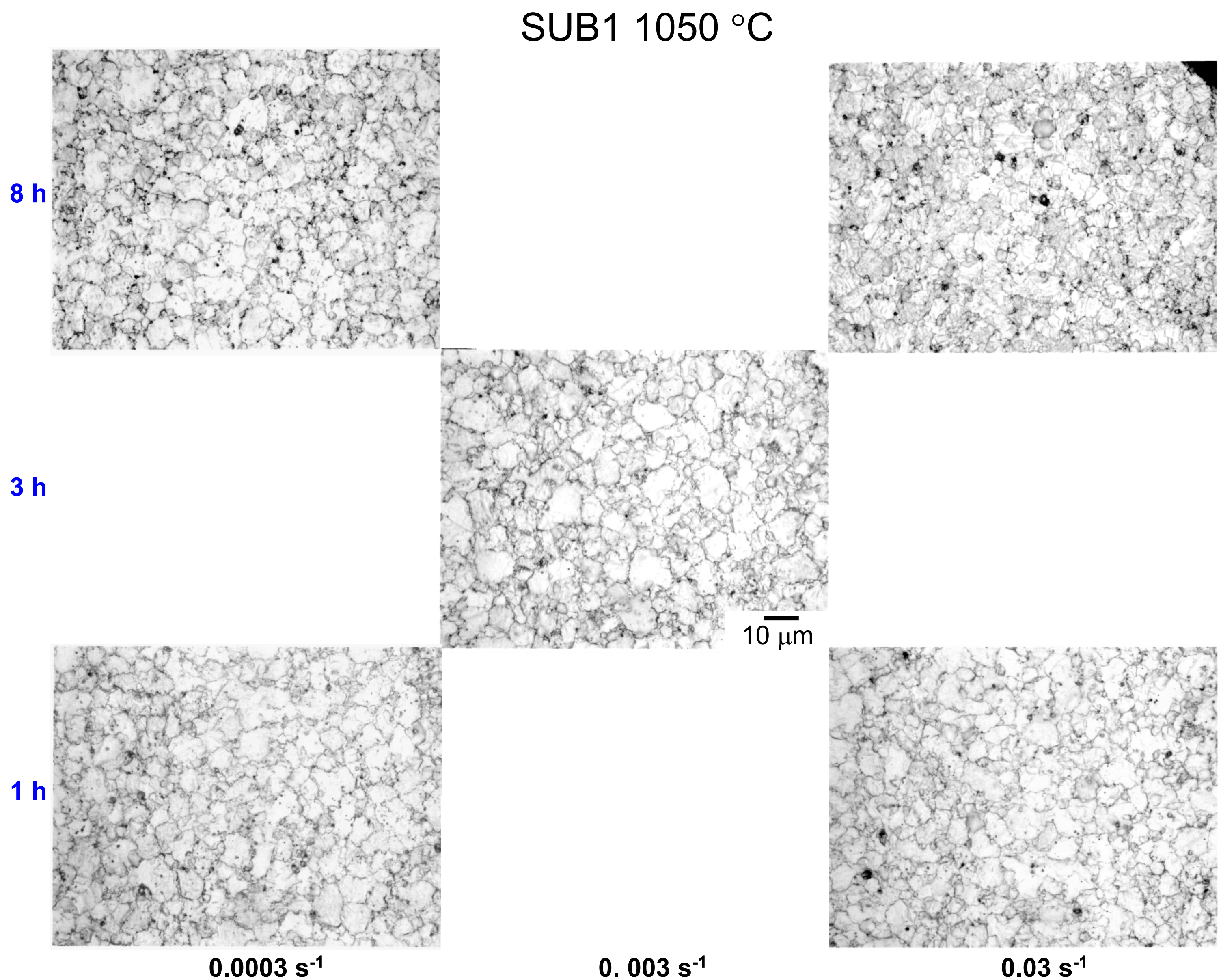

Figure 16.—Typical microstructures of specimens forged at 1050 °C with the indicated presoak times and strain rates, then subsolvus solution heat treated 1h.

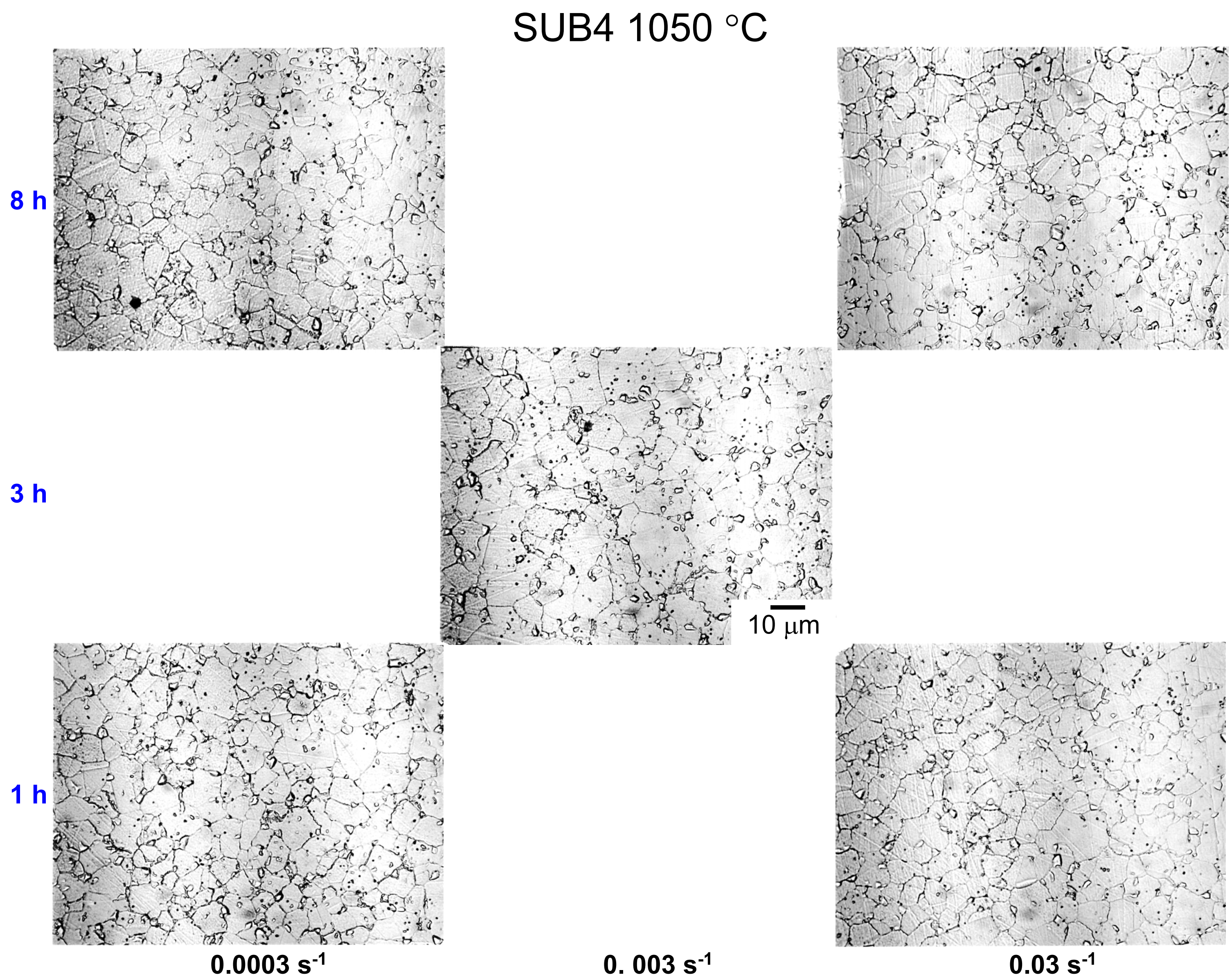

Figure 17.—Typical microstructures of specimens forged at 1050 °C with the indicated presoak times and strain rates, then subsolvus solution heat treated 4h.

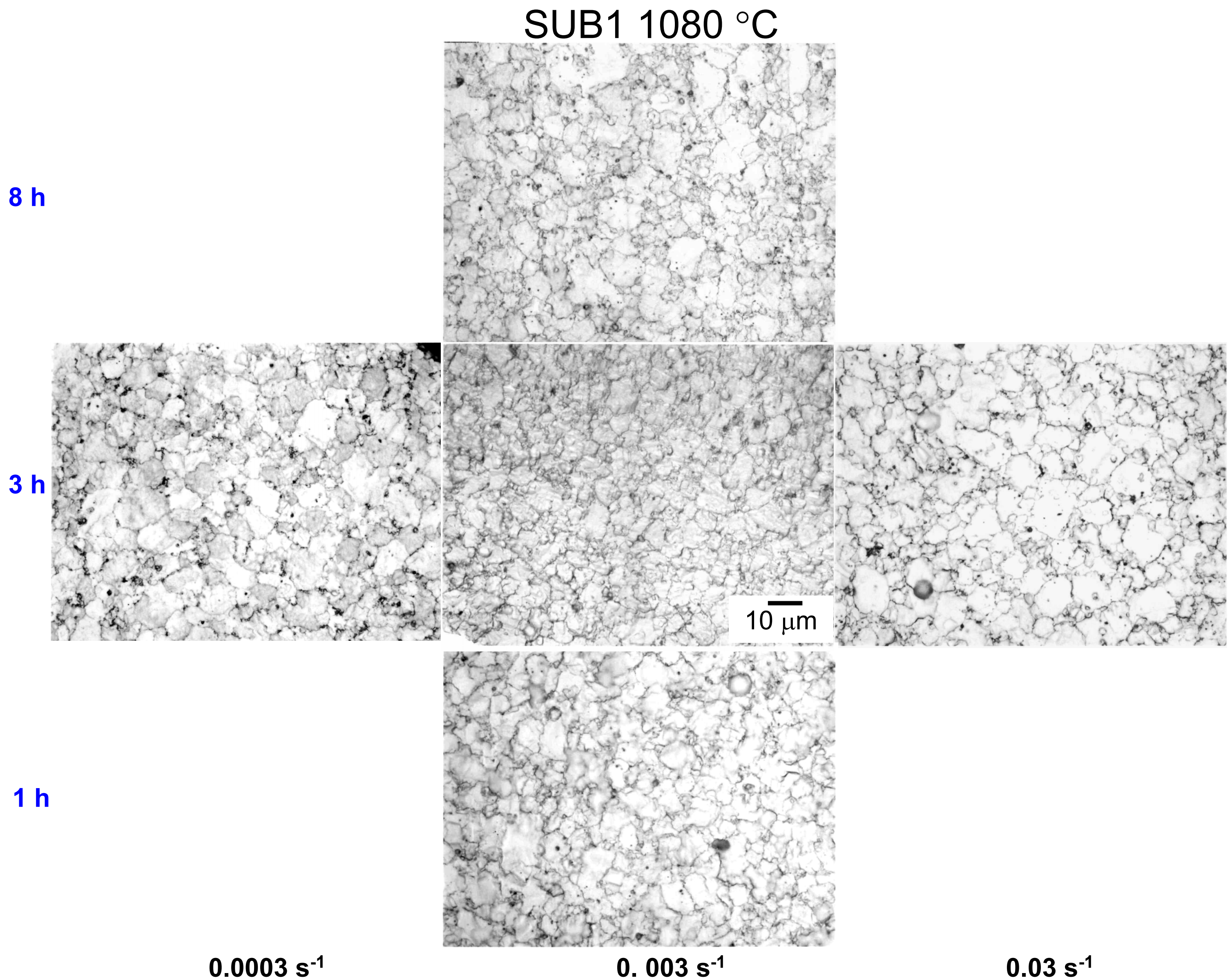

Figure 18. Typical microstructures of specimens forged at 1080 °C with the indicated presoak times and strain rates, then subsolvus solution heat treated 1h.

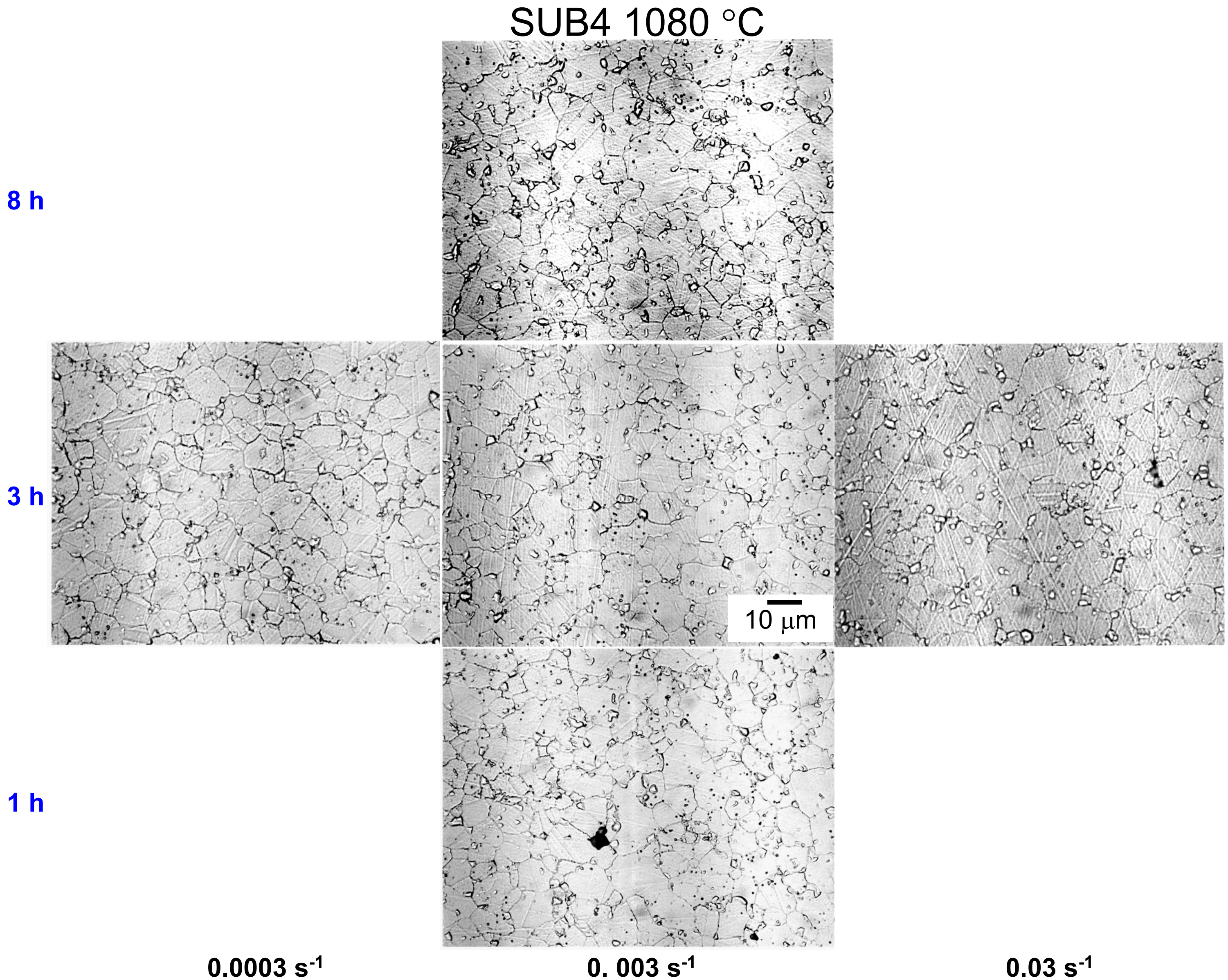

Figure 19.—Typical microstructures of specimens forged at 1080 °C with the indicated presoak times and strain rates, then subsolvus solution heat treated 4h.

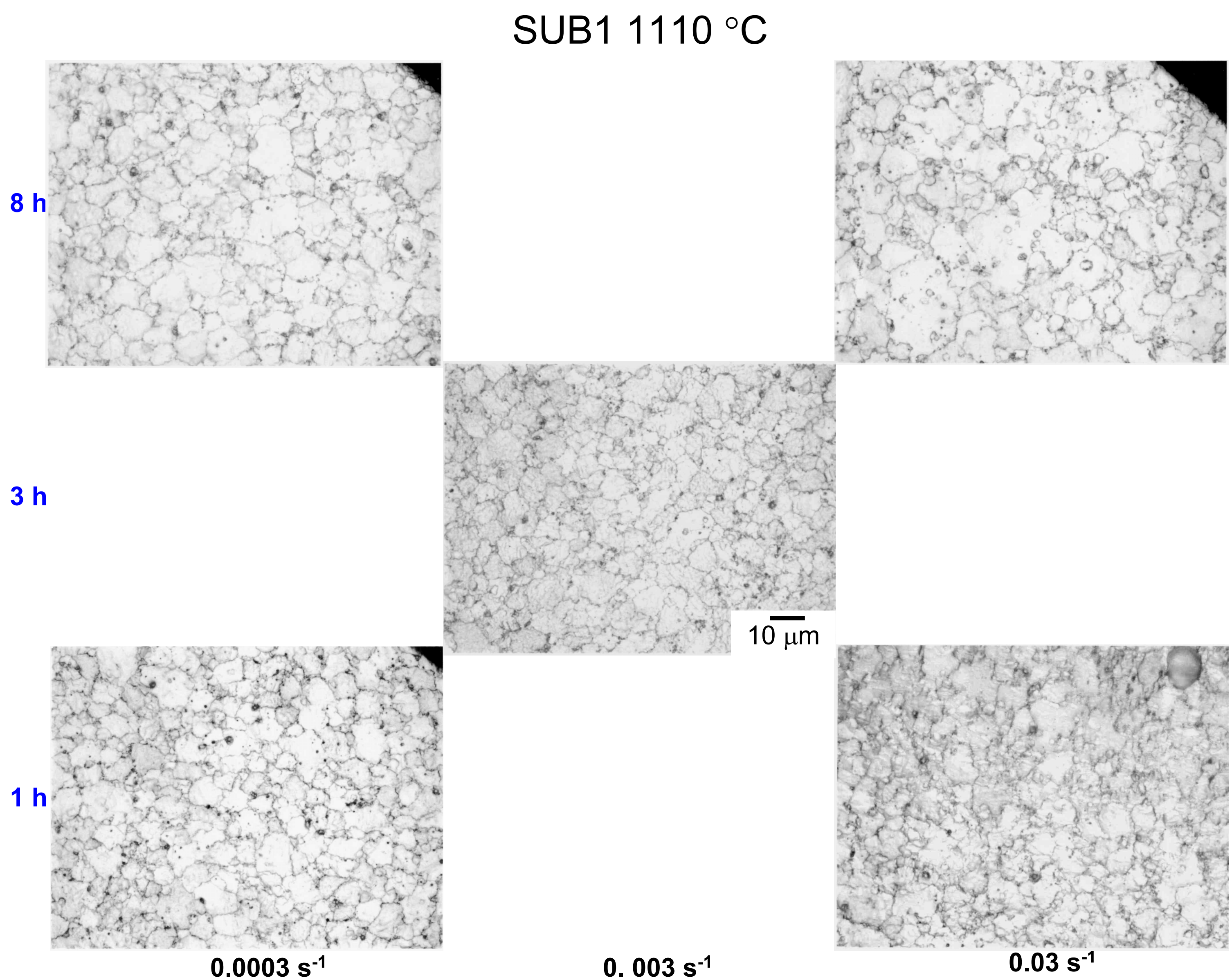

Figure 20.—Typical microstructures of specimens forged at 1110 °C with the indicated presoak times and strain rates, then subsolvus solution heat treated 1h.

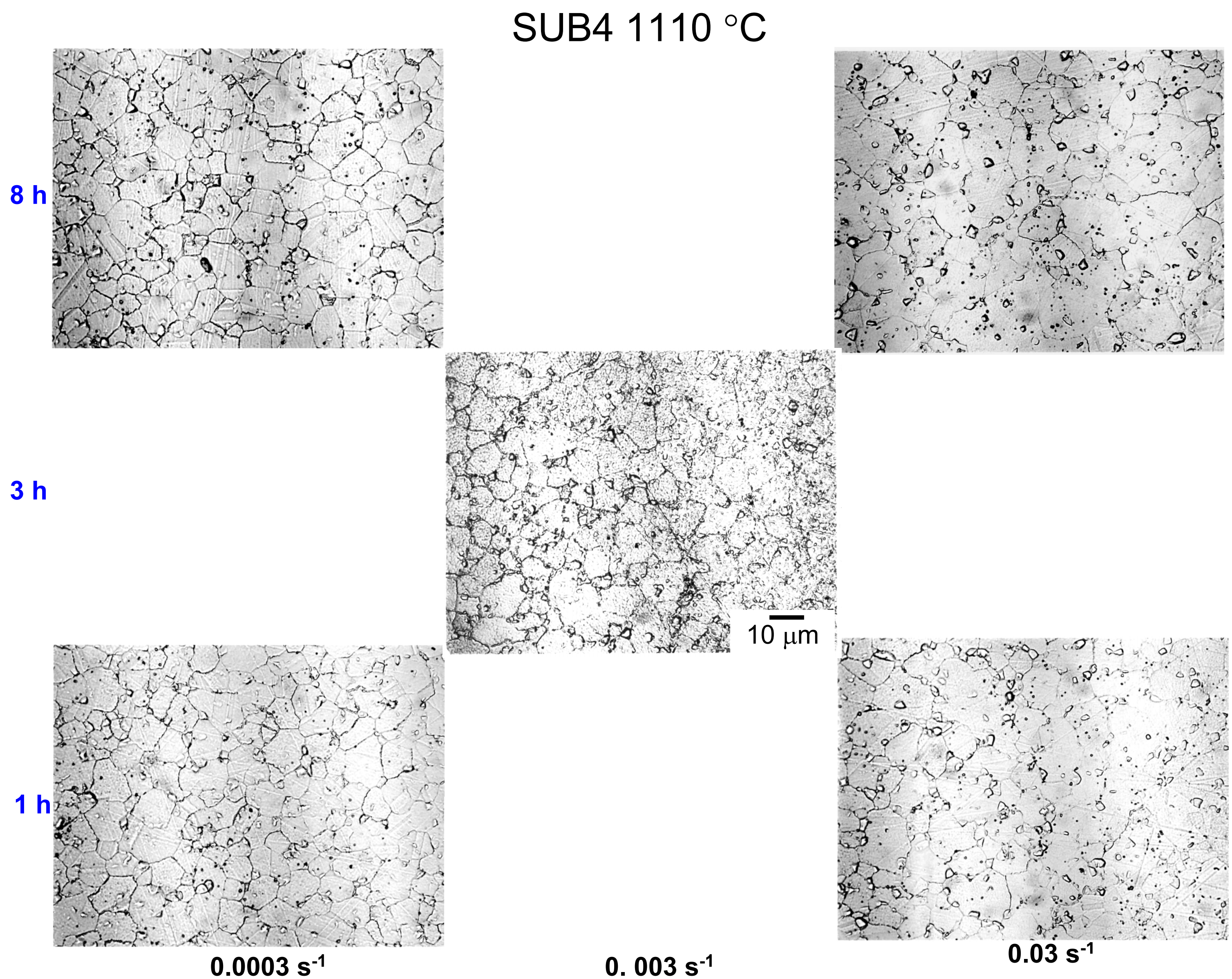

Figure 21.Typical microstructures of specimens forged at 1110 °C with the indicated presoak times and strain rates, then subsolvus solution heat treated 4h.

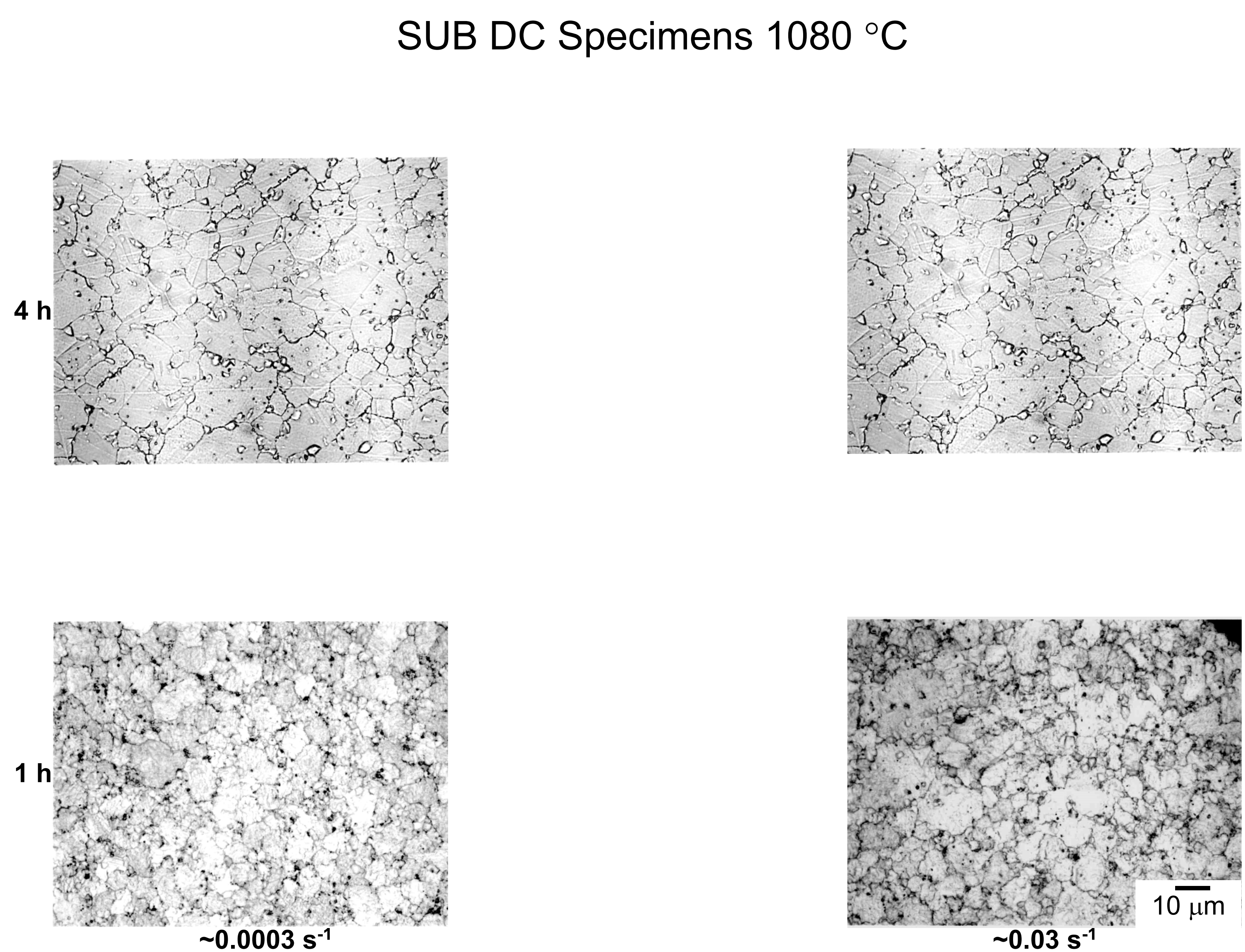

Figure 22.—Typical microstructures of double cone specimens forged at 1080 °C with the indicated approximate average strain rates, then subsolvus solution heat treated 1 and 4h.

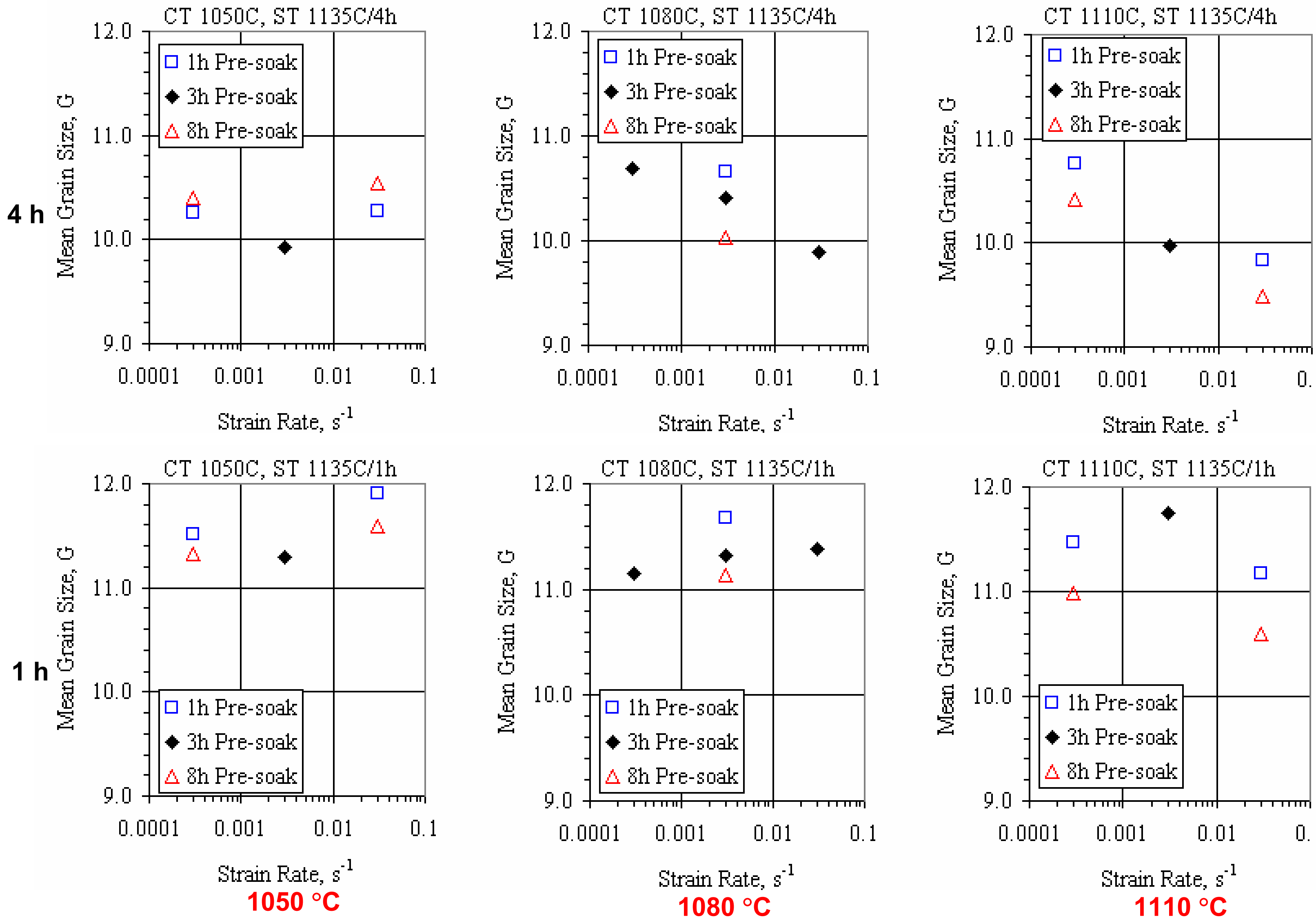

Figure 23.—Mean grain size vs. strain rate for the indicated forging presoak times and temperatures, with subsequent 1h and 4h subsolvus solution heat treatments.

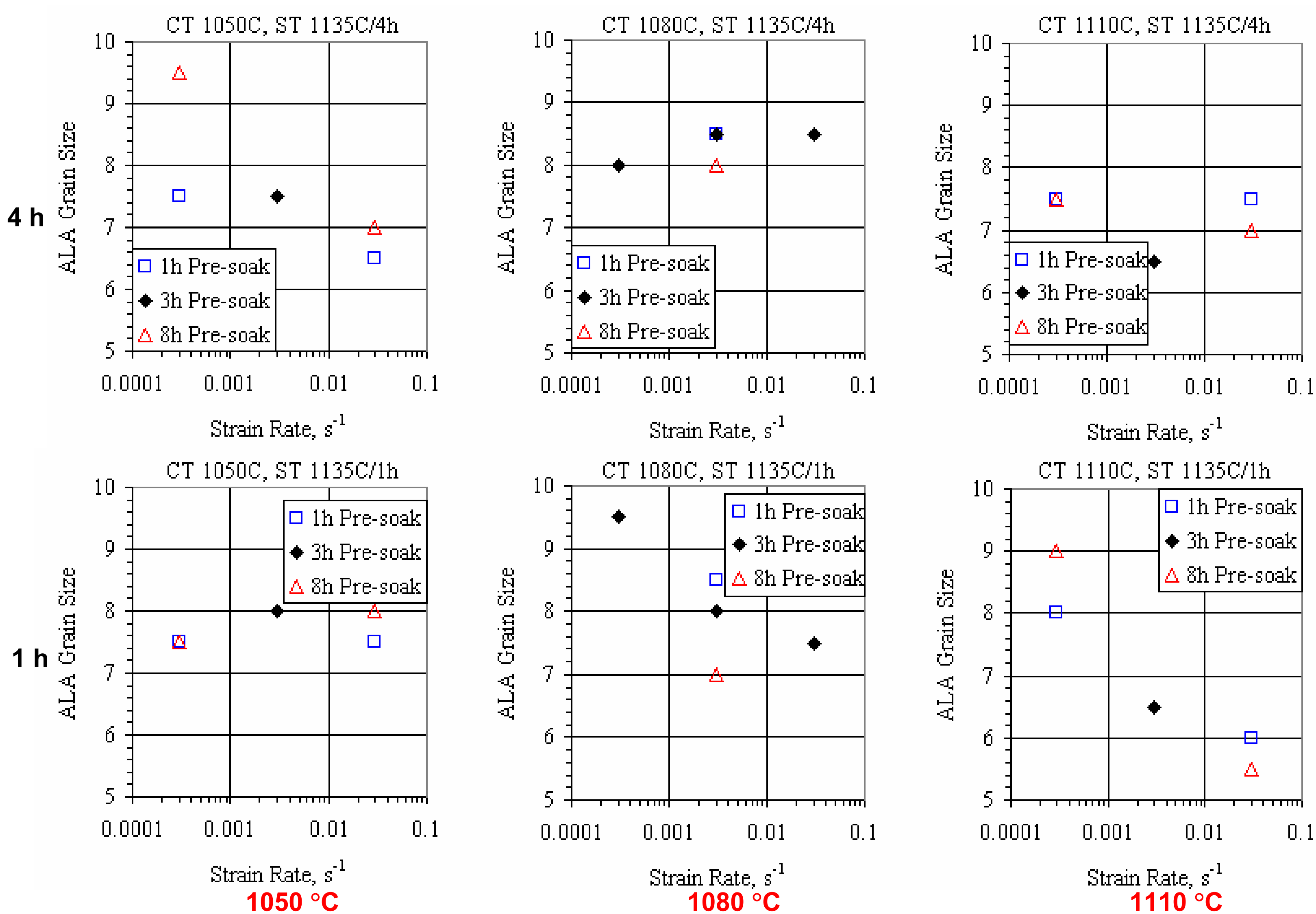

Figure 24.—As-large-as grain size vs. strain rate for the indicated forging presoak times and temperatures, with subsequent 1 and 4h subsolvus solution heat treatments.

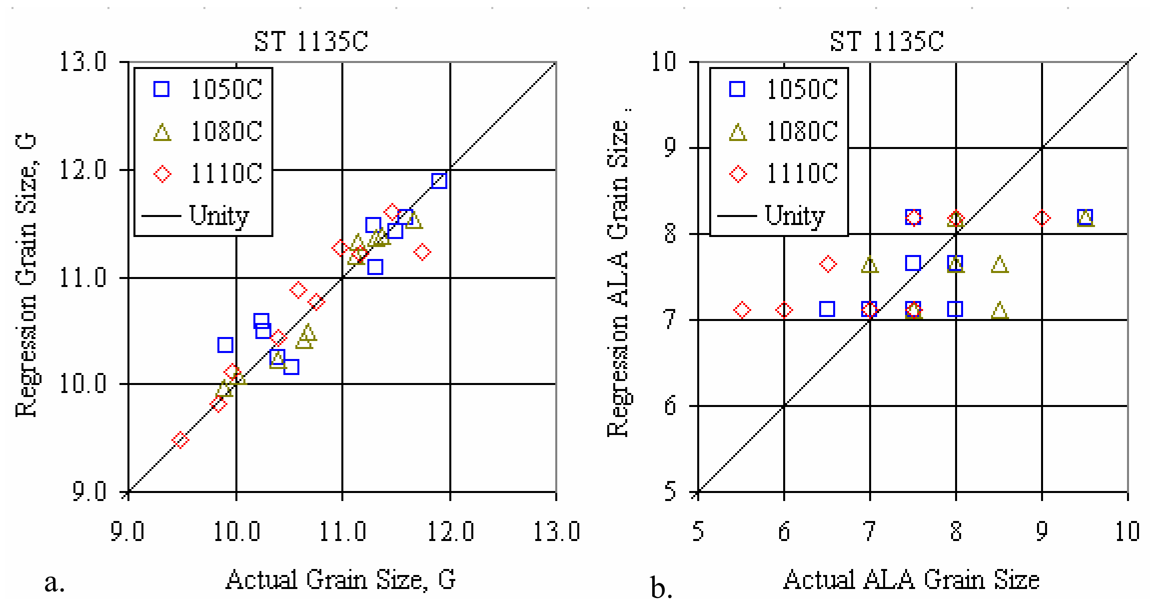

Figure 25.—Comparison of actual vs. regression subsolvus heat treated grain sizes: a) mean grain sizes, b) as-large-as grain sizes.

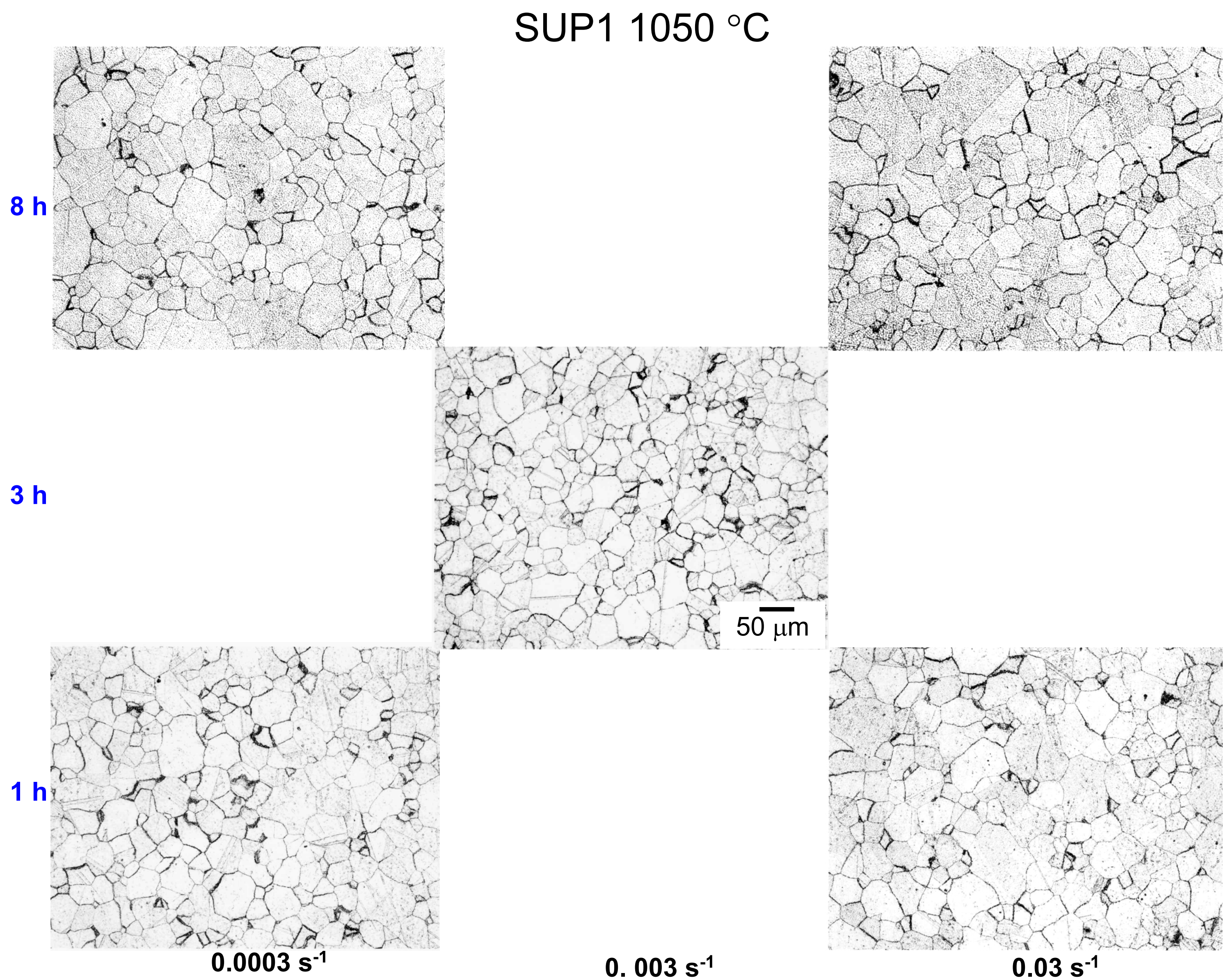

Figure 26.—Typical microstructures of specimens forged at 1050 °C with the indicated presoak times and strain rates, then supersolvus solution heat treated 1h.

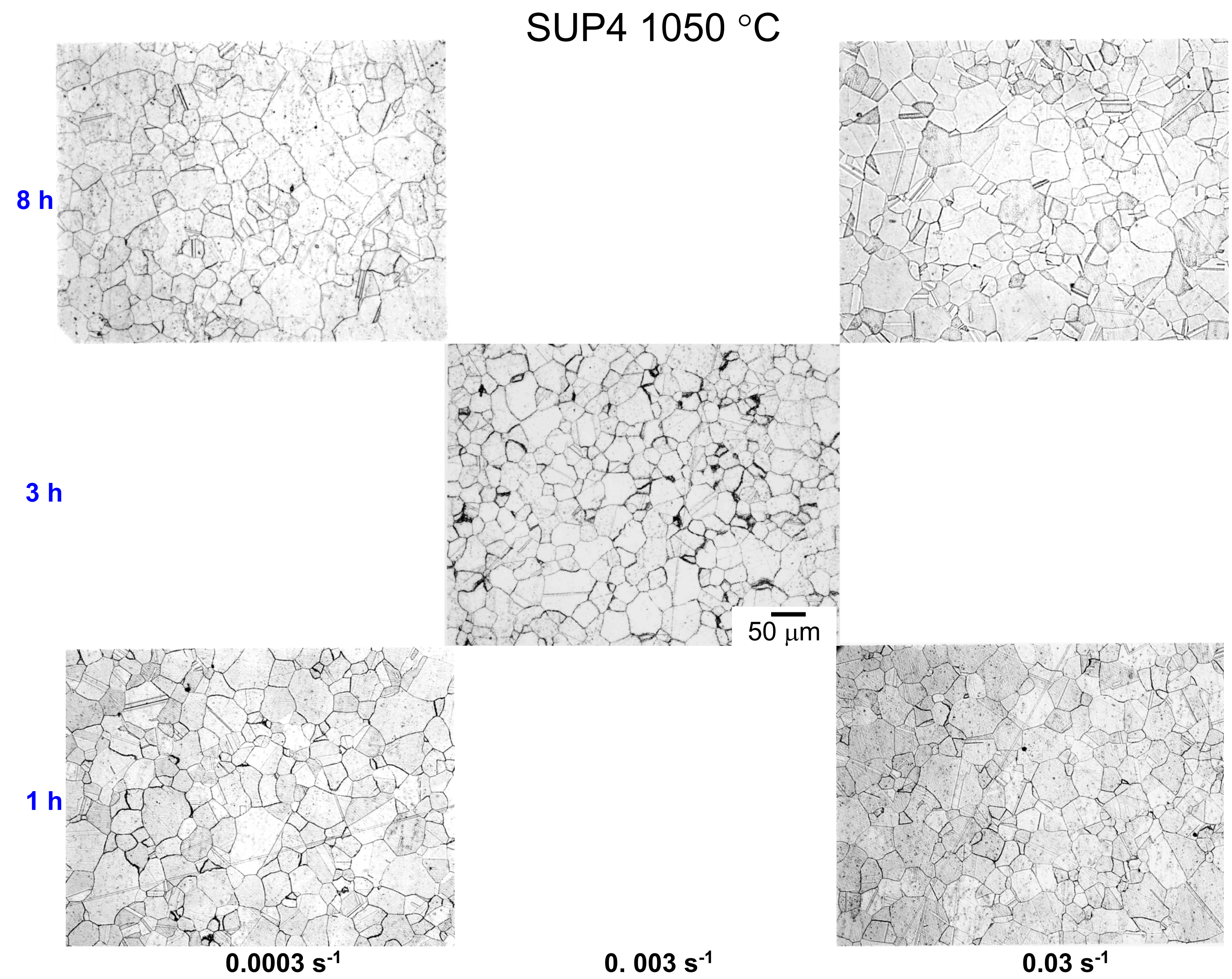

Figure 27.—Typical microstructures of specimens forged at 1050 °C with the indicated presoak times and strain rates, then supersolvus solution heat treated 4h.

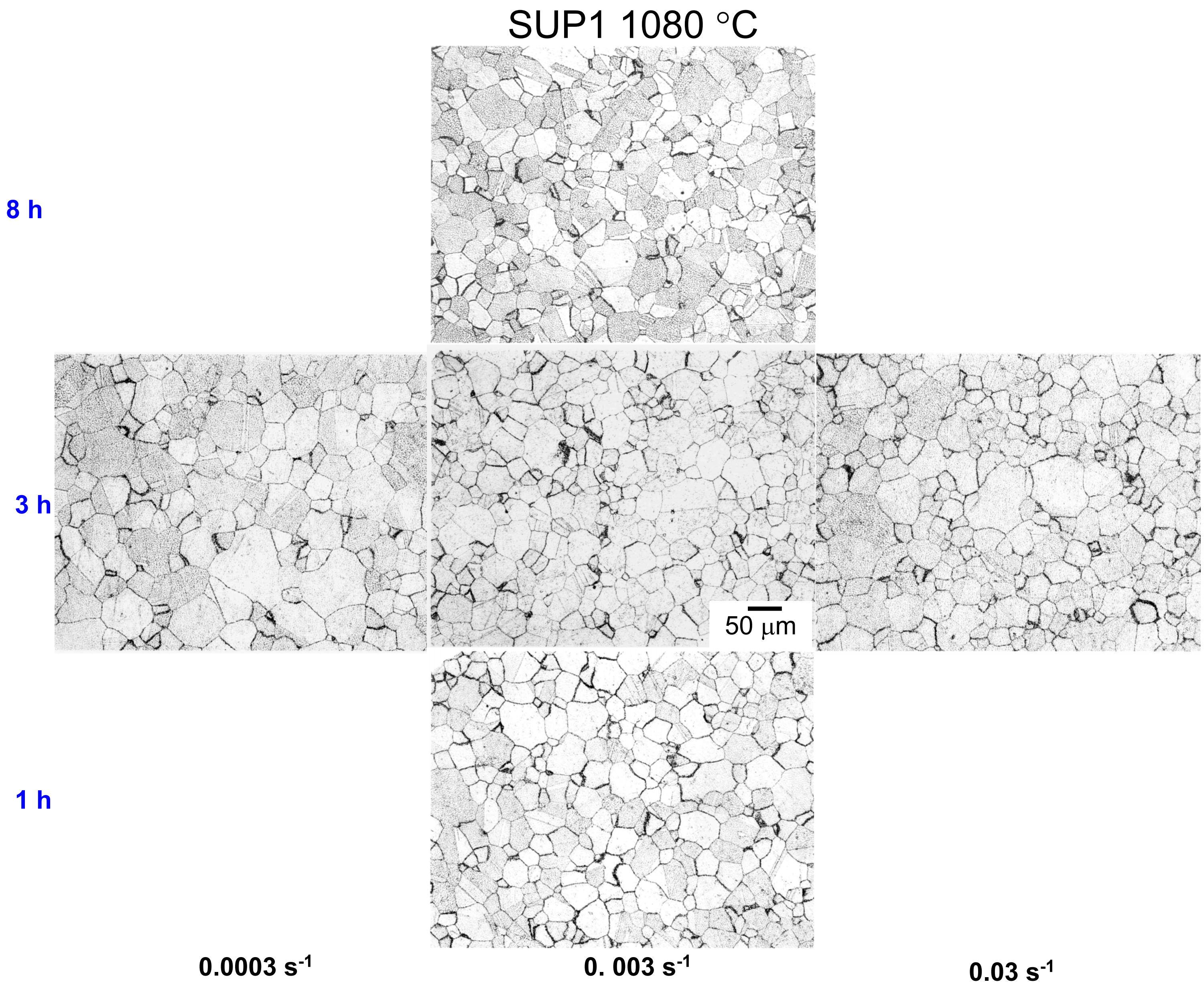

Figure 28.—Typical microstructures of specimens forged at 1080 °C with the indicated presoak times and strain rates, then supersolvus solution heat treated 1h.

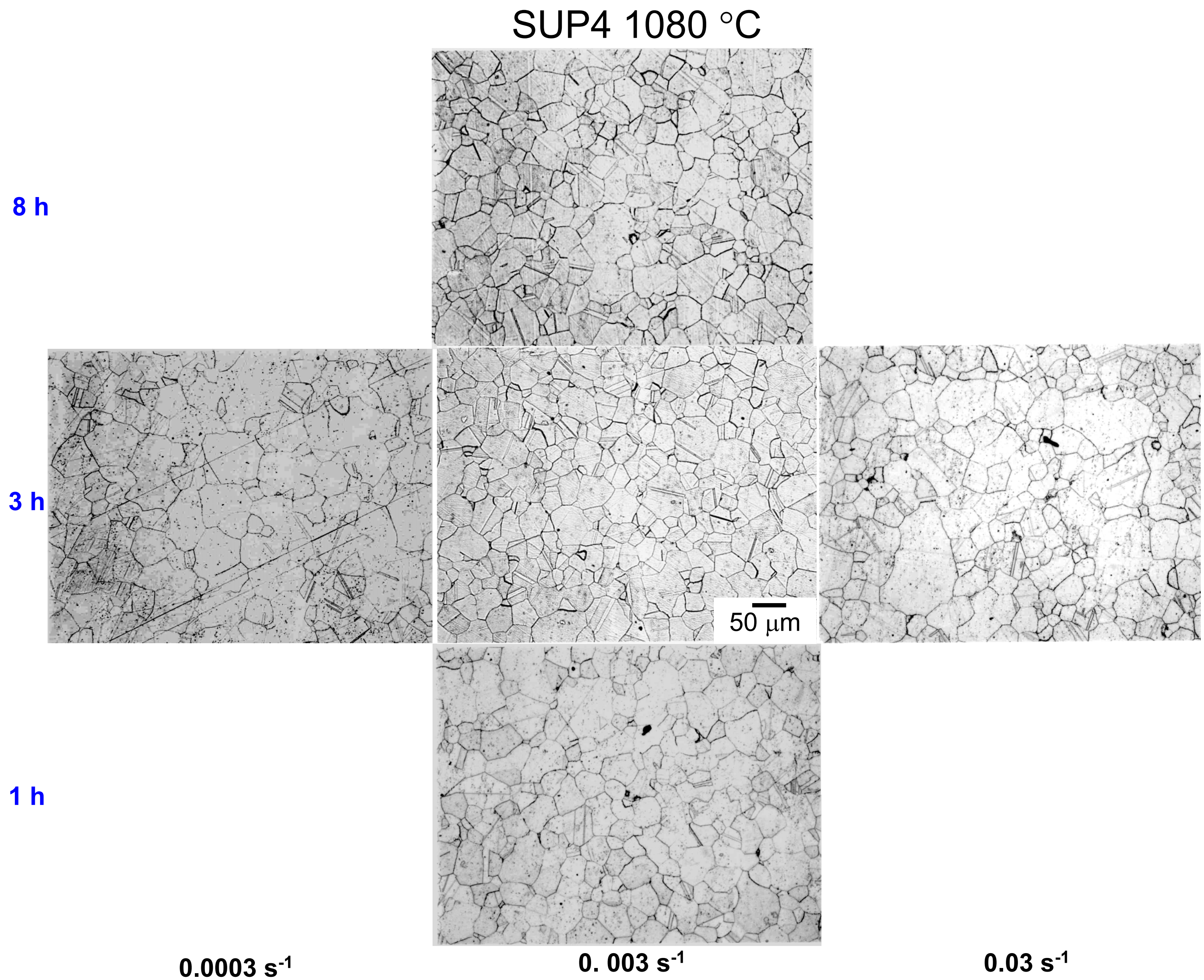

Figure 29.—Typical microstructures of specimens forged at 1080 °C with the indicated presoak times and strain rates, then supersolvus solution heat treated 4h.

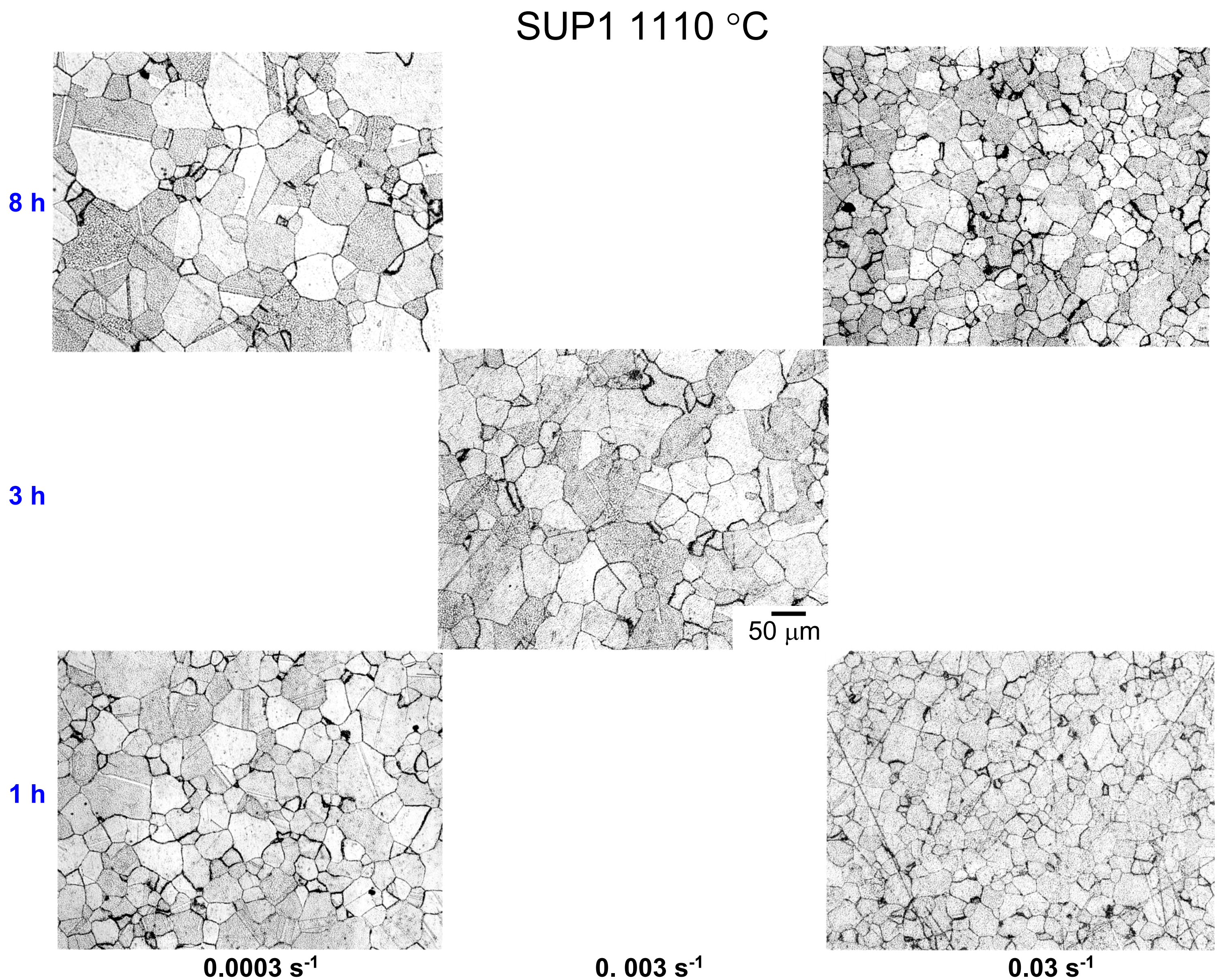

Figure 30.—Typical microstructures of specimens forged at 1110 °C with the indicated presoak times and strain rates, then supersolvus solution heat treated 1h.

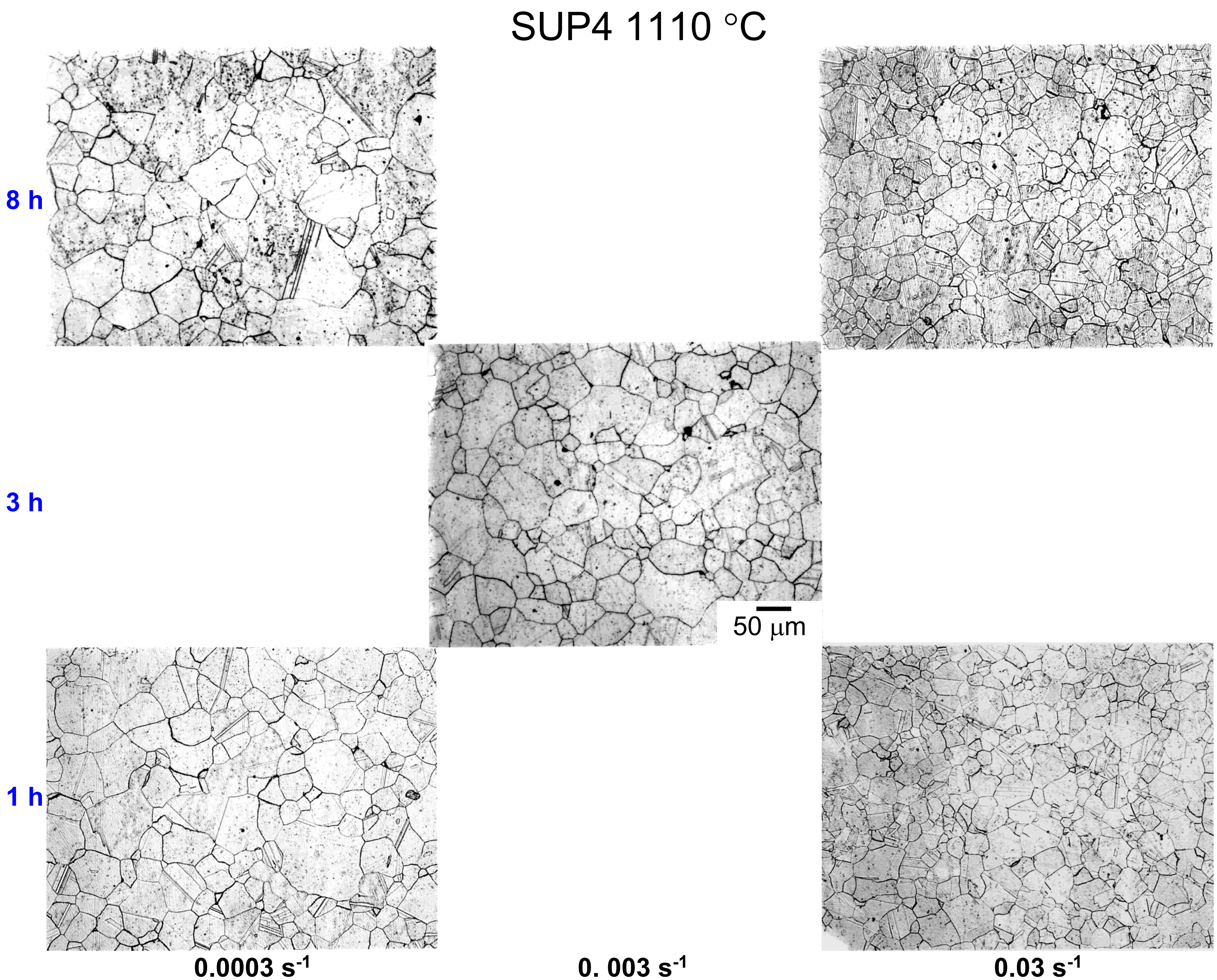

Figure 31.—Typical microstructures of specimens forged at 1110 °C with the indicated presoak times and strain rates, then supersolvus solution heat treated 4h.

SUP DC Specimens 1080 °C

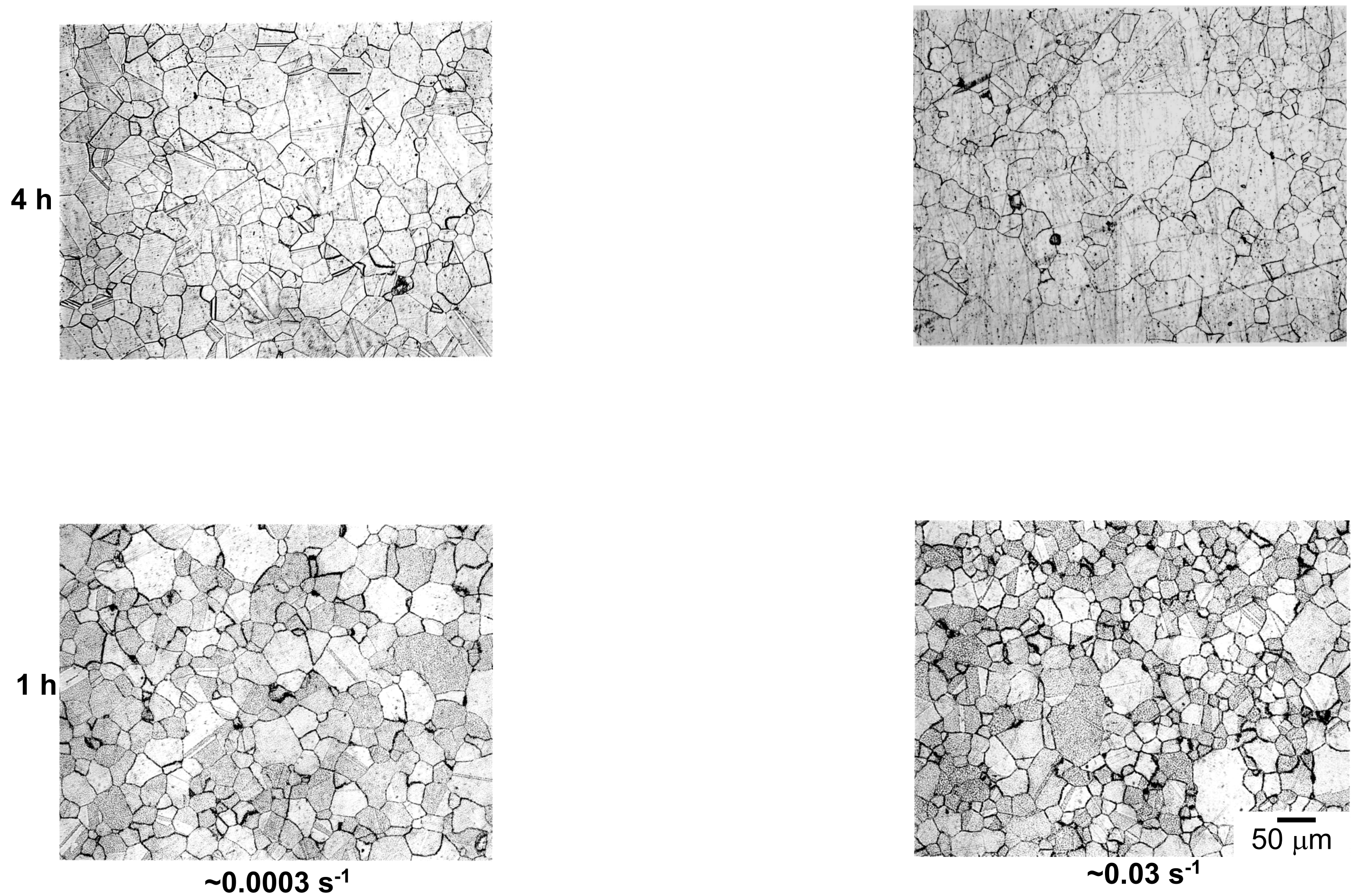

Figure 32.—Typical microstructures of double cone specimens forged at 1080 °C with the indicated approximate average strain rates, then supersolvus solution heat treated 1 and 4h.

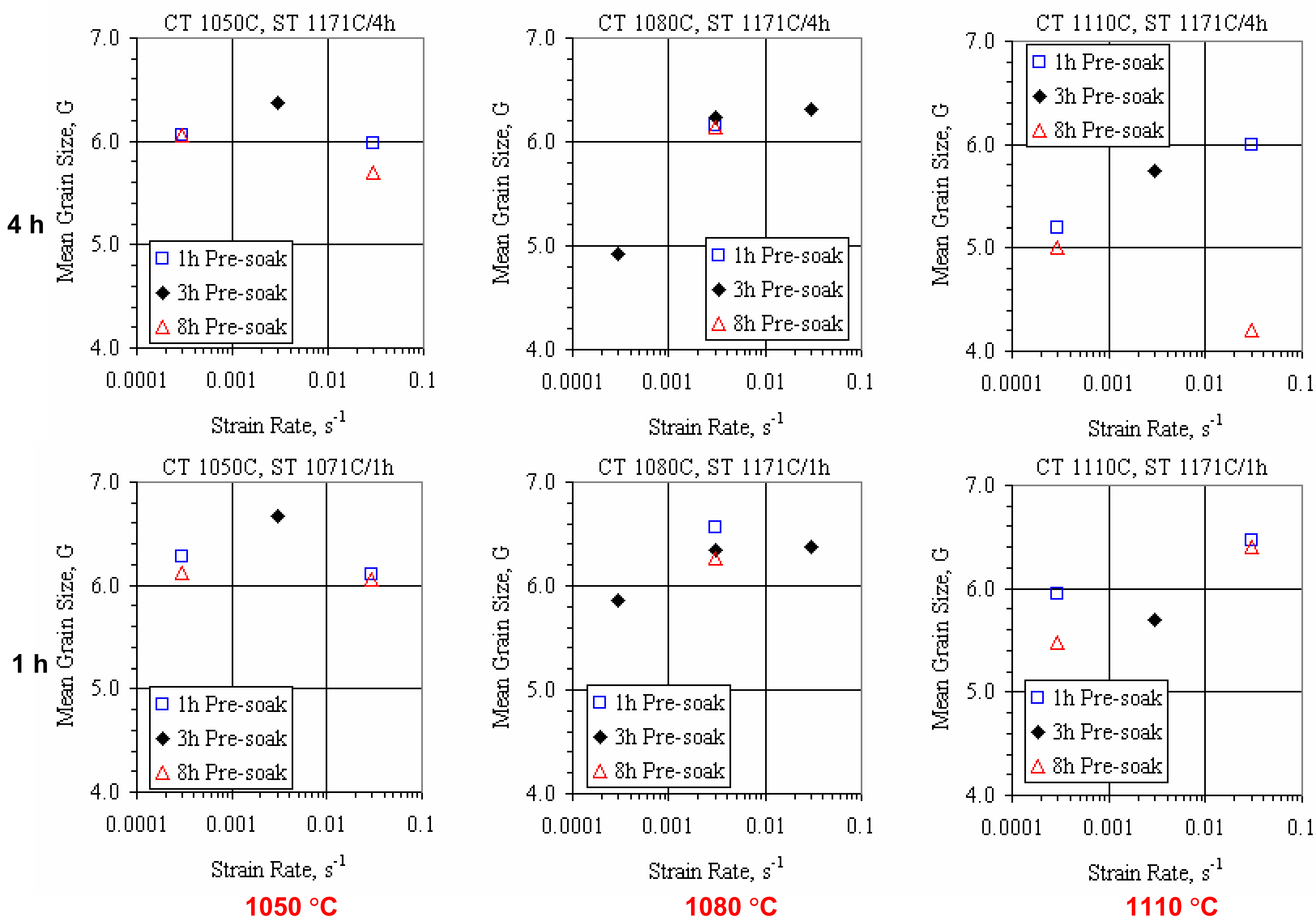

Figure 33.—Mean grain size vs. strain rate for the indicated forging presoak times and temperatures, with subsequent 1h and 4h supersolvus solution heat treatments.

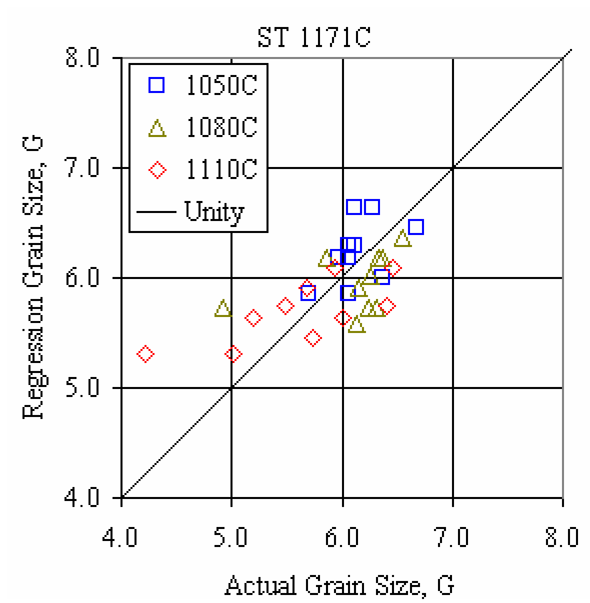

Figure 34.—Comparison of actual vs. regression supersolvus heat treated mean grain sizes.

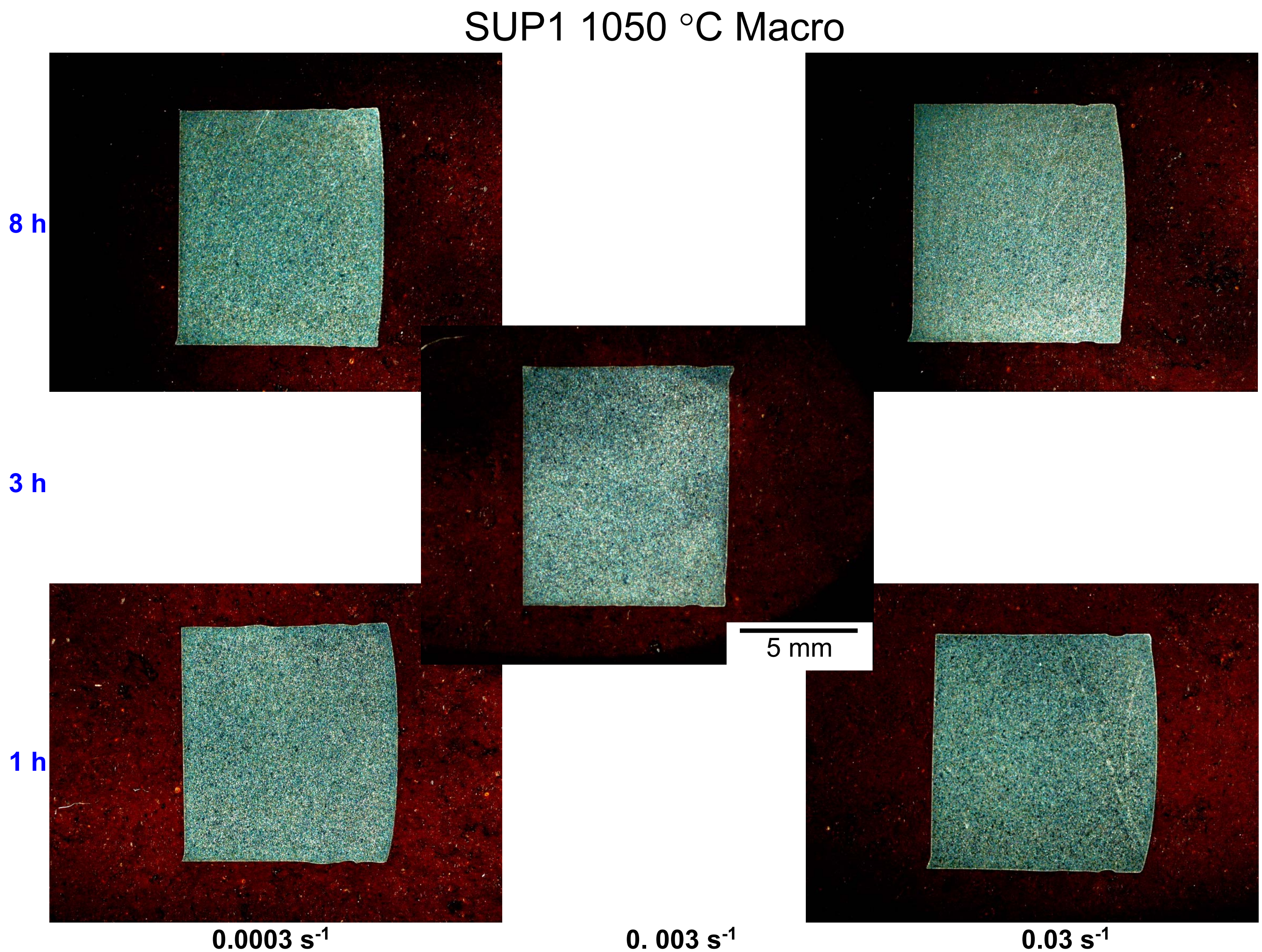

Figure 35.—Typical macrostructures of specimens forged at 1050 °C with the indicated presoak times and strain rates, then supersolvus solution heat treated 1h.

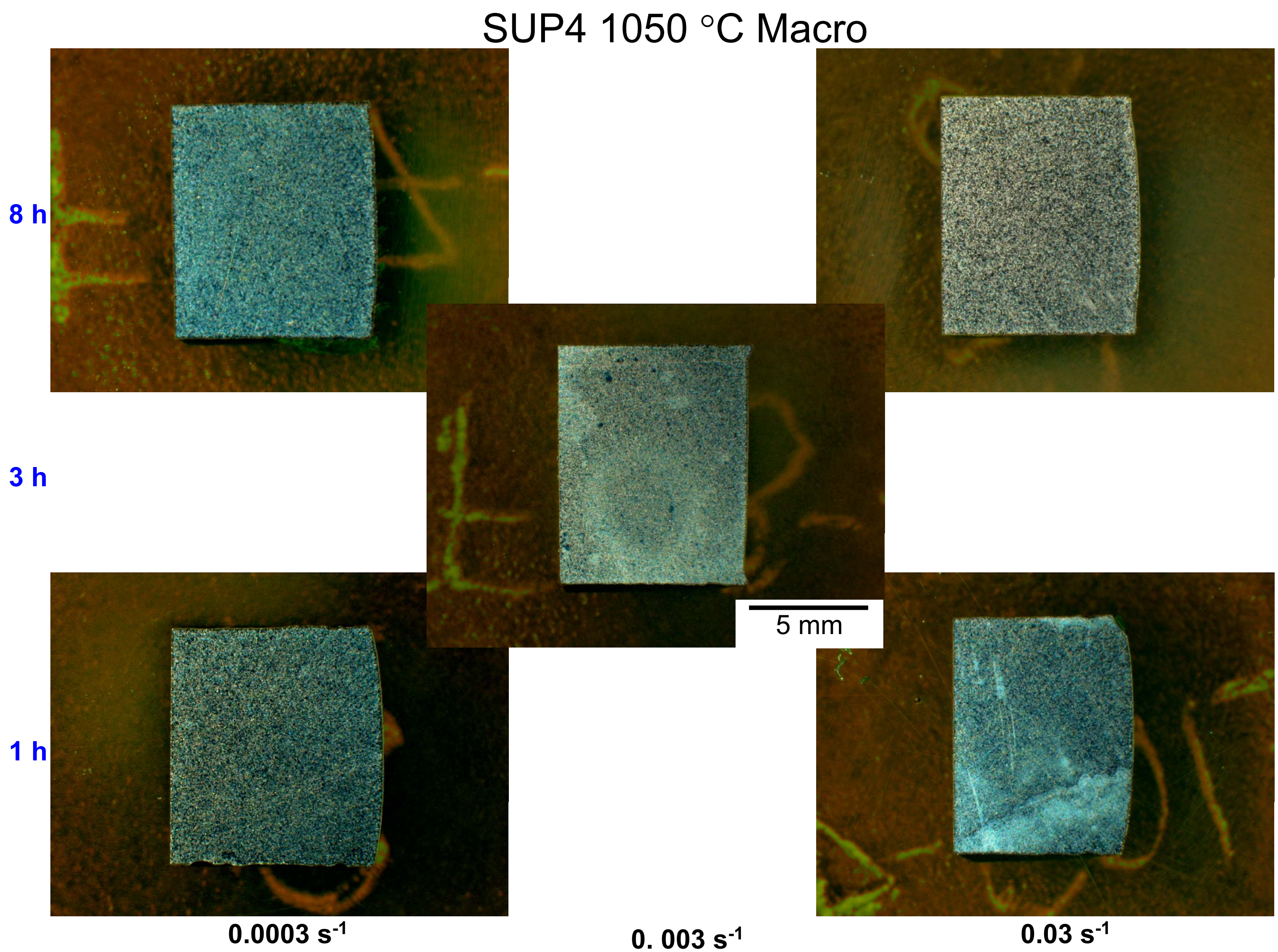

Figure 36.—Typical macrostructures of specimens forged at 1050 °C with the indicated presoak times and strain rates, then supersolvus solution heat treated 4h.

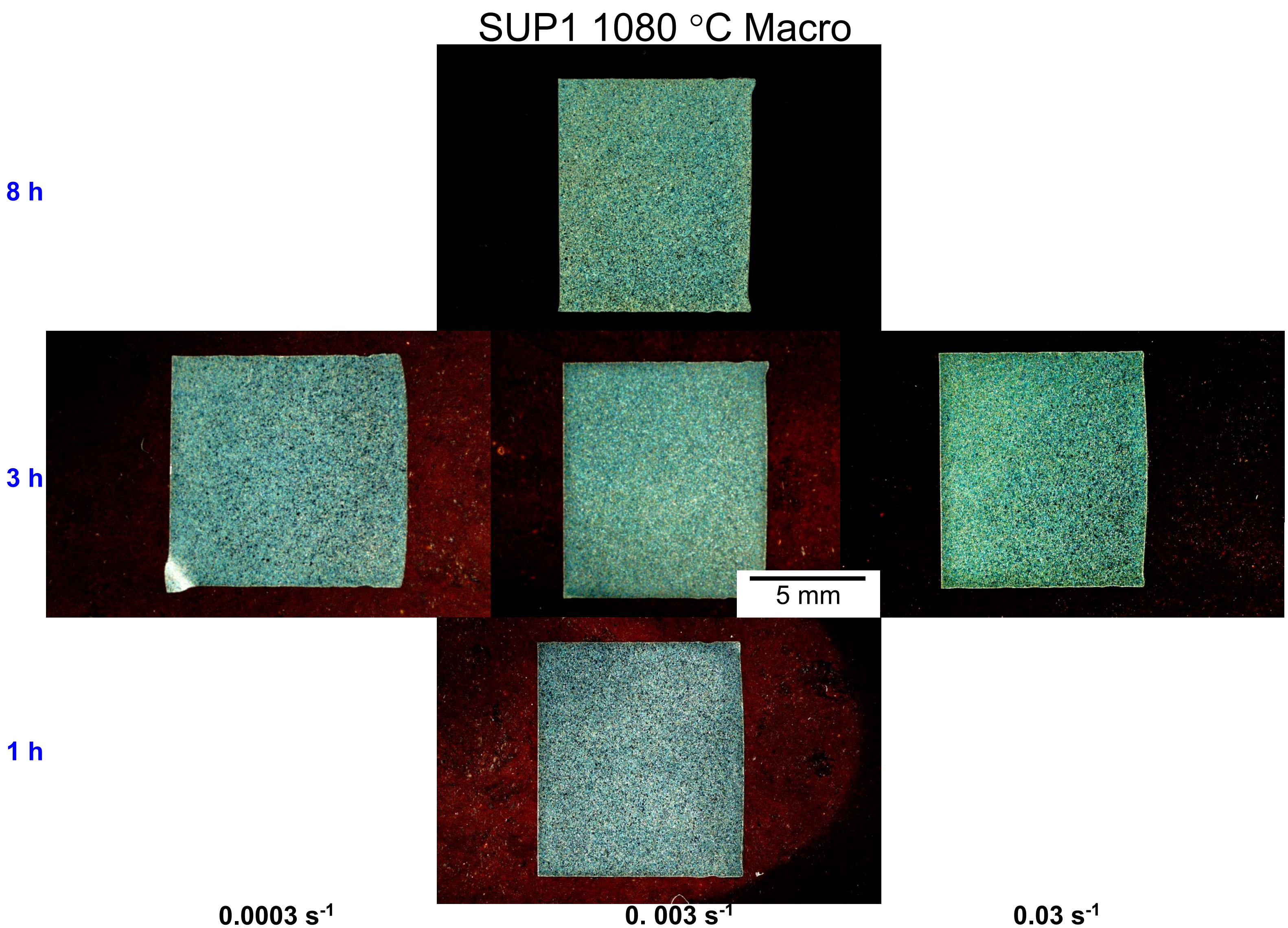

Figure 37.—Typical macrostructures of specimens forged at 1080 °C with the indicated presoak times and strain rates, then supersolvus solution heat treated 1h.

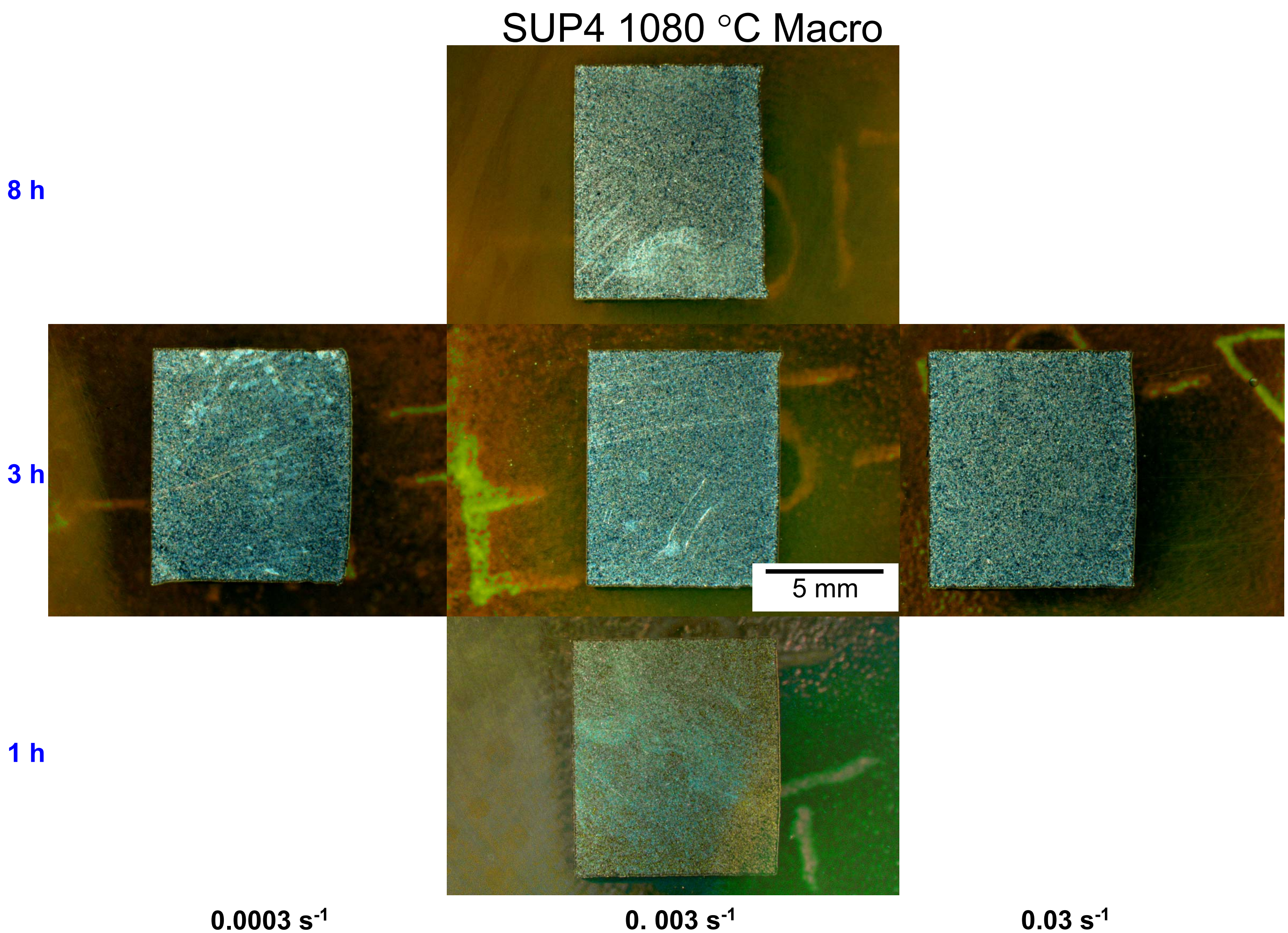

Figure 38.—Typical macrostructures of specimens forged at 1080 °C with the indicated presoak times and strain rates, then supersolvus solution heat treated 4h.

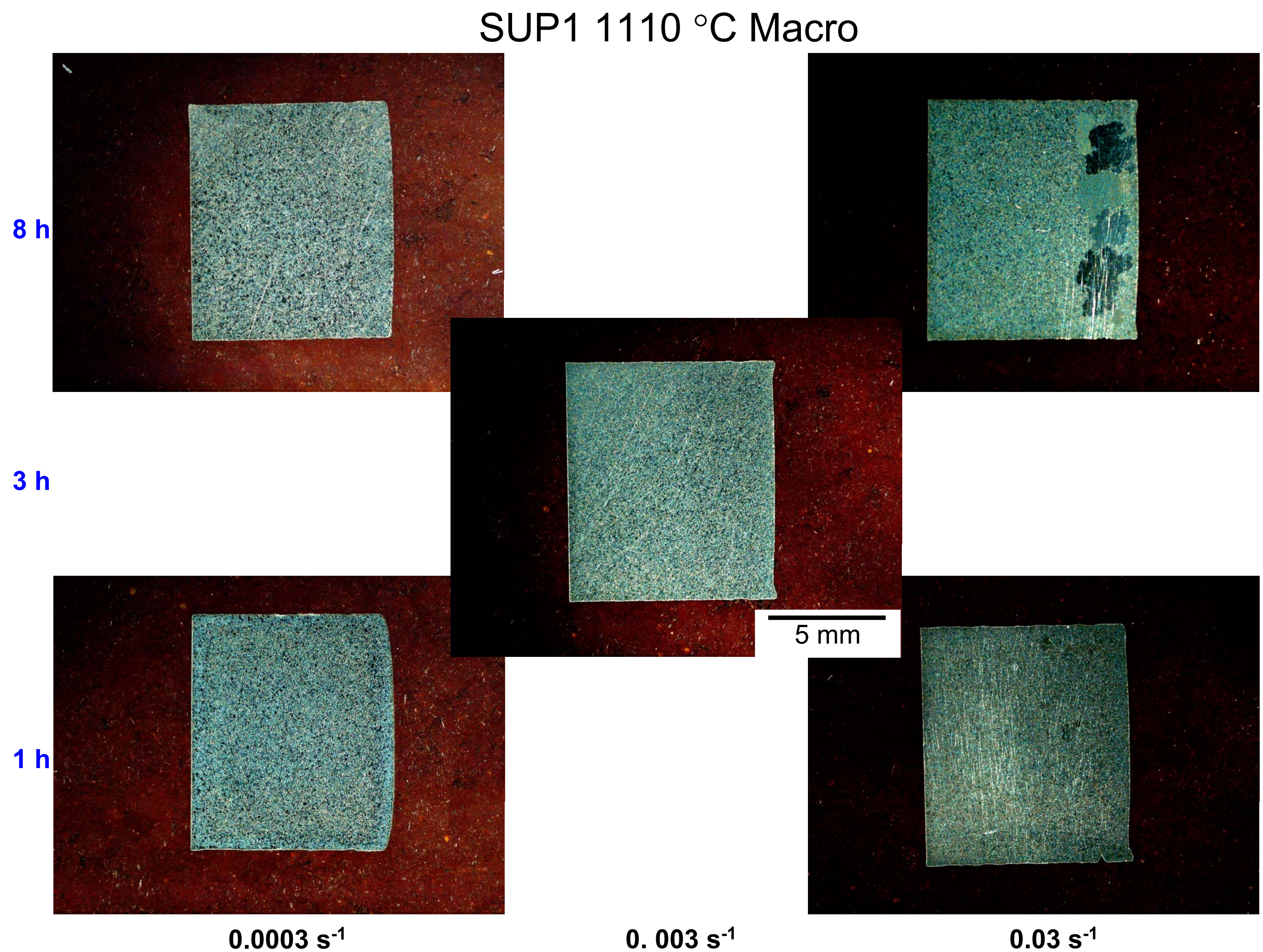

Figure 39.—Typical macrostructures of specimens forged at 1110 °C with the indicated presoak times and strain rates, then supersolvus solution heat treated 1h.

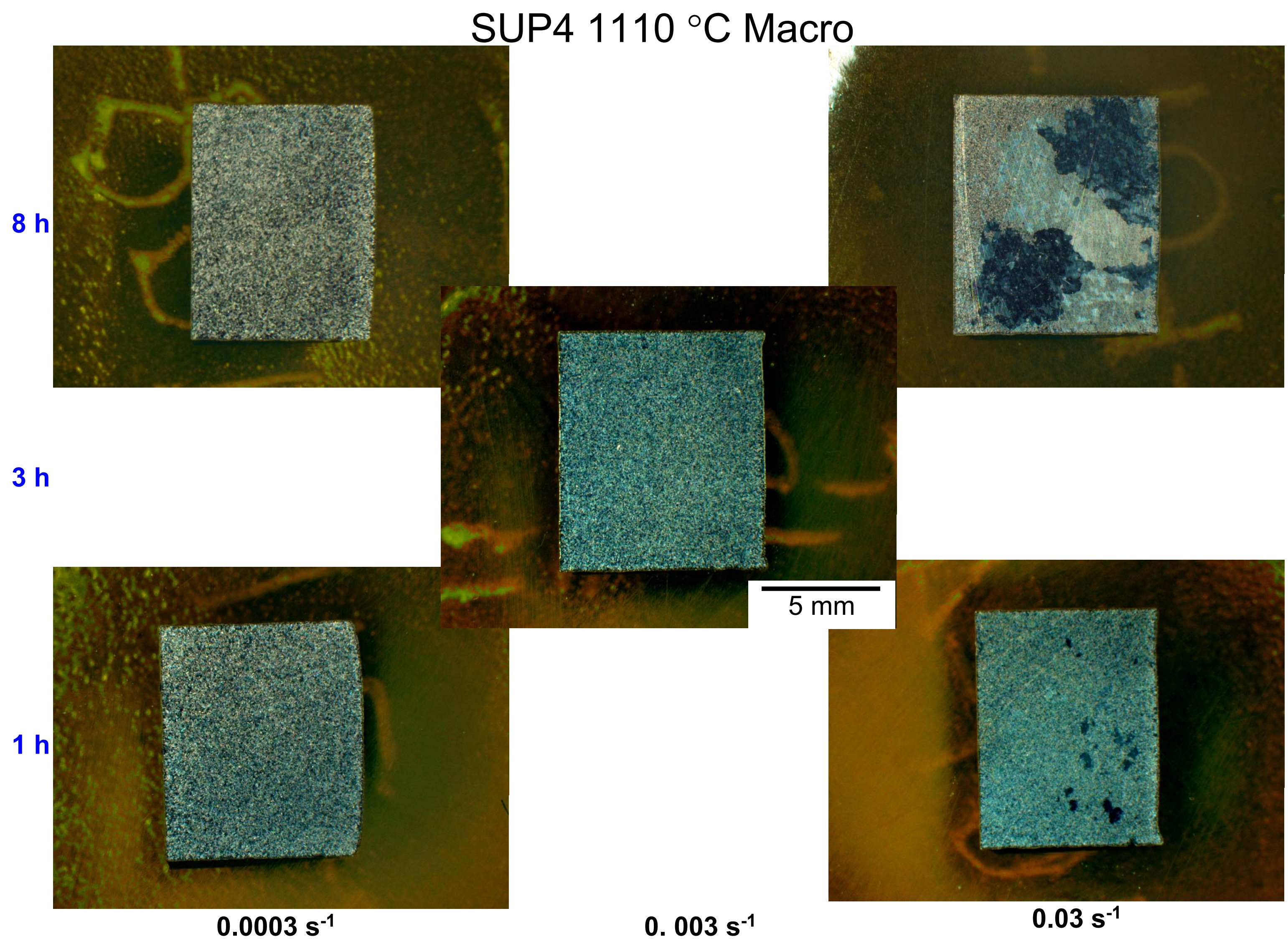

Figure 40.—Typical macrostructures of specimens forged at 1110 °C with the indicated presoak times and strain rates, then supersolvus solution heat treated 4h.

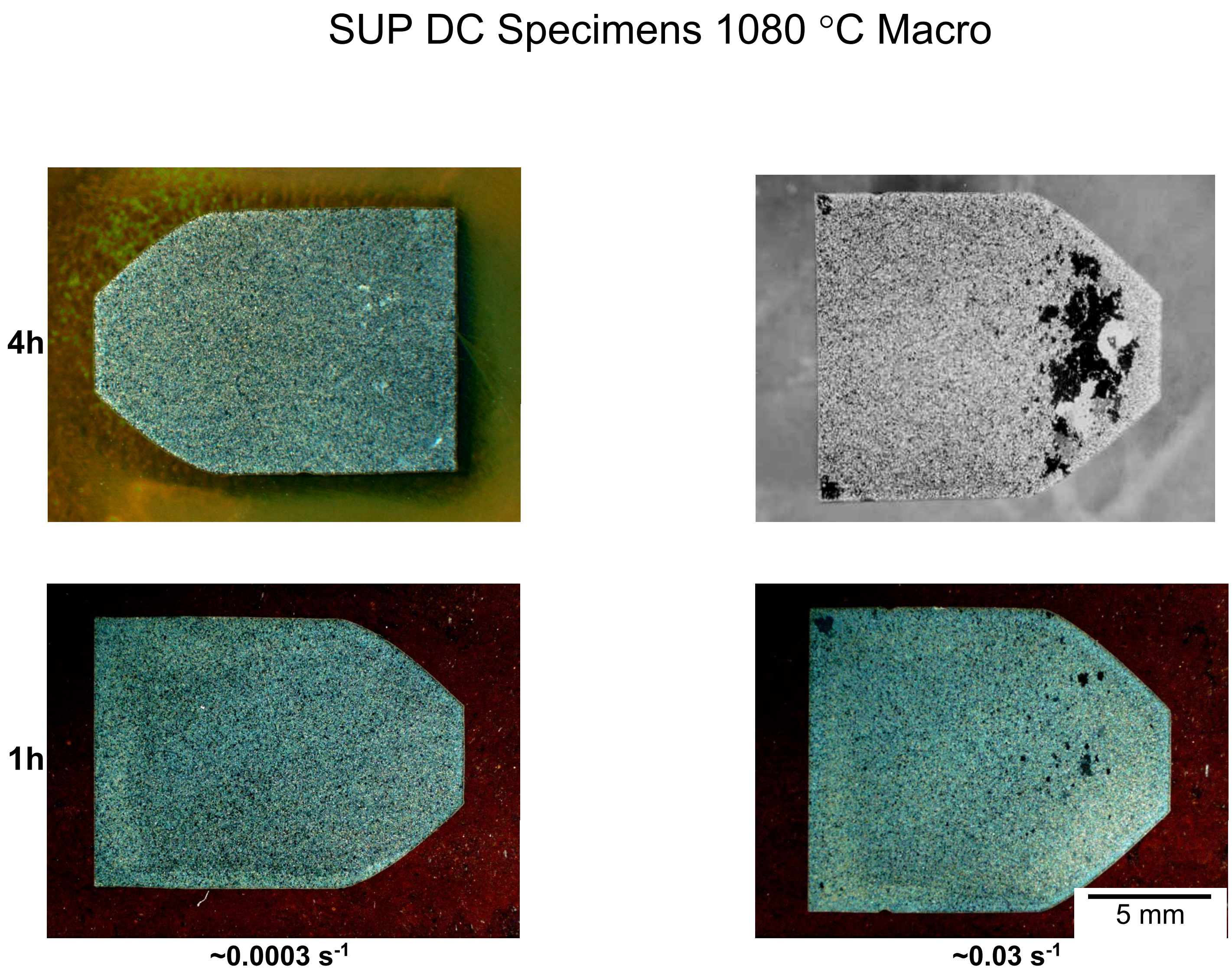

Figure 41.—Typical macrostructures of double cone specimens forged at 1080 °C with the indicated approximate average strain rates, then supersolvus solution heat treated 1 and 4h.

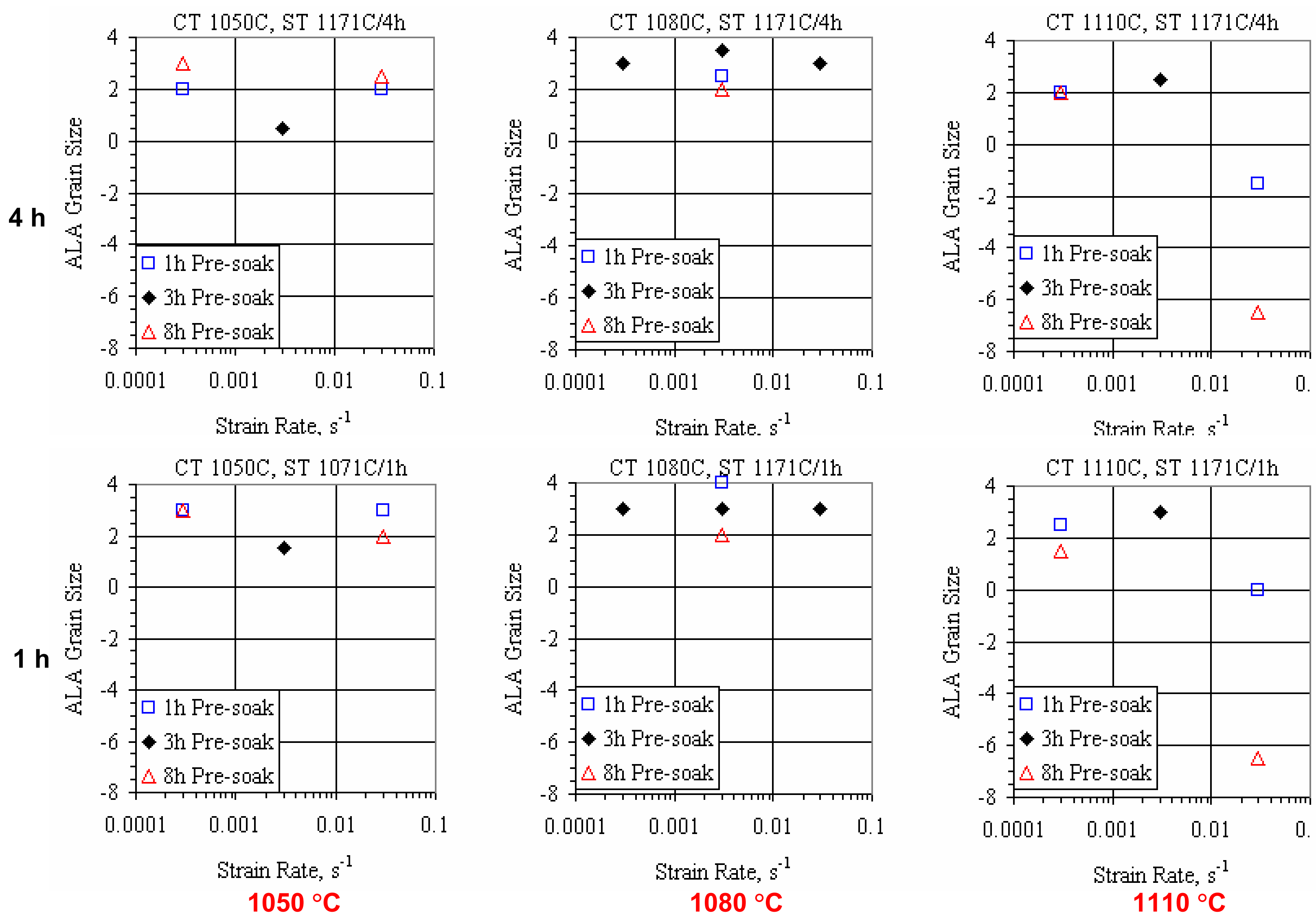

Figure 42.—As-large-as grain size vs. strain rate for the indicated forging presoak times and temperatures, with subsequent 1h and 4h supersolvus solution heat treatments.

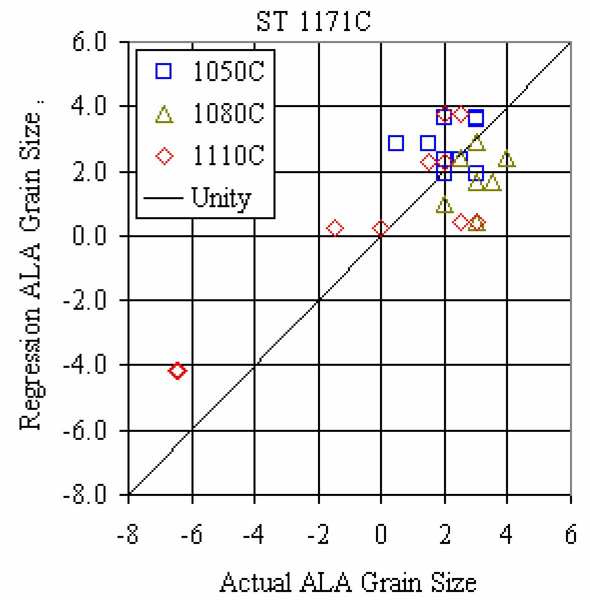

Figure 43.—Comparison of actual vs. regression supersolvus heat treated as-large-as grain sizes.

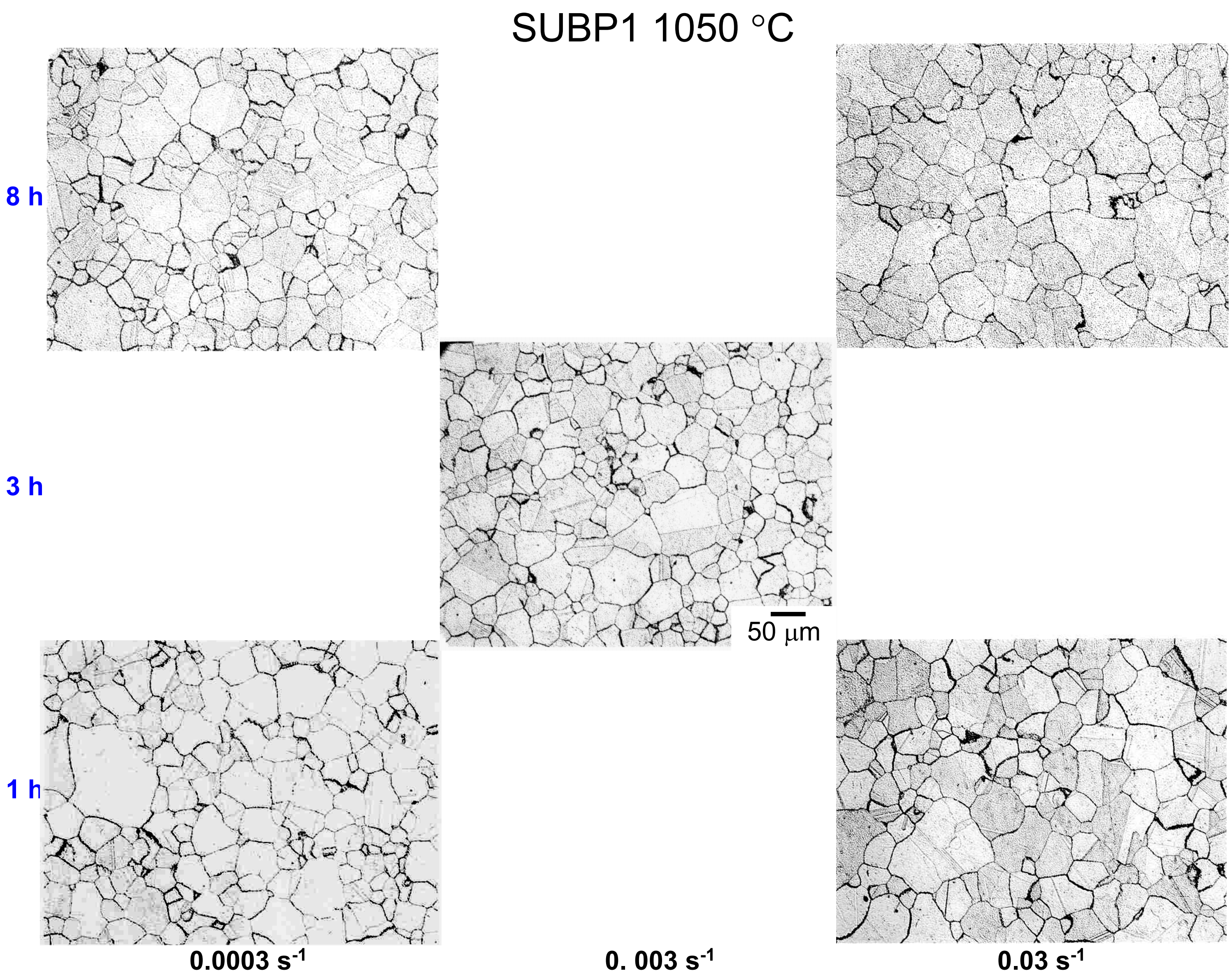

Figure 44.—Typical microstructures of specimens forged at 1050 °C with the indicated presoak times and strain rates, then 1h subsolvus plus 1h supersolvus solution heat treated.

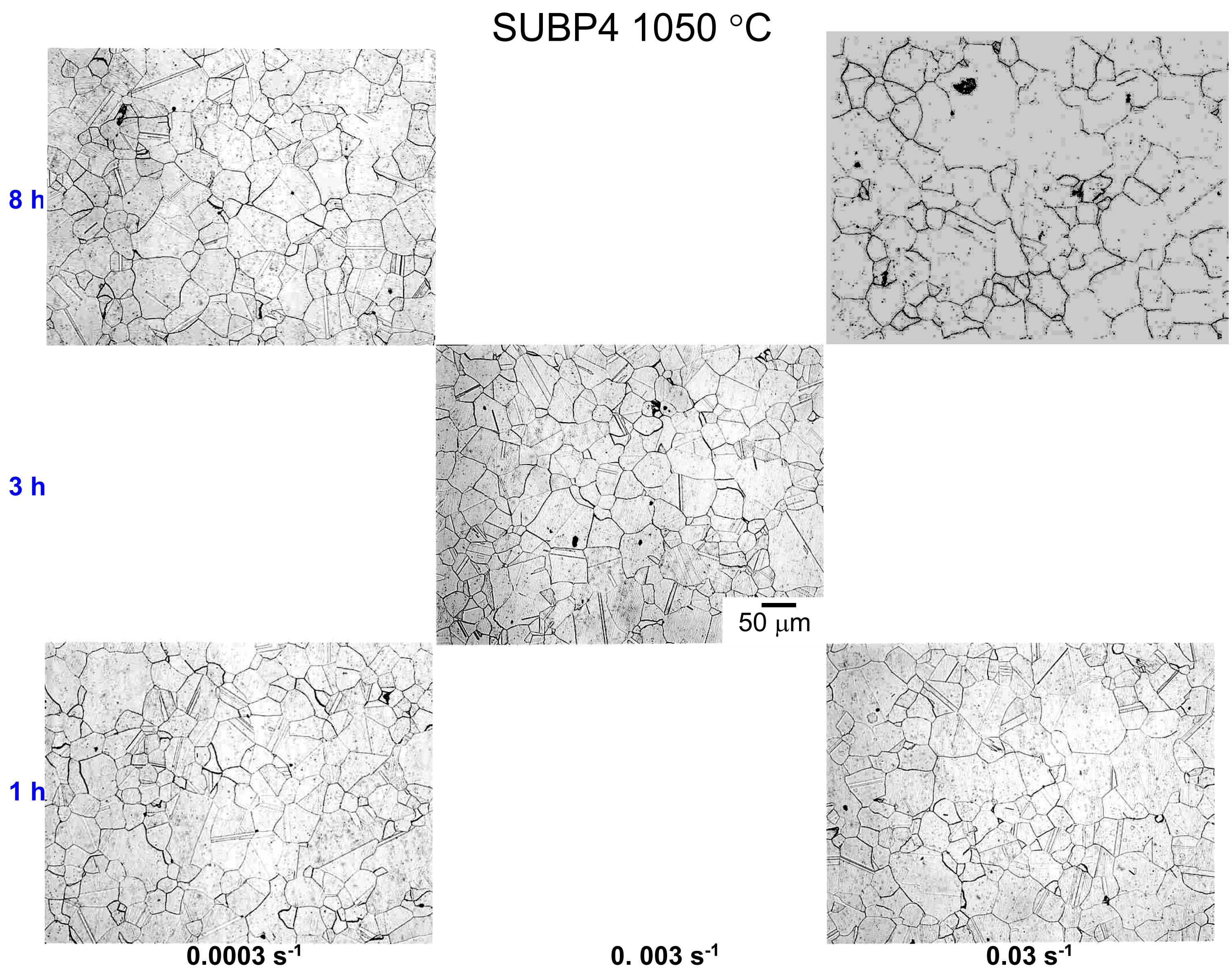

Figure 45.—Typical microstructures of specimens forged at 1050 °C with the indicated presoak times and strain rates, then 1h subsolvus plus 4h supersolvus solution heat treated.

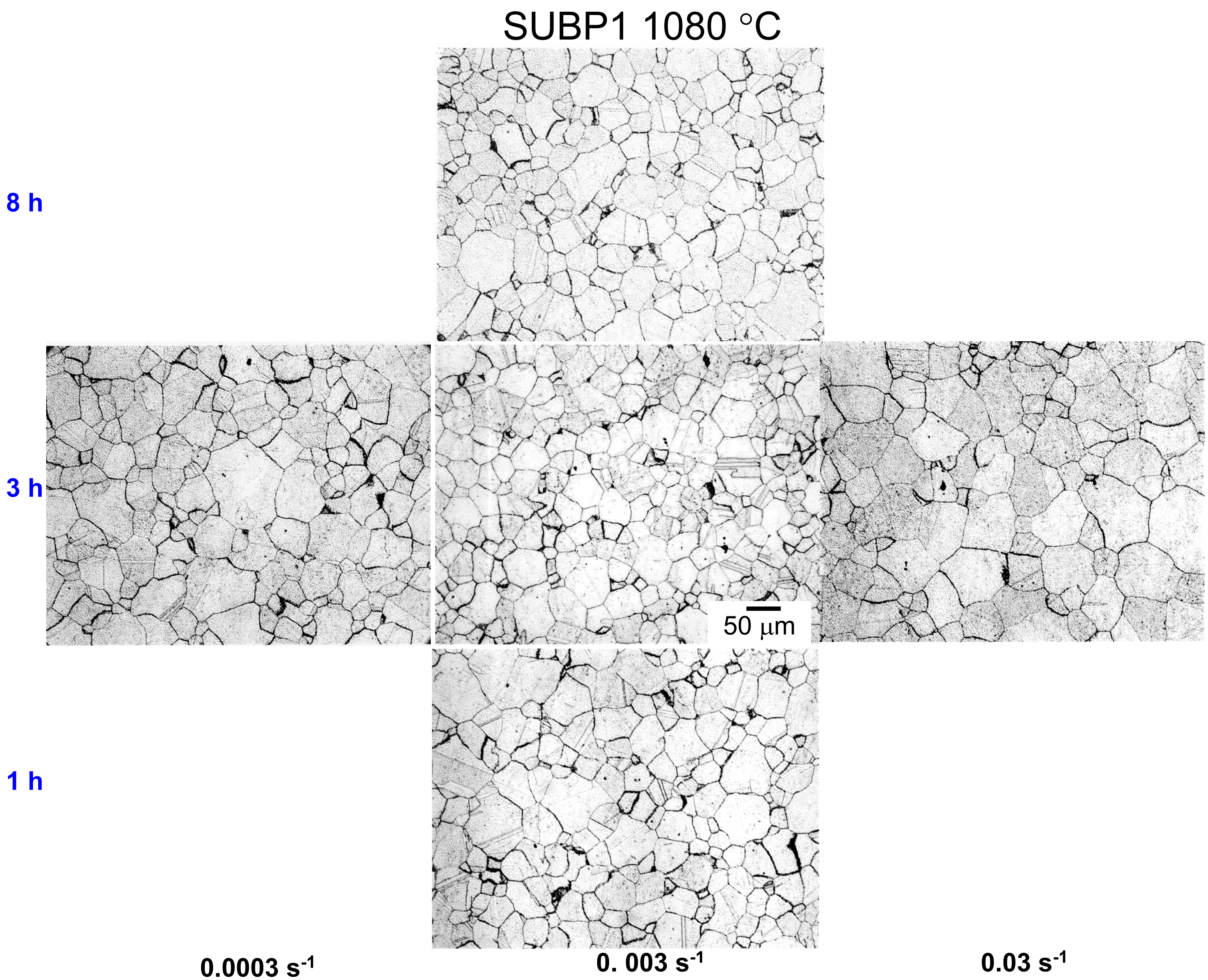

Figure 46.—Typical microstructures of specimens forged at 1080 °C with the indicated presoak times and strain rates, then 1h subsolvus plus 1h supersolvus solution heat treated.

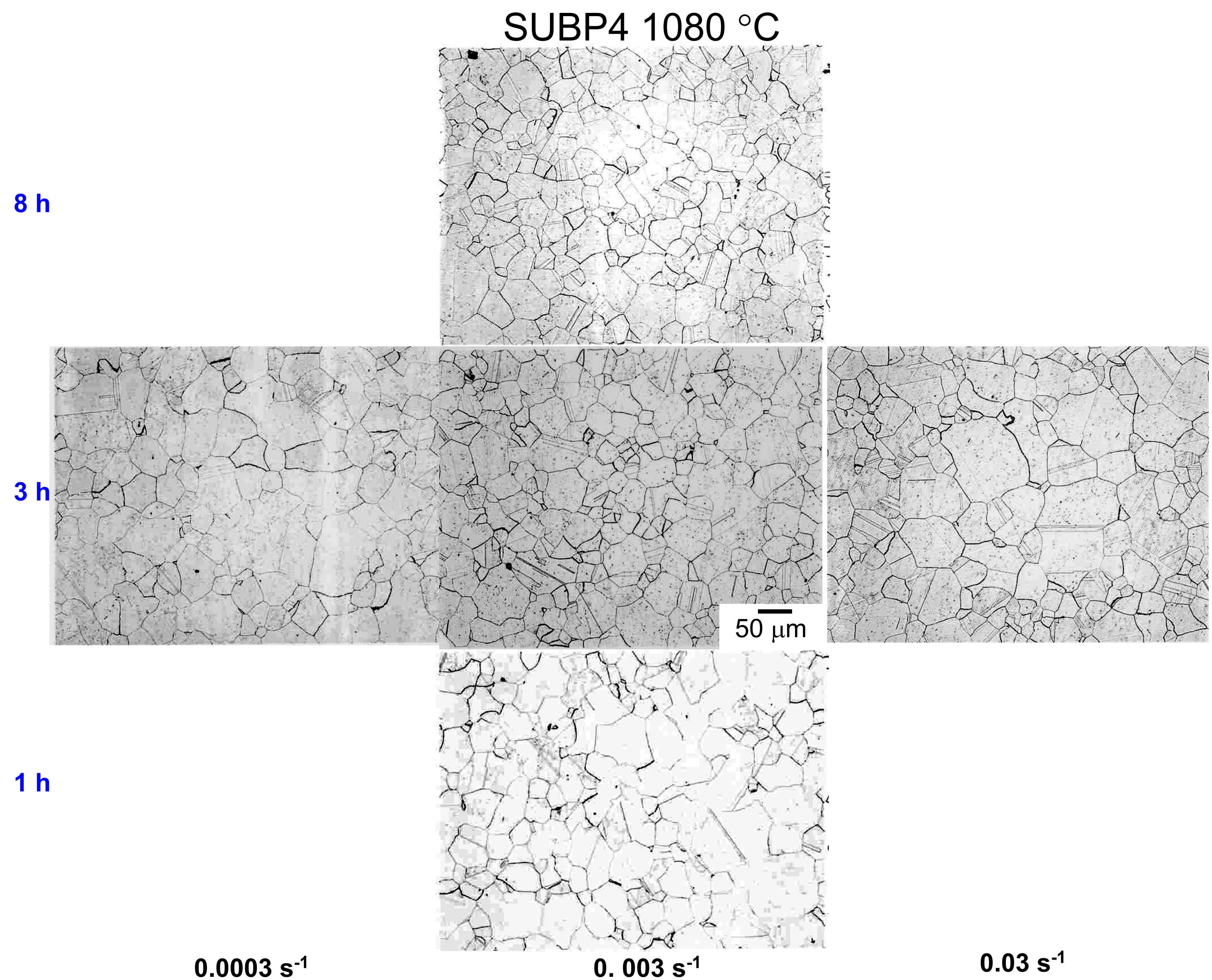

Figure 47.—Typical microstructures of specimens forged at 1080 °C with the indicated presoak times and strain rates, then 1h subsolvus plus 4h supersolvus solution heat treated.

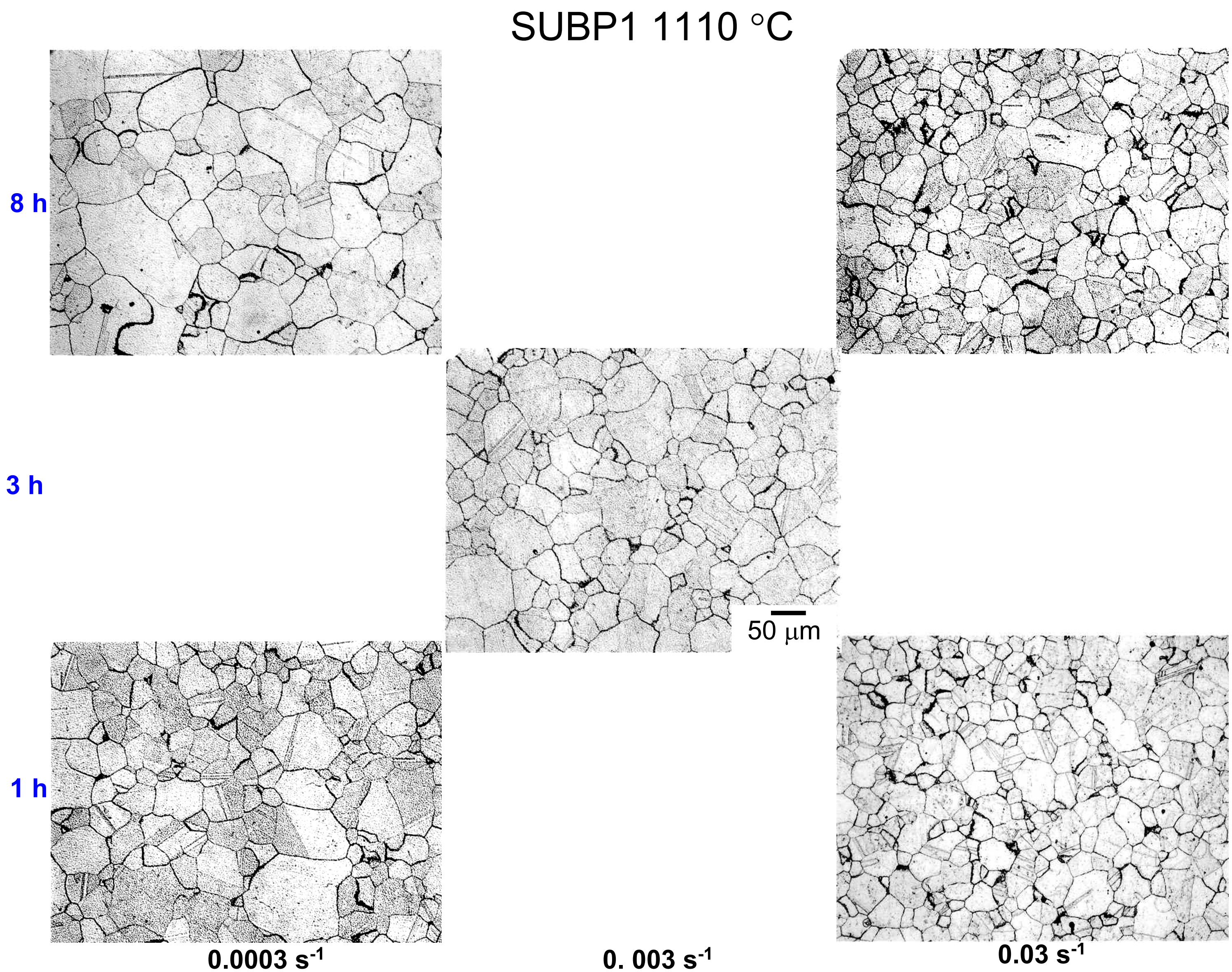

Figure 48.—Typical microstructures of specimens forged at 1110 °C with the indicated presoak times and strain rates, then 1h subsolvus plus 1h supersolvus solution heat treated.

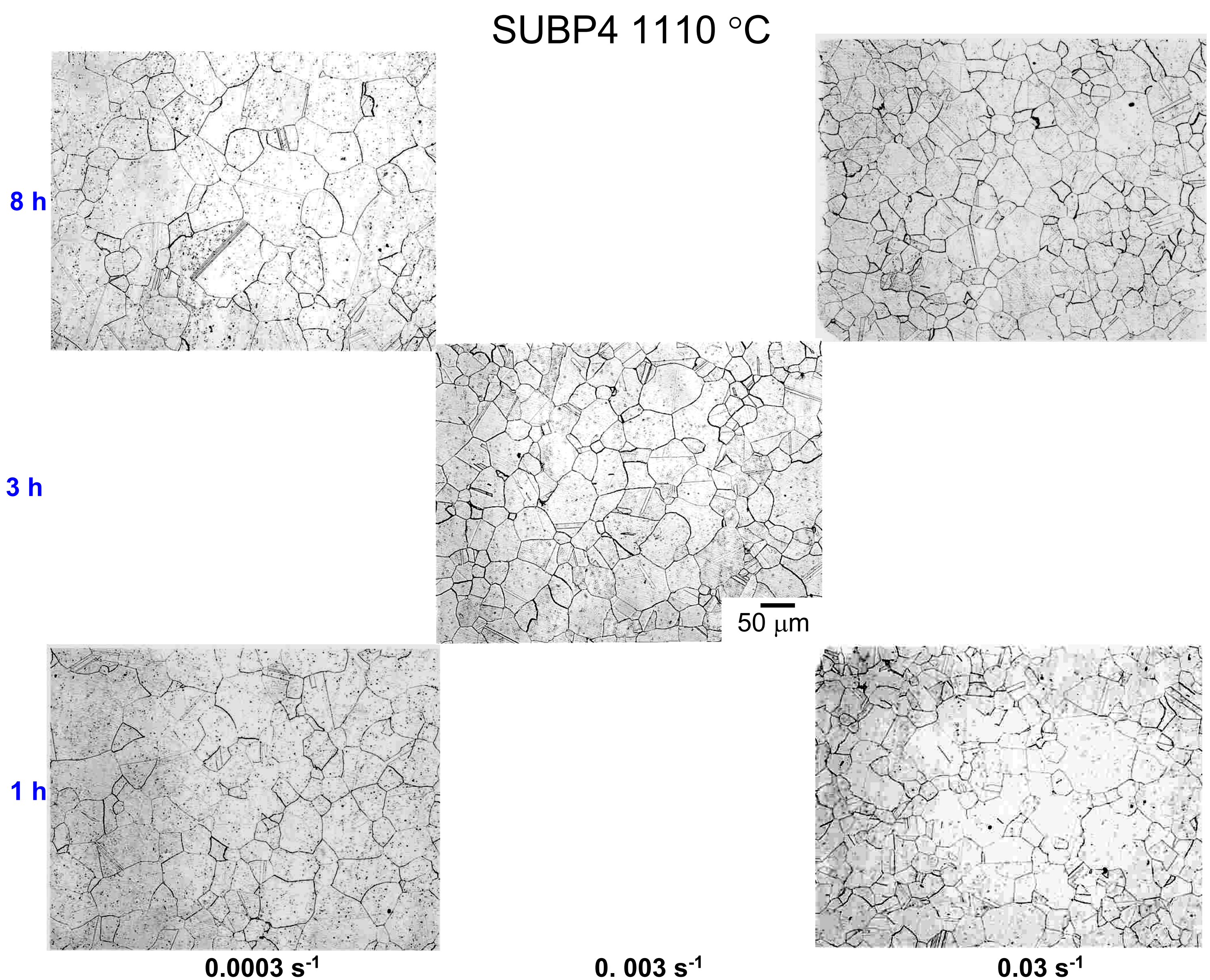

Figure 49.—Typical microstructures of specimens forged at 1110 °C with the indicated presoak times and strain rates, then 1h subsolvus plus 4h supersolvus solution heat treated.

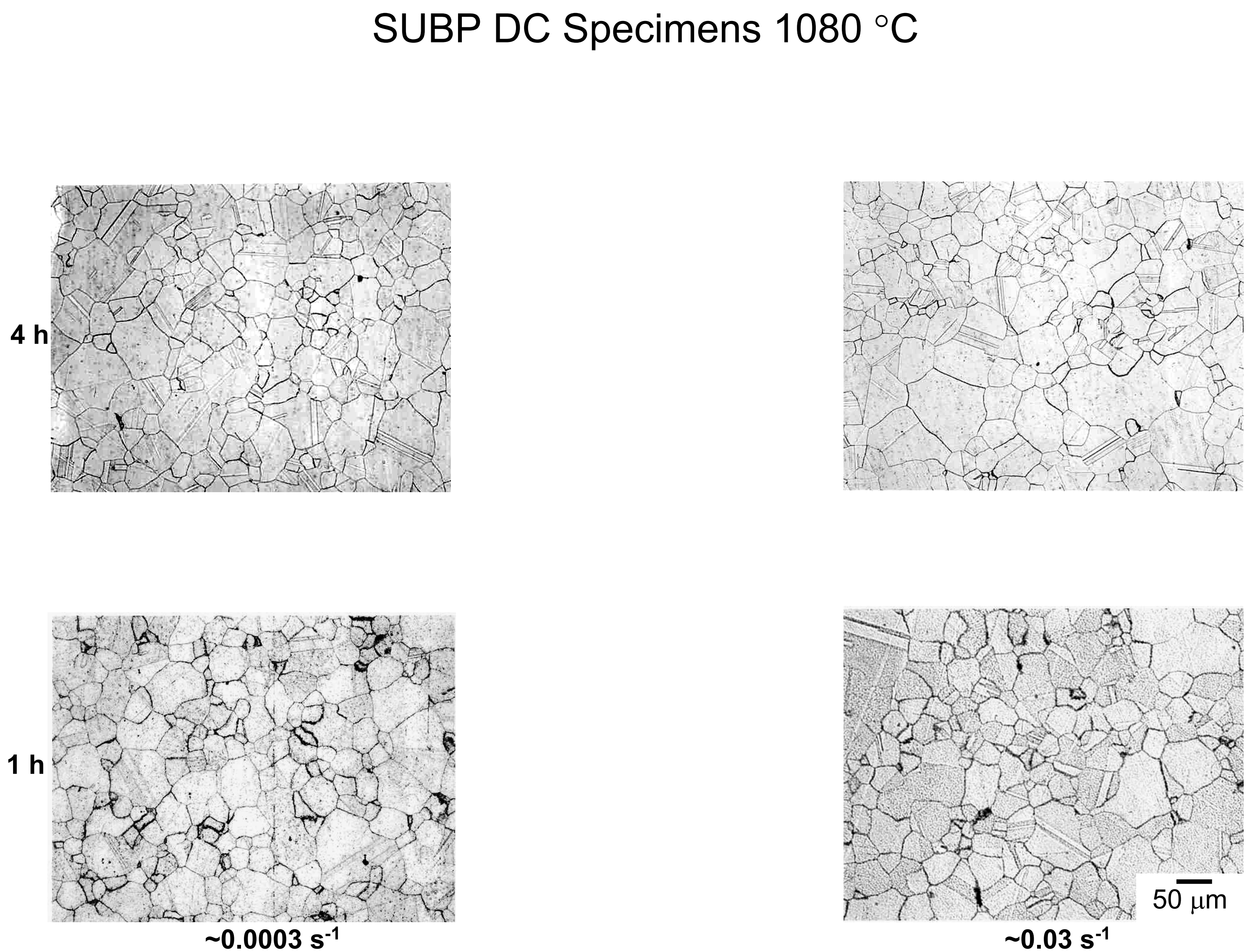

Figure 50.—Typical microstructures of double cone specimens forged at 1080 °C with the indicated approximate average strain rates, then 1h subsolvus plus 1h and 4h supersolvus solution heat treated.

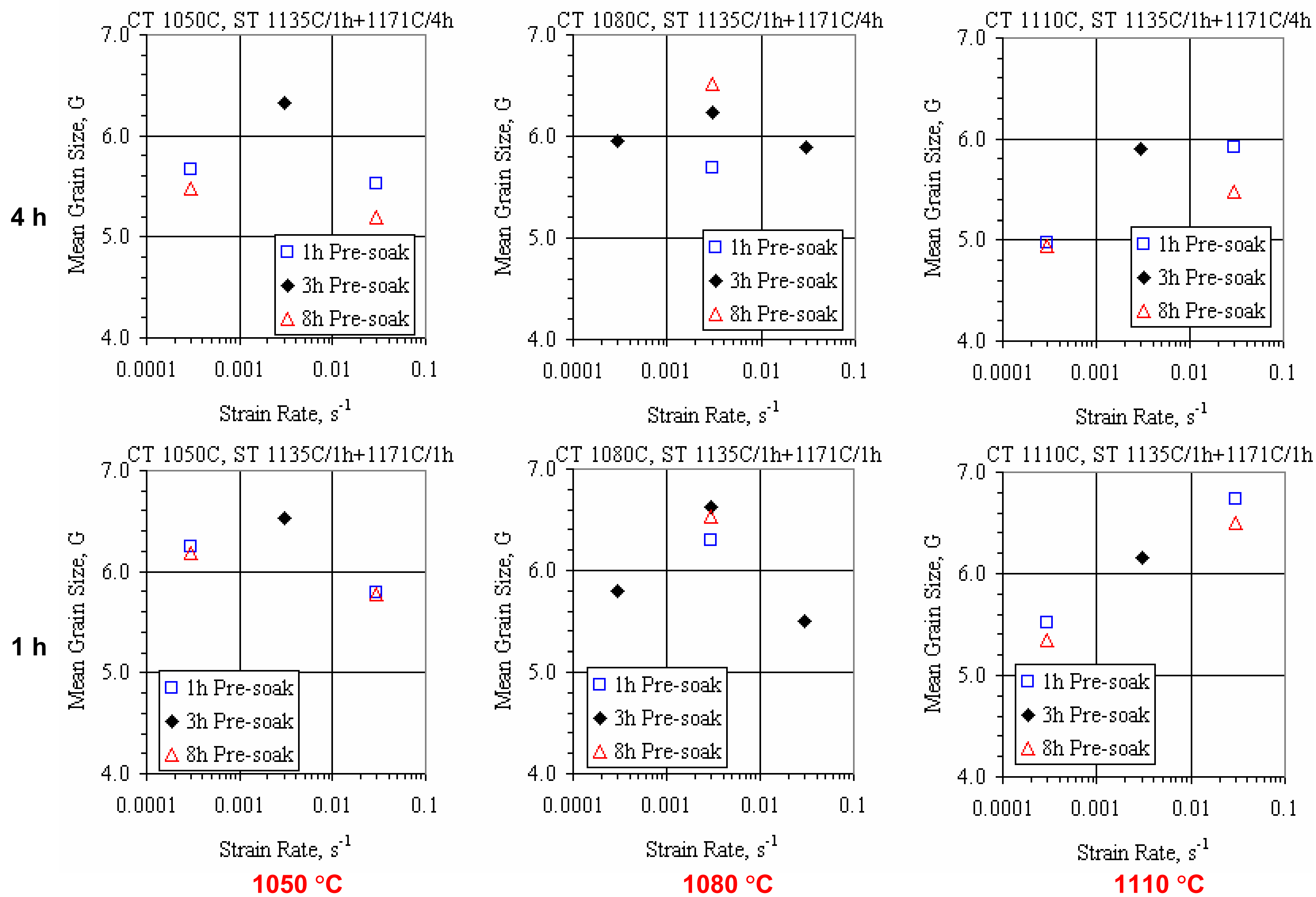

Figure 51.—Mean grain size vs. strain rate for the indicated forging presoak times and temperatures, with subsequent 1h subsolvus plus 1h and 4h supersolvus solution heat treatments.

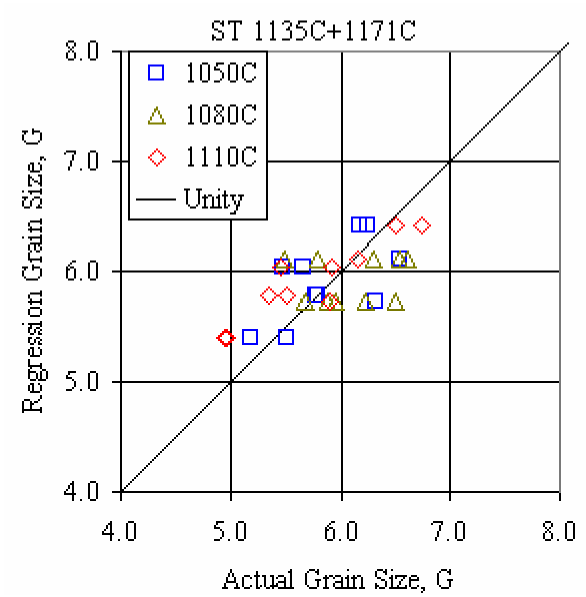

Figure 52.—Comparison of actual vs. regression subsolvus plus supersolvus heat treated mean grain sizes.

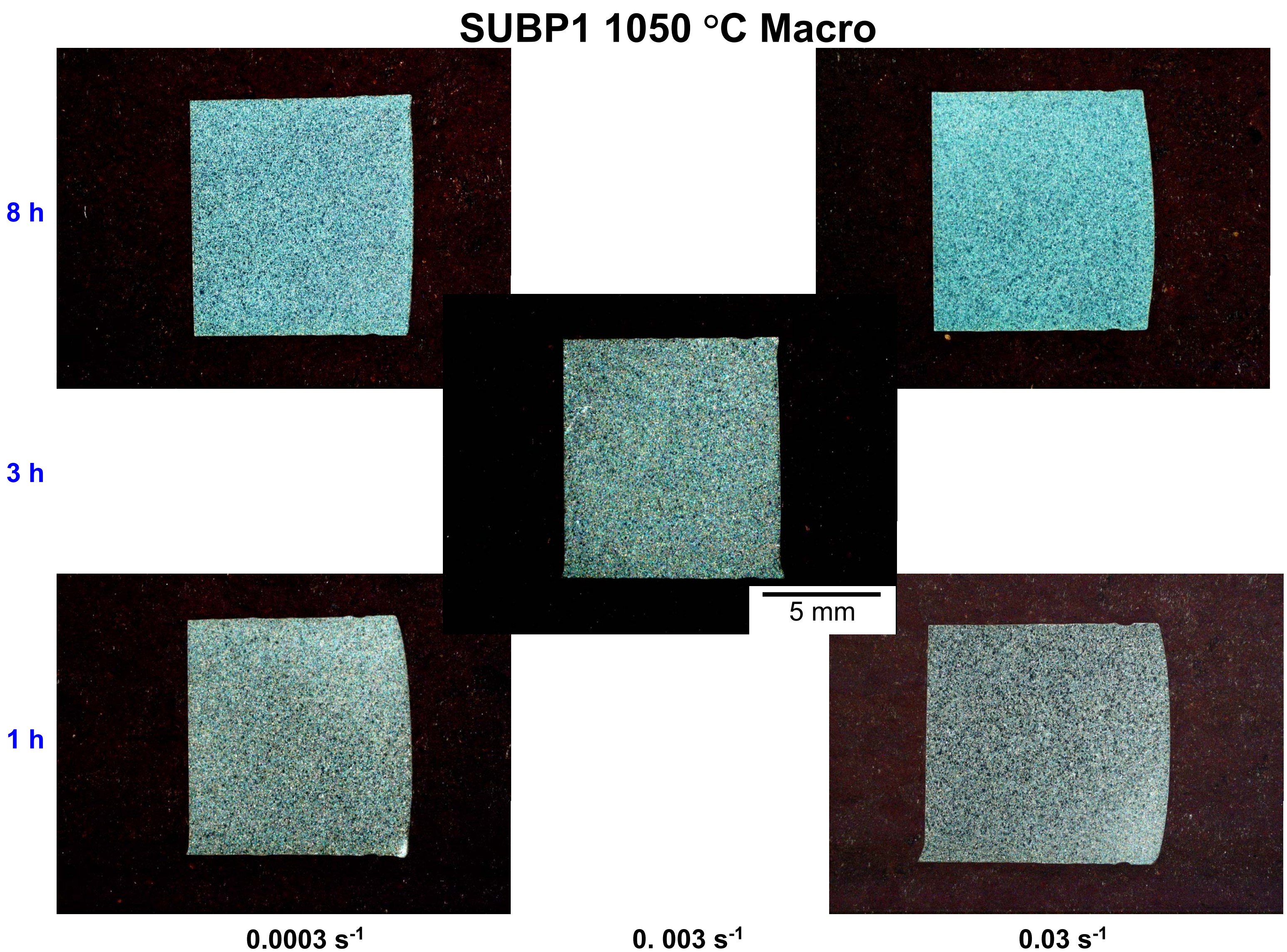

Figure 53.—Typical macrostructures of specimens forged at 1050 °C with the indicated presoak times and strain rates, then 1h subsolvus plus 1h supersolvus solution heat treated.

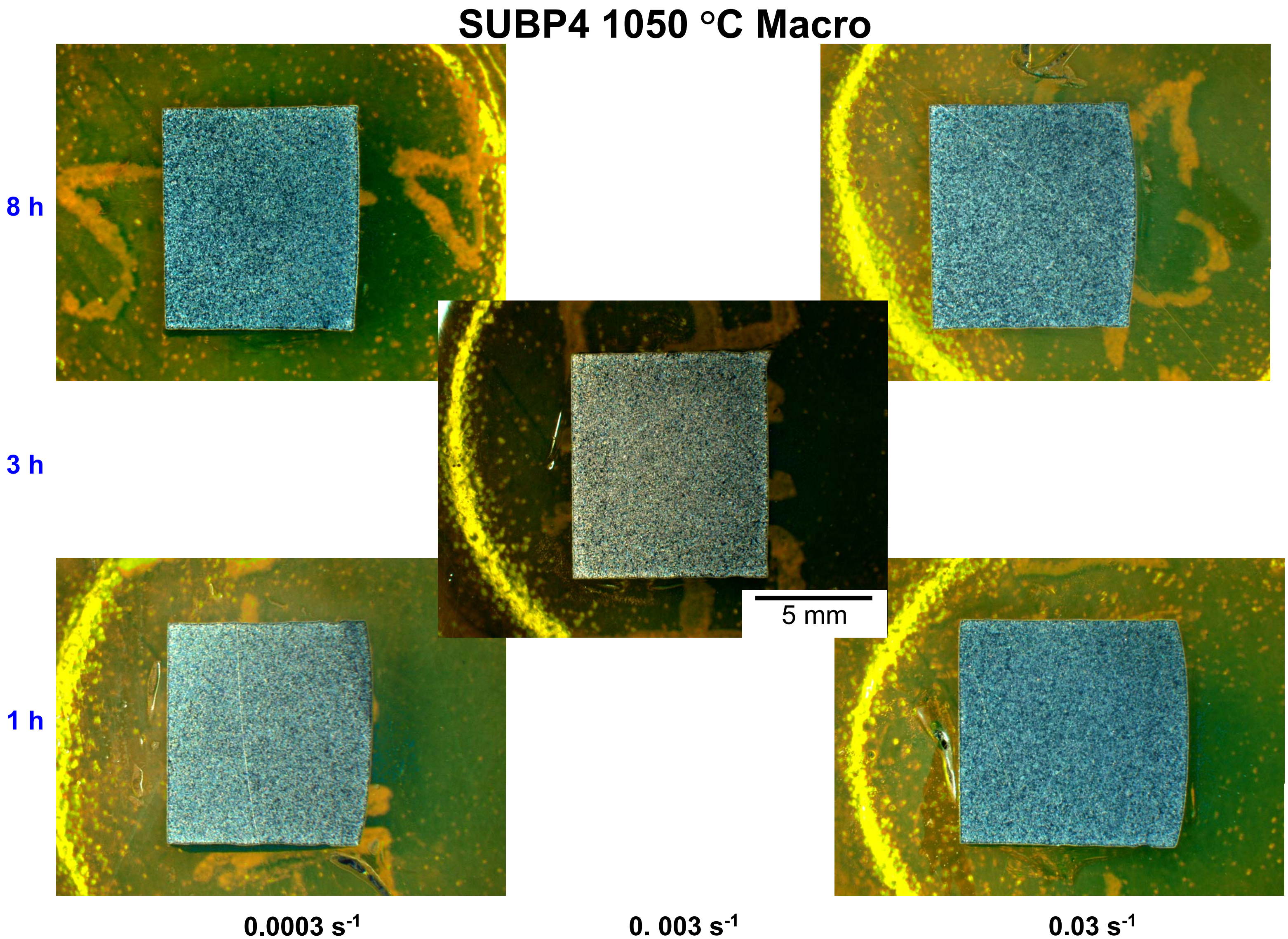

Figure 54.—Typical macrostructures of specimens forged at 1050 °C with the indicated presoak times and strain rates, then 1h subsolvus plus 4h supersolvus solution heat treated.

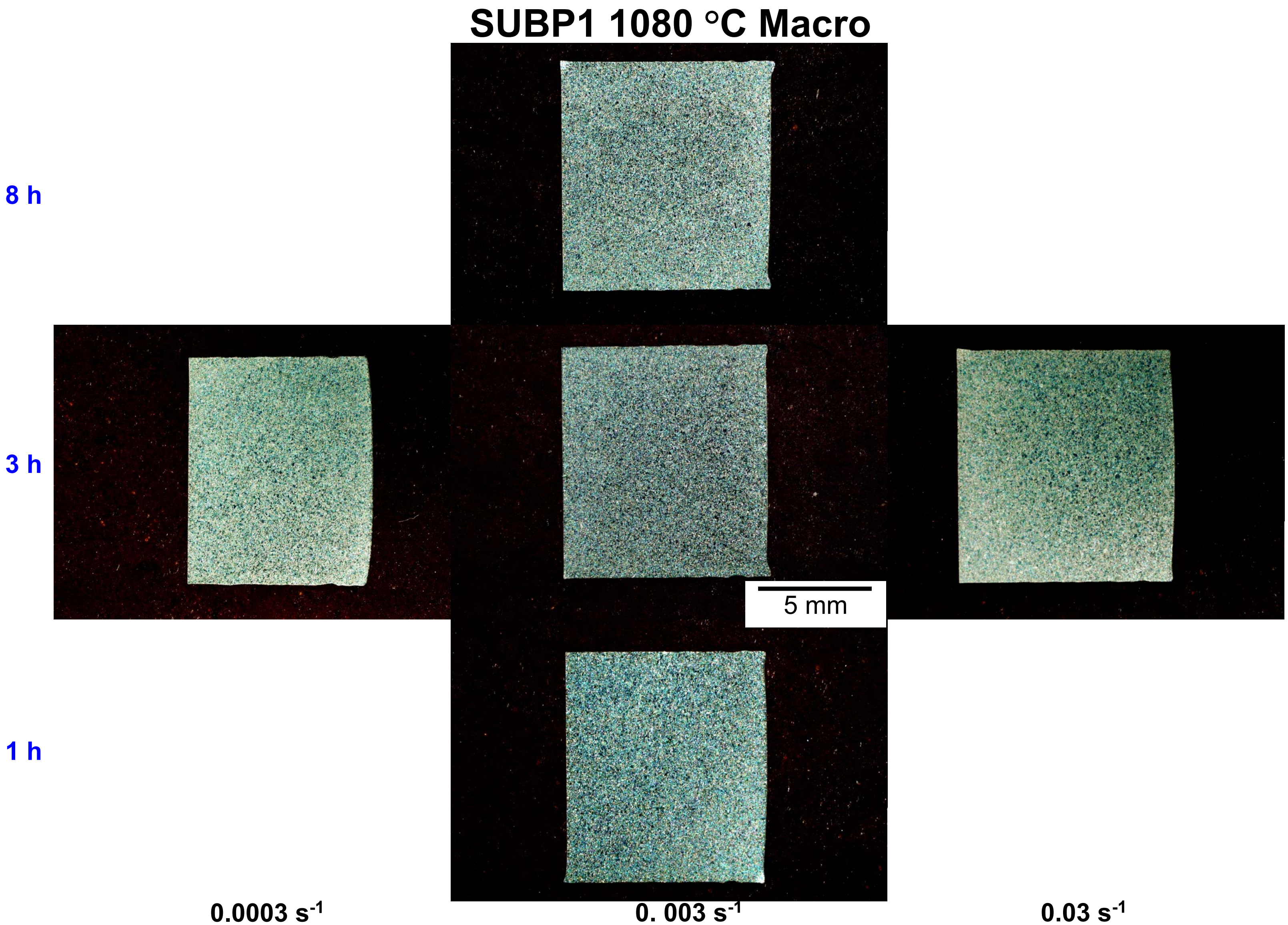

Figure 55.—Typical macrostructures of specimens forged at 1080 °C with the indicated presoak times and strain rates, then 1h subsolvus plus 1h supersolvus solution heat treated.

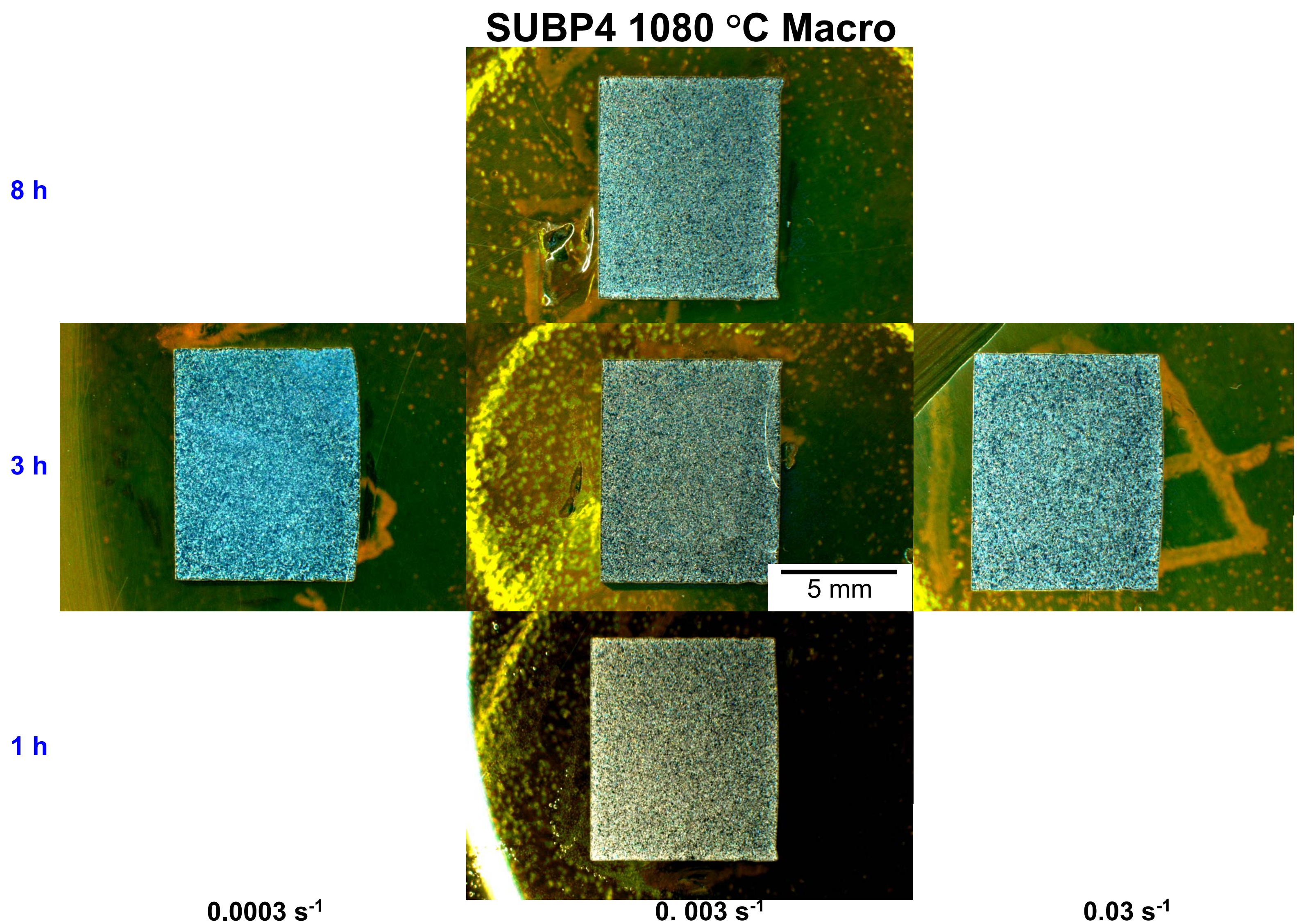

Figure 56.—Typical macrostructures of specimens forged at 1080 °C with the indicated presoak times and strain rates, then 1h subsolvus plus 4h supersolvus solution heat treated.

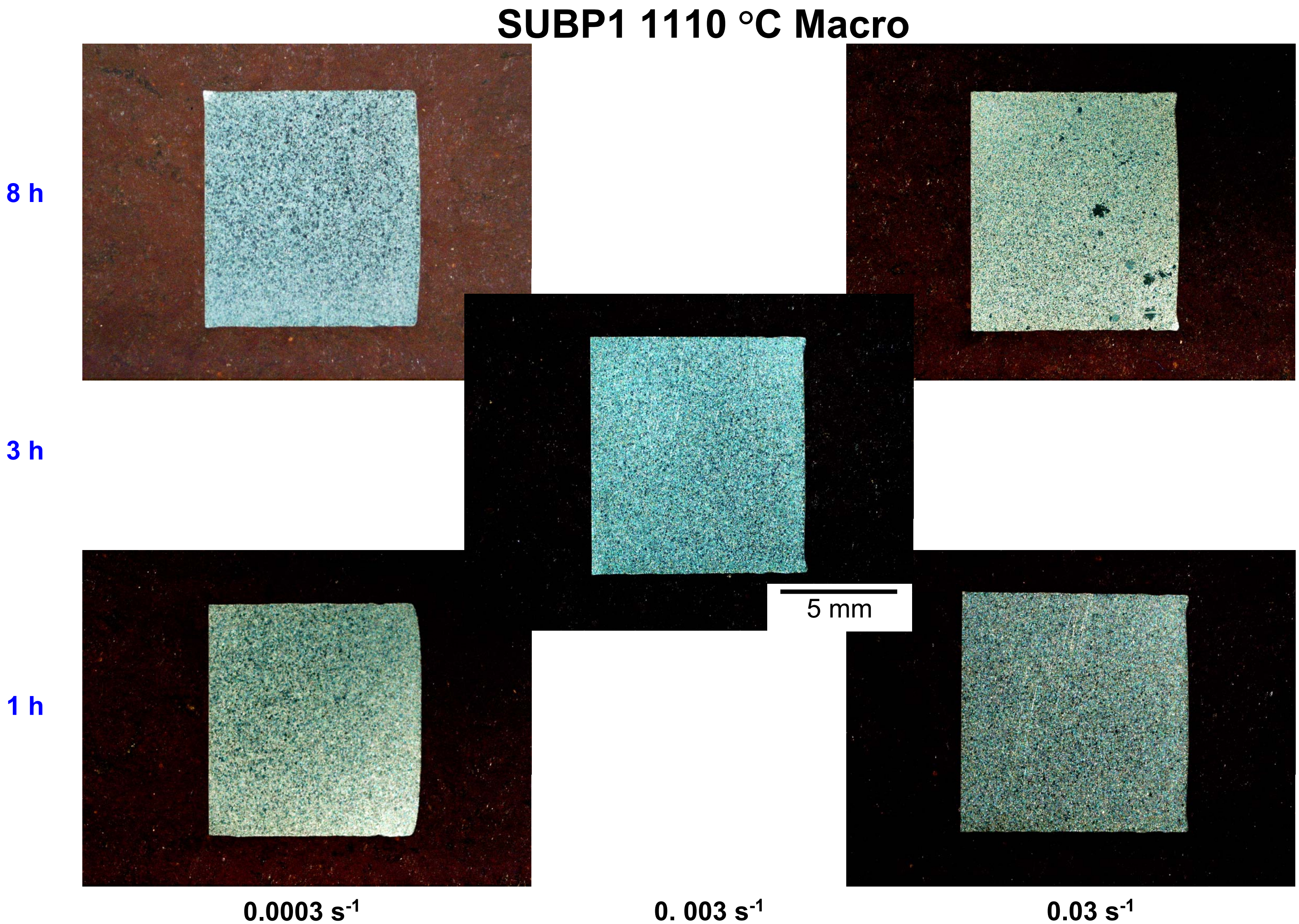

Figure 57.—Typical macrostructures of specimens forged at 1110 °C with the indicated presoak times and strain rates, then 1h subsolvus plus 1h supersolvus solution heat treated.

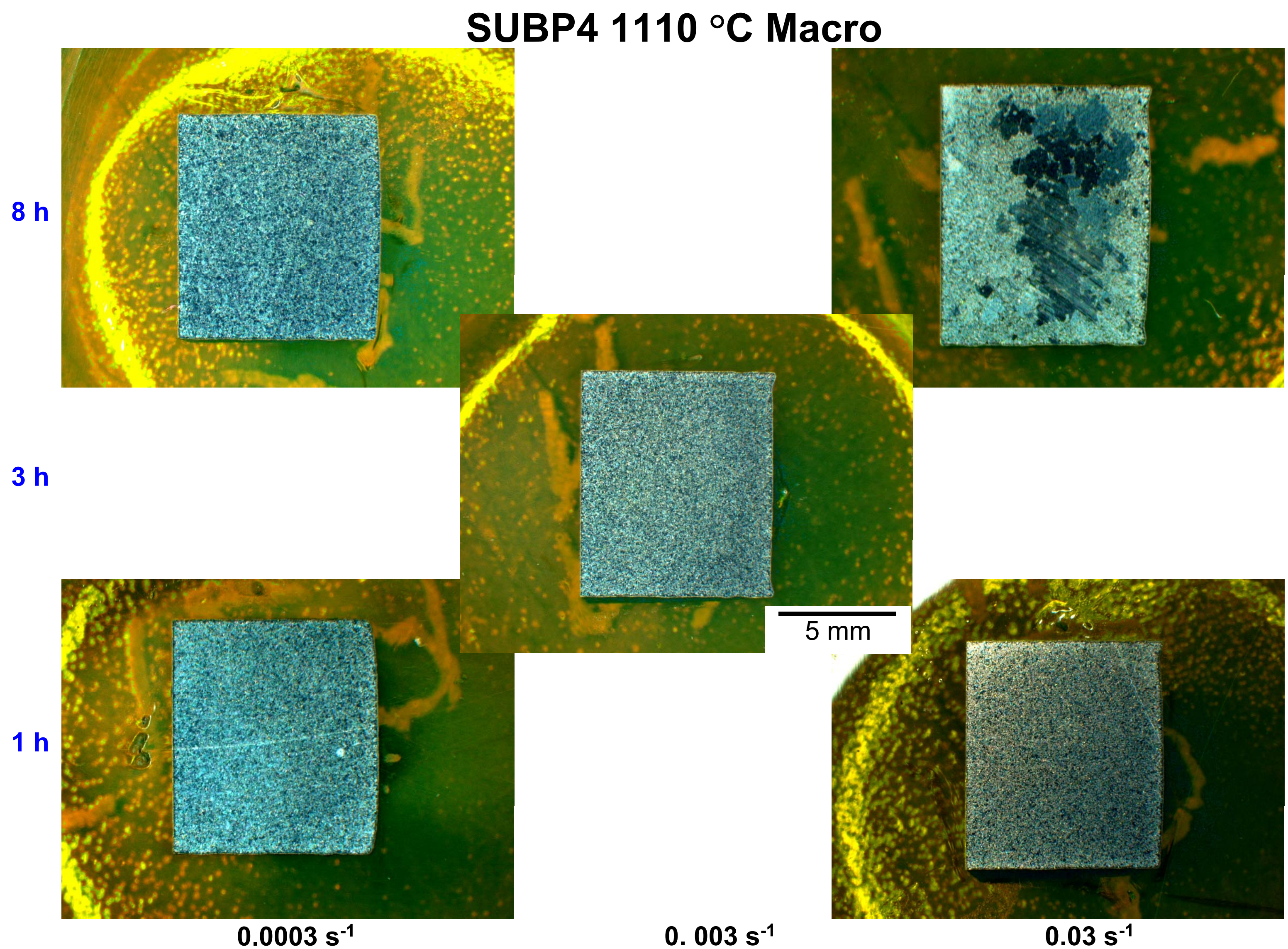

Figure 58.—Typical macrostructures of specimens forged at 1110 °C with the indicated presoak times and strain rates, then 1h subsolvus plus 4h supersolvus solution heat treated.

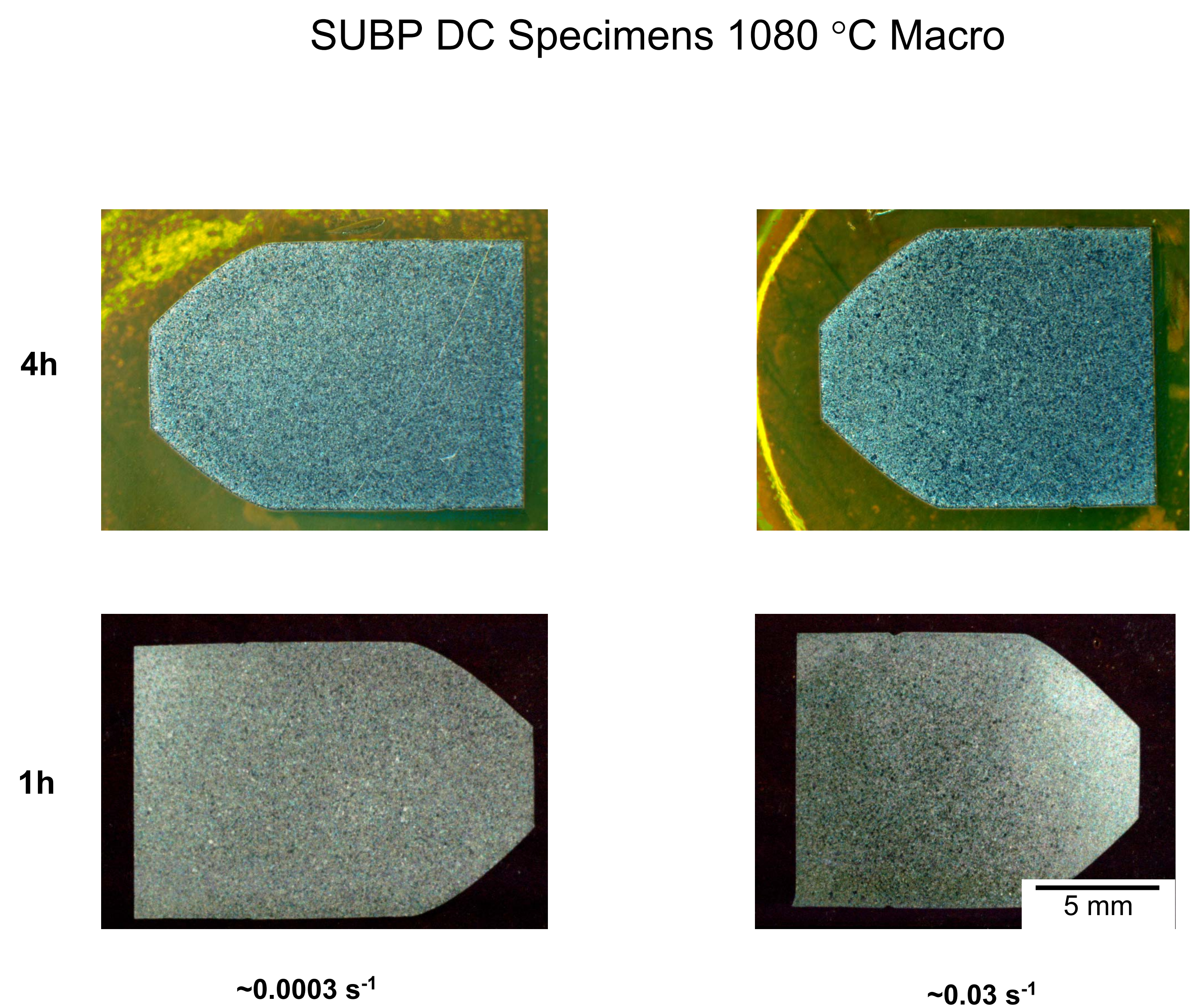

Figure 59.—Typical macrostructures of double cone specimens forged at 1080 °C with the indicated approximate average strain rates, then 1h subsolvus plus 1h and 4h supersolvus solution heat treated.

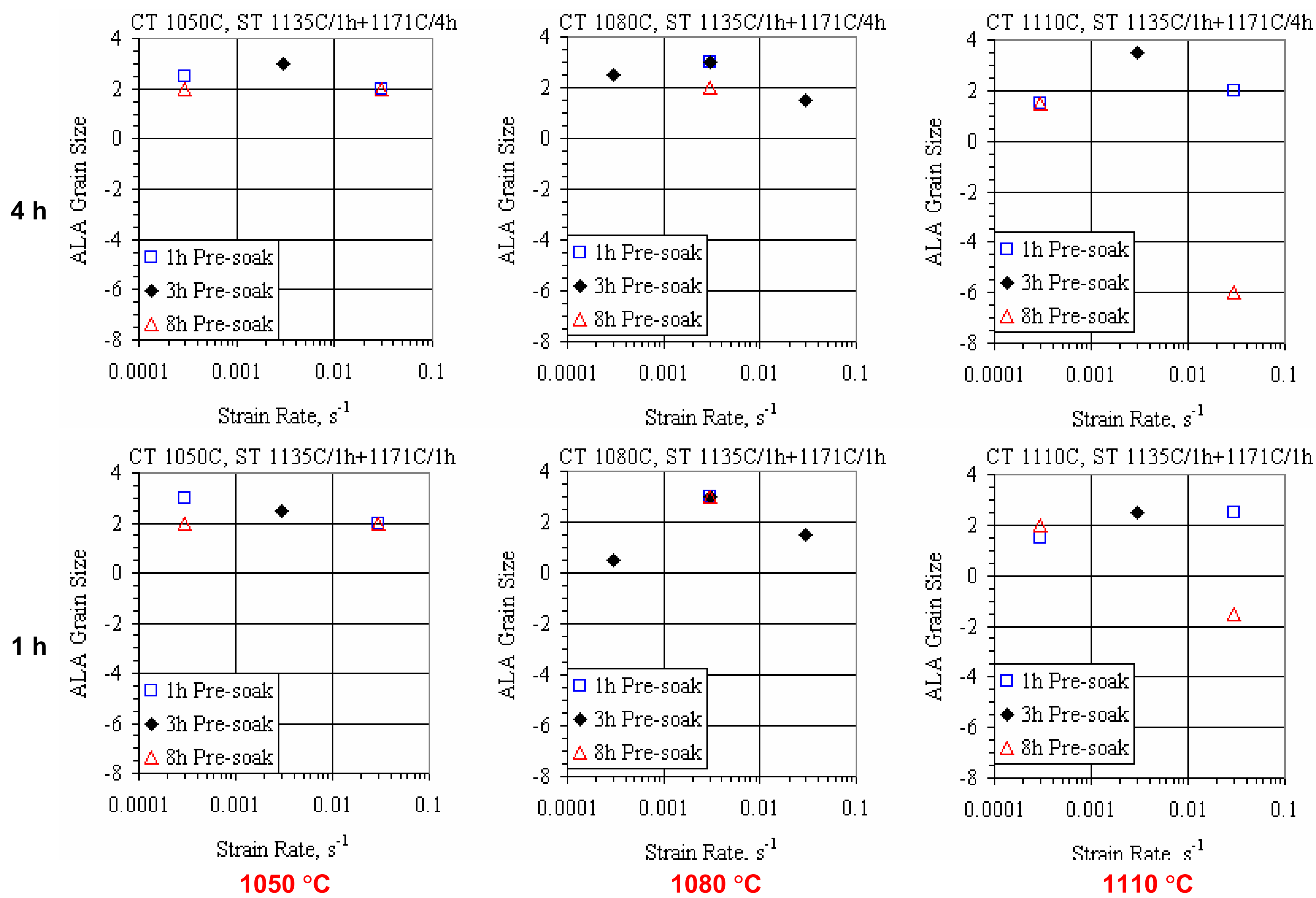

Figure 60.—As-large-as grain size vs. strain rate for the indicated forging presoak times and temperatures, with subsequent 1h subsolvus plus 1h and 4h supersolvus solution heat treatments.

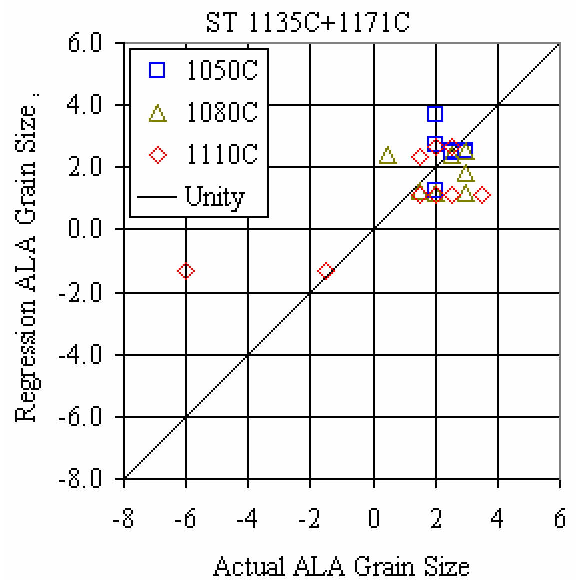

Figure 61.—Comparison of actual vs. regression subsolvus plus supersolvus heat treated as-large-as grain sizes.

Appendix A

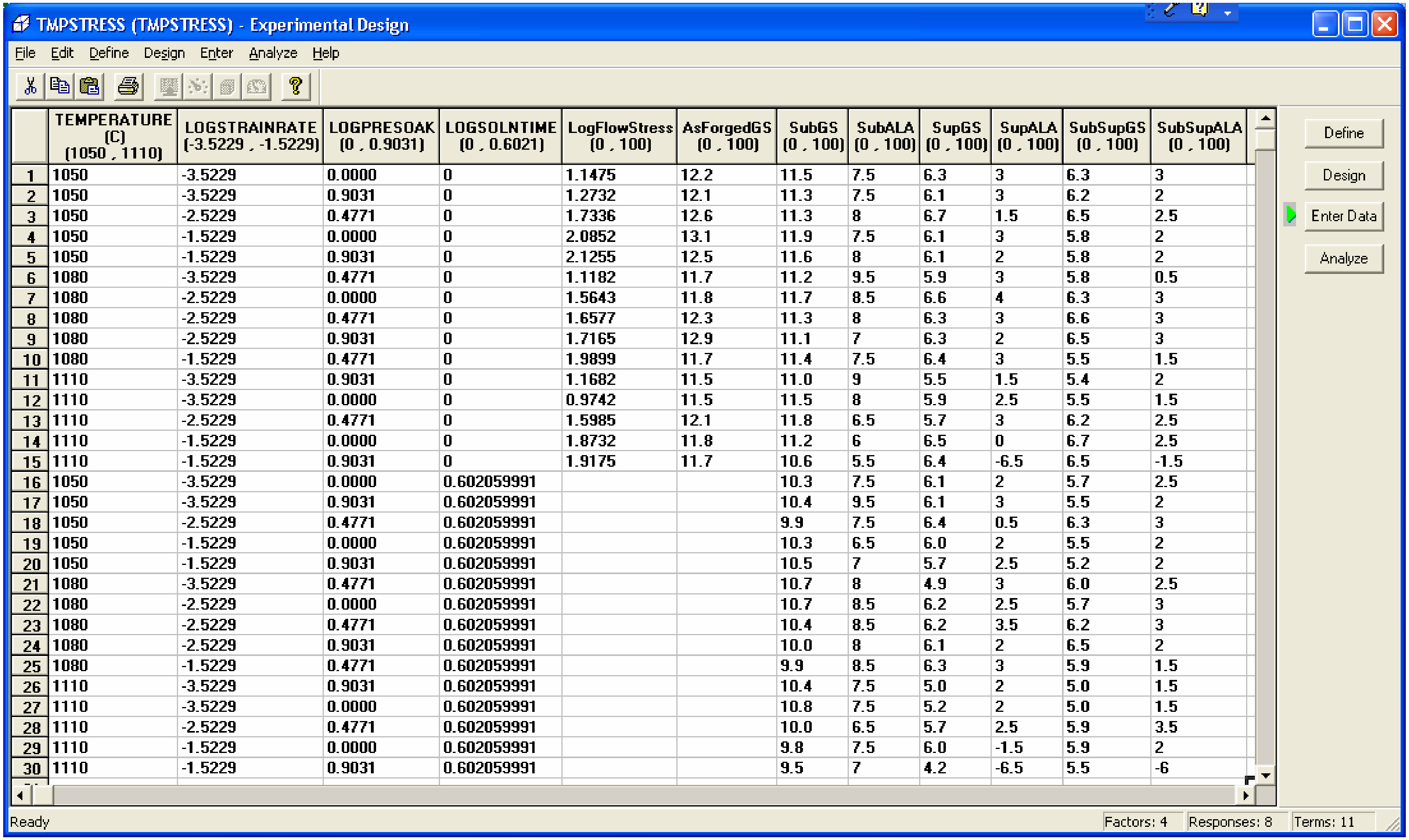

	TEMPERATURE (C) (1050 , 1110)	LOGSTRAINRATE (-3.5229 , -1.5229)	LOGPRESOAK (0 , 0.9031)	LOGSOLNTIME (0 , 0.6021)	LogFlowStress (0 , 100)	AsForgedGS (0 , 100)	SubGS (0 , 100)	SubALA (0 , 100)	SupGS (0 , 100)	SupALA (0 , 100)	SubSupGS (0 , 100)	SubSupALA (0 , 100)
1	1050	-3.5229	0.0000	0	1.1475	12.2	11.5	7.5	6.3	3	6.3	3
2	1050	-3.5229	0.9031	0	1.2732	12.1	11.3	7.5	6.1	3	6.2	2
3	1050	-2.5229	0.4771	0	1.7336	12.6	11.3	8	6.7	1.5	6.5	2.5
4	1050	-1.5229	0.0000	0	2.0852	13.1	11.9	7.5	6.1	3	5.8	2
5	1050	-1.5229	0.9031	0	2.1255	12.5	11.6	8	6.1	2	5.8	2
6	1080	-3.5229	0.4771	0	1.1182	11.7	11.2	9.5	5.9	3	5.8	0.5
7	1080	-2.5229	0.0000	0	1.5643	11.8	11.7	8.5	6.6	4	6.3	3
8	1080	-2.5229	0.4771	0	1.6577	12.3	11.3	8	6.3	3	6.6	3
9	1080	-2.5229	0.9031	0	1.7165	12.9	11.1	7	6.3	2	6.5	3
10	1080	-1.5229	0.4771	0	1.9899	11.7	11.4	7.5	6.4	3	5.5	1.5
11	1110	-3.5229	0.9031	0	1.1682	11.5	11.0	9	5.5	1.5	5.4	2
12	1110	-3.5229	0.0000	0	0.9742	11.5	11.5	8	5.9	2.5	5.5	1.5
13	1110	-2.5229	0.4771	0	1.5985	12.1	11.8	6.5	5.7	3	6.2	2.5
14	1110	-1.5229	0.0000	0	1.8732	11.8	11.2	6	6.5	0	6.7	2.5
15	1110	-1.5229	0.9031	0	1.9175	11.7	10.6	5.5	6.4	-6.5	6.5	-1.5
16	1050	-3.5229	0.0000	0.602059991			10.3	7.5	6.1	2	5.7	2.5
17	1050	-3.5229	0.9031	0.602059991			10.4	9.5	6.1	3	5.5	2
18	1050	-2.5229	0.4771	0.602059991			9.9	7.5	6.4	0.5	6.3	3
19	1050	-1.5229	0.0000	0.602059991			10.3	6.5	6.0	2	5.5	2
20	1050	-1.5229	0.9031	0.602059991			10.5	7	5.7	2.5	5.2	2
21	1080	-3.5229	0.4771	0.602059991			10.7	8	4.9	3	6.0	2.5
22	1080	-2.5229	0.0000	0.602059991			10.7	8.5	6.2	2.5	5.7	3
23	1080	-2.5229	0.4771	0.602059991			10.4	8.5	6.2	3.5	6.2	3
24	1080	-2.5229	0.9031	0.602059991			10.0	8	6.1	2	6.5	2
25	1080	-1.5229	0.4771	0.602059991			9.9	8.5	6.3	3	5.9	1.5
26	1110	-3.5229	0.9031	0.602059991			10.4	7.5	5.0	2	5.0	1.5
27	1110	-3.5229	0.0000	0.602059991			10.8	7.5	5.2	2	5.0	1.5
28	1110	-2.5229	0.4771	0.602059991			10.0	6.5	5.7	2.5	5.9	3.5
29	1110	-1.5229	0.0000	0.602059991			9.8	7.5	6.0	-1.5	5.9	2
30	1110	-1.5229	0.9031	0.602059991			9.5	7	4.2	-6.5	5.5	-6

A-1.—Input data table used for flow stress regression.

All Terms

```
                 Least Squares Coefficients, Response LFS, Model DESIGN

Term        Coeff.        Std. Error    T-value  Signif.  Transformed Term
----------------------------------------------------------------------------------
1 1             1.595152      0.015225
2 ~T           -0.083445      0.018643                    ((T-1.08e+03)/3e+01)
3 ~LSR          0.431332      0.018643                    (LSR+2.5229)
4 ~LP           0.056251      0.018632                    ((LP-4.5155e-01)/4.5155e
5 ~T*LSR       -0.017712      0.020842     -0.85   0.4201  ((T-1.08e+03)/3e+01)*(LS
6 ~T*LP         0.009255      0.020836      0.44   0.6687  ((T-1.08e+03)/3e+01)*((L
7 ~LSR*LP      -0.029300      0.020836     -1.41   0.1973  (LSR+2.5229)*((LP-4.5155

No. cases = 15       R-sq. =   0.9861    RMS Error = 0.05895
Resid. df =  8   R-sq-adj. =   0.9756      Cond. No. = 1.023
~ indicates factors are transformed.
```

FORWARD AND REVERSE STEPWISE SELECTION

```
Mulreg @TMPSTRESS@MULREG, Model DESIGN__COPY, Response LFS

Term       df  P-Remove  P-Enter
1 1         1    0.000
2 T         1    0.002
3 LSR       1    0.000
4 LP        1    0.017
5 T*LSR     1    0.420
6 T*LP      1    0.669
7 LSR*LP    1    0.197

No. cases = 15       R-sq. =   0.9861    RMS Error = 0.05895
Resid. df =  8   R-sq-adj. =   0.9756     Obey Hierarchy: no
```

```
Mulreg @TMPSTRESS@MULREG, Model DESIGN__COPY, Response LFS

Term       df  P-Remove  P-Enter
1 1         1    0.000
2 T         1    0.001
3 LSR       1    0.000
4 LP        1    0.011
5 T*LSR     1              0.419
6 T*LP      1              0.677
7 LSR*LP    1              0.167

No. cases = 15       R-sq. =   0.9810    RMS Error = 0.05867
Resid. df = 11   R-sq-adj. =   0.9759     Obey Hierarchy: no
```

A-1.—Log flow stress regression results.

MODEL TMPLPLSTRESS

Least Squares Coefficients, Response LFS, Model TMPLPLSTRESS

Term	Coeff.	Std. Error	T-value	Signif.	Transformed Term
1 1	1.595152	0.015154	105.27	0.0001	
2 ~T	-0.083340	0.018554	-4.49	0.0009	((T-1.08e+03)/3e+01)
3 ~LSR	0.431000	0.018554	23.23	0.0001	(LSR+2.5229)
4 ~LP	0.056251	0.018545	3.03	0.0114	((LP-4.5155e-01)/4.5155e

No. cases = 15 R-sq. = 0.9810 RMS Error = 0.05867
Resid. df = 11 R-sq-adj. = 0.9759 Cond. No. = 1.023
~ indicates factors are transformed.

ANOVA

Least Squares Summary ANOVA, Response LFS Model TMPLPLSTRESS

Source	df	Sum Sq.	Mean Sq.	F-Ratio	Signif.
1 Total(Corr.)	14	1.996611			
2 Regression	3	1.958741	0.652914	189.70	0.0000
3 Residual	11	0.037869	0.003443		

R-sq. = 0.9810
R-sq-adj. = 0.9759

Least Squares Components ANOVA, Response LFS Model TMPLPLSTRESS

Source	df	Sum Sq.	Mean Sq.	F-Ratio	Signif.	Transformed Term
1 Constant	1	38.147333				
2 ~T	1	0.069456	0.069456	20.17	0.0009	((T-1.08e+03)/3e+01)
3 ~LSR	1	1.857610	1.857610	539.60	0.0000	(LSR+2.5229)
4 ~LP	1	0.031676	0.031676	9.20	0.0114	((LP-4.5155e-01)/4.5155e
5 Residual	11	0.037869	0.003443			

~ indicates factors R-sq. = 0.9810
are transformed. R-sq-adj. = 0.9759
Type 3 sum of squares.

A-1.—Log flow stress regression results.

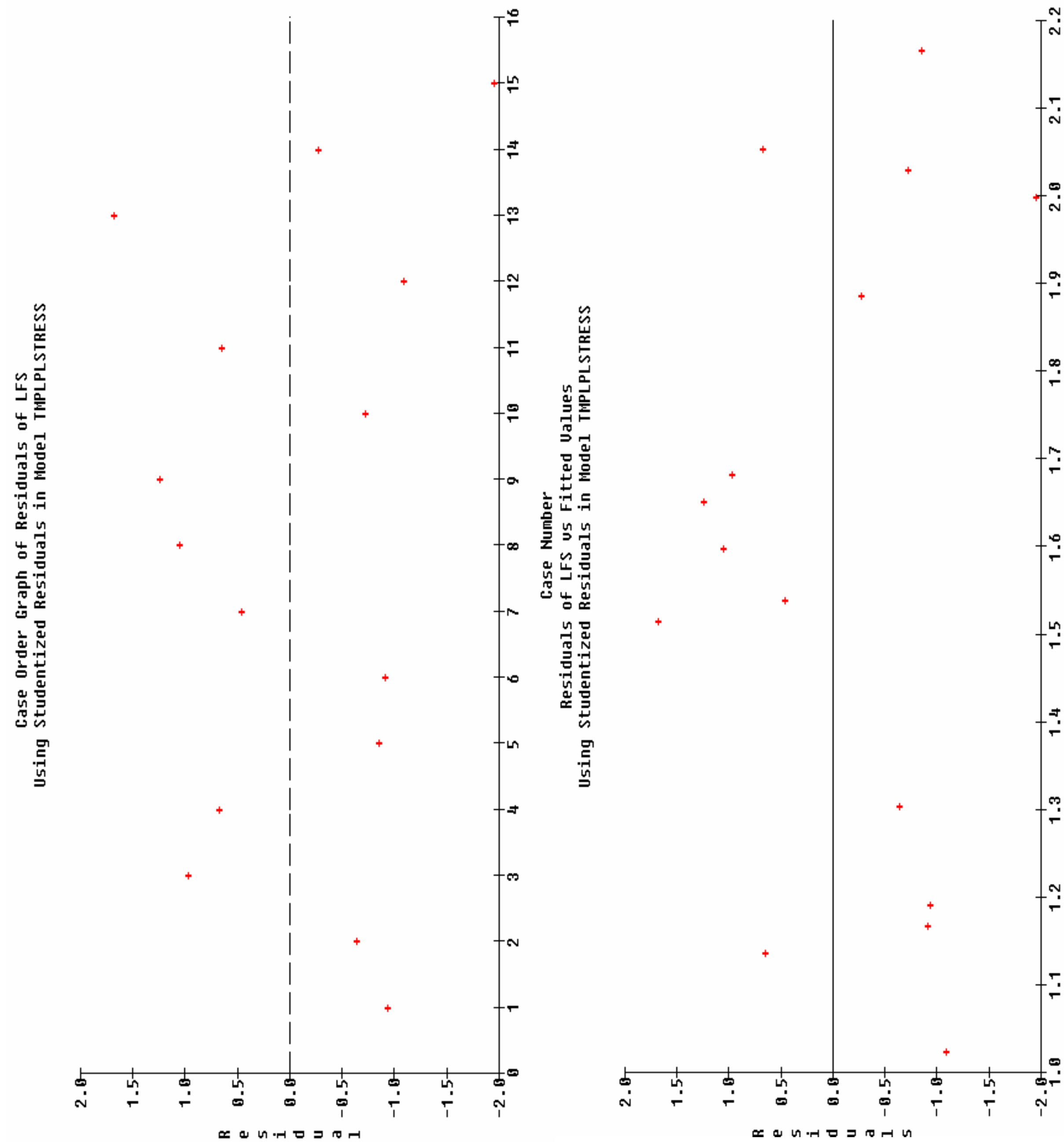

A-1.—Log flow stress regression results.

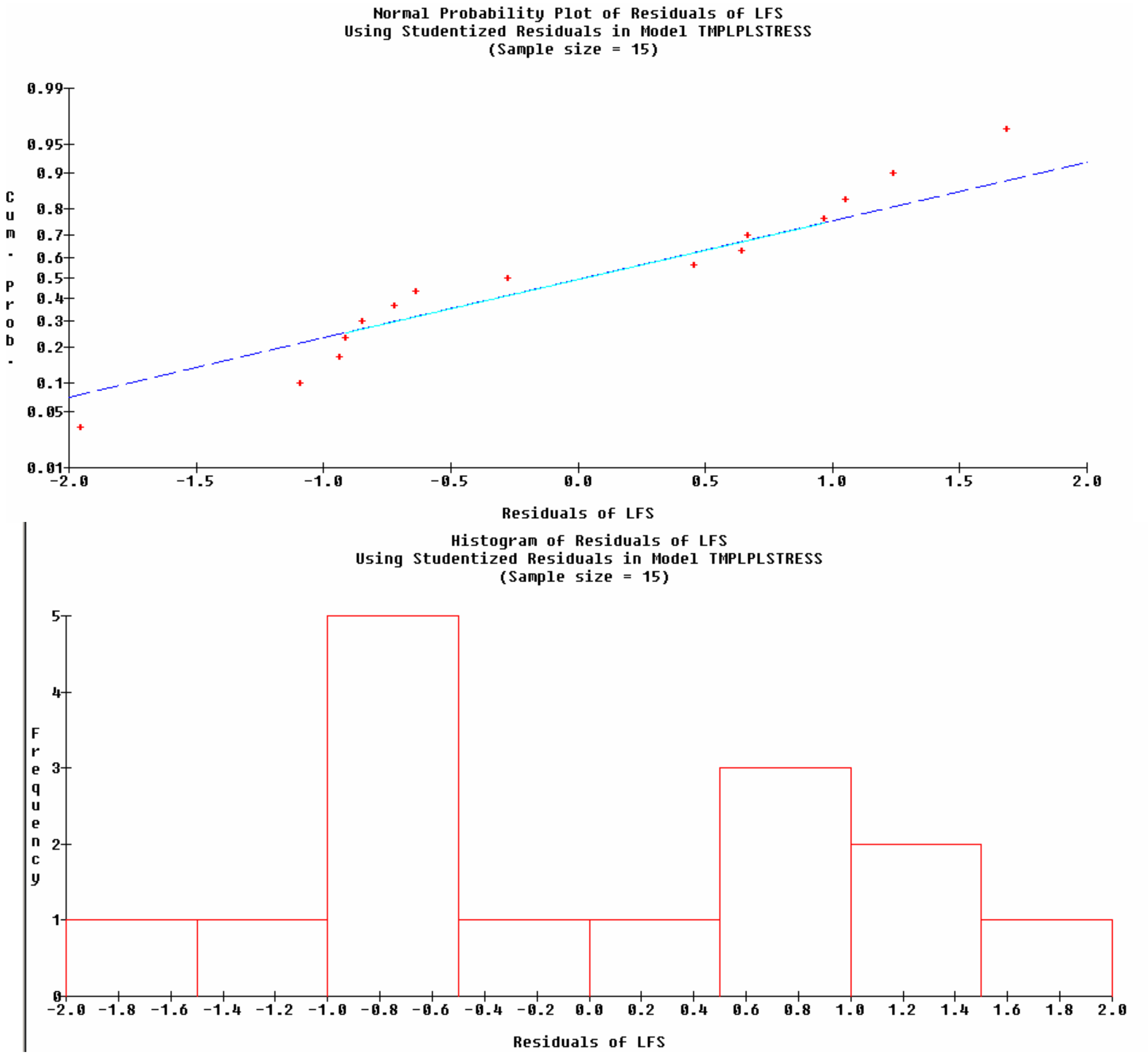

A-1.—Log flow stress regression results.

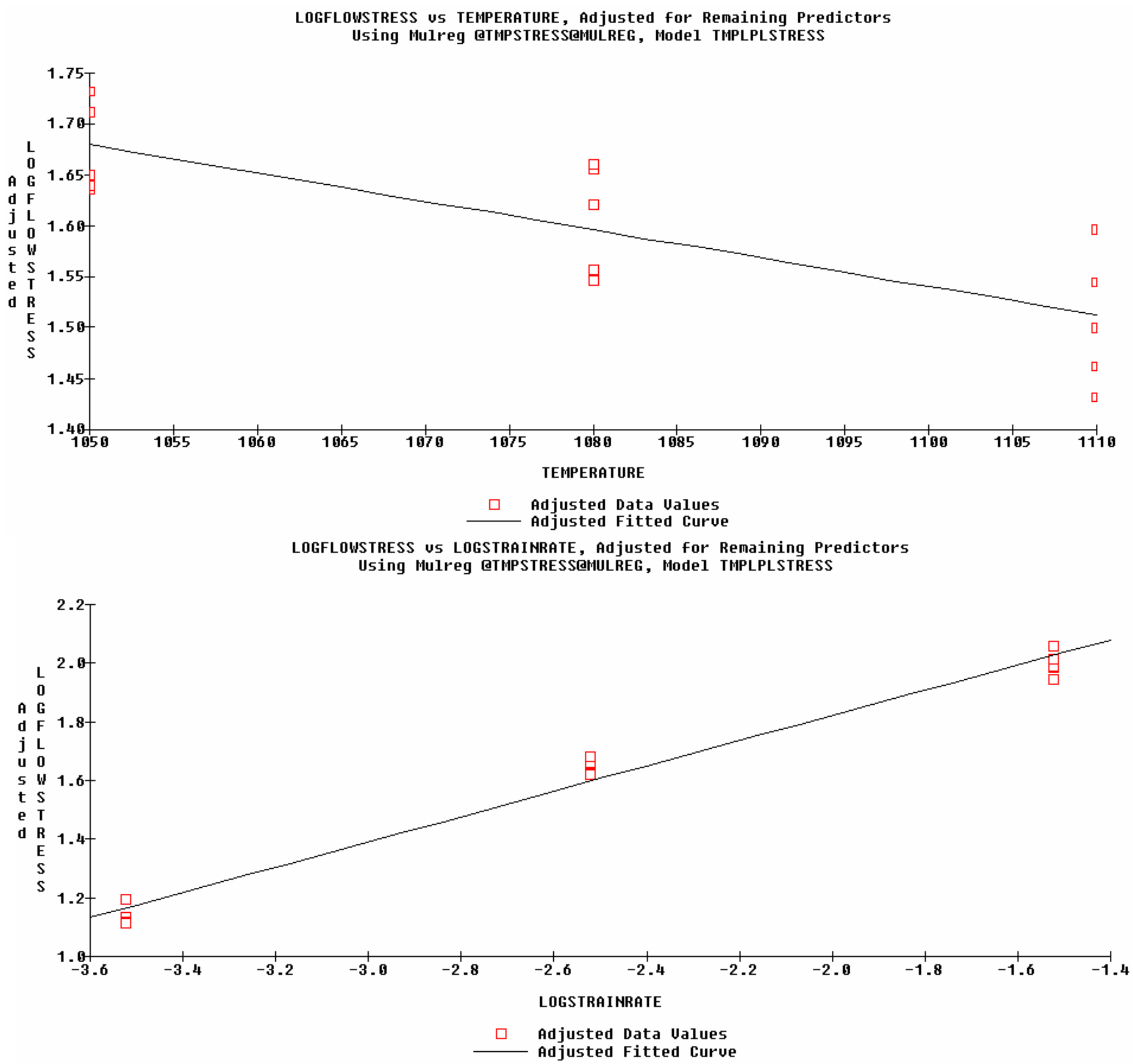

A-1.—Log flow stress regression results.

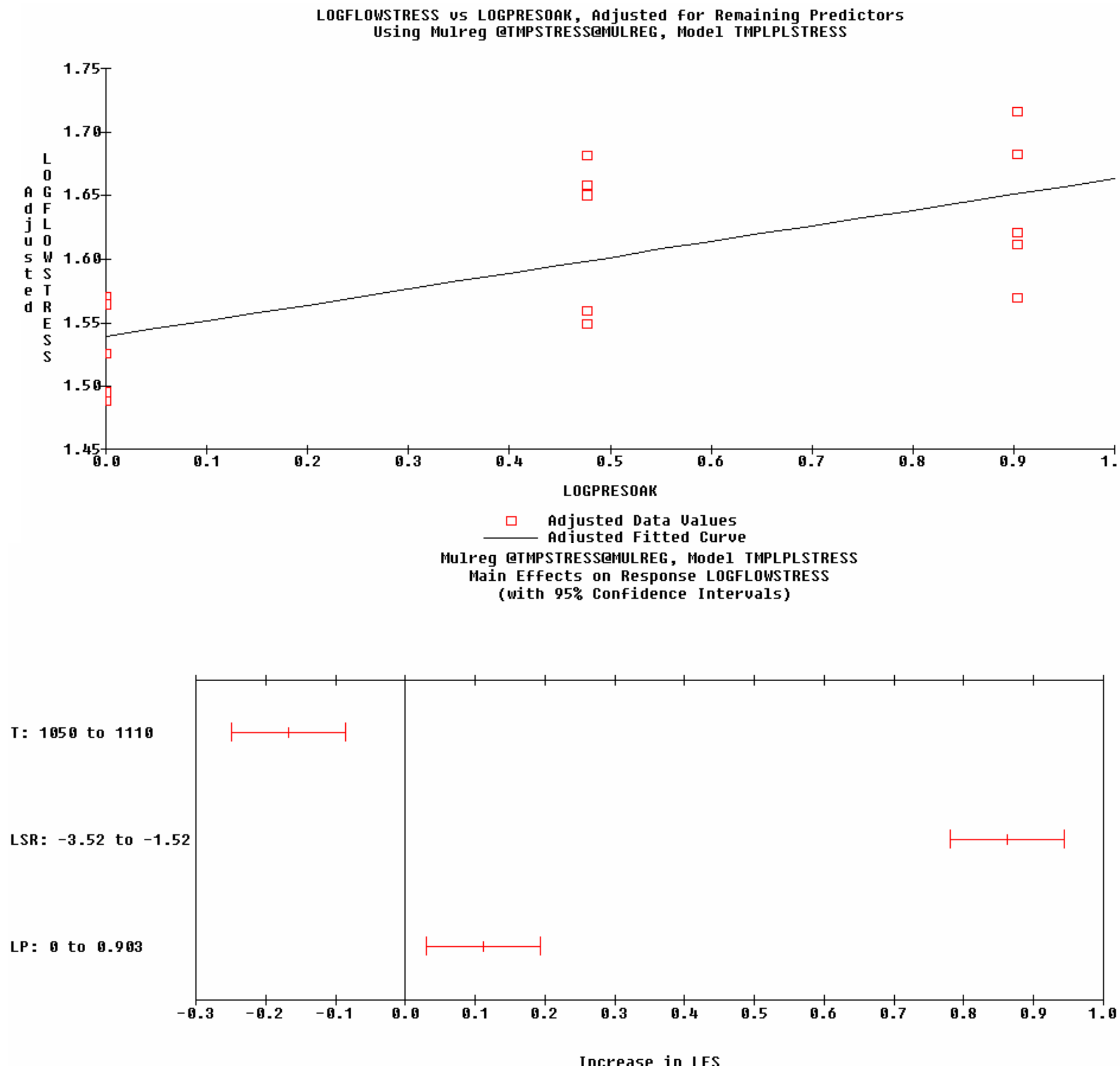

A-1.—Log flow stress regression results.

Predictions and 95% simultaneous confidence intervals
for mean responses of LOGFLOWSTRESS using model TMPLPSTRESS
LP = 0.45771

LSR		T=1050	T=1080	T=1110
	Lower	1.137235	1.077147	0.970555
-3.5229	Predicted	1.248260	1.164920	1.081580
	Upper	1.359285	1.252693	1.192605
	Lower	1.591487	1.540406	1.424807
-2.5229	Predicted	1.679260	1.595920	1.512580
	Upper	1.767033	1.651433	1.600353
	Lower	1.999235	1.939147	1.832555
-1.5229	Predicted	2.110260	2.026920	1.943580
	Upper	2.221285	2.114693	2.054605

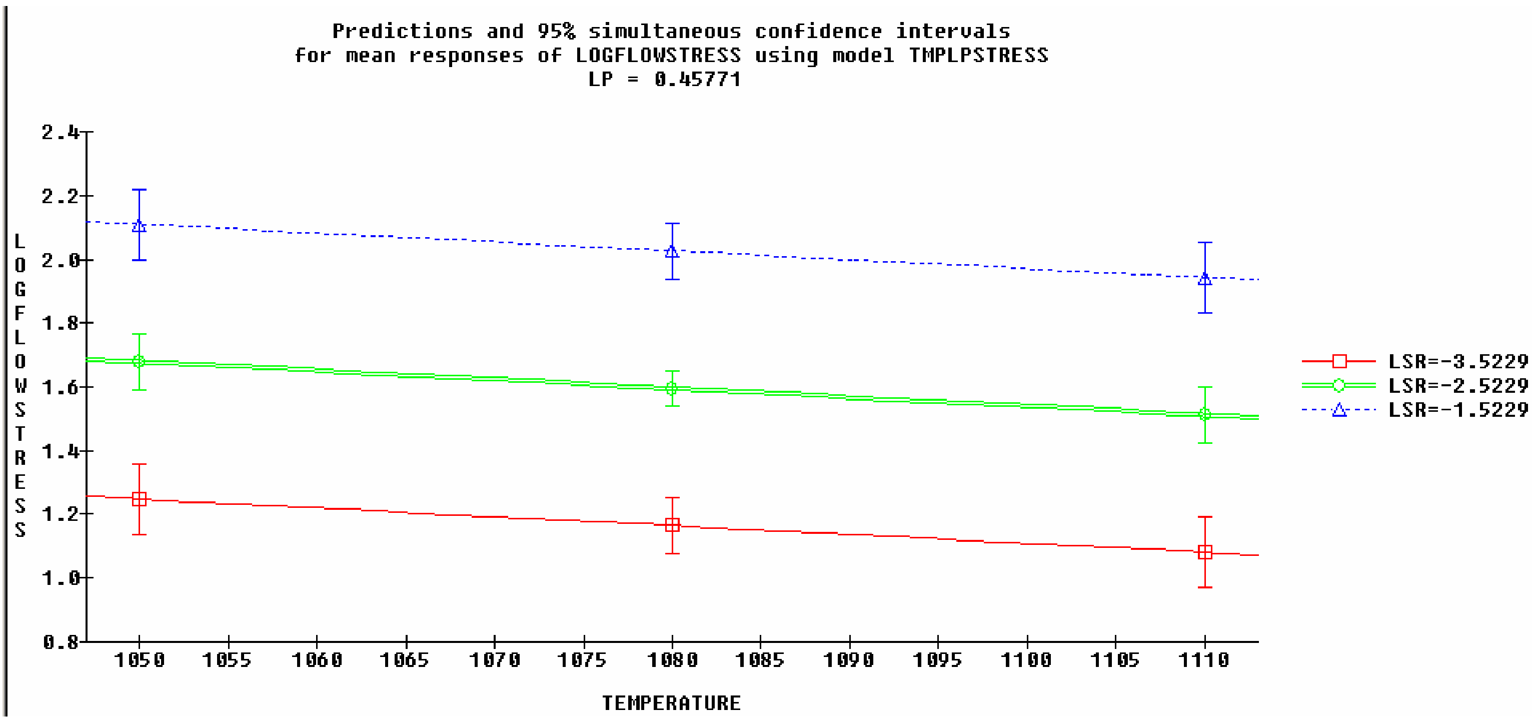

A-1.—Log flow stress regression results.

All Terms

Least Squares Coefficients, Response AFG, Model DESIGN

Term	Coeff.	Std. Error	T-value	Signif.	Transformed Term
1 1	12.099445	0.109987	110.01	0.0001	
2 ~T	-0.390871	0.134681	-2.90	0.0198	((T-1.08e+03)/3e+01)
3 ~LSR	0.180877	0.134681	1.34	0.2161	(LSR+2.5229)
4 ~LP	0.029403	0.134599	0.22	0.8325	((LP-4.5155e-01)/4.5155e
5 ~T*LSR	-0.100000	0.150566	-0.66	0.5253	((T-1.08e+03)/3e+01)*(LS
6 ~T*LP	0.076931	0.150518	0.51	0.6231	((T-1.08e+03)/3e+01)*((L
7 ~LSR*LP	-0.077497	0.150518	-0.51	0.6206	(LSR+2.5229)*((LP-4.5155

No. cases = 15 R-sq. = 0.5831 RMS Error = 0.4259
Resid. df = 8 R-sq-adj. = 0.2704 Cond. No. = 1.023
~ indicates factors are transformed.

FORWARD AND REVERSE STEPWISE SELECTION

Mulreg @TMP@MULREG, Model DESIGN__COPY, Response AFG

Term	df	P-Remove	P-Enter
1 1	1	0.000	
2 T	1	0.020	
3 LSR	1	0.216	
4 LP	1	0.833	
5 T*LSR	1	0.525	
6 T*LP	1	0.623	
7 LSR*LP	1	0.621	

No. cases = 15 R-sq. = 0.5831 RMS Error = 0.4259
Resid. df = 8 R-sq-adj. = 0.2704 Obey Hierarchy: no

Mulreg @TMP@MULREG, Model DESIGN__COPY, Response AFG

Term	df	P-Remove	P-Enter
1 1	1	0.000	
2 T	1	0.007	
3 LSR	1		0.149
4 LP	1		0.821
5 T*LSR	1		0.488
6 T*LP	1		0.595
7 LSR*LP	1		0.605

No. cases = 15 R-sq. = 0.4371 RMS Error = 0.3882
Resid. df = 13 R-sq-adj. = 0.3938 Obey Hierarchy: no

A-2.—As-Forged grain size regression results.

MODEL TMPAFG

Least Squares Coefficients, Response AFG, Model TMPAFG

Term	Coeff.	Std. Error	T-value	Signif.	Transformed Term
1 1	12.100000	0.100231	120.72	0.0001	
2 ~T	-0.390000	0.122757	-3.18	0.0073	((T-1.08e+03)/3e+01)

No. cases = 15 R-sq. = 0.4371 RMS Error = 0.3882
Resid. df = 13 R-sq-adj. = 0.3938 Cond. No. = 1
~ indicates factors are transformed.

ANOVA

Least Squares Summary ANOVA, Response AFG Model TMPAFG

Source	df	Sum Sq.	Mean Sq.	F-Ratio	Signif.
1 Total(Corr.)	14	3.480000			
2 Regression	1	1.521000	1.521000	10.09	0.0073
3 Residual	13	1.959000	0.150692		

R-sq. = 0.4371
R-sq-adj. = 0.3938

Least Squares Components ANOVA, Response AFG Model TMPAFG

Source	df	Sum Sq.	Mean Sq.	F-Ratio	Signif.	Transformed Term
1 Constant	1	2196				
2 ~T	1	1.521000	1.521000	10.09	0.0073	((T-1.08e+03)/3e+01)
3 Residual	13	1.959000	0.150692			

~ indicates factors are transformed. R-sq. = 0.4371
R-sq-adj. = 0.3938
Type 3 sum of squares.

A-2.—As-Forged grain size regression results.

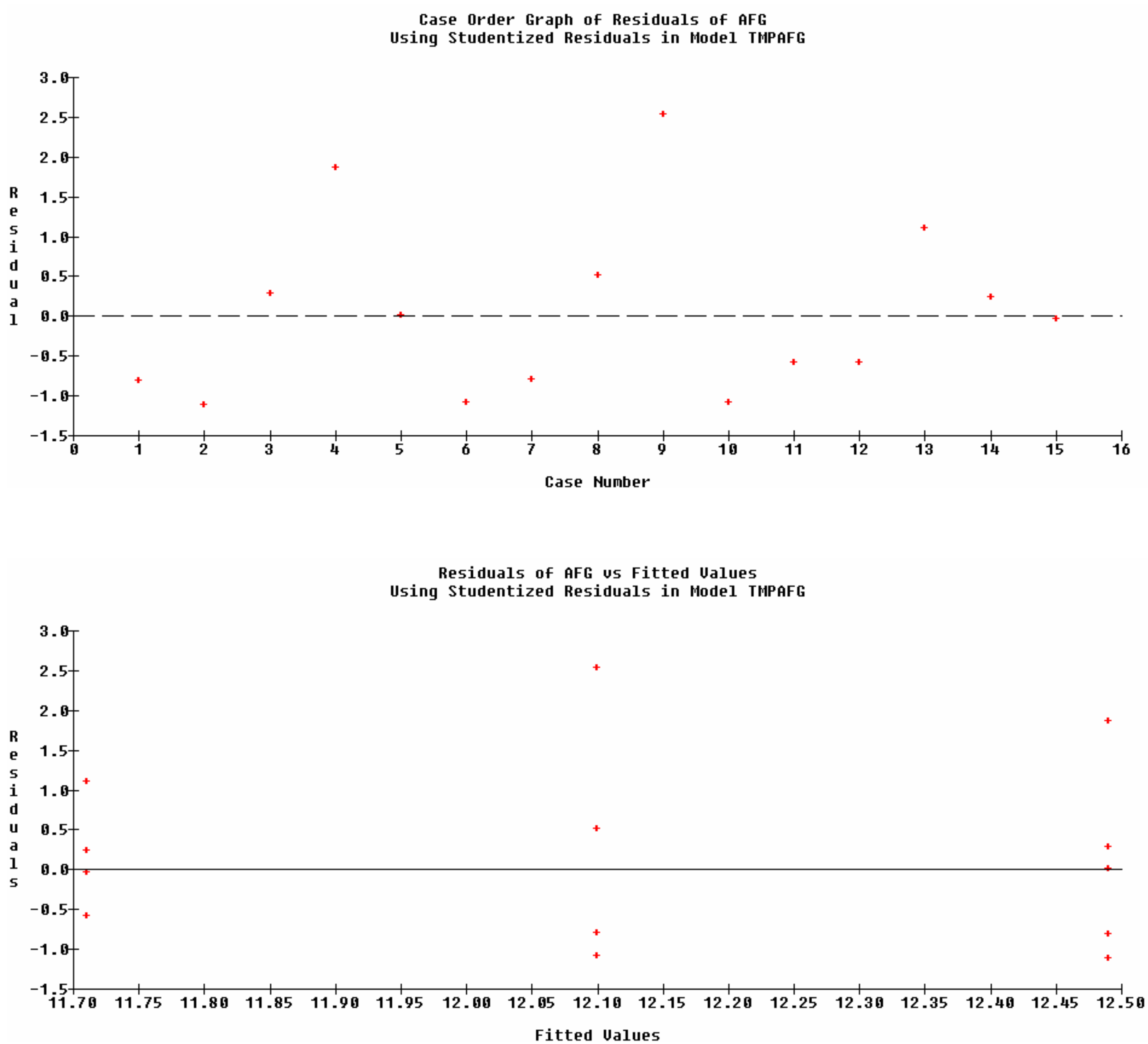

A-2.—As-Forged grain size regression results.

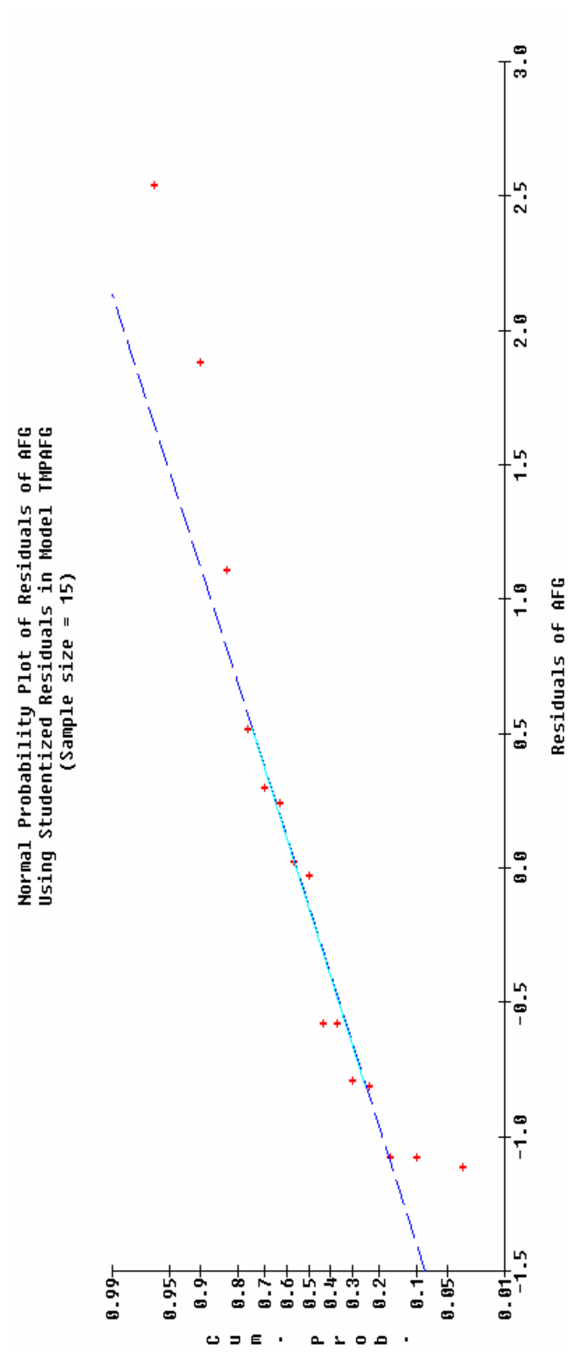

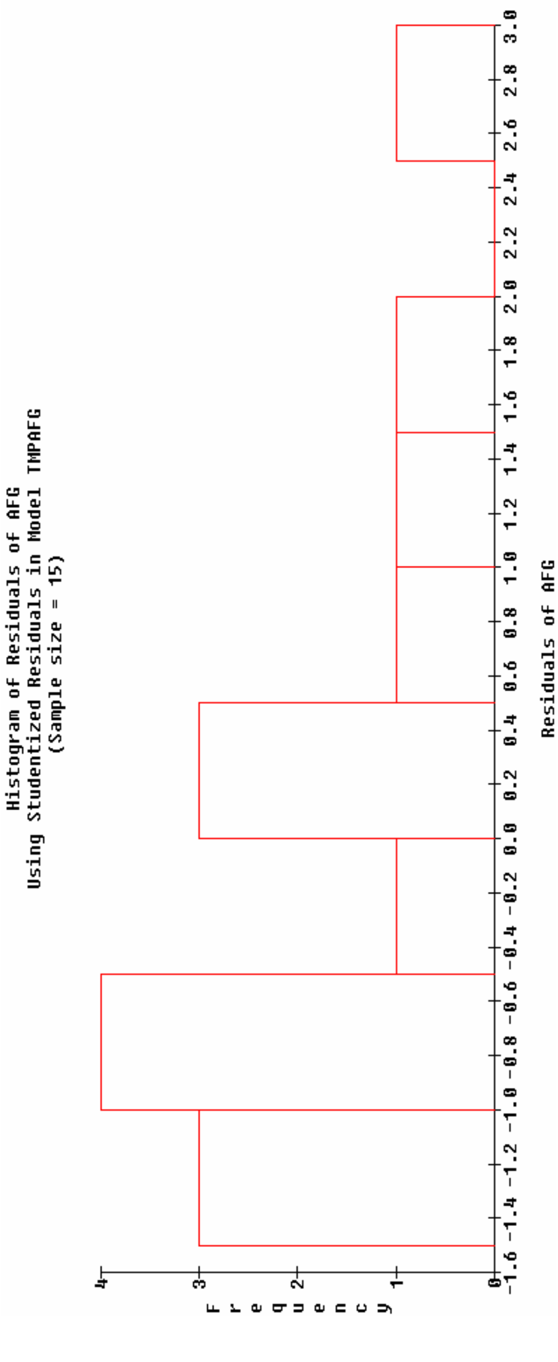

A-2.—As-Forged grain size regression results.

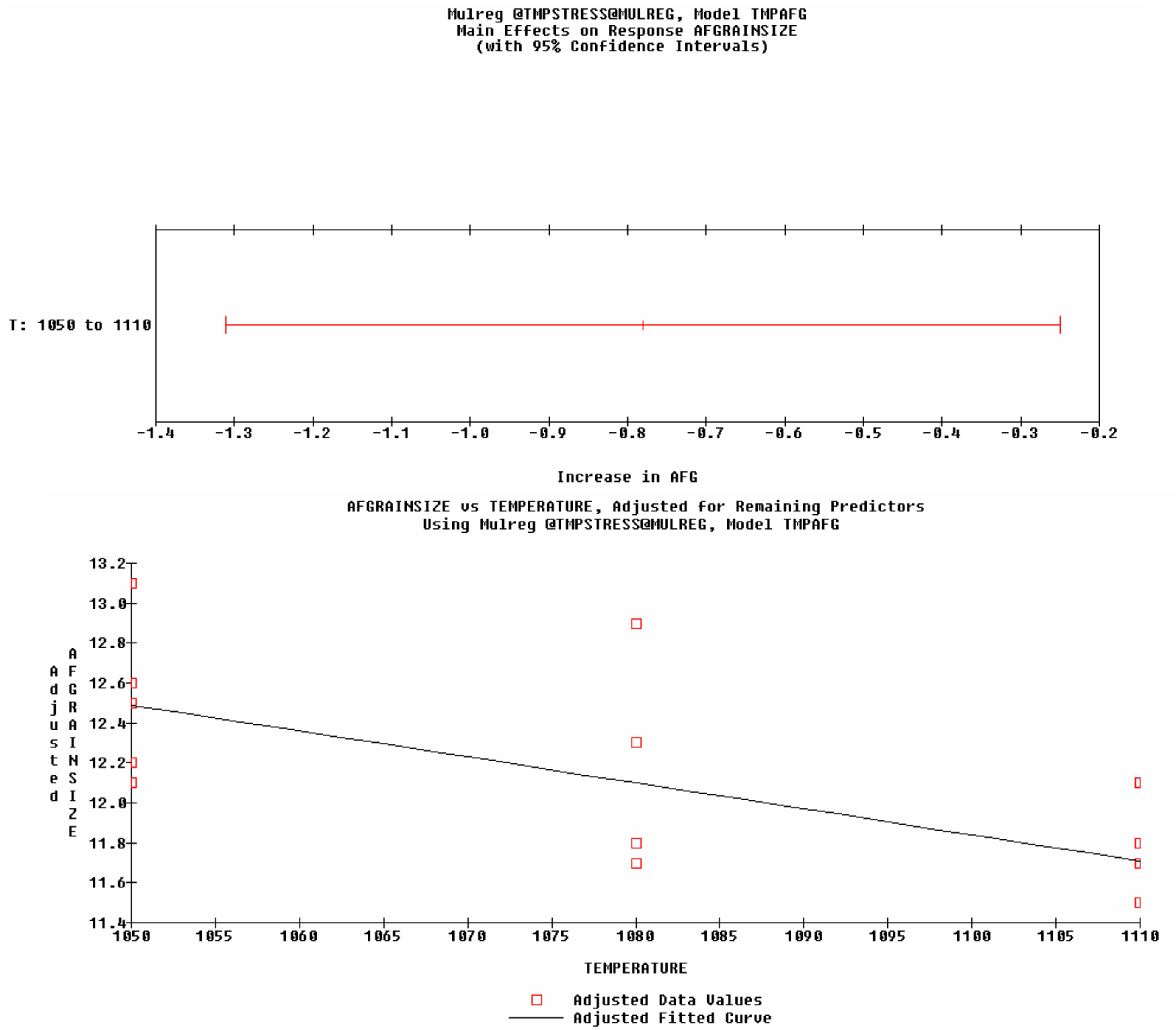

A-2.—As-Forged grain size regression results.

Predictions and 95% simultaneous confidence intervals
for mean responses of ASFORGEGS using model TMPAFG

T:	1050	1080	1110
Lower	12.052786	11.823481	11.272786
Predicted	12.490000	12.100000	11.710000
Upper	12.927214	12.376519	12.147214

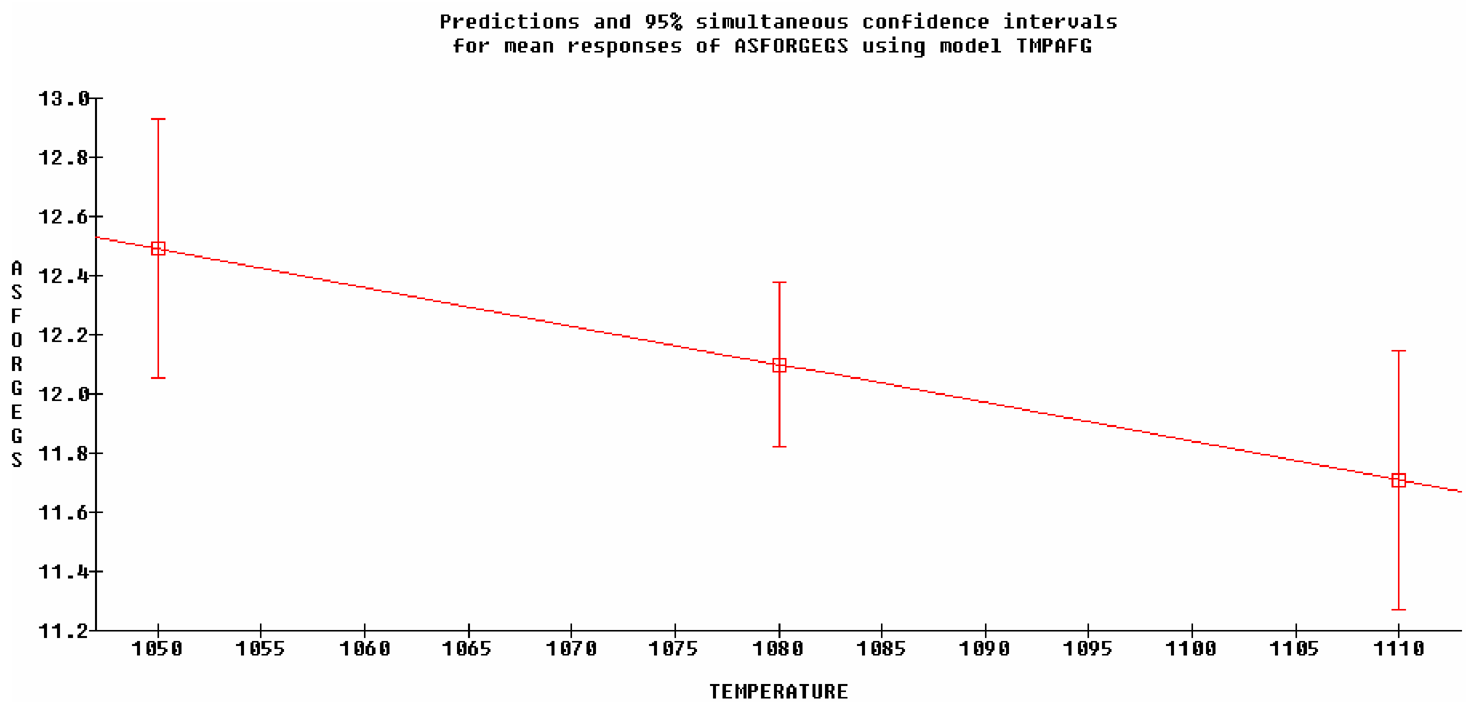

A-2.—As-Forged grain size regression results.

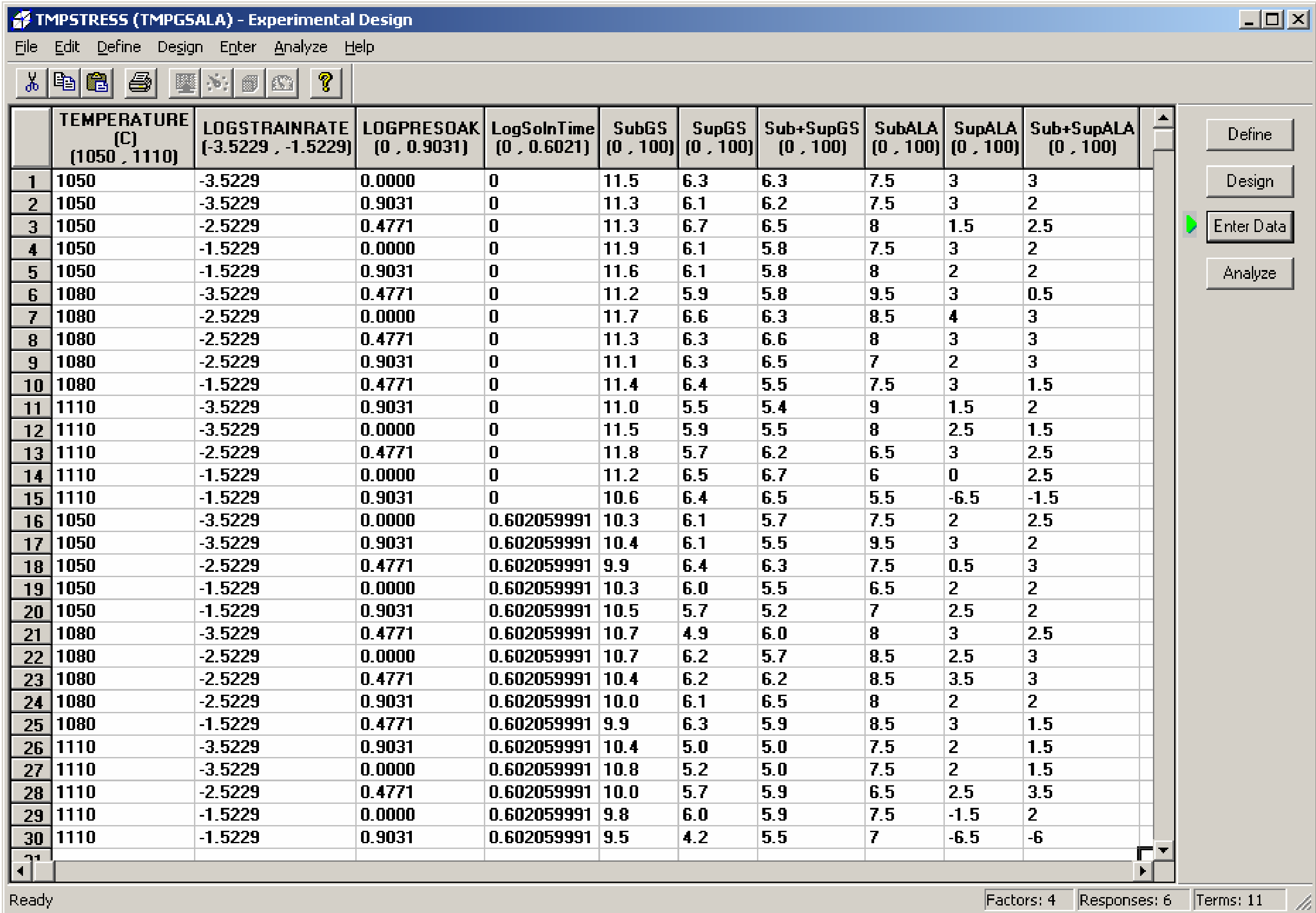

	TEMPERATURE (C) (1050 , 1110)	LOGSTRAINRATE (-3.5229 , -1.5229)	LOGPRESOAK (0 , 0.9031)	LogSolnTime (0 , 0.6021)	SubGS (0 , 100)	SupGS (0 , 100)	Sub+SupGS (0 , 100)	SubALA (0 , 100)	SupALA (0 , 100)	Sub+SupALA (0 , 100)
1	1050	-3.5229	0.0000	0	11.5	6.3	6.3	7.5	3	3
2	1050	-3.5229	0.9031	0	11.3	6.1	6.2	7.5	3	2
3	1050	-2.5229	0.4771	0	11.3	6.7	6.5	8	1.5	2.5
4	1050	-1.5229	0.0000	0	11.9	6.1	5.8	7.5	3	2
5	1050	-1.5229	0.9031	0	11.6	6.1	5.8	8	2	2
6	1080	-3.5229	0.4771	0	11.2	5.9	5.8	9.5	3	0.5
7	1080	-2.5229	0.0000	0	11.7	6.6	6.3	8.5	4	3
8	1080	-2.5229	0.4771	0	11.3	6.3	6.6	8	3	3
9	1080	-2.5229	0.9031	0	11.1	6.3	6.5	7	2	3
10	1080	-1.5229	0.4771	0	11.4	6.4	5.5	7.5	3	1.5
11	1110	-3.5229	0.9031	0	11.0	5.5	5.4	9	1.5	2
12	1110	-3.5229	0.0000	0	11.5	5.9	5.5	8	2.5	1.5
13	1110	-2.5229	0.4771	0	11.8	5.7	6.2	6.5	3	2.5
14	1110	-1.5229	0.0000	0	11.2	6.5	6.7	6	0	2.5
15	1110	-1.5229	0.9031	0	10.6	6.4	6.5	5.5	-6.5	-1.5
16	1050	-3.5229	0.0000	0.602059991	10.3	6.1	5.7	7.5	2	2.5
17	1050	-3.5229	0.9031	0.602059991	10.4	6.1	5.5	9.5	3	2
18	1050	-2.5229	0.4771	0.602059991	9.9	6.4	6.3	7.5	0.5	3
19	1050	-1.5229	0.0000	0.602059991	10.3	6.0	5.5	6.5	2	2
20	1050	-1.5229	0.9031	0.602059991	10.5	5.7	5.2	7	2.5	2
21	1080	-3.5229	0.4771	0.602059991	10.7	4.9	6.0	8	3	2.5
22	1080	-2.5229	0.0000	0.602059991	10.7	6.2	5.7	8.5	2.5	3
23	1080	-2.5229	0.4771	0.602059991	10.4	6.2	6.2	8.5	3.5	3
24	1080	-2.5229	0.9031	0.602059991	10.0	6.1	6.5	8	2	2
25	1080	-1.5229	0.4771	0.602059991	9.9	6.3	5.9	8.5	3	1.5
26	1110	-3.5229	0.9031	0.602059991	10.4	5.0	5.0	7.5	2	1.5
27	1110	-3.5229	0.0000	0.602059991	10.8	5.2	5.0	7.5	2	1.5
28	1110	-2.5229	0.4771	0.602059991	10.0	5.7	5.9	6.5	2.5	3.5
29	1110	-1.5229	0.0000	0.602059991	9.8	6.0	5.9	7.5	-1.5	2
30	1110	-1.5229	0.9031	0.602059991	9.5	4.2	5.5	7	-6.5	-6

A-3.—Subsolvus mean grain size regression results.

All Terms

```
                 Least Squares Coefficients, Response SBG, Model DESIGN

Term          Coeff.        Std. Error    T-value  Signif.  Transformed Term
----------------------------------------------------------------------------------
 1 1             10.803077      0.042981
 2 ~T            -0.118910      0.052631                    ((T-1.08e+03)/3e+01)
 3 ~LSR          -0.120005      0.052631                    (LSR+2.5229)
 4 ~LP           -0.165103      0.052598                    ((LP-4.5155e-01)/4.5155e
 5 ~LST          -0.561047      0.042984                    ((LST-3.0105e-01)/3.0105
 6 ~T*LSR        -0.212500      0.058838    -3.61   0.0019  ((T-1.08e+03)/3e+01)*(LS
 7 ~T*LP         -0.096119      0.058819    -1.63   0.1187  ((T-1.08e+03)/3e+01)*((L
 8 ~T*LST         0.030002      0.052630     0.57   0.5753  ((T-1.08e+03)/3e+01)*((L
 9 ~LSR*LP       -0.000424      0.058819    -0.01   0.9943  (LSR+2.5229)*((LP-4.5155
10 ~LSR*LST      -0.140009      0.052630    -2.66   0.0155  (LSR+2.5229)*((LST-3.010
11 ~LP*LST        0.053532      0.052602     1.02   0.3216  ((LP-4.5155e-01)/4.5155e

No. cases = 30       R-sq. =  0.9185     RMS Error = 0.2354
Resid. df = 19   R-sq-adj. =  0.8757      Cond. No. = 1.023
~ indicates factors are transformed.
```

FORWARD AND REVERSE STEPWISE SELECTION

```
Mulreg @TMPSTRESS@MULREG, Model DESIGN__COPY, Response SBG

Term         df  P-Remove  P-Enter
 1 1          1     0.000
 2 T          1     0.036
 3 LSR        1     0.034
 4 LP         1     0.005
 5 LST        1     0.000
 6 T*LSR      1     0.002
 7 T*LP       1     0.119
 8 T*LST      1     0.575
 9 LSR*LP     1     0.994
10 LSR*LST    1     0.015
11 LP*LST     1     0.322

No. cases = 30       R-sq. =  0.9185     RMS Error = 0.2354
Resid. df = 19   R-sq-adj. =  0.8757     Obey Hierarchy: no
```

```
Mulreg @TMPSTRESS@MULREG, Model DESIGN__COPY, Response SBG

Term         df  P-Remove  P-Enter
 1 1          1     0.000
 2 T          1     0.032
 3 LSR        1     0.032
 4 LP         1     0.005
 5 LST        1     0.000
 6 T*LSR      1     0.001
 7 T*LP       1               0.104
 8 T*LST      1               0.580
 9 LSR*LP     1               0.994
10 LSR*LST    1     0.014
11 LP*LST     1               0.320

No. cases = 30       R-sq. =  0.9013     RMS Error = 0.2355
Resid. df = 23   R-sq-adj. =  0.8755     Obey Hierarchy: no
```

A-3.—Subsolvus mean grain size regression results.

MODEL TMPSUBGS

Least Squares Coefficients, Response SBG, Model TMPSUBGS

Term	Coeff.	Std. Error	T-value	Signif.	Transformed Term
1 1	10.803077	0.043010	251.18	0.0001	
2 ~T	-0.120000	0.052662	-2.28	0.0323	((T-1.08e+03)/3e+01)
3 ~LSR	-0.120009	0.052662	-2.28	0.0323	(LSR+2.5229)
4 ~LP	-0.165107	0.052634	-3.14	0.0046	((LP-4.5155e-01)/4.5155e
5 ~LST	-0.560037	0.043001	-13.02	0.0001	((LST-3.0105e-01)/3.0105
6 ~T*LSR	-0.212500	0.058878	-3.61	0.0015	((T-1.08e+03)/3e+01)*(LS
7 ~LSR*LST	-0.140009	0.052666	-2.66	0.0140	(LSR+2.5229)*((LST-3.010

No. cases = 30 R-sq. = 0.9013 RMS Error = 0.2355
Resid. df = 23 R-sq-adj. = 0.8755 Cond. No. = 1.023
~ indicates factors are transformed.

ANOVA

Least Squares Summary ANOVA, Response SBG Model TMPSUBGS

Source	df	Sum Sq.	Mean Sq.	F-Ratio	Signif.
1 Total(Corr.)	29	12.92000			
2 Regression	6	11.64429	1.94071	34.99	0.0000
3 Linear	4	10.52983	2.63246	47.46	0.0000
4 Non-linear	2	1.11450	0.55725	10.05	0.0007
5 Residual	23	1.27571	0.05547		

R-sq. = 0.9013
R-sq-adj. = 0.8755

Least Squares Components ANOVA, Response SBG Model TMPSUBGS

Source	df	Sum Sq.	Mean Sq.	F-Ratio	Signif.	Transformed Term
1 Constant	1	3499				
2 ~T	1	0.28800	0.28800	5.19	0.0323	((T-1.08e+03)/3e+01)
3 ~LSR	1	0.28804	0.28804	5.19	0.0323	(LSR+2.5229)
4 ~LP	1	0.54579	0.54579	9.84	0.0046	((LP-4.5155e-01)/4.5155e
5 ~LST	1	9.40800	9.40800	169.60	0.0000	((LST-3.0105e-01)/3.0105
6 ~T*LSR	1	0.72250	0.72250	13.03	0.0015	((T-1.08e+03)/3e+01)*(LS
7 ~LSR*LST	1	0.39200	0.39200	7.07	0.0140	(LSR+2.5229)*((LST-3.010
8 Residual	23	1.27571	0.05547			

~ indicates factors R-sq. = 0.9013
are transformed. R-sq-adj. = 0.8755
Type 3 sum of squares.

A-3.—Subsolvus mean grain size regression results.

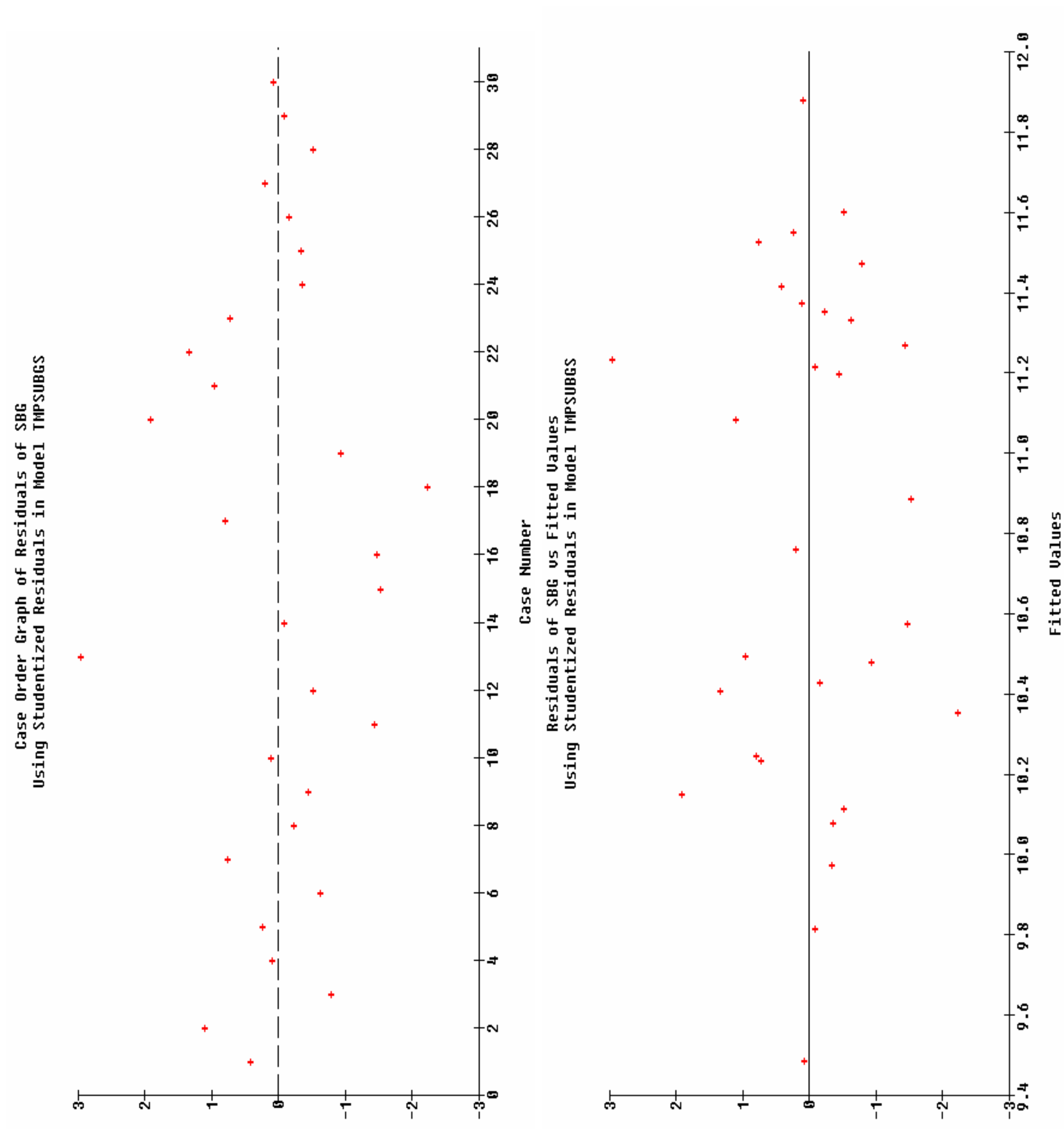

A-3.—Subsolvus mean grain size regression results.

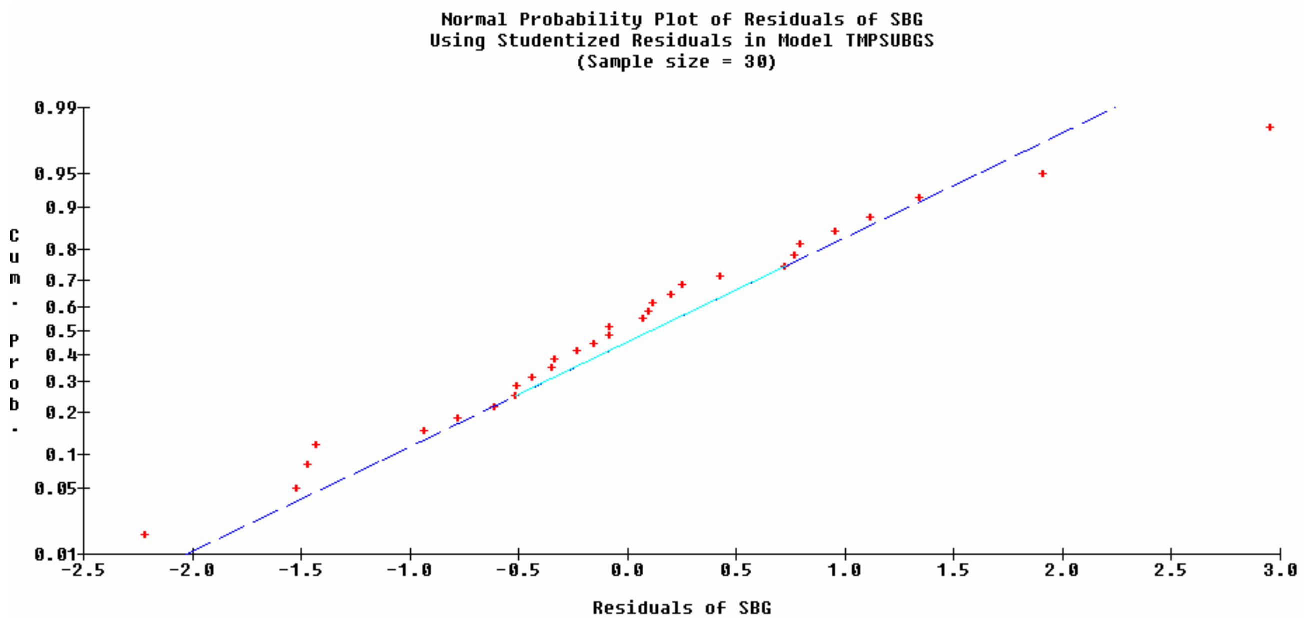

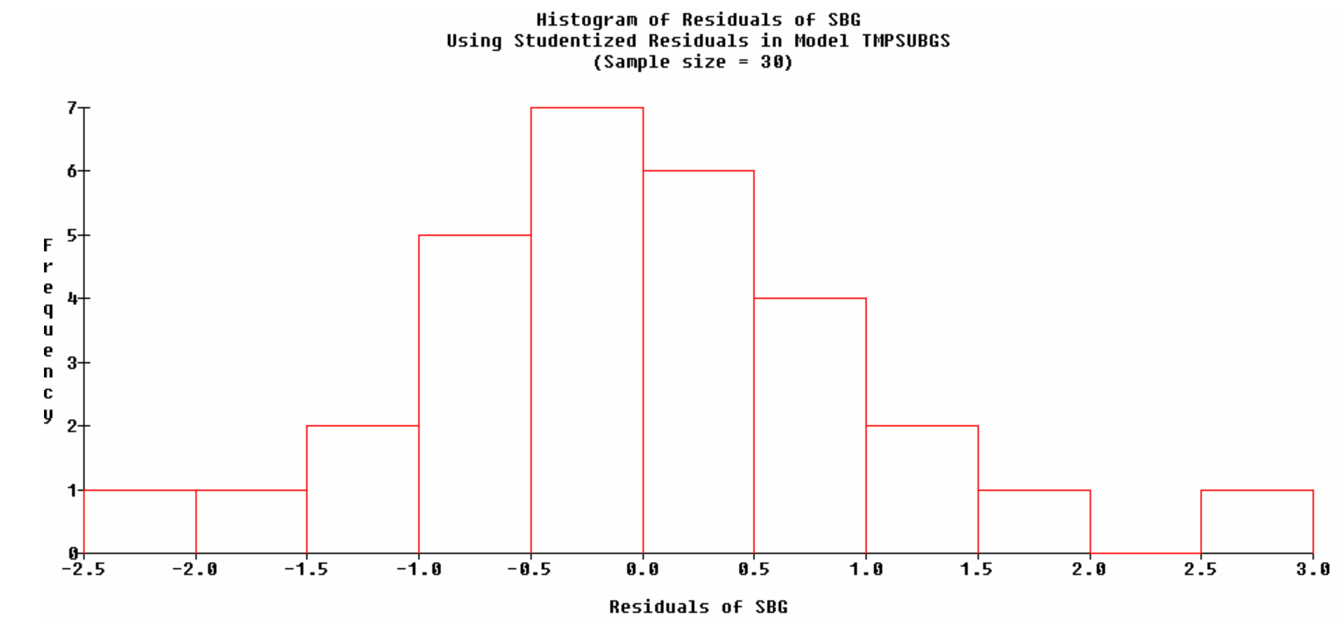

A-3.—Subsolvus mean grain size regression results.

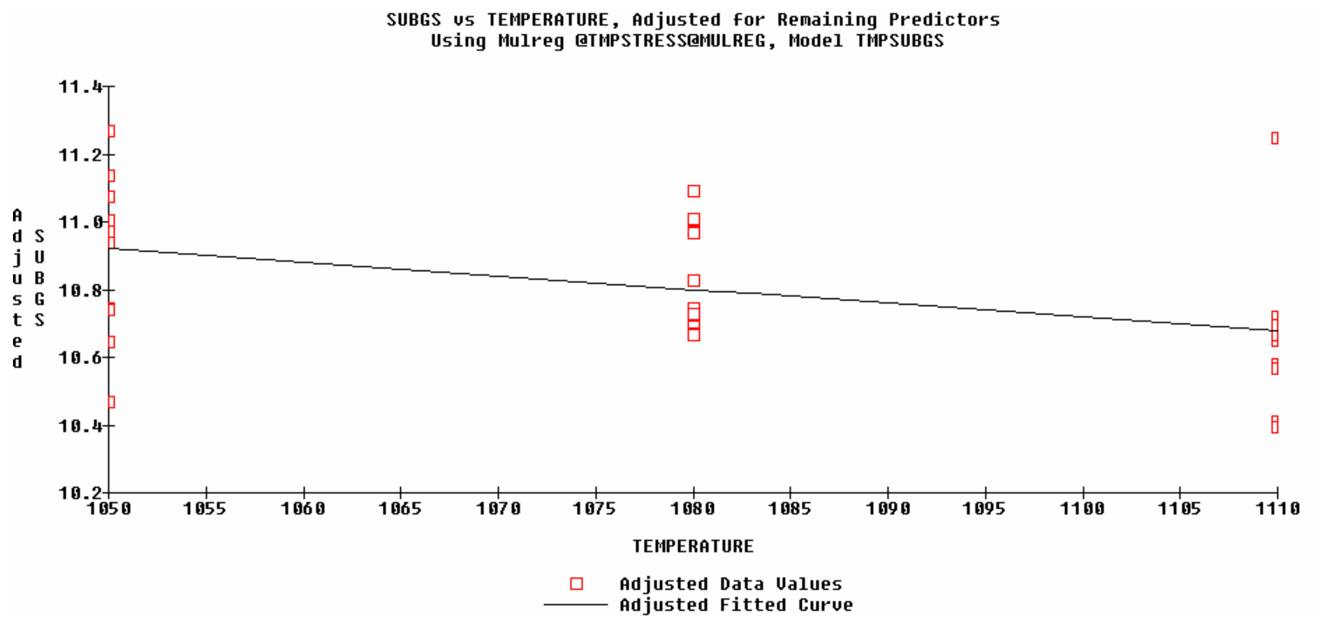

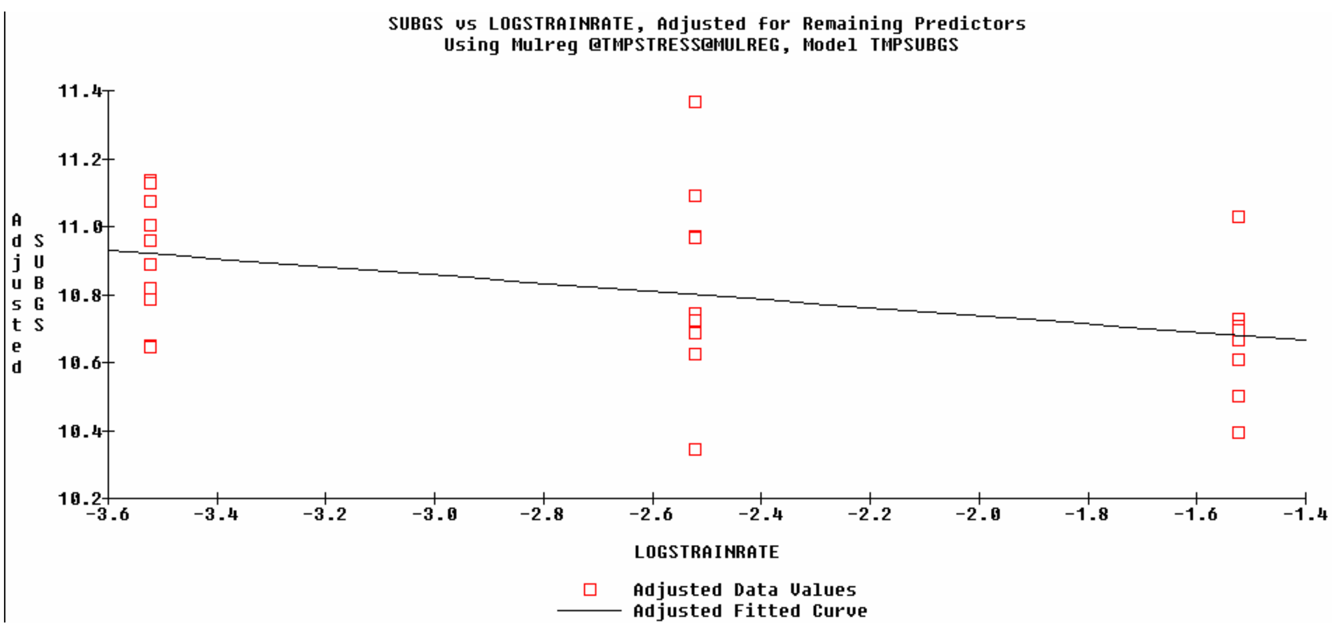

A-3.—Subsolvus mean grain size regression results.

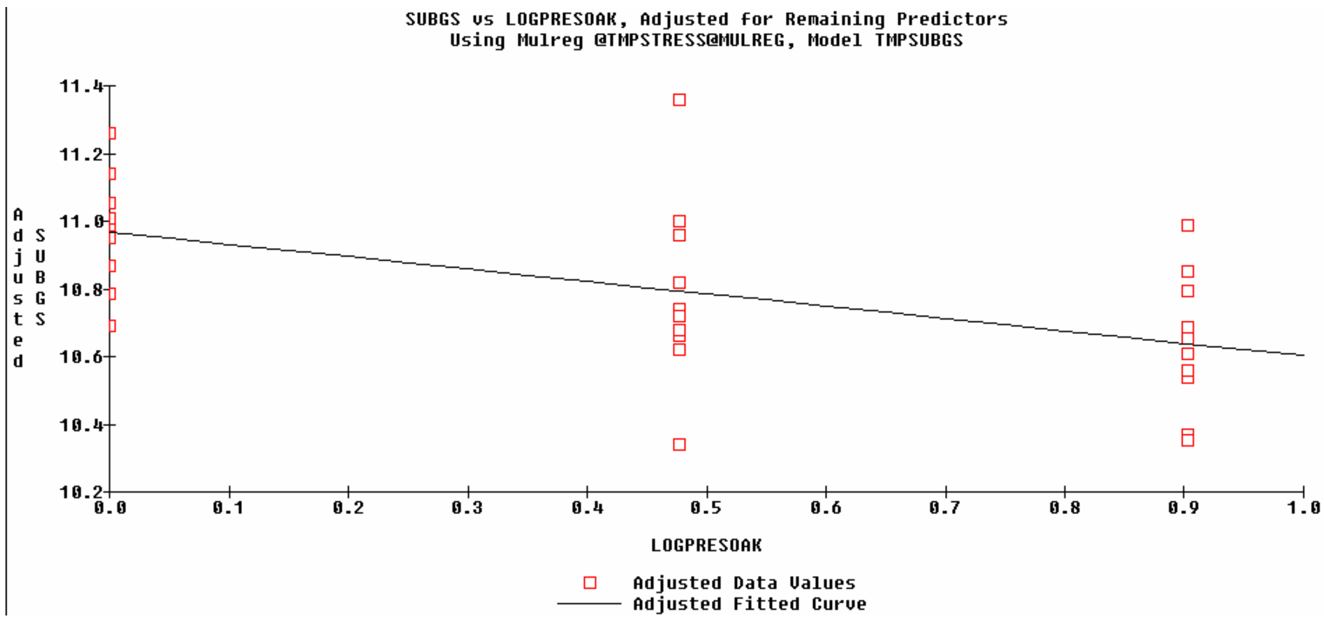

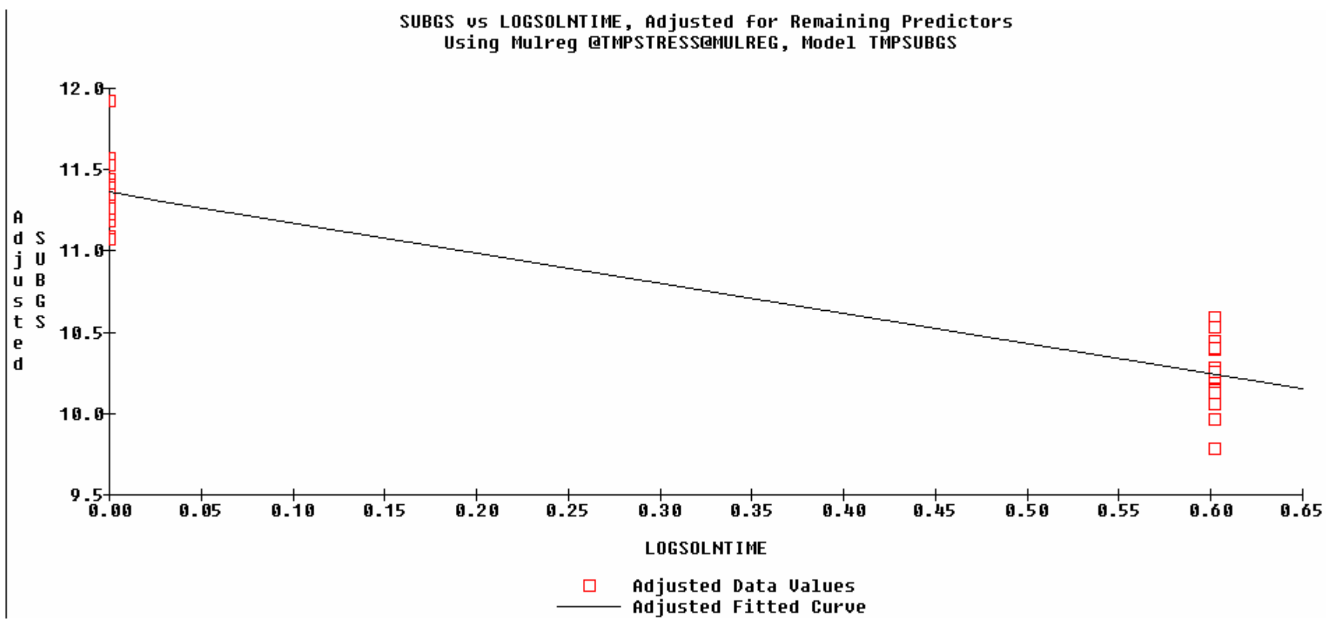

A-3.—Subsolvus mean grain size regression results.

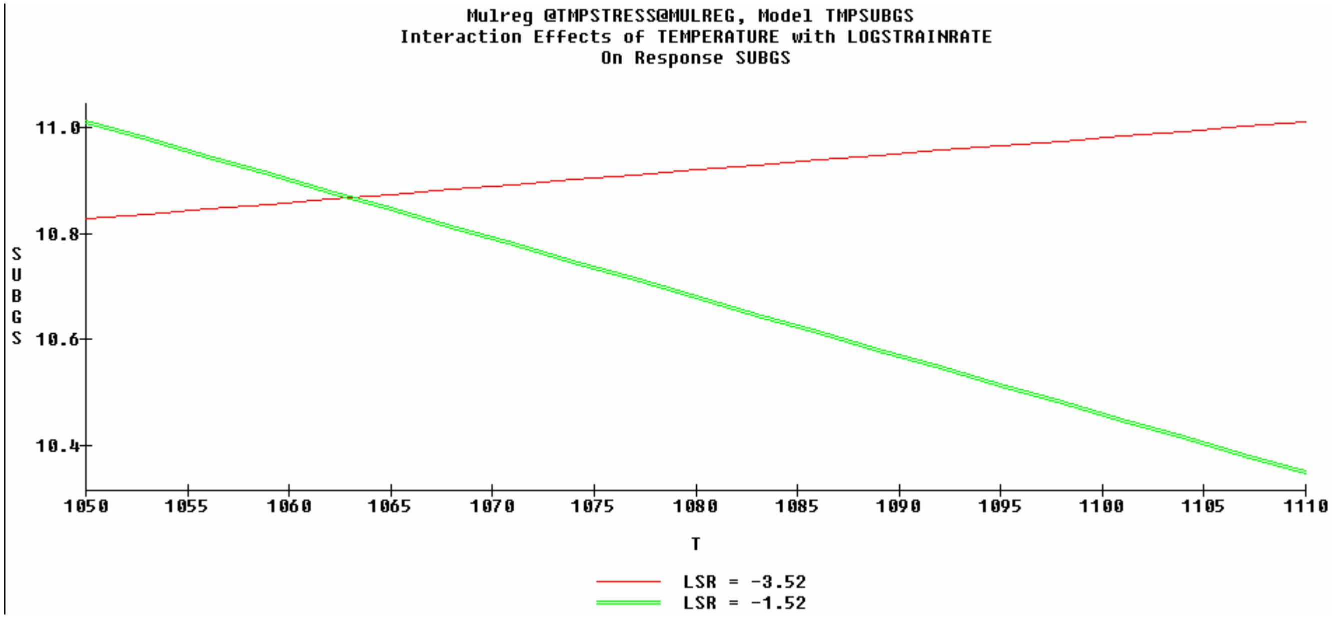

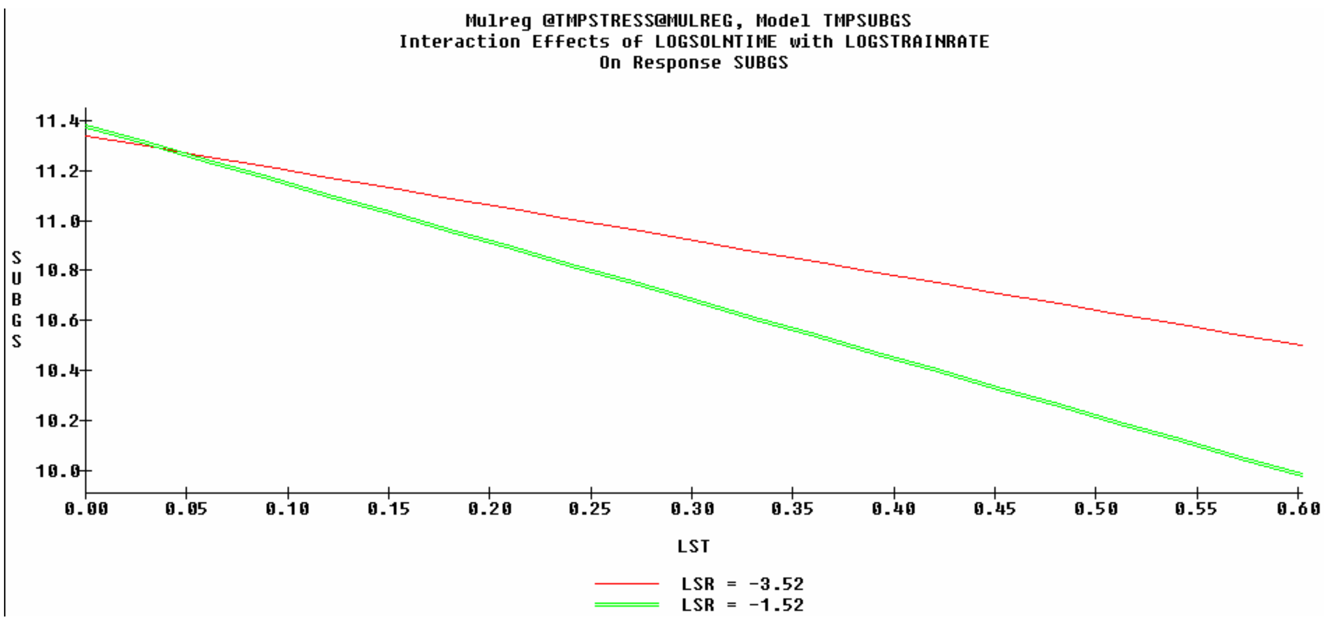

A-3.—Subsolvus mean grain size regression results.

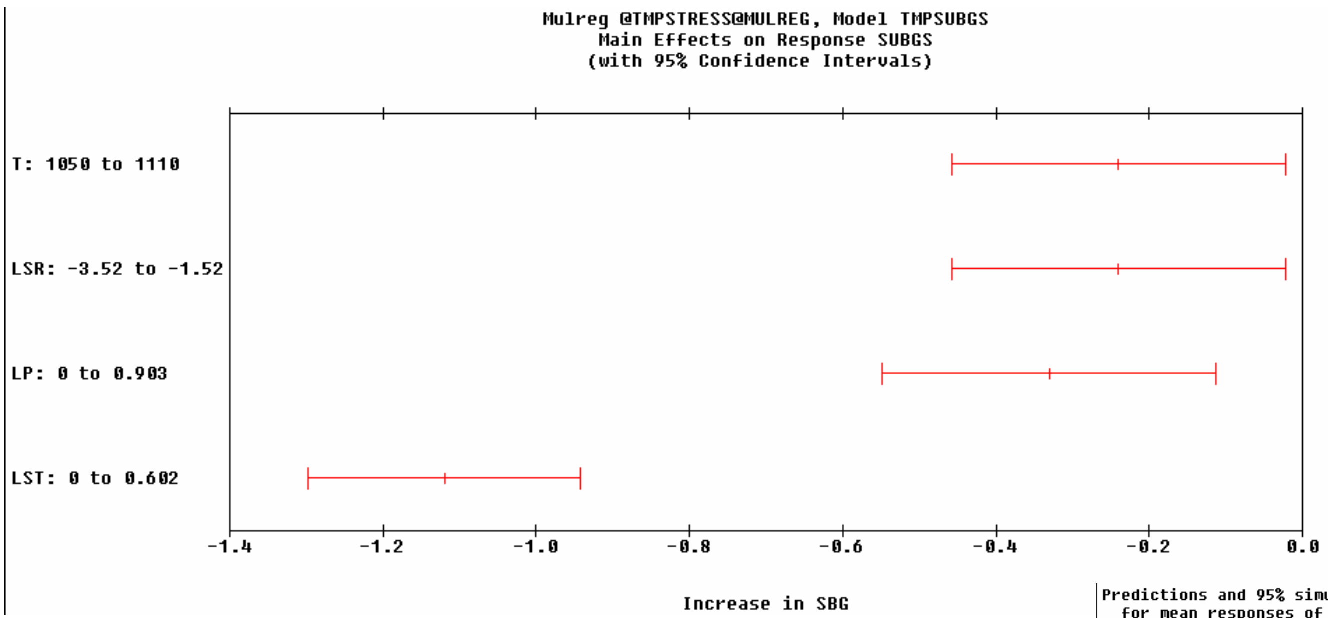

Predictions and 95% simultaneous confidence intervals
for mean responses of SUBGS using model TMPSUBGS
LP = 0.45771, LST = 0.30103

LSR		T=1050	T=1080	T=1110
	Lower	10.397439	10.639757	10.582439
-3.5229	Predicted	10.828362	10.920862	11.013362
	Upper	11.259284	11.201966	11.444284
	Lower	10.639757	10.623074	10.399757
-2.5229	Predicted	10.920862	10.800862	10.680862
	Upper	11.201966	10.978650	10.961966
	Lower	10.582439	10.399757	9.917439
-1.5229	Predicted	11.013362	10.680862	10.348362
	Upper	11.444284	10.961966	10.779284

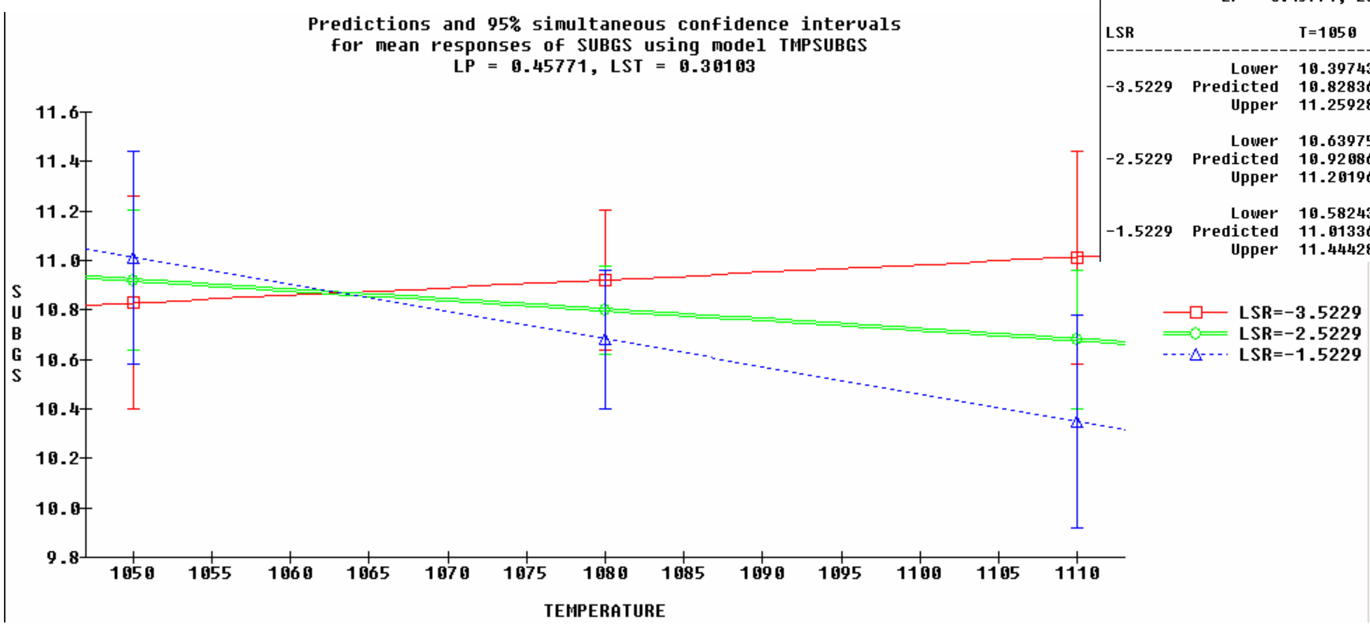

A-3.—Subsolvus mean grain size regression results.

All Terms

Least Squares Coefficients, Response SBA, Model DESIGN

Term	Coeff.	Std. Error	T-value	Signif.	Transformed Term
1 1	7.648955	0.163854	46.68	0.0001	
2 ~T	-0.272819	0.200642	-1.36	0.1898	((T-1.08e+03)/3e+01)
3 ~LSR	-0.522892	0.200642	-2.61	0.0174	(LSR+2.5229)
4 ~LP	0.055605	0.200519	0.28	0.7845	((LP-4.5155e-01)/4.5155e
5 ~LST	0.048172	0.163865	0.29	0.7720	((LST-3.0105e-01)/3.0105
6 ~T*LSR	-0.187500	0.224306	-0.84	0.4136	((T-1.08e+03)/3e+01)*(LS
7 ~T*LP	-0.192328	0.224235	-0.86	0.4017	((T-1.08e+03)/3e+01)*((L
8 ~T*LST	0.075005	0.200639	0.37	0.7127	((T-1.08e+03)/3e+01)*((L
9 ~LSR*LP	-0.185260	0.224235	-0.83	0.4190	(LSR+2.5229)*((LP-4.5155
10 ~LSR*LST	0.175012	0.200639	0.87	0.3940	(LSR+2.5229)*((LST-3.010
11 ~LP*LST	0.097074	0.200532	0.48	0.6339	((LP-4.5155e-01)/4.5155e

No. cases = 30 R-sq. = 0.3900 RMS Error = 0.8972
Resid. df = 19 R-sq-adj. = 0.0690 Cond. No. = 1.023
~ indicates factors are transformed.

FORWARD AND REVERSE STEPWISE SELECTION

Mulreg @TMPSTRESS@MULREG, Model DESIGN__COPY, Response SBA

Term	df	P-Remove	P-Enter
1 1	1	0.000	
2 T	1	0.190	
3 LSR	1	0.017	
4 LP	1	0.785	
5 LST	1	0.772	
6 T*LSR	1	0.414	
7 T*LP	1	0.402	
8 T*LST	1	0.713	
9 LSR*LP	1	0.419	
10 LSR*LST	1	0.394	
11 LP*LST	1	0.634	

No. cases = 30 R-sq. = 0.3900 RMS Error = 0.8972
Resid. df = 19 R-sq-adj. = 0.0690 Obey Hierarchy: no

Mulreg @TMPSTRESS@MULREG, Model DESIGN__COPY, Response SBA

Term	df	P-Remove	P-Enter
1 1	1	0.000	
2 T	1		0.144
3 LSR	1	0.009	
4 LP	1		0.772
5 LST	1		0.750
6 T*LSR	1		0.379
7 T*LP	1		0.357
8 T*LST	1		0.696
9 LSR*LP	1		0.385
10 LSR*LST	1		0.359
11 LP*LST	1		0.607

No. cases = 30 R-sq. = 0.2198 RMS Error = 0.8359
Resid. df = 28 R-sq-adj. = 0.1920 Obey Hierarchy: no

A-4.—Subsolvus as-large-as grain size regression results.

MODEL TMPSUBALA

Least Squares Coefficients, Response SBA, Model TMPSUBALA

Term	Coeff.	Std. Error	T-value	Signif.	Transformed Term
1 1	7.650000	0.152606	50.13	0.0001	
2 ~LSR	-0.525000	0.186904	-2.81	0.0090	(LSR+2.5229)

No. cases = 30 R-sq. = 0.2198 RMS Error = 0.8359
Resid. df = 28 R-sq-adj. = 0.1920 Cond. No. = 1
~ indicates factors are transformed.

ANOVA

Least Squares Summary ANOVA, Response SBA Model TMPSUBALA

Source	df	Sum Sq.	Mean Sq.	F-Ratio	Signif.
1 Total(Corr.)	29	25.07500			
2 Regression	1	5.51250	5.51250	7.89	0.0090
3 Residual	28	19.56250	0.69866		

R-sq. = 0.2198
R-sq-adj. = 0.1920

Least Squares Components ANOVA, Response SBA Model TMPSUBALA

Source	df	Sum Sq.	Mean Sq.	F-Ratio	Signif.	Transformed Term
1 Constant	1	1756				
2 ~LSR	1	5.51250	5.51250	7.89	0.0090	(LSR+2.5229)
3 Residual	28	19.56250	0.69866			

~ indicates factors R-sq. = 0.2198
are transformed. R-sq-adj. = 0.1920
Type 3 sum of squares.

A-4.—Subsolvus as-large-as grain size regression results.

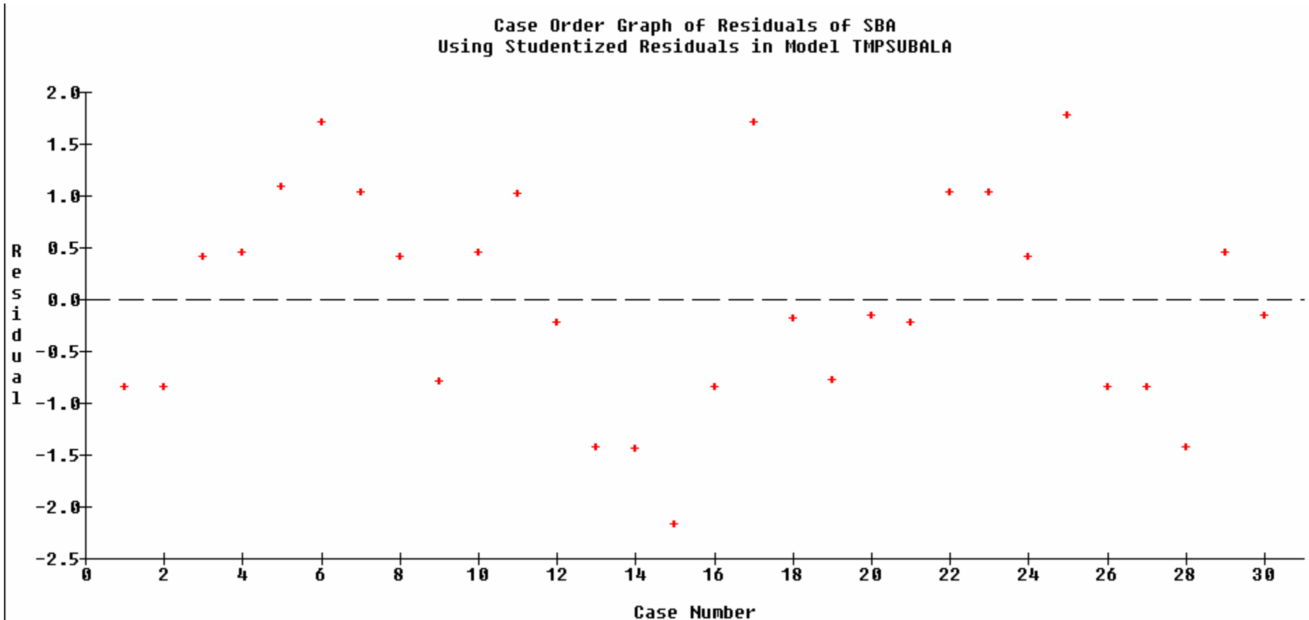

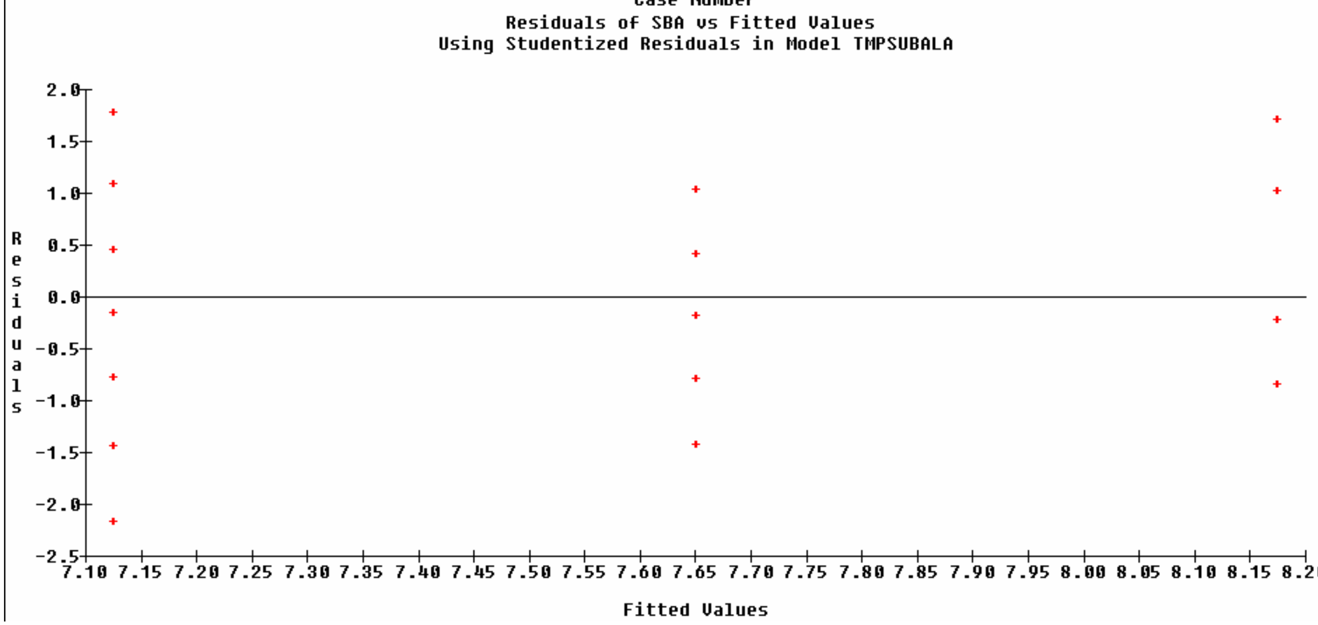

A-4.—Subsolvus as-large-as grain size regression results.

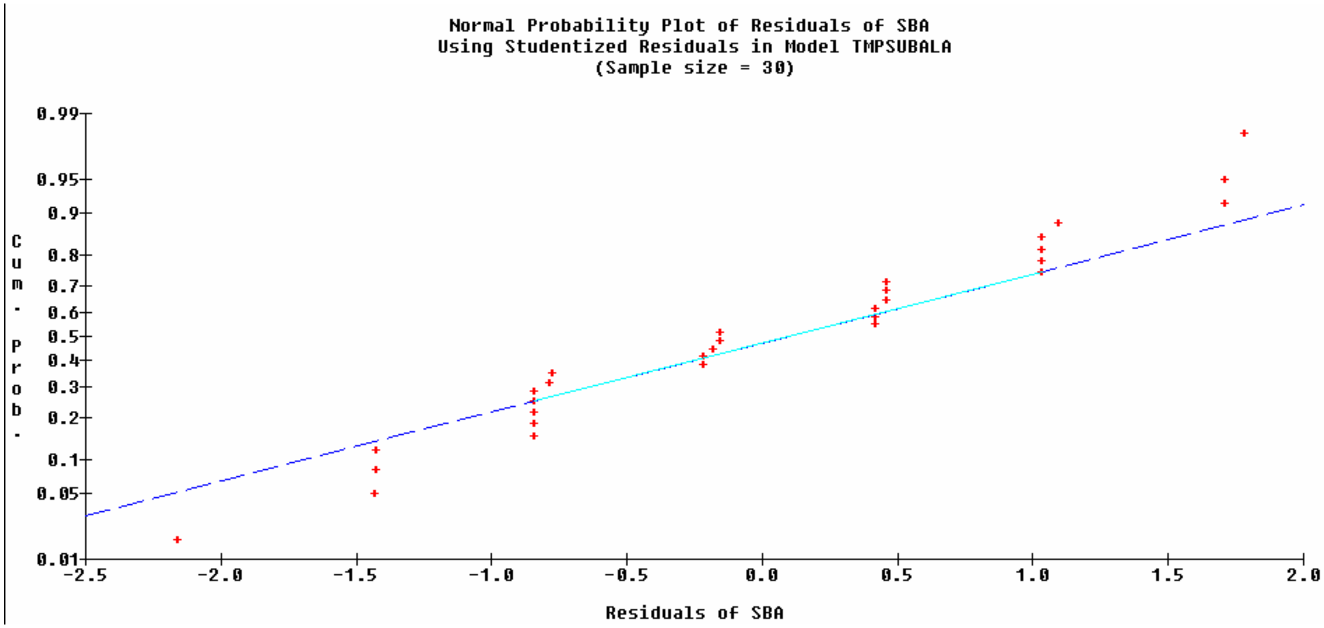

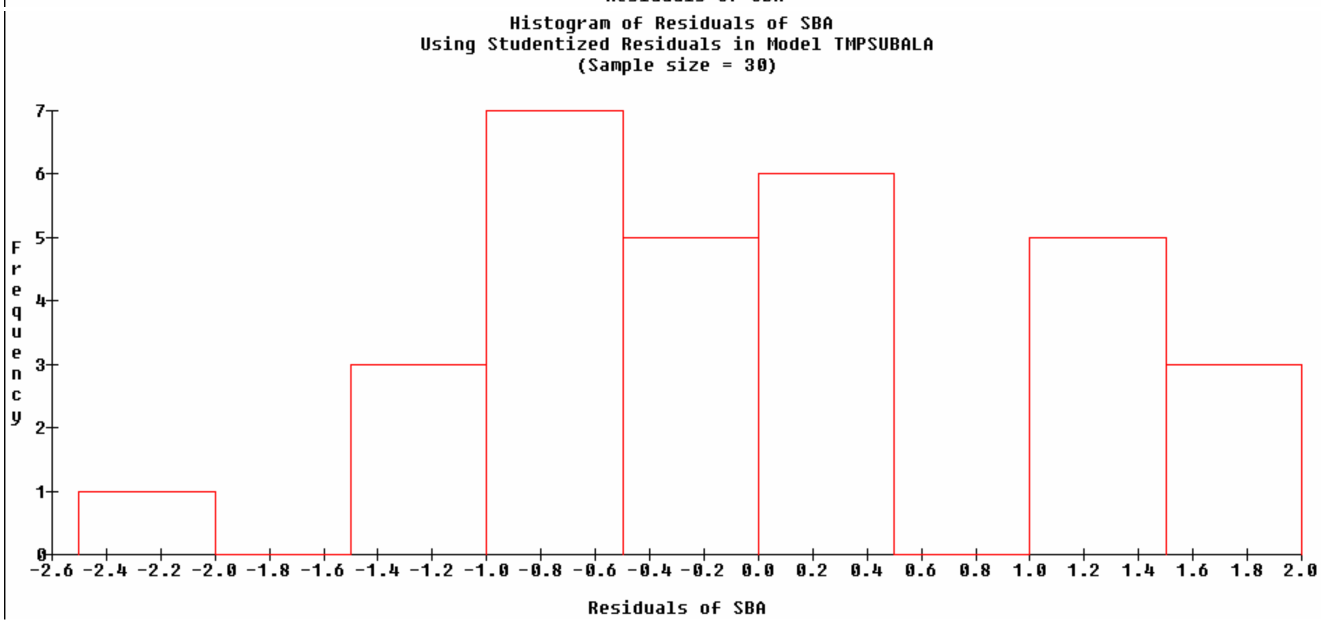

A-4.—Subsolvus as-large-as grain size regression results.

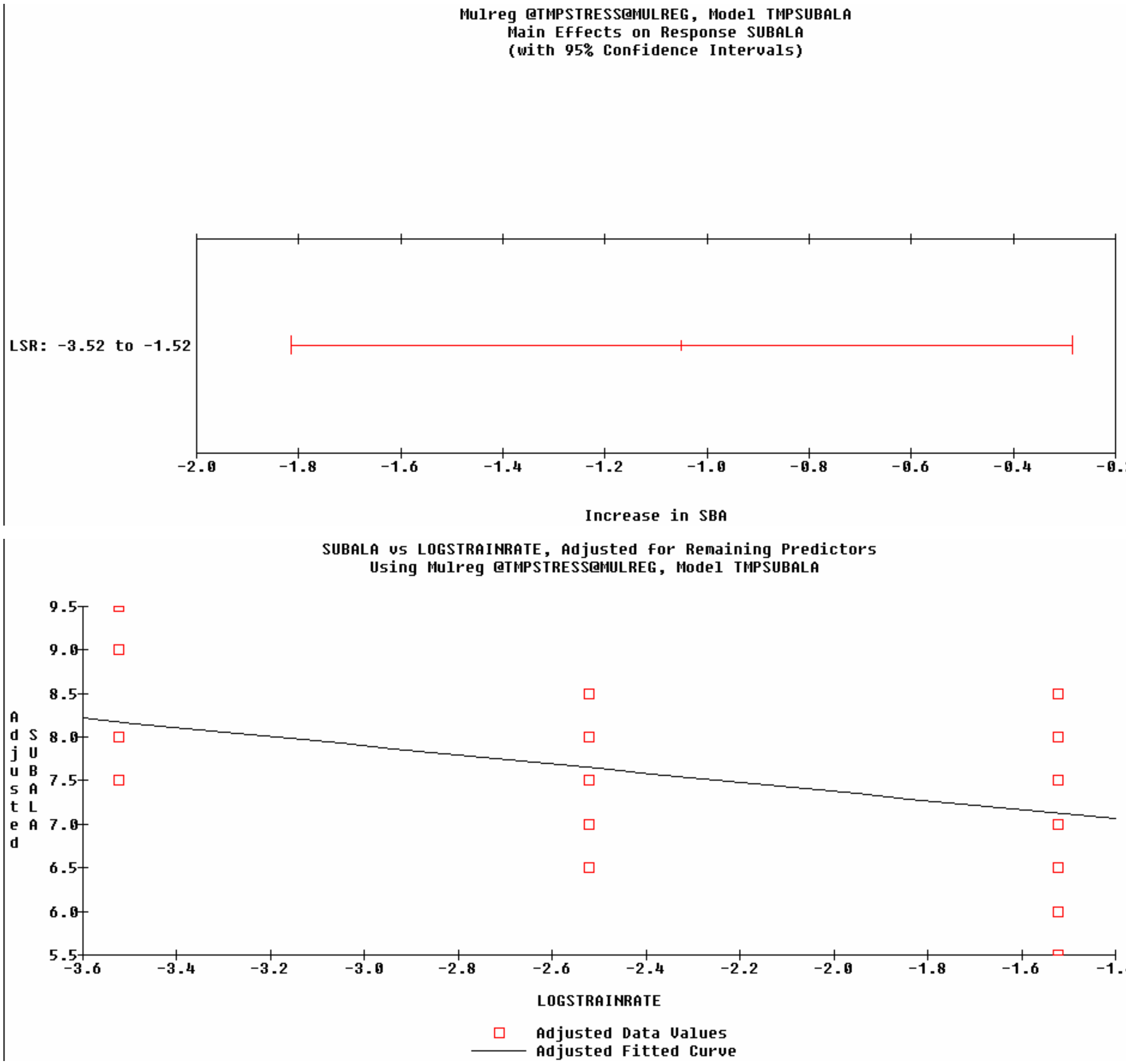

A-4.—Subsolvus as-large-as grain size regression results.

Predictions and 95% simultaneous confidence intervals
for mean responses of SUBALA using model TMPSUBALA

LSR:	-3.5229	-2.5229	-1.5229
Lower	7.551329	7.255556	6.501329
Predicted	8.175000	7.650000	7.125000
Upper	8.798671	8.044444	7.748671

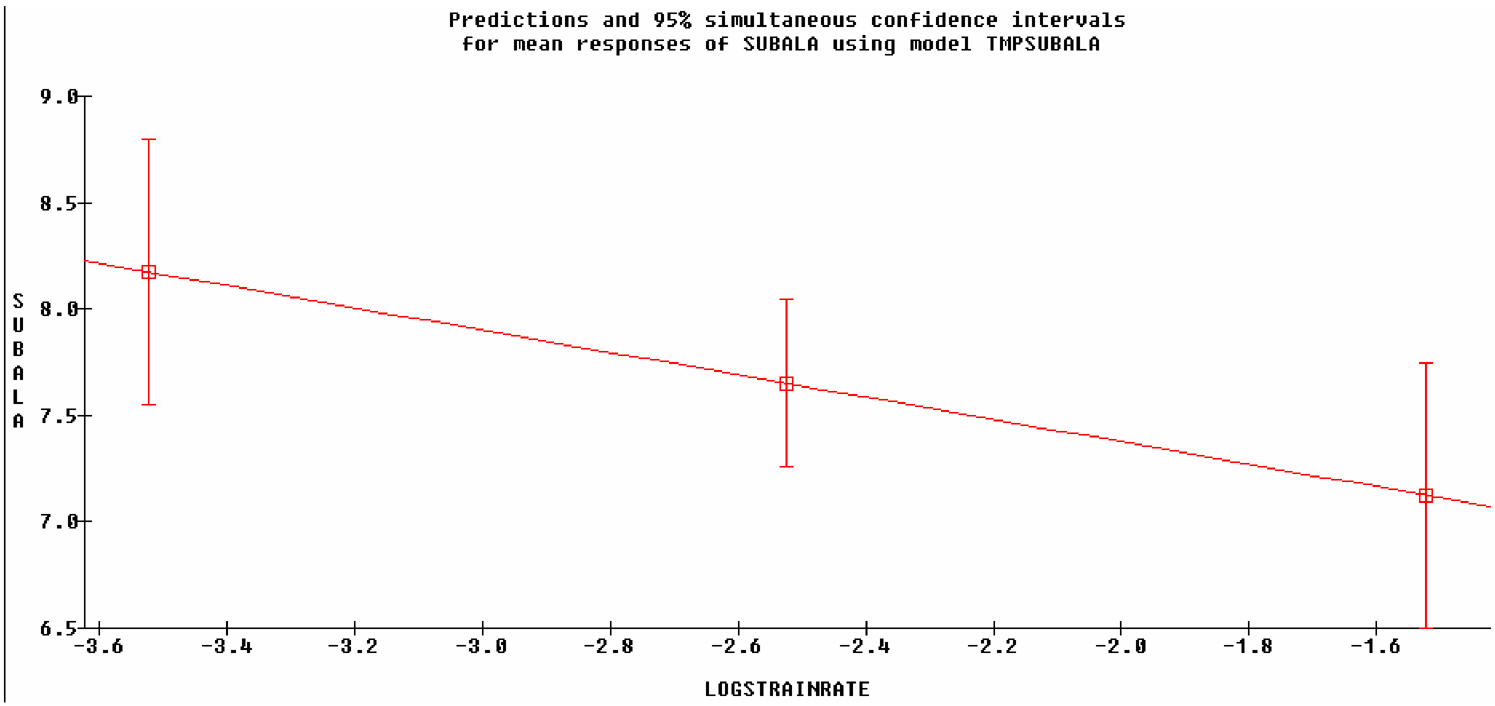

A-4.—Subsolvus as-large-as grain size regression results.

All Terms

Least Squares Coefficients, Response SPG, Model DESIGN

Term	Coeff.	Std. Error	T-value	Signif.	Transformed Term
1 1	5.966475	0.078516	75.99	0.0001	
2 ~T	-0.273572	0.096145	-2.85	0.0103	((T-1.08e+03)/3e+01)
3 ~LSR	0.135932	0.096145	1.41	0.1736	(LSR+2.5229)
4 ~LP	-0.167374	0.096086	-1.74	0.0977	((LP-4.5155e-01)/4.5155e
5 ~LST	-0.222068	0.078522	-2.83	0.0107	((LST-3.0105e-01)/3.0105
6 ~T*LSR	0.137500	0.107484	1.28	0.2162	((T-1.08e+03)/3e+01)*(LS
7 ~T*LP	-0.127041	0.107450	-1.18	0.2517	((T-1.08e+03)/3e+01)*((L
8 ~T*LST	-0.145010	0.096143	-1.51	0.1479	((T-1.08e+03)/3e+01)*((L
9 ~LSR*LP	-0.082638	0.107450	-0.77	0.4513	(LSR+2.5229)*((LP-4.5155
10 ~LSR*LST	-0.045003	0.096143	-0.47	0.6451	(LSR+2.5229)*((LST-3.010
11 ~LP*LST	-0.067857	0.096092	-0.71	0.4887	((LP-4.5155e-01)/4.5155e

No. cases = 30 R-sq. = 0.5949 RMS Error = 0.4299
Resid. df = 19 R-sq-adj. = 0.3817 Cond. No. = 1.023
~ indicates factors are transformed.

FORWARD AND REVERSE STEPWISE SELECTION

Mulreg @TMPSTRESS@MULREG, Model DESIGN__COPY, Response SPG

Term	df	P-Remove	P-Enter
1 1	1	0.000	
2 T	1	0.010	
3 LSR	1	0.174	
4 LP	1	0.098	
5 LST	1	0.011	
6 T*LSR	1	0.216	
7 T*LP	1	0.252	
8 T*LST	1	0.148	
9 LSR*LP	1	0.451	
10 LSR*LST	1	0.645	
11 LP*LST	1	0.489	

No. cases = 30 R-sq. = 0.5949 RMS Error = 0.429
Resid. df = 19 R-sq-adj. = 0.3817 Obey Hierarchy: n

Mulreg @TMPSTRESS@MULREG, Model DESIGN__COPY, Response SPG

Term	df	P-Remove	P-Enter
1 1	1	0.000	
2 T	1	0.010	
3 LSR	1		0.178
4 LP	1	0.103	
5 LST	1	0.010	
6 T*LSR	1		0.221
7 T*LP	1		0.259
8 T*LST	1		0.146
9 LSR*LP	1		0.477
10 LSR*LST	1		0.658
11 LP*LST	1		0.504

No. cases = 30 R-sq. = 0.4117 RMS Error = 0.4429
Resid. df = 26 R-sq-adj. = 0.3439 Obey Hierarchy: no

MODEL TMPSUPGS

Least Squares Coefficients, Response SPG, Model TMPSUPGS

Term	Coeff.	Std. Error	T-value	Signif.	Transformed Term
1 1	5.966475	0.080882	73.77	0.0001	
2 ~T	-0.275000	0.099034	-2.78	0.0100	((T-1.08e+03)/3e+01)
3 ~LP	-0.167369	0.098981	-1.69	0.1028	((LP-4.5155e-01)/4.5155e
4 ~LST	-0.223348	0.080866	-2.76	0.0104	((LST-3.0105e-01)/3.0105

No. cases = 30 R-sq. = 0.4117 RMS Error = 0.4429
Resid. df = 26 R-sq-adj. = 0.3439 Cond. No. = 1.023
~ indicates factors are transformed.

A-5.—Supersolvus mean grain size regression results.

ANOVA

Least Squares Summary ANOVA, Response SPG Model TMPSUPGS

Source	df	Sum Sq.	Mean Sq.	F-Ratio	Signif.
1 Total(Corr.)	29	8.669667			
2 Regression	3	3.569682	1.189894	6.07	0.0028
3 Residual	26	5.099985	0.196153		

R-sq. = 0.4117
R-sq-adj. = 0.3439

Least Squares Components ANOVA, Response SPG Model TMPSUPGS

Source	df	Sum Sq.	Mean Sq.	F-Ratio	Signif.	Transformed Term
1 Constant	1	1067				
2 ~T	1	1.512500	1.512500	7.71	0.0100	((T-1.08e+03)/3e+01)
3 ~LP	1	0.560849	0.560849	2.86	0.1028	((LP-4.5155e-01)/4.5155e
4 ~LST	1	1.496333	1.496333	7.63	0.0104	((LST-3.0105e-01)/3.0105
5 Residual	26	5.099985	0.196153			

~ indicates factors R-sq. = 0.4117
are transformed. R-sq-adj. = 0.3439
Type 3 sum of squares.

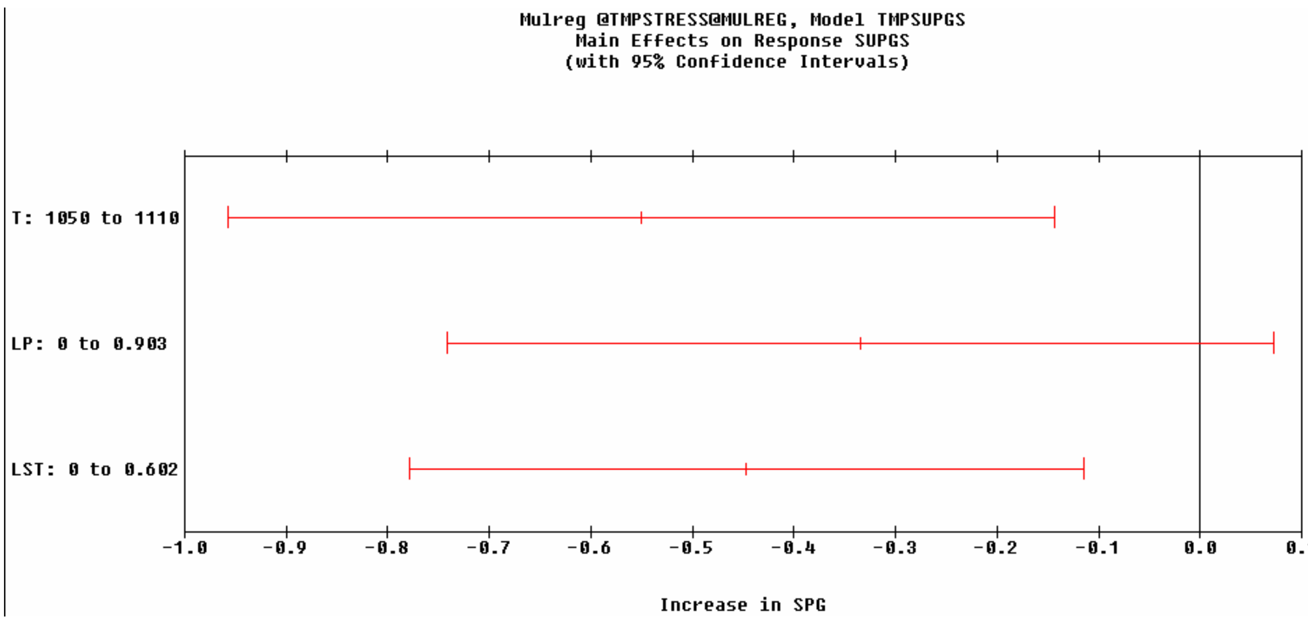

A-5.—Supersolvus mean grain size regression results.

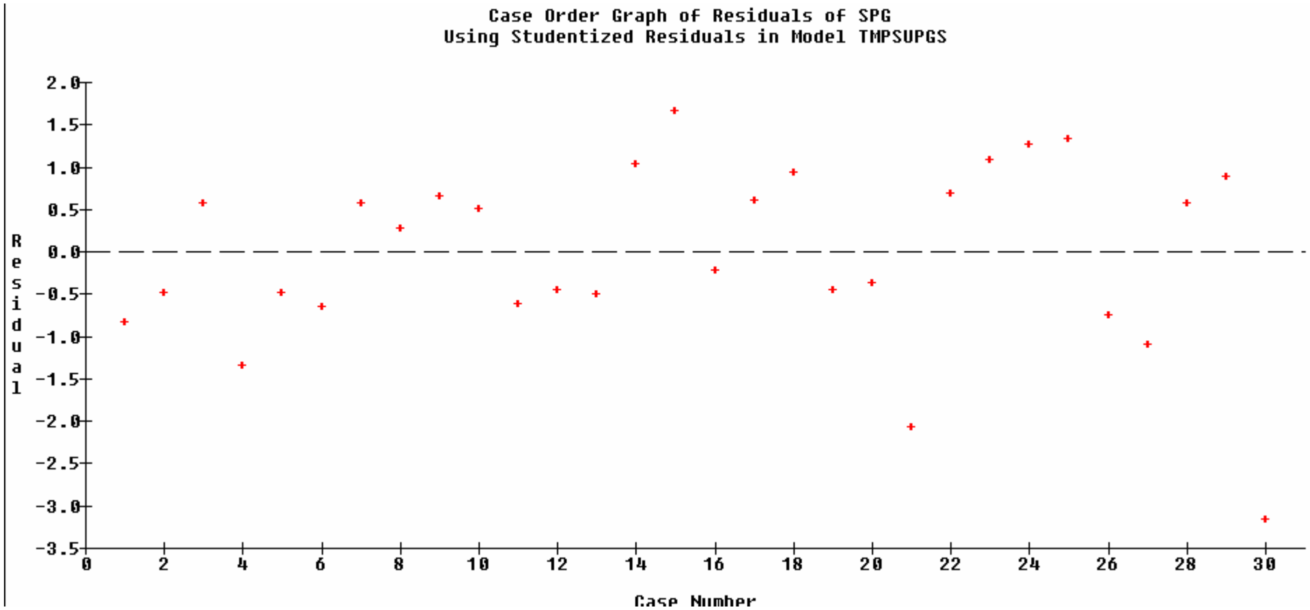

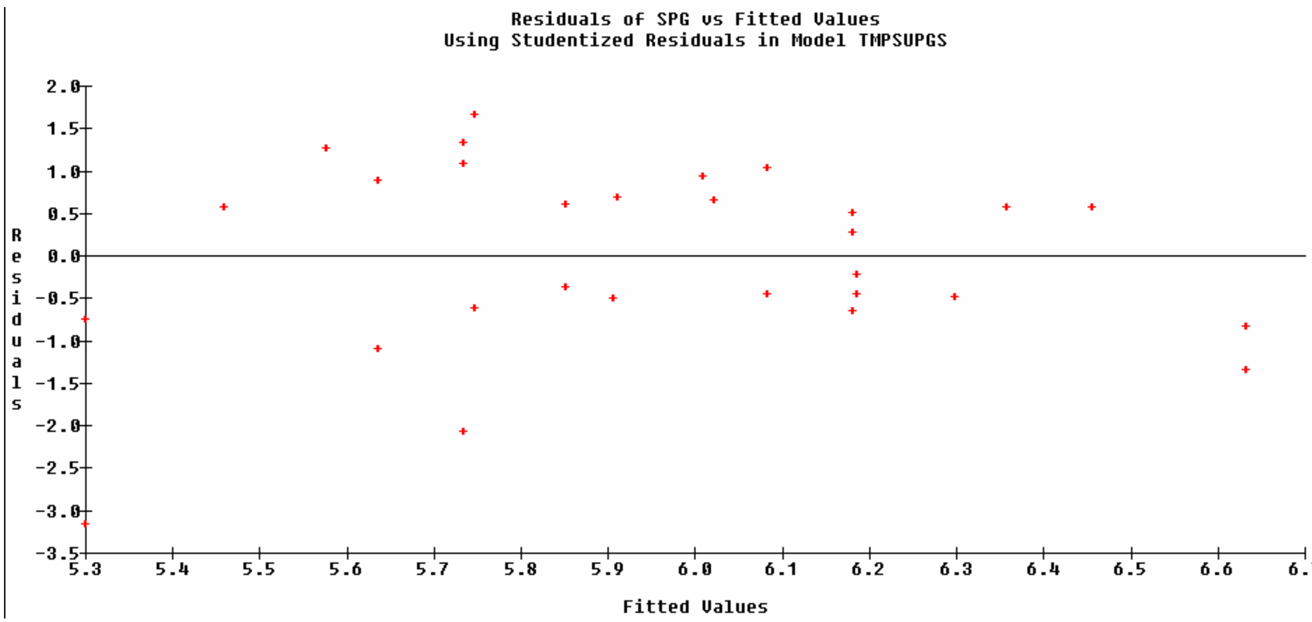

A-5.—Supersolvus mean grain size regression results.

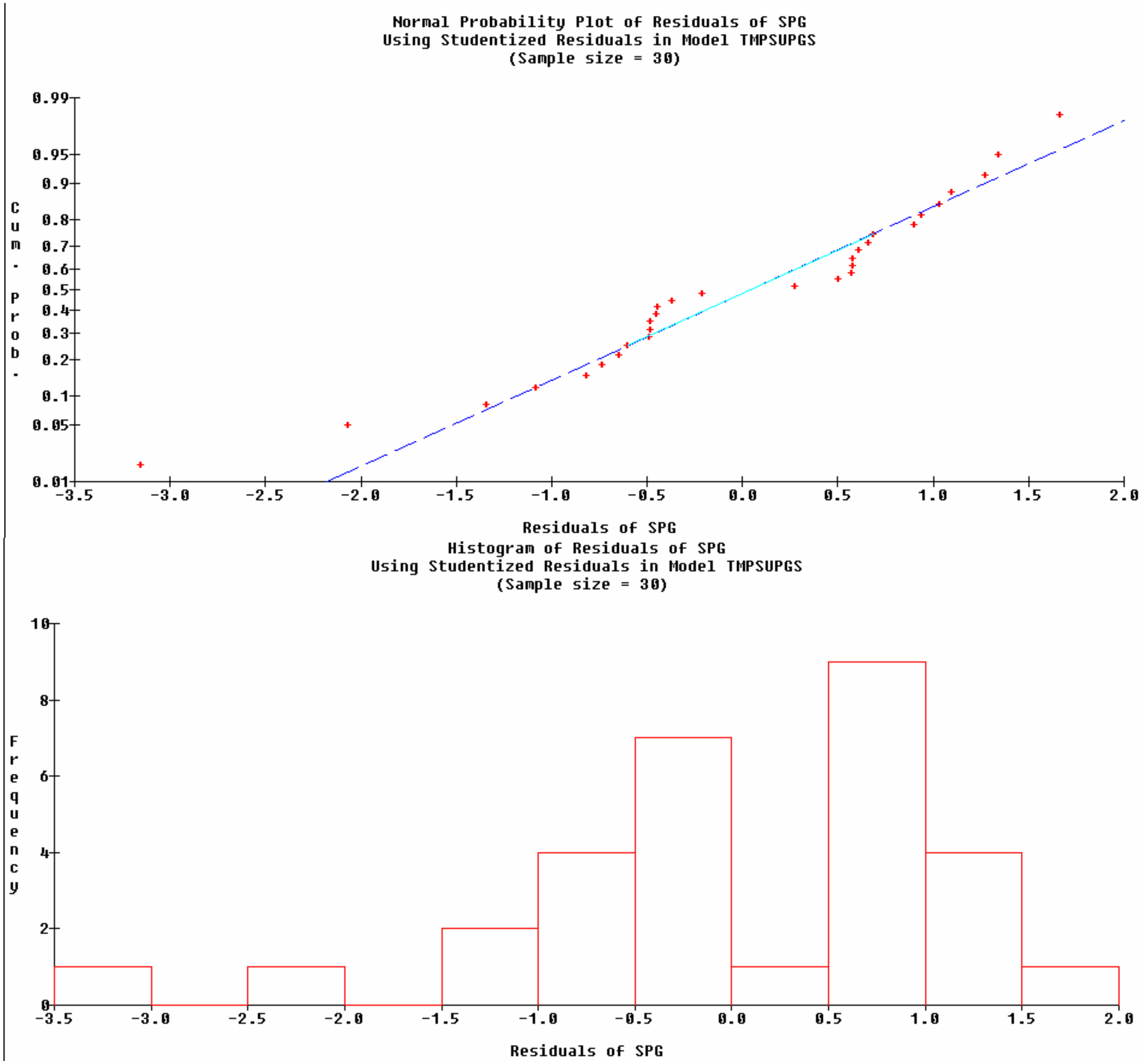

A-5.—Supersolvus mean grain size regression results.

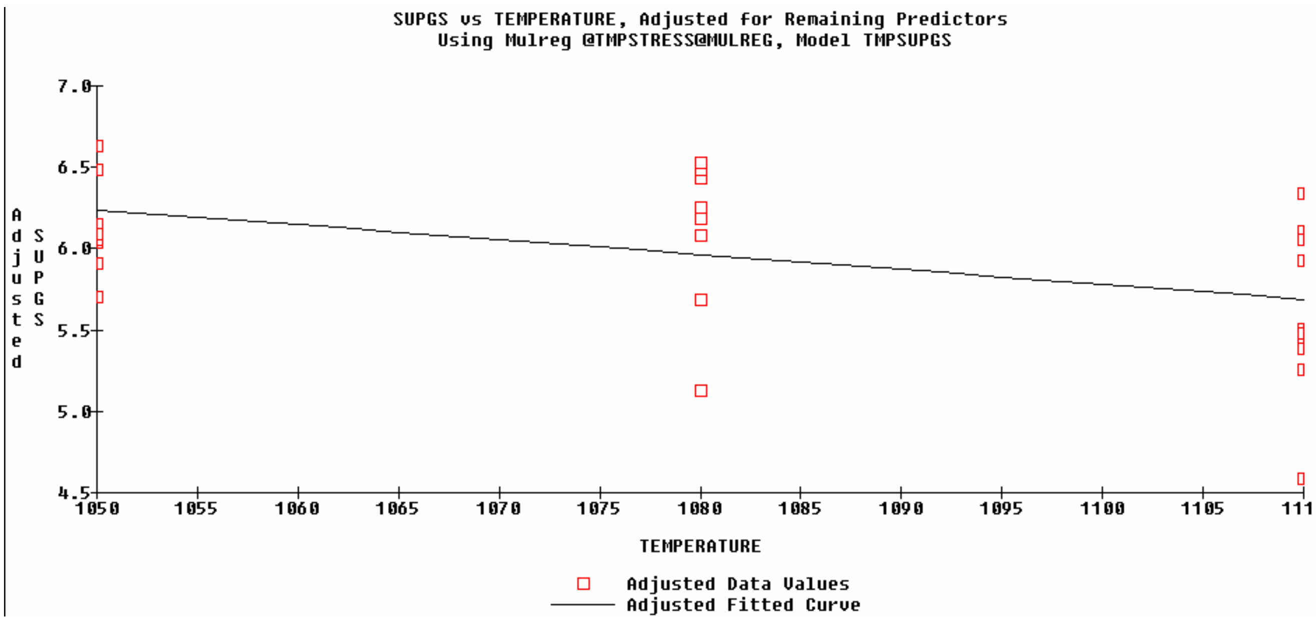

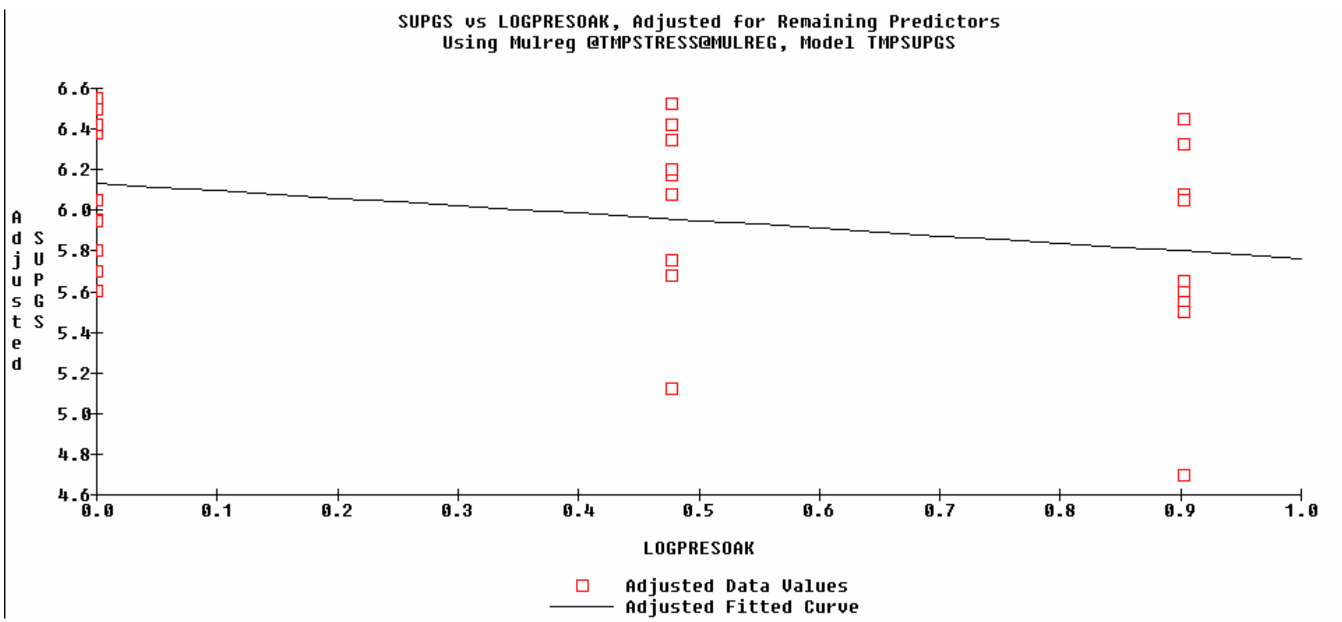

A-5.—Supersolvus mean grain size regression results.

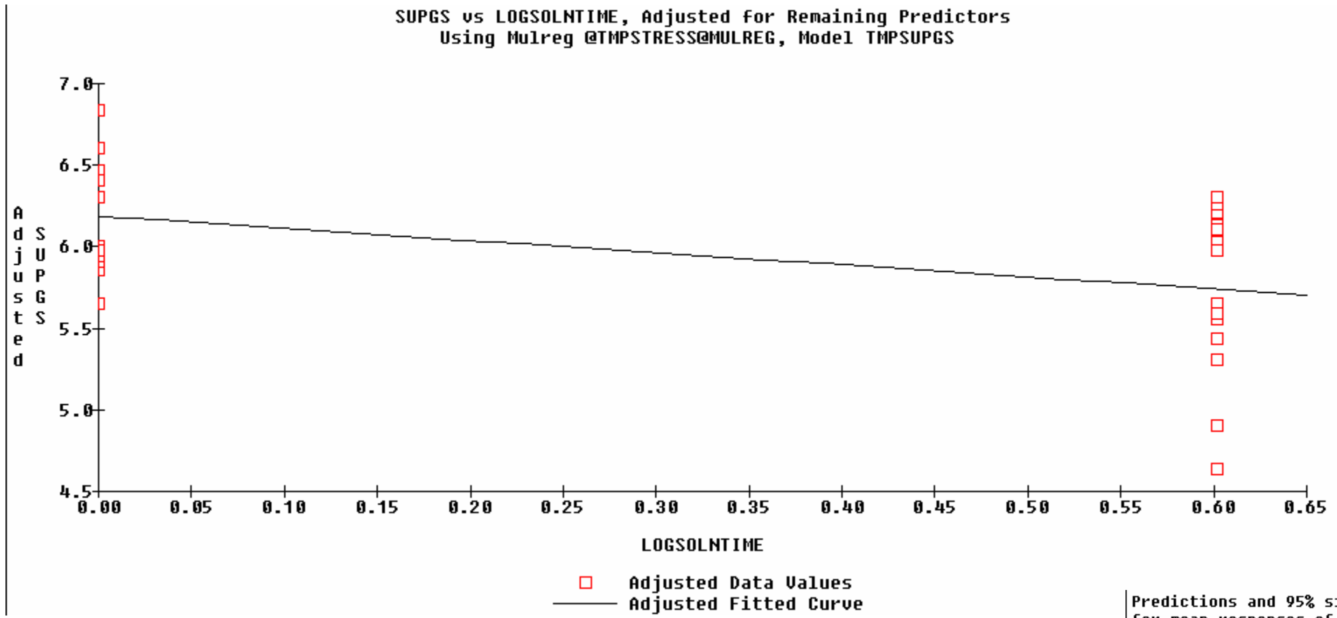

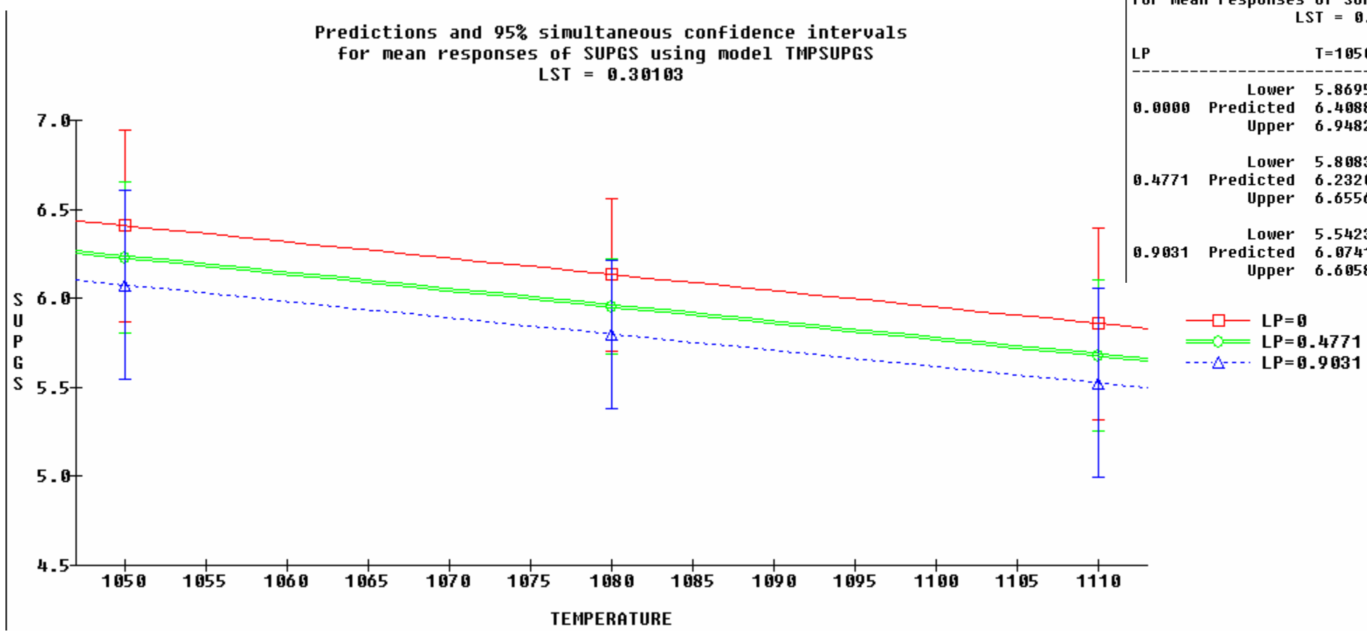

Predictions and 95% simultaneous confidence intervals
for mean responses of SUPGS using model TMPSUPGS
LST = 0.30103

LP		T=1050	T=1080	T=1110
	Lower	5.869513	5.705723	5.319513
0.0000	Predicted	6.408860	6.133860	5.858860
	Upper	6.948206	6.561996	6.398206
	Lower	5.808374	5.688911	5.258374
0.4771	Predicted	6.232020	5.957020	5.682020
	Upper	6.655666	6.225128	6.105666
	Lower	5.542344	5.380561	4.992344
0.9031	Predicted	6.074121	5.799121	5.524121
	Upper	6.605897	6.217680	6.055897

A-5.—Supersolvus mean grain size regression results.

ALL TERMS

```
                 Least Squares Coefficients, Response SPA, Model DESIGN

Term          Coeff.         Std. Error    T-value   Signif.  Transformed Term
-------------------------------------------------------------------------------------
 1 1              1.696492      0.330914     5.13    0.0001
 2 ~T            -1.166137      0.405209    -2.88    0.0096  ((T-1.08e+03)/3e+01)
 3 ~LSR          -1.191713      0.405209    -2.94    0.0084  (LSR+2.5229)
 4 ~LP           -0.698299      0.404961    -1.72    0.1009  ((LP-4.5155e-01)/4.5155e
 5 ~LST          -0.189514      0.330936    -0.57    0.5736  ((LST-3.0105e-01)/3.0105
 6 ~T*LSR        -1.312500      0.453002    -2.90    0.0092  ((T-1.08e+03)/3e+01)*(LS
 7 ~T*LP         -0.783000      0.452857    -1.73    0.1000  ((T-1.08e+03)/3e+01)*((L
 8 ~T*LST         0.025002      0.405204     0.06    0.9514  ((T-1.08e+03)/3e+01)*((L
 9 ~LSR*LP       -0.732556      0.452857    -1.62    0.1222  (LSR+2.5229)*((LP-4.5155
10 ~LSR*LST      -0.050003      0.405204    -0.12    0.9031  (LSR+2.5229)*((LST-3.010
11 ~LP*LST        0.327030      0.404988     0.81    0.4294  ((LP-4.5155e-01)/4.5155e

No. cases = 30       R-sq. =  0.6490      RMS Error = 1.812
Resid. df = 19   R-sq-adj. =  0.4643      Cond. No. = 1.023
~ indicates factors are transformed.
```

FORWARD AND REVERSE STEPWISE SELECTION

```
Mulreg @TMPSTRESS@MULREG, Model DESIGN__COPY, Response SPA

Term        df  P-Remove  P-Enter
 1 1         1     0.000
 2 T         1     0.010
 3 LSR       1     0.008
 4 LP        1     0.101
 5 LST       1     0.574
 6 T*LSR     1     0.009
 7 T*LP      1     0.100
 8 T*LST     1     0.951
 9 LSR*LP    1     0.122
10 LSR*LST   1     0.903
11 LP*LST    1     0.429

No. cases = 30       R-sq. =  0.6490      RMS Error = 1.812
Resid. df = 19   R-sq-adj. =  0.4643     Obey Hierarchy: no
```

```
Mulreg @TMPSTRESS@MULREG, Model DESIGN__COPY, Response SPA

Term        df  P-Remove  P-Enter
 1 1         1     0.000
 2 T         1     0.005
 3 LSR       1     0.004
 4 LP        1     0.077
 5 LST       1              0.564
 6 T*LSR     1     0.005
 7 T*LP      1     0.076
 8 T*LST     1              0.949
 9 LSR*LP    1     0.096
10 LSR*LST   1              0.898
11 LP*LST    1              0.406

No. cases = 30       R-sq. =  0.6309      RMS Error = 1.689
Resid. df = 23   R-sq-adj. =  0.5347     Obey Hierarchy: no
```

A-6.—Supersolvus as-large-as grain size regression results.

MODEL TMPSUPALA

Least Squares Coefficients, Response SPA, Model TMPSUPALA

Term	Coeff.	Std. Error	T-value	Signif.	Transformed Term
1 1	1.696504	0.308411	5.50	0.0001	
2 ~T	-1.166139	0.377654	-3.09	0.0052	((T-1.08e+03)/3e+01)
3 ~LSR	-1.191710	0.377654	-3.16	0.0044	(LSR+2.5229)
4 ~LP	-0.698321	0.377422	-1.85	0.0772	((LP-4.5155e-01)/4.5155e
5 ~T*LSR	-1.312500	0.422196	-3.11	0.0049	((T-1.08e+03)/3e+01)*(LS
6 ~T*LP	-0.783000	0.422061	-1.86	0.0764	((T-1.08e+03)/3e+01)*((L
7 ~LSR*LP	-0.732556	0.422061	-1.74	0.0960	(LSR+2.5229)*((LP-4.5155

No. cases = 30   R-sq. = 0.6309   RMS Error = 1.689
Resid. df = 23   R-sq-adj. = 0.5347   Cond. No. = 1.023
~ indicates factors are transformed.

ANOVA

Least Squares Summary ANOVA, Response SPA Model TMPSUPALA

Source	df	Sum Sq.	Mean Sq.	F-Ratio	Signif.
1 Total(Corr.)	29	177.7417			
2 Regression	6	112.1459	18.6910	6.55	0.0004
3 Linear	3	65.3556	21.7852	7.64	0.0010
4 Non-linear	3	45.9699	15.3233	5.37	0.0059
5 Residual	23	65.5958	2.8520		

R-sq. = 0.6309
R-sq-adj. = 0.5347

Least Squares Components ANOVA, Response SPA Model TMPSUPALA

Source	df	Sum Sq.	Mean Sq.	F-Ratio	Signif.	Transformed Term
1 Constant	1	86.2978				
2 ~T	1	27.1933	27.1933	9.54	0.0052	((T-1.08e+03)/3e+01)
3 ~LSR	1	28.3989	28.3989	9.96	0.0044	(LSR+2.5229)
4 ~LP	1	9.7635	9.7635	3.42	0.0772	((LP-4.5155e-01)/4.5155e
5 ~T*LSR	1	27.5625	27.5625	9.66	0.0049	((T-1.08e+03)/3e+01)*(LS
6 ~T*LP	1	9.8157	9.8157	3.44	0.0764	((T-1.08e+03)/3e+01)*((L
7 ~LSR*LP	1	8.5917	8.5917	3.01	0.0960	(LSR+2.5229)*((LP-4.5155
8 Residual	23	65.5958	2.8520			

~ indicates factors   R-sq. = 0.6309
are transformed. R-sq-adj. = 0.5347
Type 3 sum of squares.

A-6.—Supersolvus as-large-as grain size regression results.

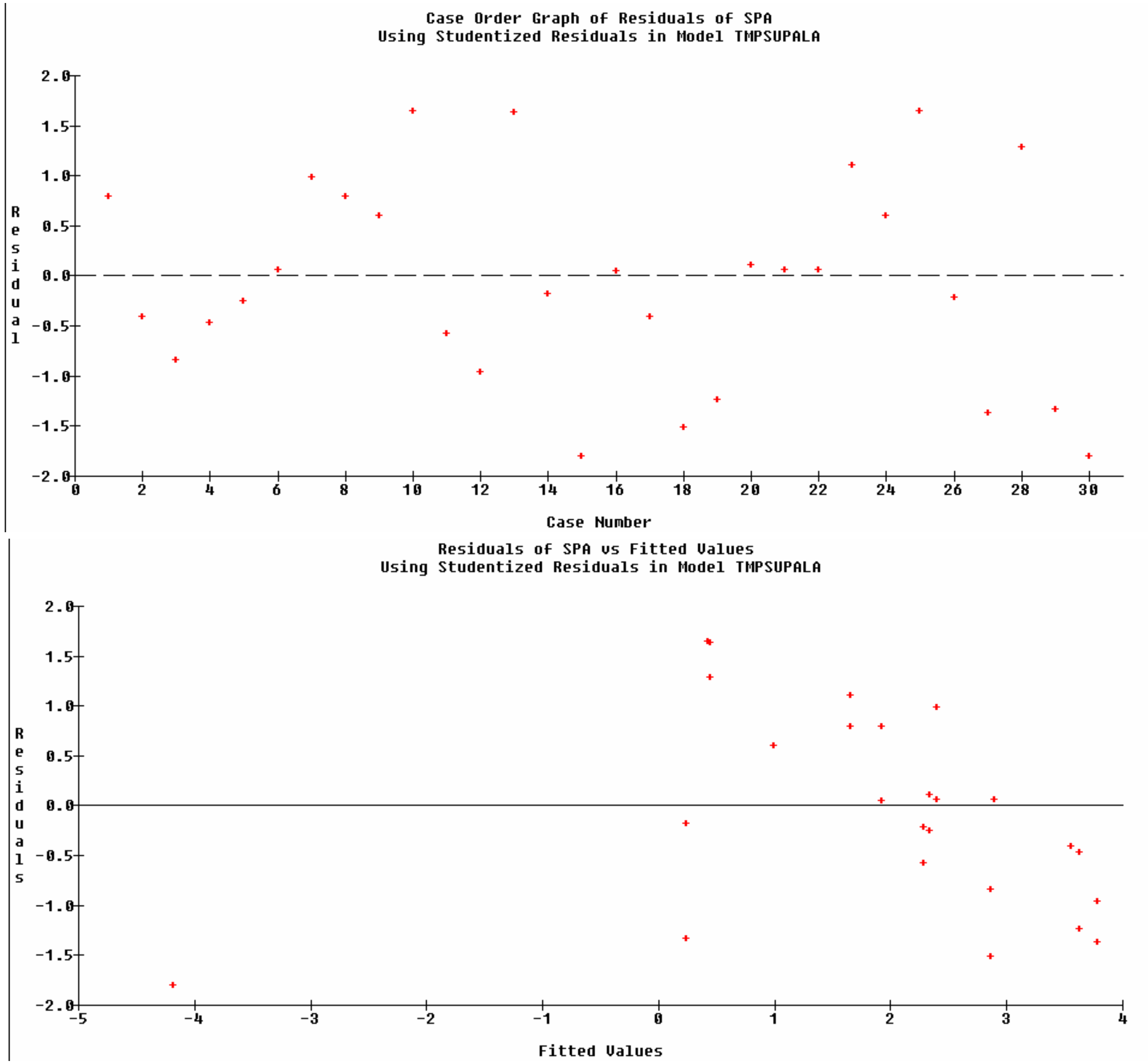

A-6.—Supersolvus as-large-as grain size regression results.

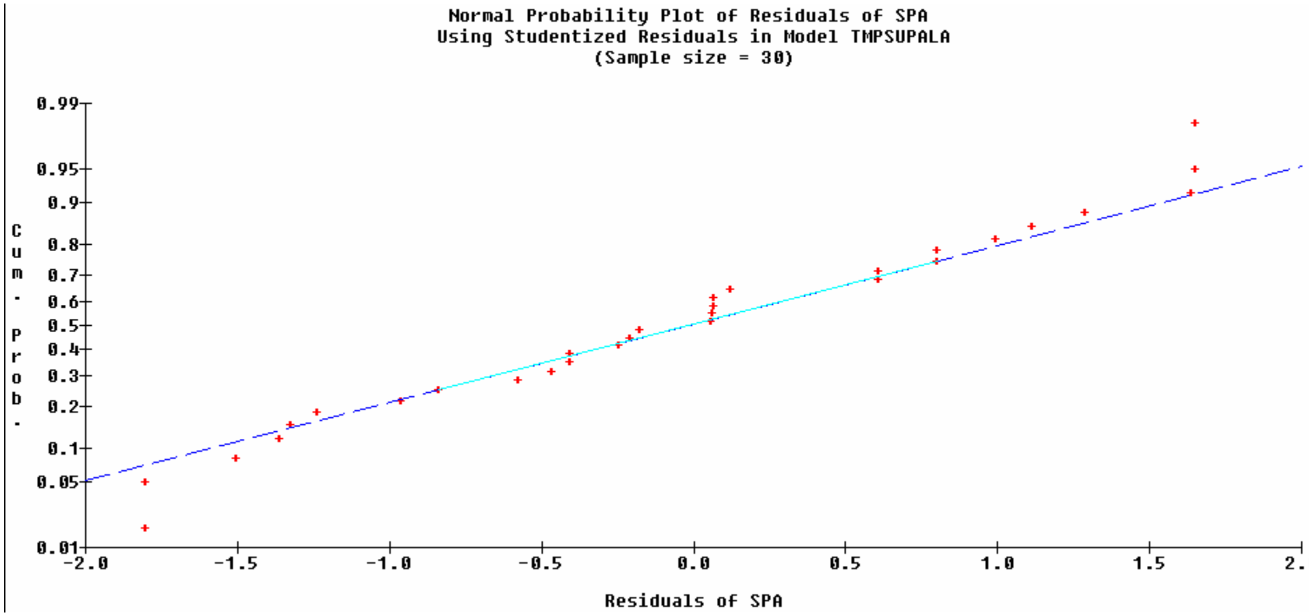

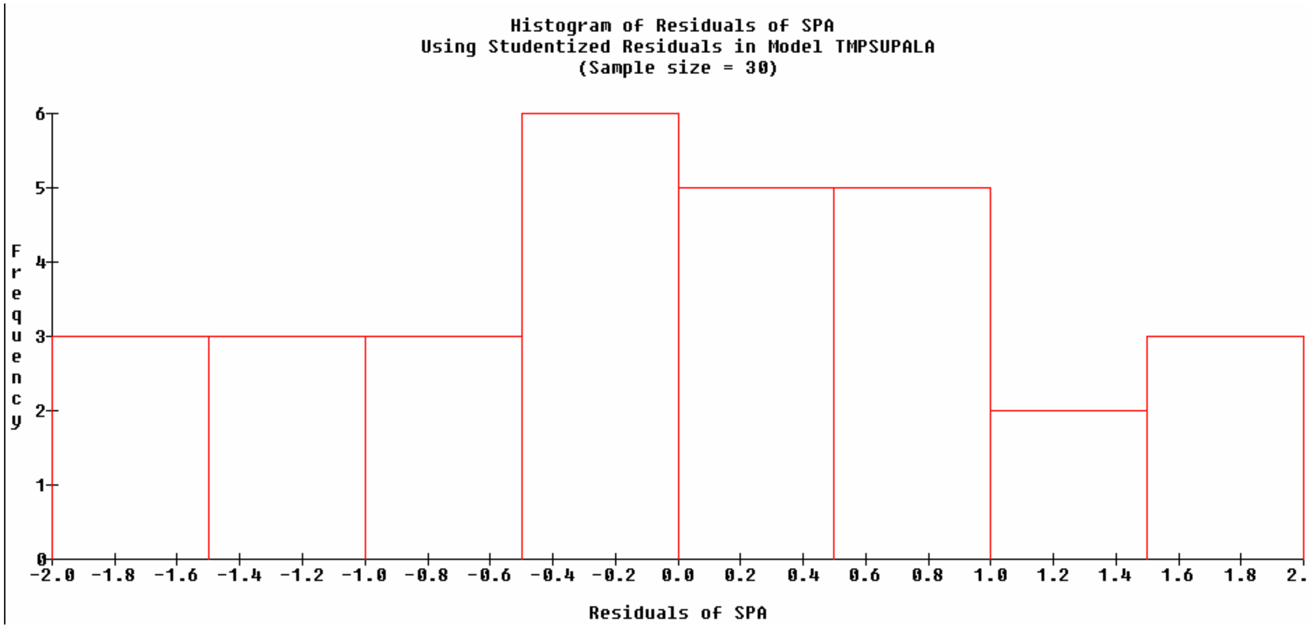

A-6.—Supersolvus as-large-as grain size regression results.

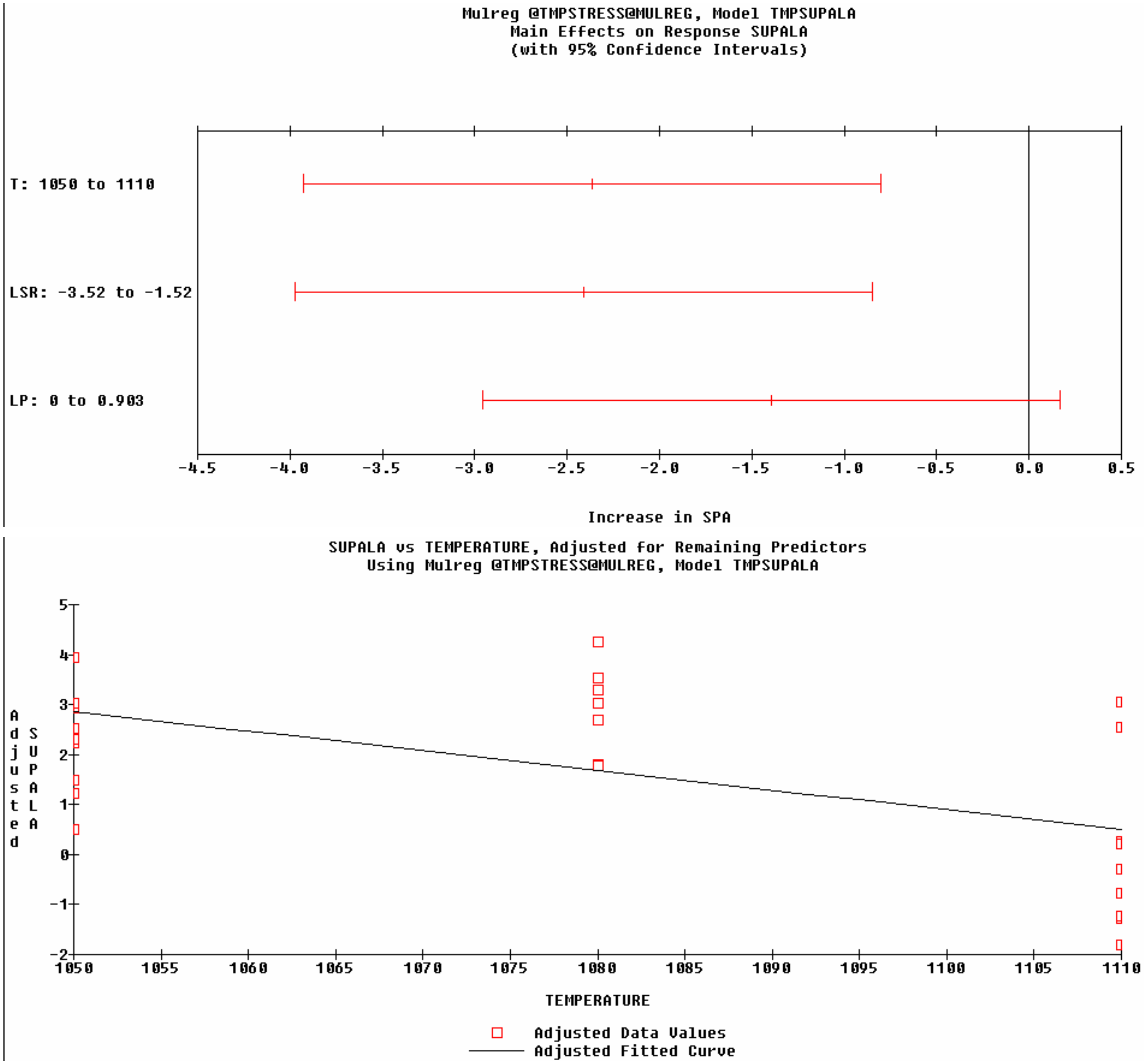

A-6.—Supersolvus as-large-as grain size regression results.

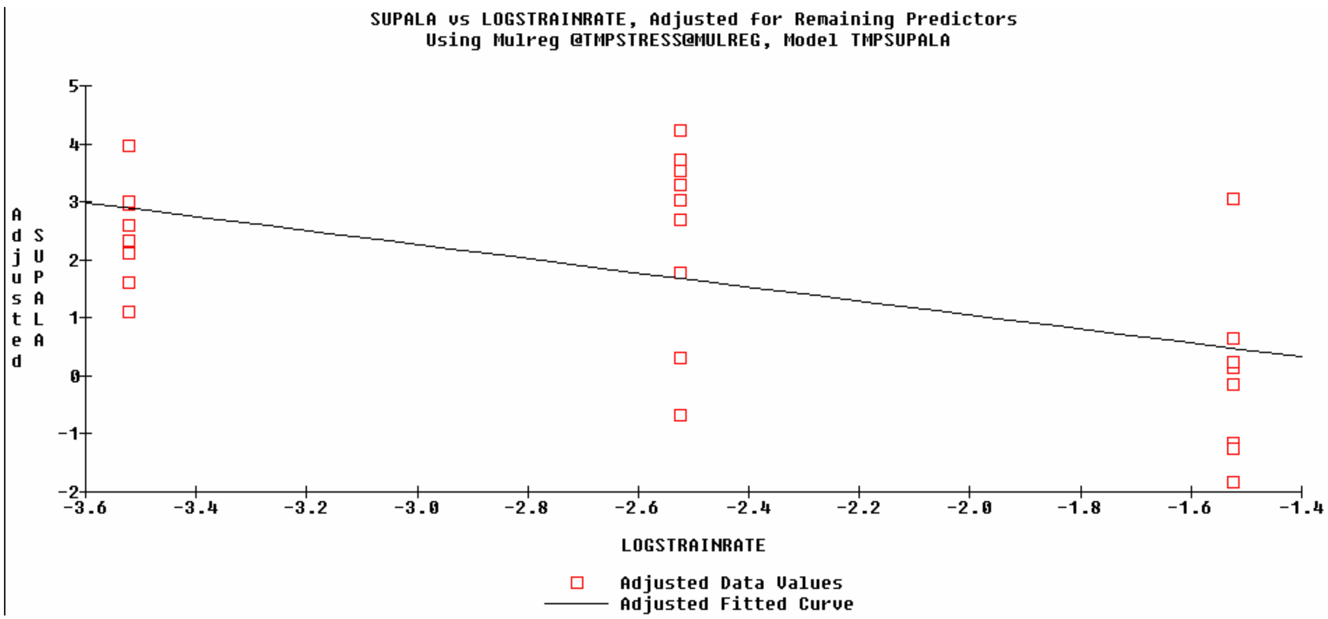

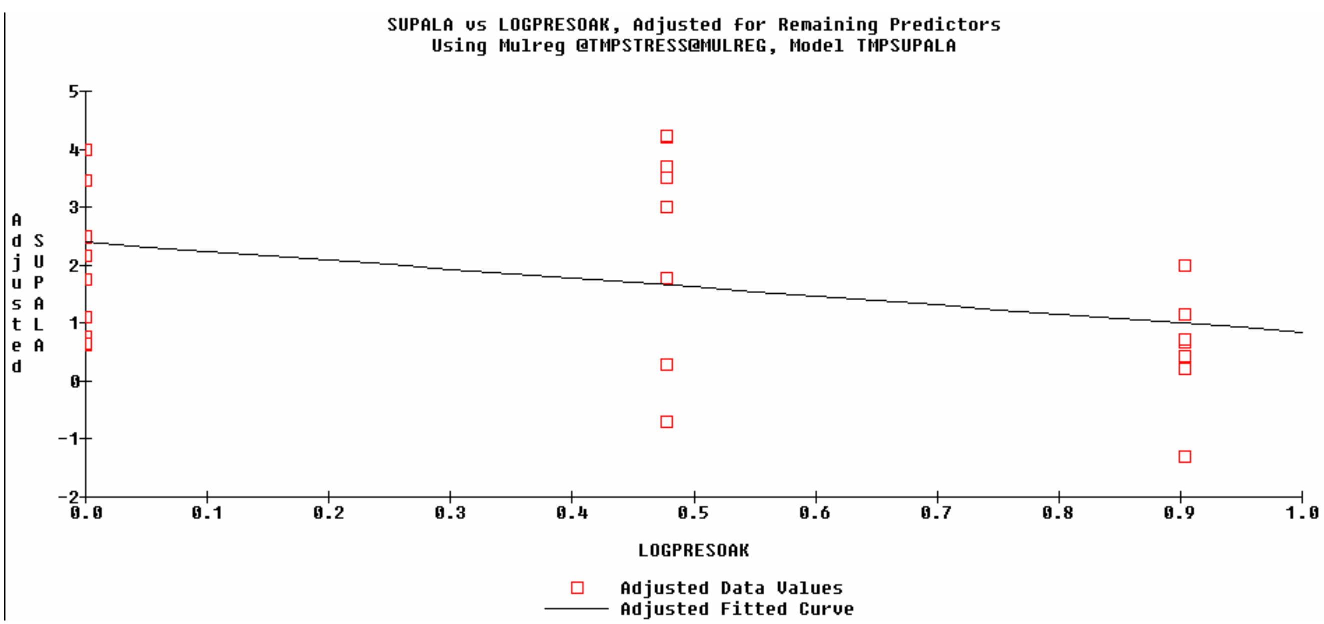

A-6.—Supersolvus as-large-as grain size regression results.

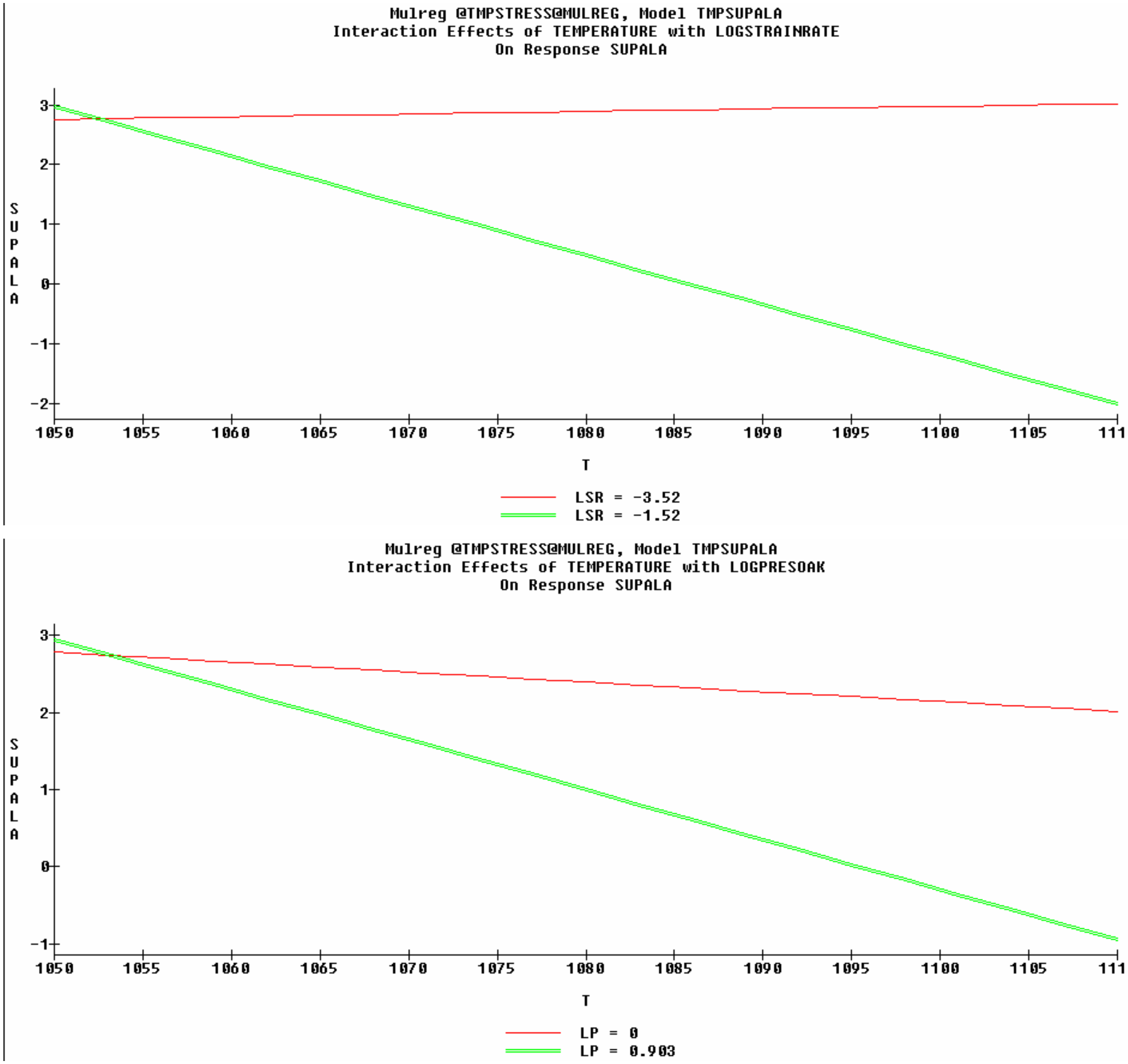

A-6.—Supersolvus as-large-as grain size regression results.

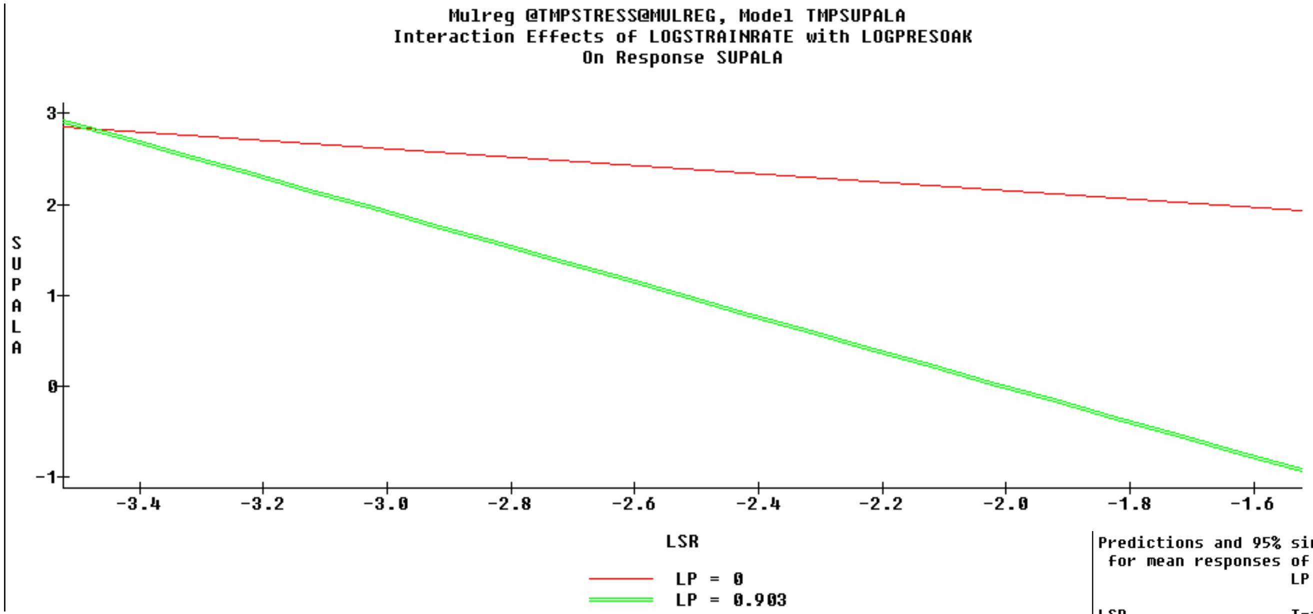

Predictions and 95% simultaneous confidence intervals
for mean responses of SUPALA using model TMPSUPALA
LP = 0.4771

LSR		T=1050	T=1080	T=1110
	Lower	-0.304490	0.872048	-0.100377
-3.5229	Predicted	2.788095	2.890151	2.992208
	Upper	5.880680	4.908255	6.084793
	Lower	0.849331	0.380794	-1.571556
-2.5229	Predicted	2.867435	1.656991	0.446548
	Upper	4.885539	2.933189	2.464652
	Lower	-0.145811	-1.594273	-5.191698
-1.5229	Predicted	2.946775	0.423831	-2.099112
	Upper	6.039360	2.441935	0.993473

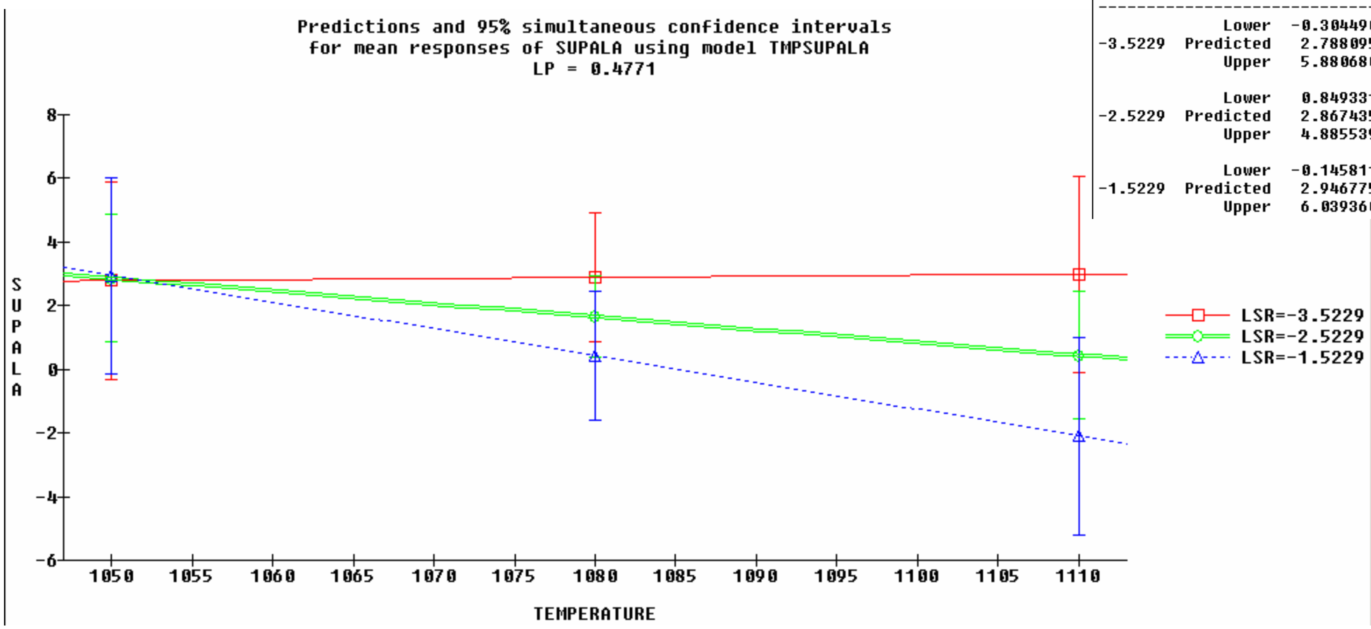

A-6.—Supersolvus as-large-as grain size regression results.

All Terms

Least Squares Coefficients, Response SBPG, Model DESIGN

Term	Coeff.	Std. Error	T-value	Signif.	Transformed Term
1 1	5.913509	0.078932	74.92	0.0001	
2 ~T	-0.059913	0.096654	-0.62	0.5427	((T-1.08e+03)/3e+01)
3 ~LSR	0.095384	0.096654	0.99	0.3361	(LSR+2.5229)
4 ~LP	-0.009991	0.096595	-0.10	0.9187	((LP-4.5155e-01)/4.5155e
5 ~LST	-0.193527	0.078937	-2.45	0.0241	((LST-3.0105e-01)/3.0105
6 ~T*LSR	0.318750	0.108054	2.95	0.0082	((T-1.08e+03)/3e+01)*(LS
7 ~T*LP	-0.007872	0.108019	-0.07	0.9427	((T-1.08e+03)/3e+01)*((L
8 ~T*LST	-0.030002	0.096652	-0.31	0.7596	((T-1.08e+03)/3e+01)*((L
9 ~LSR*LP	-0.033987	0.108019	-0.31	0.7565	(LSR+2.5229)*((LP-4.5155
10 ~LSR*LST	-0.015001	0.096652	-0.16	0.8783	(LSR+2.5229)*((LST-3.010
11 ~LP*LST	0.009611	0.096601	0.10	0.9218	((LP-4.5155e-01)/4.5155e

No. cases = 30 R-sq. = 0.4618 RMS Error = 0.4322
Resid. df = 19 R-sq-adj. = 0.1785 Cond. No. = 1.023
~ indicates factors are transformed.

FORWARD AND REVERSE STEPWISE SELECTION

Mulreg @TMPSTRESS@MULREG, Model DESIGN__COPY, Response SBPG

Term	df	P-Remove	P-Enter
1 1	1	0.000	
2 T	1	0.543	
3 LSR	1	0.336	
4 LP	1	0.919	
5 LST	1	0.024	
6 T*LSR	1	0.008	
7 T*LP	1	0.943	
8 T*LST	1	0.760	
9 LSR*LP	1	0.757	
10 LSR*LST	1	0.878	
11 LP*LST	1	0.922	

No. cases = 30 R-sq. = 0.4618 RMS Error = 0.4322
Resid. df = 19 R-sq-adj. = 0.1785 Obey Hierarchy: no

Mulreg @TMPSTRESS@MULREG, Model DESIGN__COPY, Response SBPG

Term	df	P-Remove	P-Enter
1 1	1	0.000	
2 T	1		0.488
3 LSR	1		0.268
4 LP	1		0.908
5 LST	1	0.009	
6 T*LSR	1	0.002	
7 T*LP	1		0.928
8 T*LST	1		0.730
9 LSR*LP	1		0.736
10 LSR*LST	1		0.863
11 LP*LST	1		0.912

No. cases = 30 R-sq. = 0.4165 RMS Error = 0.3775
Resid. df = 27 R-sq-adj. = 0.3733 Obey Hierarchy: no

A-7.—Subsolvus plus supersolvus mean grain size regression results.

MODEL TMPSUBPGS

Least Squares Coefficients, Response SBPG, Model TMPSUBPGS

Term	Coeff.	Std. Error	T-value	Signif.	Transformed Term
1 1	5.913320	0.068922	85.80	0.0001	
2 ~LST	-0.193346	0.068927	-2.81	0.0092	((LST-3.0105e-01)/3.0105
3 ~T*LSR	0.318750	0.094375	3.38	0.0022	((T-1.08e+03)/3e+01)*(LS

No. cases = 30 R-sq. = 0.4165 RMS Error = 0.3775
Resid. df = 27 R-sq-adj. = 0.3733 Cond. No. = 1
~ indicates factors are transformed.

ANOVA

Least Squares Summary ANOVA, Response SBPG Model TMPSUBPGS

Source	df	Sum Sq.	Mean Sq.	F-Ratio	Signif.
1 Total(Corr.)	29	6.594667			
2 Regression	2	2.746958	1.373479	9.64	0.0007
3 Linear	1	1.121333	1.121333	7.87	0.0092
4 Non-linear	1	1.625625	1.625625	11.41	0.0022
5 Residual	27	3.847708	0.142508		

R-sq. = 0.4165
R-sq-adj. = 0.3733

Least Squares Components ANOVA, Response SBPG Model TMPSUBPGS

Source	df	Sum Sq.	Mean Sq.	F-Ratio	Signif.	Transformed Term
1 Constant	1	1049				
2 ~LST	1	1.121333	1.121333	7.87	0.0092	((LST-3.0105e-01)/3.0105
3 ~T*LSR	1	1.625625	1.625625	11.41	0.0022	((T-1.08e+03)/3e+01)*(LS
4 Residual	27	3.847708	0.142508			

~ indicates factors R-sq. = 0.4165
are transformed. R-sq-adj. = 0.3733
Type 3 sum of squares.

A-7.—Subsolvus plus supersolvus mean grain size regression results.

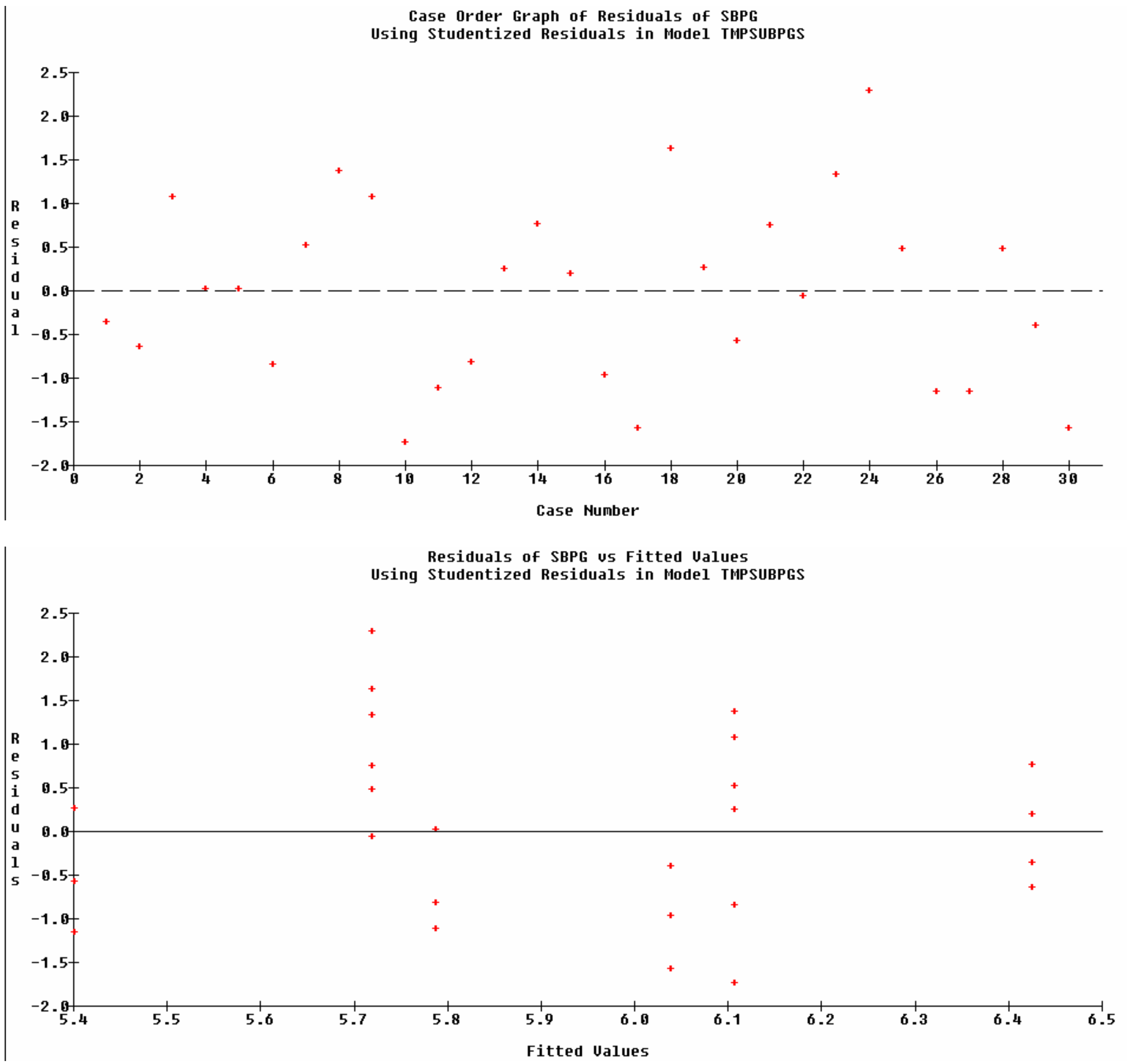

A-7.—Subsolvus plus supersolvus mean grain size regression results.

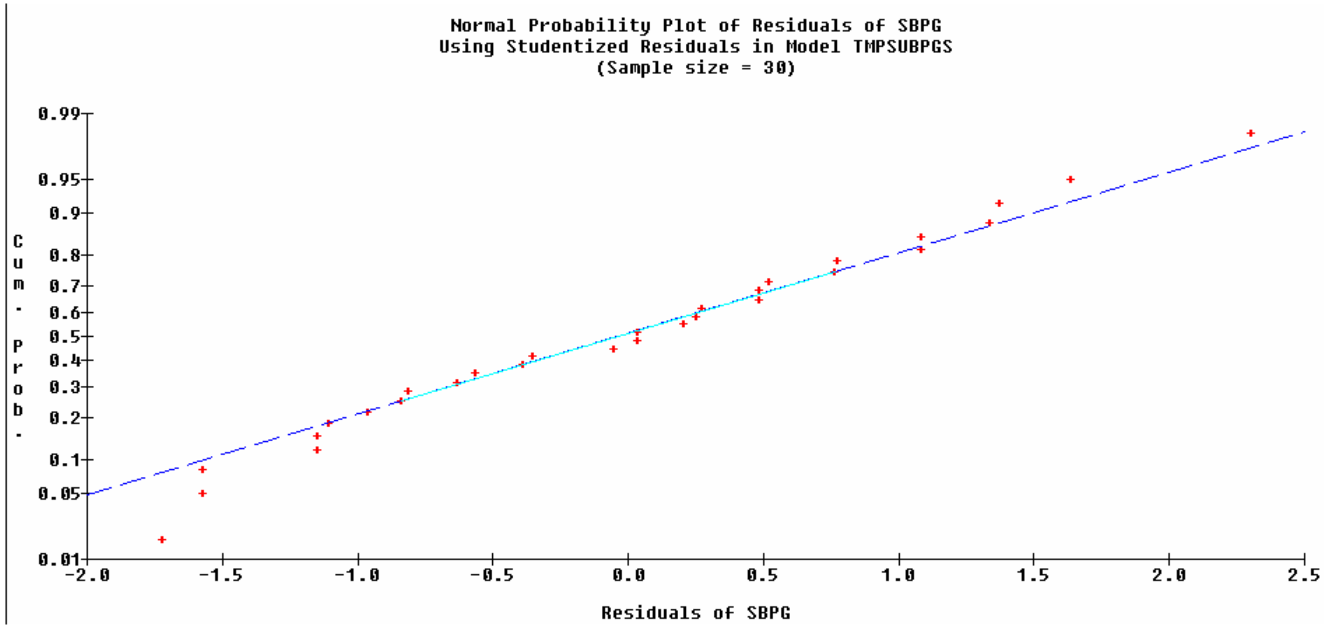

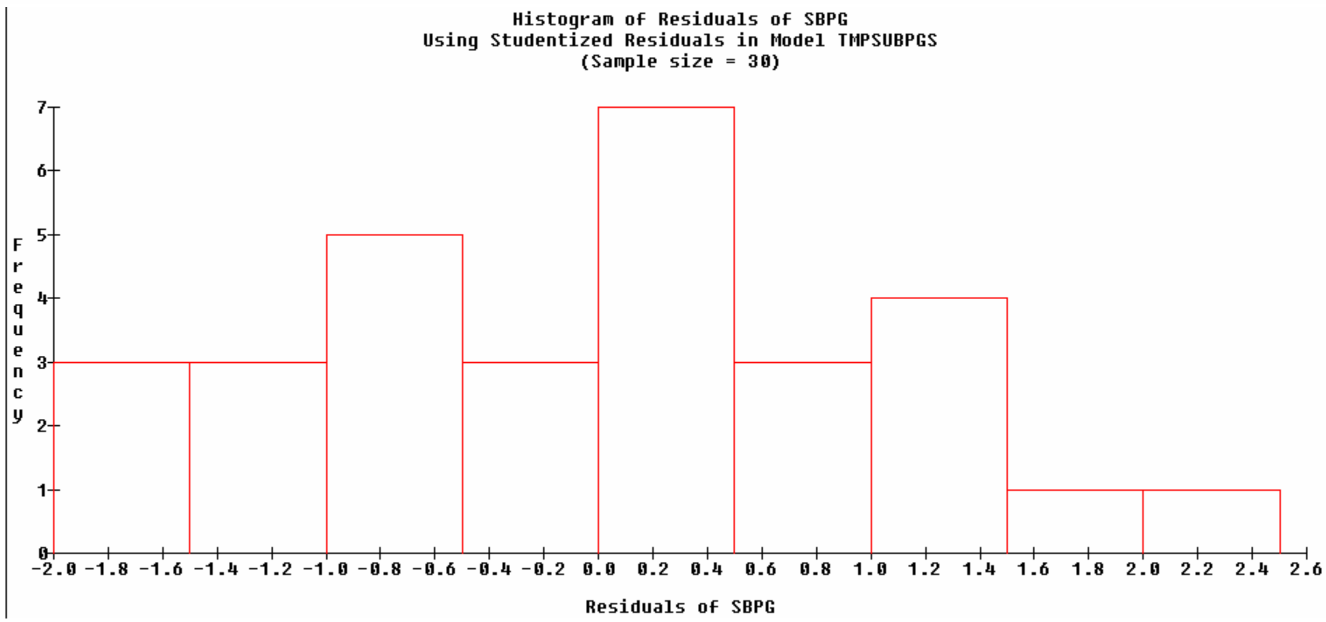

A-7.—Subsolvus plus supersolvus mean grain size regression results.

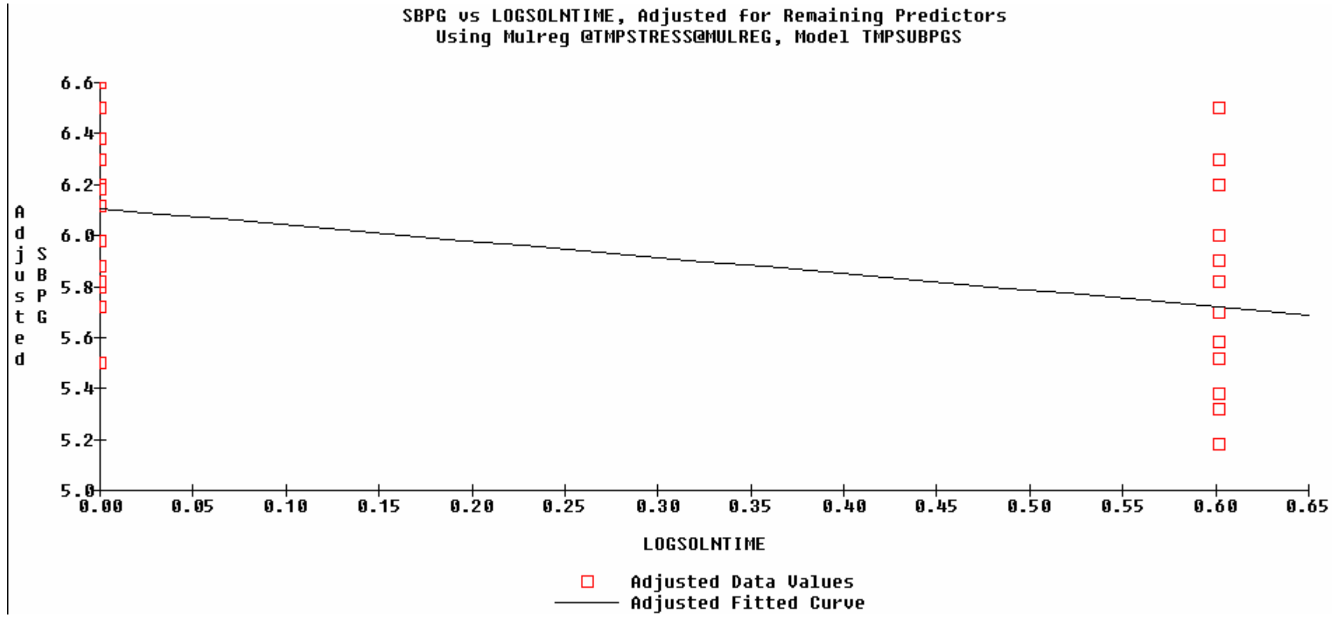

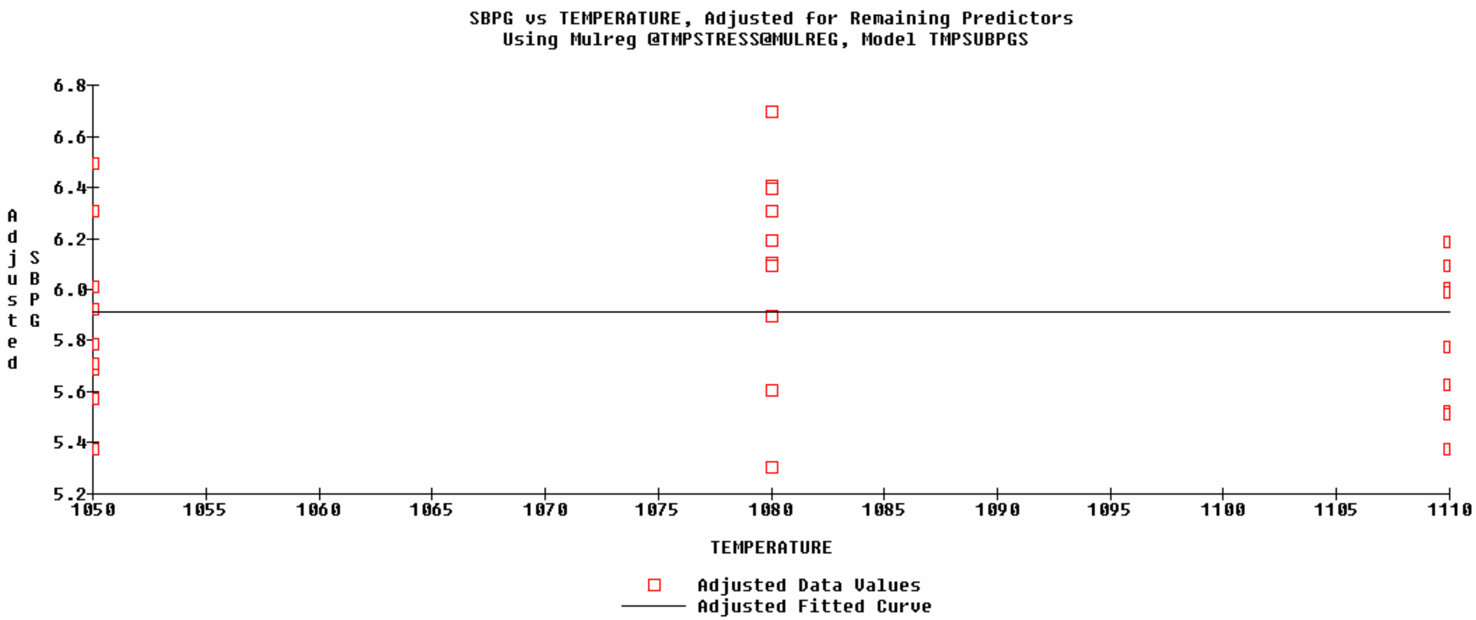

A-7.—Subsolvus plus supersolvus mean grain size regression results.

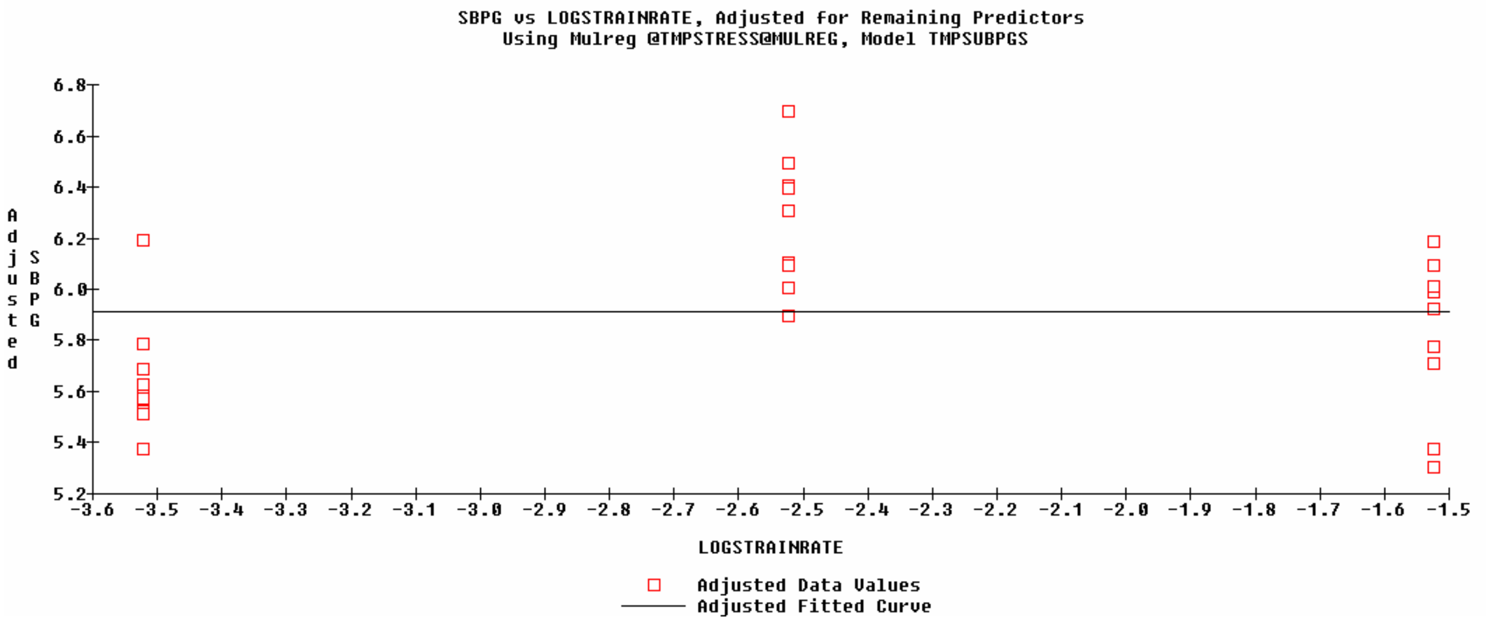

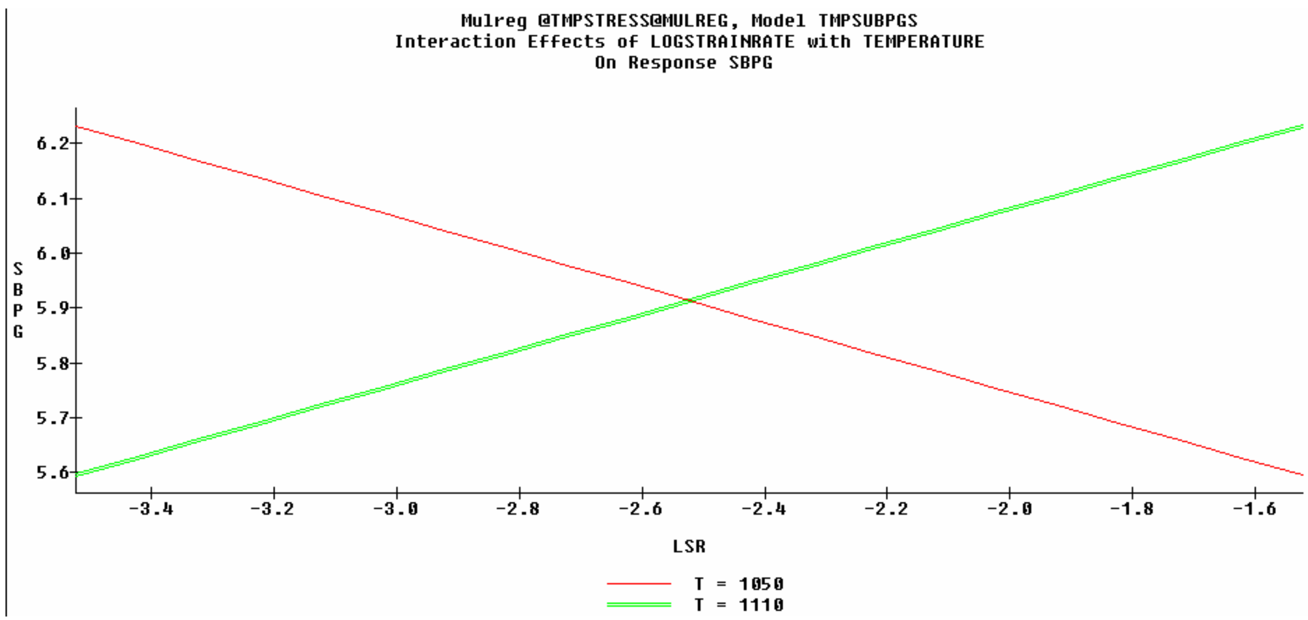

A-7.—Subsolvus plus supersolvus mean grain size regression results.

Predictions and 95% simultaneous confidence intervals
for mean responses of SBPG using model TMPSUBPGS
LST = 0.30103

LSR		T=1050	T=1080	T=1110
	Lower	5.883818	5.707938	5.246318
-3.5229	Predicted	6.232083	5.913333	5.594583
	Upper	6.580348	6.118729	5.942848
	Lower	5.707938	5.707938	5.707938
-2.5229	Predicted	5.913333	5.913333	5.913333
	Upper	6.118729	6.118729	6.118729
	Lower	5.246318	5.707938	5.883818
-1.5229	Predicted	5.594583	5.913333	6.232083
	Upper	5.942848	6.118729	6.580348

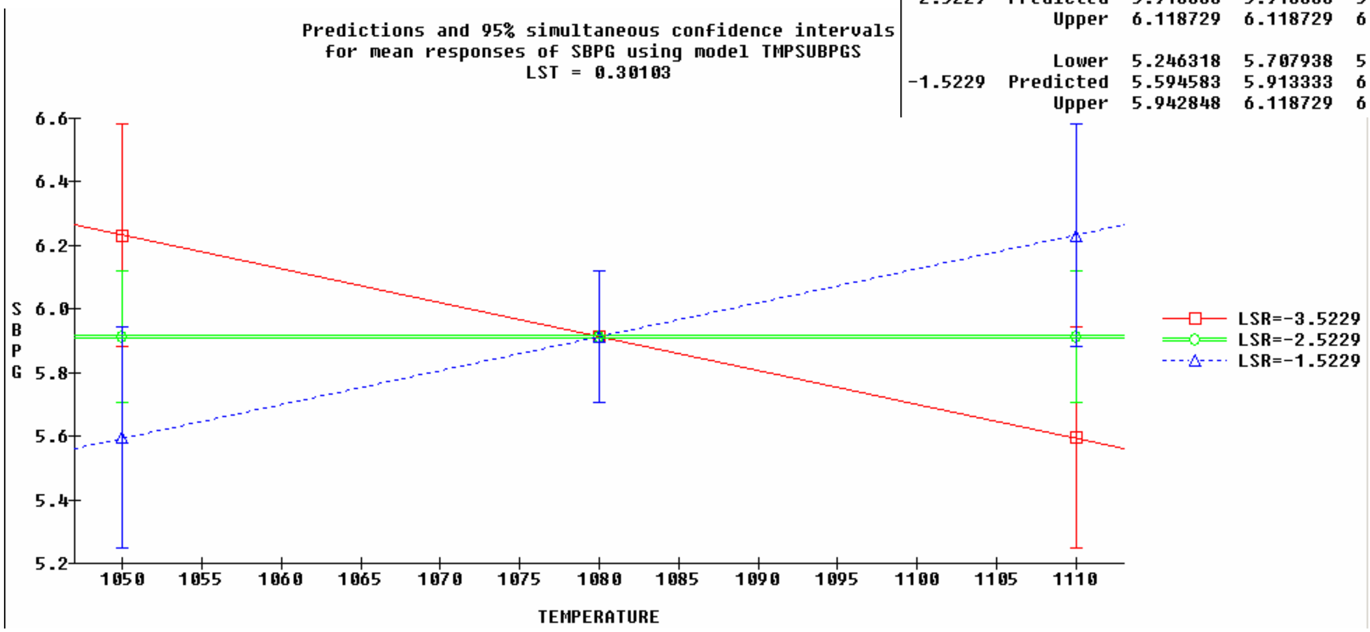

A-7.—Subsolvus plus supersolvus mean grain size regression results.

All Terms

```
          Least Squares Coefficients, Response SBPA, Model TMPSUBSUPALA

Term         Coeff.        Std. Error    T-value  Signif.  Transformed Term
-------------------------------------------------------------------------------------
 1 1            1.862915      0.275576
 2 ~T          -0.668075      0.337448                     ((T-1.08e+03)/3e+01)
 3 ~LSR        -0.542333      0.337448                     (LSR+2.5229)
 4 ~LP         -0.685139      0.337241                     ((LP-4.5155e-01)/4.5155e
 5 ~LST        -0.112213      0.275595                     ((LST-3.0105e-01)/3.0105
 6 ~T*LSR      -0.500000      0.377248     -1.33   0.2008  ((T-1.08e+03)/3e+01)*(LS
 7 ~T*LP       -0.613291      0.377127     -1.63   0.1204  ((T-1.08e+03)/3e+01)*((L
 8 ~T*LST      -0.225015      0.337443     -0.67   0.5129  ((T-1.08e+03)/3e+01)*((L
 9 ~LSR*LP     -0.679285      0.377127     -1.80   0.0876  (LSR+2.5229)*((LP-4.5155
10 ~LSR*LST    -0.300020      0.337443     -0.89   0.3851  (LSR+2.5229)*((LST-3.010
11 ~LP*LST     -0.236561      0.337263     -0.70   0.4915  ((LP-4.5155e-01)/4.5155e

No. cases = 30       R-sq. =  0.5170      RMS Error = 1.509
Resid. df = 19   R-sq-adj. =  0.2628      Cond. No. = 1.023
~ indicates factors are transformed.
```

FORWARD AND REVERSE STEPWISE SELECTION

```
Mulreg @TMPSTRESS@MULREG, Model TMPSUBSUPALA__COPY, Response SBPA

Term        df  P-Remove  P-Enter
 1 1         1     0.000
 2 T         1     0.062
 3 LSR       1     0.125
 4 LP        1     0.056
 5 LST       1     0.688
 6 T*LSR     1     0.201
 7 T*LP      1     0.120
 8 T*LST     1     0.513
 9 LSR*LP    1     0.088
10 LSR*LST   1     0.385
11 LP*LST    1     0.492

No. cases = 30       R-sq. =  0.5170      RMS Error = 1.509
Resid. df = 19   R-sq-adj. =  0.2628     Obey Hierarchy: no
```

```
Mulreg @TMPSTRESS@MULREG, Model TMPSUBSUPALA__COPY, Response SBPA

Term        df  P-Remove  P-Enter
 1 1         1     0.000
 2 T         1     0.053
 3 LSR       1     0.111
 4 LP        1     0.047
 5 LST       1              0.672
 6 T*LSR     1              0.178
 7 T*LP      1     0.107
 8 T*LST     1              0.504
 9 LSR*LP    1     0.076
10 LSR*LST   1              0.371
11 LP*LST    1              0.476

No. cases = 30       R-sq. =  0.4239      RMS Error = 1.466
Resid. df = 24   R-sq-adj. =  0.3039     Obey Hierarchy: no
```

A-8.—Subsolvus plus supersolvus as-large-as grain size regression results.

MODEL TMPSUBSUPALA

Least Squares Coefficients, Response SBPA, Model TMPSUBSUPALA

Term	Coeff.	Std. Error	T-value	Signif.	Transformed Term
1 1	1.862922	0.267791	6.96	0.0001	
2 ~T	-0.668060	0.327915	-2.04	0.0528	((T-1.08e+03)/3e+01)
3 ~LSR	-0.542313	0.327915	-1.65	0.1112	(LSR+2.5229)
4 ~LP	-0.685123	0.327714	-2.09	0.0473	((LP-4.5155e-01)/4.5155e
5 ~T*LP	-0.613291	0.366473	-1.67	0.1072	((T-1.08e+03)/3e+01)*((L
6 ~LSR*LP	-0.679285	0.366473	-1.85	0.0761	(LSR+2.5229)*((LP-4.5155

No. cases = 30   R-sq. = 0.4239   RMS Error = 1.466
Resid. df = 24   R-sq-adj. = 0.3039   Cond. No. = 1.023
~ indicates factors are transformed.

ANOVA

Least Squares Summary ANOVA, Response SBPA Model TMPSUBSUPALA

Source	df	Sum Sq.	Mean Sq.	F-Ratio	Signif.
1 Total(Corr.)	29	89.57500			
2 Regression	5	37.96983	7.59397	3.53	0.0156
3 Linear	3	24.20366	8.06789	3.75	0.0243
4 Non-linear	2	13.40944	6.70472	3.12	0.0625
5 Residual	24	51.60517	2.15022		

R-sq. = 0.4239
R-sq-adj. = 0.3039

Least Squares Components ANOVA, Response SBPA Model TMPSUBSUPALA

Source	df	Sum Sq.	Mean Sq.	F-Ratio	Signif.	Transformed Term
1 Constant	1	104.05889				
2 ~T	1	8.92465	8.92465	4.15	0.0528	((T-1.08e+03)/3e+01)
3 ~LSR	1	5.88112	5.88112	2.73	0.1112	(LSR+2.5229)
4 ~LP	1	9.39789	9.39789	4.37	0.0473	((LP-4.5155e-01)/4.5155e
5 ~T*LP	1	6.02186	6.02186	2.80	0.1072	((T-1.08e+03)/3e+01)*((L
6 ~LSR*LP	1	7.38757	7.38757	3.44	0.0761	(LSR+2.5229)*((LP-4.5155
7 Residual	24	51.60517	2.15022			

~ indicates factors   R-sq. = 0.4239
are transformed.   R-sq-adj. = 0.3039
Type 3 sum of squares.

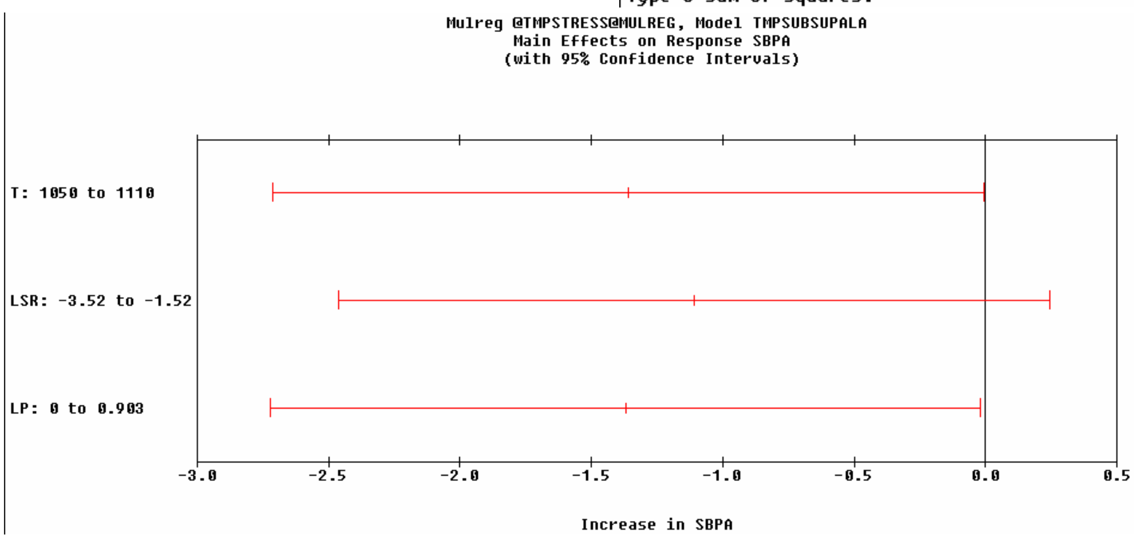

A-8.—Subsolvus plus supersolvus as-large-as grain size regression results.

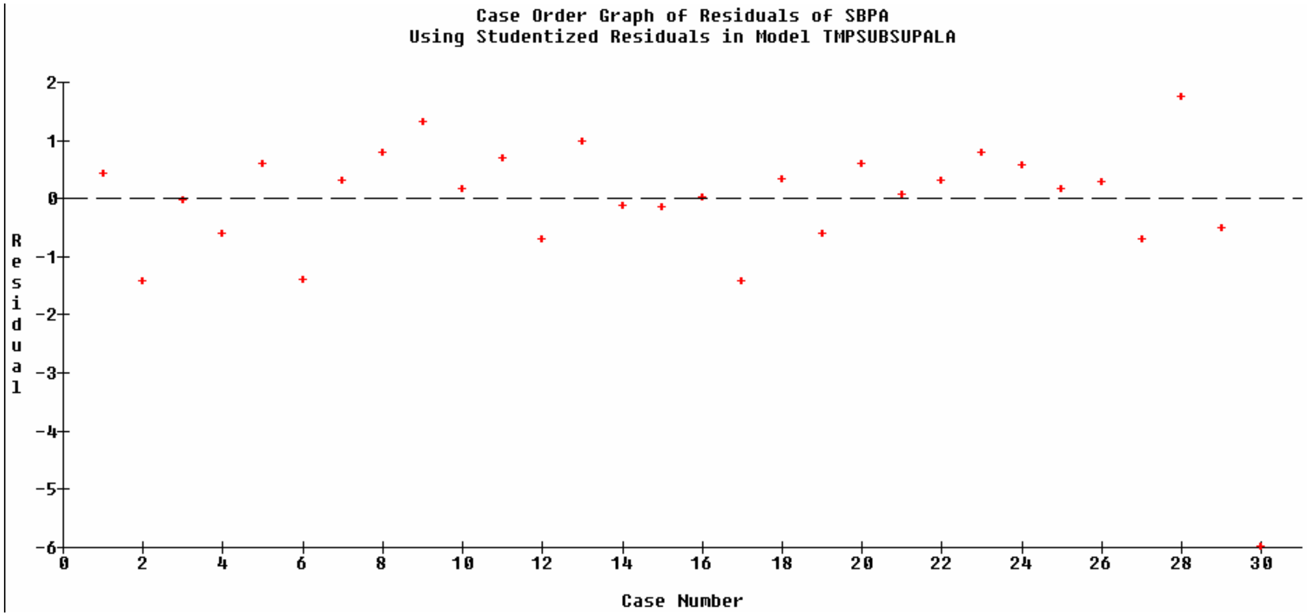

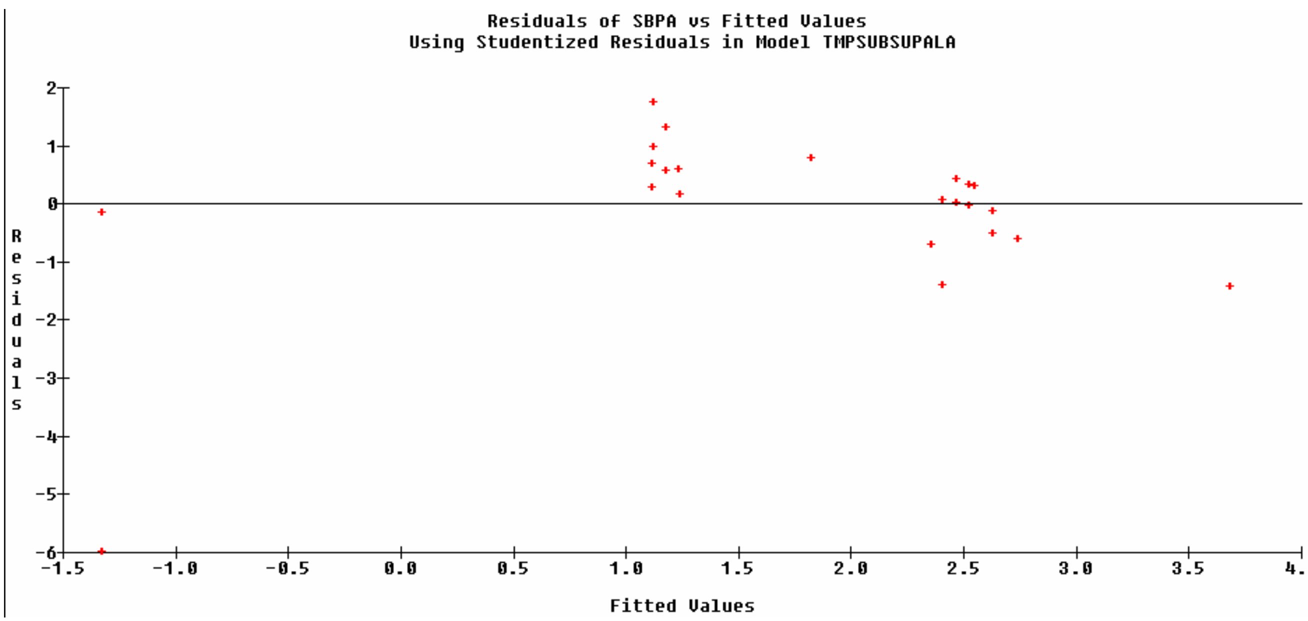

A-8.—Subsolvus plus supersolvus as-large-as grain size regression results.

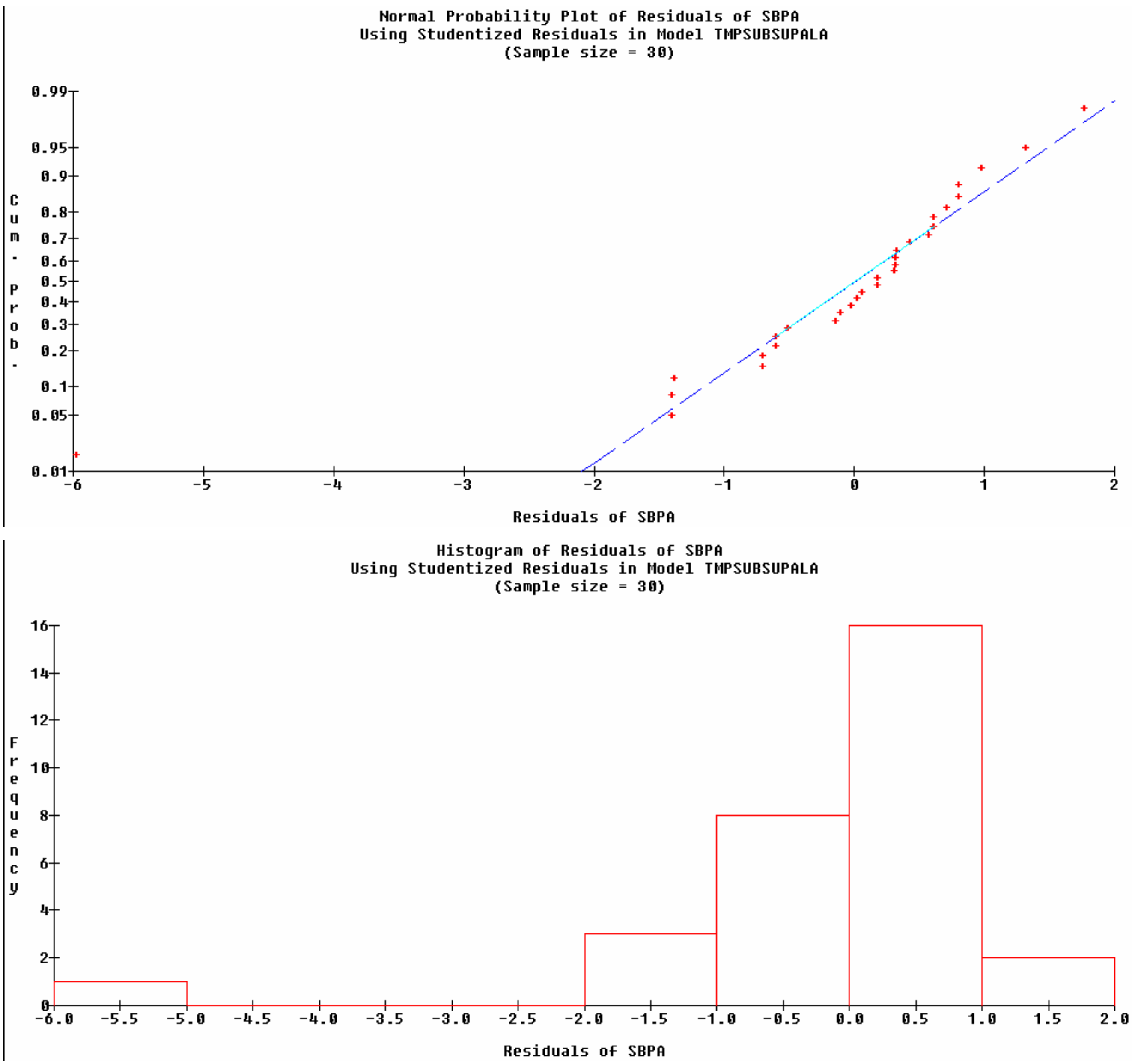

A-8.—Subsolvus plus supersolvus as-large-as grain size regression results.

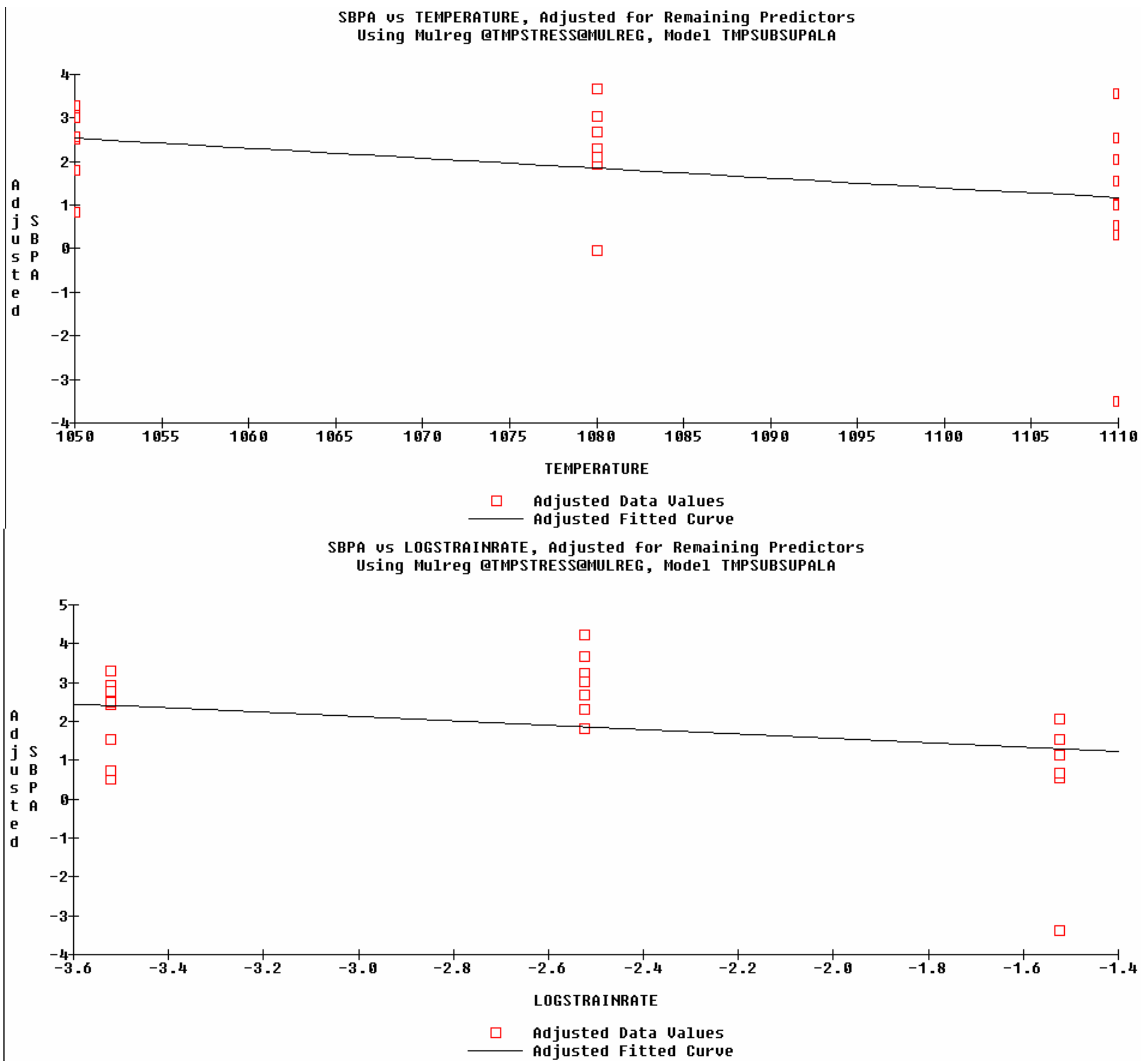

A-8.—Subsolvus plus supersolvus as-large-as grain size regression results.

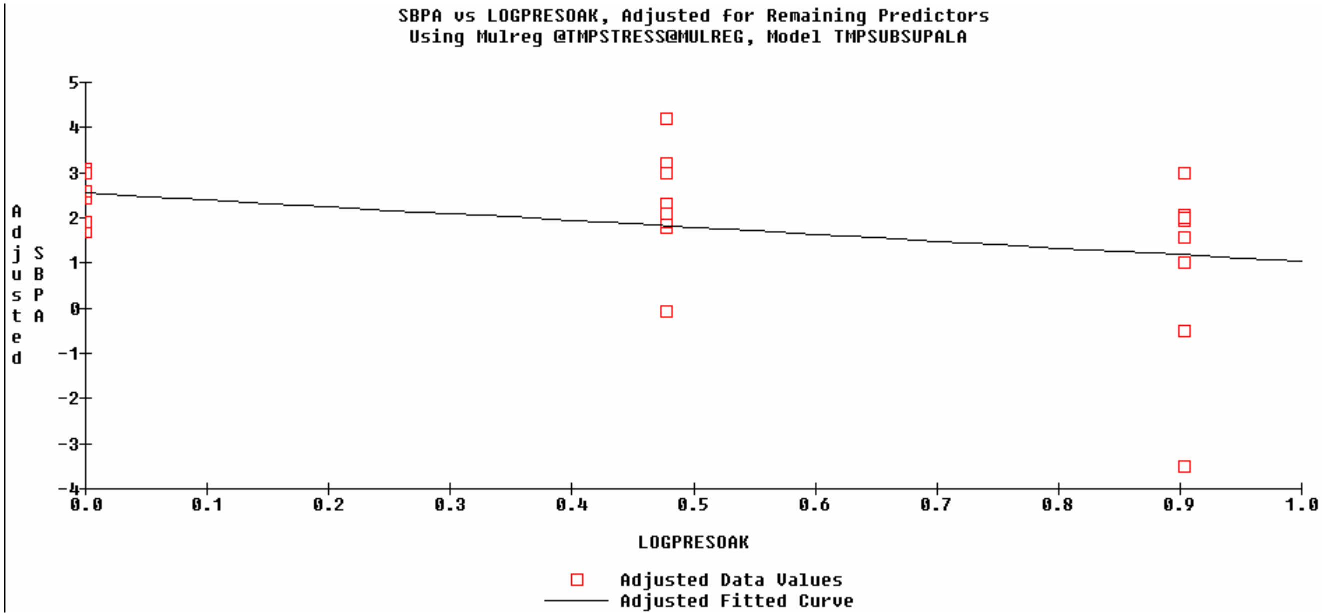

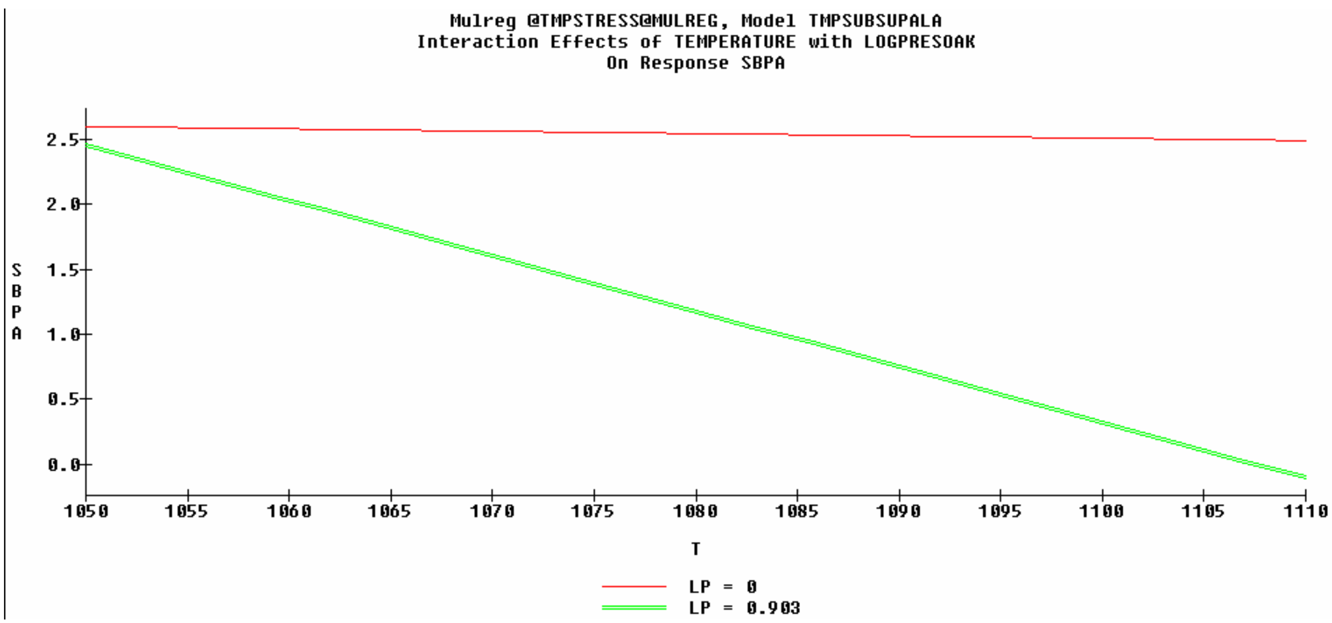

A-8.—Subsolvus plus supersolvus as-large-as grain size regression results.

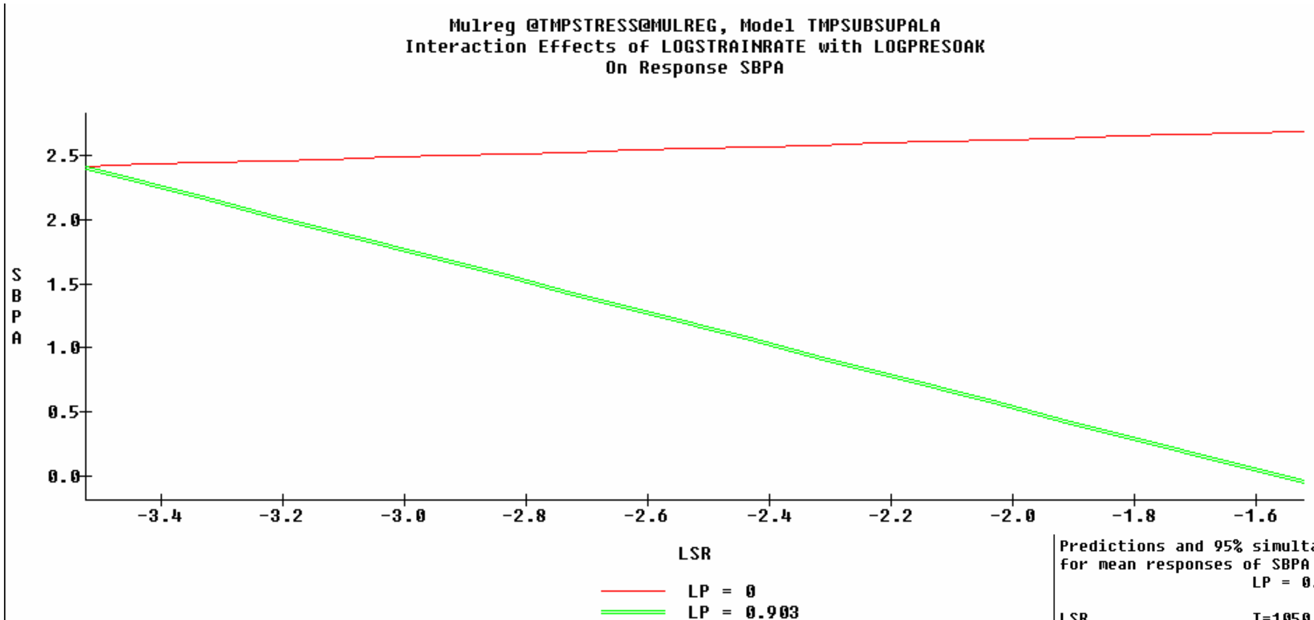

Predictions and 95% simultaneous confidence intervals
for mean responses of SBPA using model TMPSUBSUPALA
LP = 0.4771

LSR		T=1050	T=1080	T=1110
	Lower	1.027979	0.760820	-0.377544
-3.5229	Predicted	3.107666	2.404905	1.702143
	Upper	5.187353	4.048989	3.781831
	Lower	0.882833	0.784478	-0.522690
-2.5229	Predicted	2.526917	1.824156	1.121394
	Upper	4.171002	2.863833	2.765479
	Lower	-0.133519	-0.400678	-1.539042
-1.5229	Predicted	1.946169	1.243407	0.540646
	Upper	4.025856	2.887492	2.620333

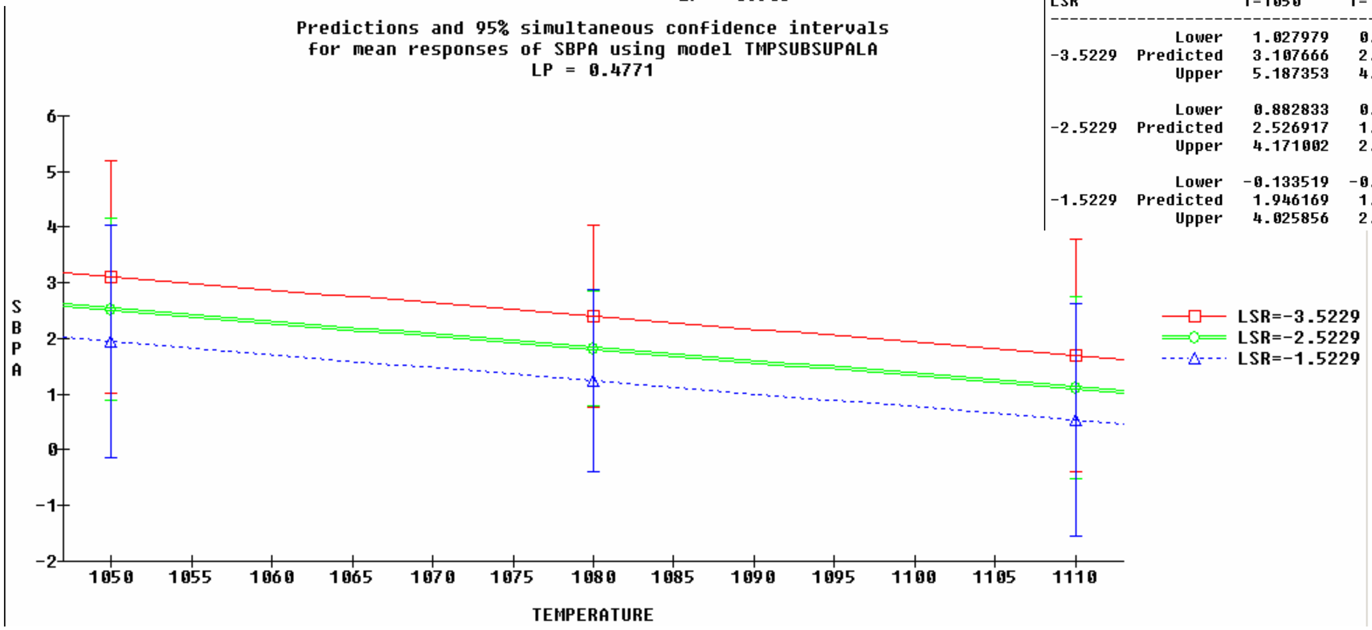

A-8.—Subsolvus plus supersolvus as-large-as grain size regression results.

REPORT DOCUMENTATION PAGE

Form Approved
OMB No. 0704-0188

1. AGENCY USE ONLY (*Leave blank*)

2. REPORT DATE
June 2005

3. REPORT TYPE AND DATES COVERED
Technical Memorandum

4. TITLE AND SUBTITLE
Forging of Advanced Disk Alloy LSHR

5. FUNDING NUMBERS
WBS–22–079–30–09

6. AUTHOR(S)
Timothy P. Gabb, John Gayda, and John Falsey

7. PERFORMING ORGANIZATION NAME(S) AND ADDRESS(ES)
National Aeronautics and Space Administration
John H. Glenn Research Center at Lewis Field
Cleveland, Ohio 44135–3191

8. PERFORMING ORGANIZATION REPORT NUMBER
E–15138

9. SPONSORING/MONITORING AGENCY NAME(S) AND ADDRESS(ES)
National Aeronautics and Space Administration
Washington, DC 20546–0001

10. SPONSORING/MONITORING AGENCY REPORT NUMBER
NASA TM—2005-213649

11. SUPPLEMENTARY NOTES
Timothy P. Gabb and John Gayda, NASA Glenn Research Center; and John Falsey, Cleveland State University, 2121 Euclid Ave., Cleveland, Ohio 44115–2214. Responsible person, Timothy P. Gabb, organization code RMM, 216–433–3272.

12a. DISTRIBUTION/AVAILABILITY STATEMENT
Unclassified - Unlimited
Subject Category: 07

Available electronically at http://gltrs.grc.nasa.gov
This publication is available from the NASA Center for AeroSpace Information, 301–621–0390.

12b. DISTRIBUTION CODE

13. ABSTRACT ***(Maximum 200 words)***
The powder metallurgy disk alloy LSHR was designed with a relatively low γ′ precipitate solvus temperature and high refractory element content to allow versatile heat treatment processing combined with high tensile, creep and fatigue properties. Grain size can be chiefly controlled through proper selection of solution heat treatment temperatures relative to the γ′ precipitate solvus temperature. However, forging process conditions can also significantly influence solution heat treatment-grain size response. Therefore, it is necessary to understand the relationships between forging process conditions and the eventual grain size of solution heat treated material. A series of forging experiments were performed with subsequent subsolvus and supersolvus heat treatments, in search of suitable forging conditions for producing uniform fine grain and coarse grain microstructures. Subsolvus, supersolvus, and combined subsolvus plus supersolvus heat treatments were then applied. Forging and subsequent heat treatment conditions were identified allowing uniform fine and coarse grain microstructures.

14. SUBJECT TERMS
Gas turbine engines; Rotating disks; Heat resistant alloys; Fatigue (materials)

15. NUMBER OF PAGES
131

16. PRICE CODE

17. SECURITY CLASSIFICATION OF REPORT	18. SECURITY CLASSIFICATION OF THIS PAGE	19. SECURITY CLASSIFICATION OF ABSTRACT	20. LIMITATION OF ABSTRACT
Unclassified	Unclassified	Unclassified	